APTAMERS FOR ADULTERANT DETECTION AND NANOBASED STRATEGIES FOR PATHOGEN CONTROL

Ph.D. THESIS

by

LAMBADI PARAMESH RAMULU

DEPARTMENT OF BIOTECHNOLOGY
INDIAN INSTITUTE OF TECHNOLOGY ROORKEE
ROORKEE-247 667 (INDIA)
OCTOBER, 2014

APTAMERS FOR ADULTERANT DETECTION AND NANOBASED STRATEGIES FOR PATHOGEN CONTROL

A THESIS

Submitted in partial fulfilment of the
Requirements for the award of the degree
of

DOCTOR OF PHILOSOPHY
in

BIOTECHNOLOGY

by

LAMBADI PARAMESH RAMULU

DEPARTMENT OF BIOTECHNOLOGY
INDIAN INSTITUTE OF TECHNOLOGY ROORKEE
ROORKEE-247 667 (INDIA)
OCTOBER, 2014

INDIAN INSTITUTE OF TECHNOLOGY ROORKEE
ROORKEE

CANDIDATE'S DECLARATION

I hereby certify that the work which is being presented in the thesis entitled **"APTAMERS FOR ADULTERANT DETECTION AND NANOBASED STRATEGIES FOR PATHOGEN CONTROL"** is in partial fulfilment of the requirements for the award of the Degree of Doctor of Philosophy and submitted in the Department of Biotechnology of the Indian Institute of Technology Roorkee, Roorkee is an authentic record of my own work carried out during a period from August, 2008 to October, 2014 under the supervision of Dr. Naveen Kumar Navani, Associate Professor, Department of Biotechnology, Indian Institute of Technology Roorkee, Roorkee.

The matter presented in this thesis has not been submitted by me for the award of any other degree of this or any other Institute.

(Lambadi Paramesh Ramulu)

This is to certify that the above statement made by the candidate is correct to the best of my knowledge.

Dated: October 2014

(Naveen Kumar Navani)
Supervisor

The Ph.D. Viva-Voce Examination of **Mr**. **Lambadi Paramesh Ramulu**, Research Scholar, has been held on..... .

Signature of Supervisor Signature of Chairman, SRC Signature of External Examiner

Signature of Head of the Dept/Chairman, ODC

ABSTRACT

With ever increasing population and rapid urbanization, the food handling system has changed enormously across the globe to meet the demand of the population. Outbreak of diseases due to contamination of food by chemicals, microbial pathogens, and toxins represents a serious threat to human health and imposes economic burden on individuals, families, industries and eventually countries. Therefore, screening of food items meant for human consumption for presence of undesirable species and adulterants are of immense significance in agriculture, industrial and healthcare sectors.

Urea is amongst the most commonly used adulterant in preparation of synthetic milk. A chemical biology approach was adopted for generation of urea specific aptamer by performing Flu-Mag SELEX and an aptamer-AuNPs based assay was developed for urea detection. The fluorescence assay demonstrated highest binding affinity for U38 aptamer with a dissociation constant of 238 nM. Circular dichroism study of U38 aptamer showed significant structural changes and an increase in the melting temperature by 9°C with urea, thus confirming stronger binding interactions. Based on the observation of ligand induced structural changes, the U38 aptamer was taken further for the development of an aptamer-AuNP based optical detection assay for urea in milk. A simple, rapid and user friendly method for milk sample preparation by methanol precipitation was standardized. Regions of U38 aptamer interacting with urea were determined by carrying out truncation studies, which highlighted the role of hair-pin motif in the forward region to be responsible optimum performance for the aptamer-gold nanoparticles assay. The aptamer-AuNPs biosensor developed in this study was specific for urea as compared to structural analogs *viz* glycine, alanine, serine and tyrosine. A urea dependent fluorescence recovery of gold nanoparticle quenched FITC-U38 aptamer further confirmed the specificity of the assay. In presence of 100 mM urea 85.5% fluorescence was recovered, while no significant recovery was observed with 100 mM glycine, confirming the specificity of the U38 aptamer for urea. Further, the robustness of the developed assay for other adulterants added to milk was evaluated and it was found to be unaffected in presence of salt (500 µM), sodium bicarbonate (20 mM), glucose (600 µM) and tween-20 (1%). The aptasensor demonstrated a linear range of detection of 20-150 mM, with a lower visual detection limit of 50 mM. While the method offers advantages of being rapid, simple and specific for detecting high concentration of urea in milk, it can be further improved for increasing the sensitivity. This method can also be adapted for detecting urea in clinical samples since urea is a pathological marker in several renal associated diseases.

Apart from adulteration of food, diseases caused by foodborne pathogens are worldwide problem. *E. coli* O157:H7 is declared by Centre for Disease Control and Prevention (CDC) amongst the most dreadful foodborne pathogen, causing haemolytic uremic syndrome, characterized by bloody diarrhea. *E. coli* O157:H7 is known to produce type IV pilus (TFP) called as hemorrhagic pilus (HCP), which plays a central role in attachment to the mucosal epithelial cells. Amplification of *hcpA* locus from *E. coli* O157:H7 genomic DNA was performed and was cloned in pET28(a) vector. The expressed His-tagged protein His-HcpA was immobilized to the nickel NTA agarose beads for carrying out an affinity chromatography based SELEX for the selection of HcpA specific aptamers. An initial binding study of different selection round by electrophoretic mobility shift assay (EMSA) demonstrated binding in 10^{th} round population. Further cloning and sequencing of the 10^{th} round of population was done and sequences were grouped in to different categories. Based on the structural folding, eight putative aptamers were selected based on the stability in terms of free energy. Preliminary binding study for the putative aptamers by EMSA demonstrated binding of HcpA-38, 41, 64 and 75 aptamers with target HcpA protein. Further, the best binding aptamer sequences can be coupled to different transducing elements like gold nanoparticles, single walled carbon nanotubes for detecting *E. coli* O157:H7.

Bacterial infections are not only limited to foodborne diseases, but also have been extensively associated with nosocomial infection due to surgical devices and medical implants. Excessive use of antibiotics in hospitals has led to the emergence of antibiotic resistance among different nosocomial bacteria. Since the pace of conventional drug discovery is slow, there is urgent need for devise new strategies to kill or curb the growth of the antibiotic resistance microbes. In the present study, silver nanoparticles were bio-functionalized with polymyxin B antibacterial peptide using a facile method. The bio-functionalized nanoparticles (PBSNPs) were assessed for antibacterial activity against multiple drug resistant clinical strain *Vibrio fluvialis* and *Pseudomonas aeruginosa*. The results of antibacterial assay revealed that PBSNPs had ~3 fold higher antibacterial effect than the citrate capped nanoparticles (CSNPs). Morphological damage to the cell membrane was studied by scanning electron microscopy, testifying PBSNPs to be more potent in controlling the bacterial growth as compared to CSNPs. Bactericidal effect of PBSNPs was further confirmed by Live/Dead staining assays. Apart from the antibacterial activity, the bio-functionalized nanoparticles were also found to resist biofilm formation. Electroplating of PBSNPs onto stainless steel surgical blades retained the antibacterial activity against *Pseudomonas aeruginosa*. Further, the affinity of polymyxin for endotoxin was exploited for its neutralization using PBSNPs. It was found that the prepared

nanoparticles removed 97% of the endotoxin from the solution. Such multifarious uses of metal nanoparticles can be explored as viable means of enhancing the potency of antimicrobial agents to control infections.

LIST OF PATENTS AND PUBLICATIONS

PATENT

- Nucleotide sequences specific for detection of urea. Applied at Indian patent office (**Application number 901 /DEL/2014).**

PUBLICATION

- **Paramesh Ramulu Lambadi**, Tarun Kumar Sharma, Piyush Kumar, Priyanka Vasnani, Sitaramanjaneya M Thalluri, Ranjana Pathania, Naveen Kumar Navani (2014). *Facile bio-functionalization of silver nanoparticles for enhanced antibacterial properties, endotoxin removal and biofilm control*. Colloids and Surfaces B: Biointerfaces. **(Communicated)**

CONFERENCE

- Piyush Kumar, **Paramesh Ramulu Lambadi**, Tarun Kumar Sharma and Naveen Kumar Navani **(2013)**. *A Biotechnological Approach for Detection of Synthetic Milk Components; Urea Detection*. Challenges in disaster mitigation and management. Organized by Centre of Excellence in Disaster Mitigation and Management, IIT Roorkee from February 15-17, 2013.

ACKNOWLEDGEMENT

This thesis is an outcome of the past five years, wherein I grew stronger, accepted failures and strived harder for success. I have been accompanied and supported by many people during this journey. I feel honoured that I have now the opportunity to express my gratitude to all those people who contributed directly or indirectly to this endeavour.

I would start with thanking GOD, for bestowing his choicest blessings on me and always providing a guiding light for me to walk on the right path of life. Without his grace, this would not have been possible.

My sincere gratitude and heartfelt thanks to my guide and mentor Dr. Naveen Kumar Navani, Assistant Professor, Department of Biotechnology, IIT Roorkee. I am fortunate to be given an opportunity to work under his supervision. His mentorship was paramount in providing a well rounded experience consistent my long-term career goals. His constant focus on precision, enlightening ideas, constructive criticism and scientific freedom helped me pave my way towards becoming an independent researcher. I am deeply indebted to him for believing that a hypothesis which was put forth as being implausible could actually be validated. His unfaltering encouragement to pursue challenges throughout this program helped me immensely. I owe him more than words express.

I am grateful to Dr. Ranjana Pathania for her invaluable suggestions and inputs in shaping my work. Her ideas and encouragement towards my work proved very helpful.

I feel overwhelmed in thanking Dr. R. Prasad, Professor and Head Department of Biotechnology for providing necessary facilities, support and cooperation in the Department for research.

I extend my heartfelt thanks to my student research committee (SRC) Dr. A.K. Sharma, Chairman SRC, Professor R. Prasad, Associate Professor, Department of Biotechnology and Professor Shishir Sinha, Professor Department of Chemical Engineering for their encouragement and suggestions.

I extend a note of thanks to the staff members of my lab and department Mr. Jain , Mr. V.P Saini, Shashi madam, Mohan, Akshay, Anil ji and Ravi for providing technical assistance and care .

I seize the opportunity to express my special thanks to Dr. Santosh, Dr. Piyush,, Manasi, Rekha, Tapas, Tamoghna, Pardeep and Abhijeet, for their kind support for the completion of the thesis.

The members of my lab contributed immensely to my personal and professional time at IIT Roorkee. The group has been a source of friendships as well as good advice, collaboration and providing a stimulating and fun filled environment. I want to thank all the members of my lab CBDD Dr. Rajnikant, Dr. Supriya, Dr. Tarun, Dr. Jitendra, Atin, Anjul, Timsy and Dr.Ila for providing a helping hand during my research work.

I am grateful to my friends Pradeep, Dr.Selvakumar, Dr.Shivender, Dr.Aditya, Manju, Prabhat, Bibekanand for all the emotional support and camaraderie during this period.

I am also indebted to the students I have had the pleasure to work with.

Last but not the least I owe it to my family for believing in me and supporting me throughout my life. I fall short of words when I come to think of my family's contribution. Their endless patience and priceless words of advice have helped me make it so far.

Besides this, several people have knowingly and unknowingly helped me in the successful completion of this project. I thank all of them.

Financial assistance provided by CSIR is gratefully acknowledged.

Roorkee ***(Lambadi Paramesh Ramulu)***

CONTENTS

LIST OF FIGURES

LIST OF TABLES

ABBREVIATIONS

AFM	Atomic microscopy
Amp	Ampicilin
ATP	Adenosine Triphosphate
AuNPs	Gold nanoparticles
BME	*β-Mercaptoethanol*
BSA	Bovine serum albumine
CD	Circular dichroism
CFU	Colony forming unit
CSNPs	Citrate capped nanoparticles
CV	Crystal violet
DLS	Dynamic light scattering
DNA	Deoxyribonucleic acid
DNA	Dexoy-ribonuleic acid
dsDNA	double stranded DNA
EDC	N-(3-dimethylaminopropyl)-N-ethylcarbodiimide
EDTA	Ethylene diamine tetra acetic acid
EHEC	Entero hemorrhagic *Escherichia coli*
EMSA	Electrophoretic mobility shift assay
FITC	Fluorescein isothiocynate
FITC-RDL	FITC labelled random DNA library
FITC-U38	5' FITC labeled U38 aptamer
FRTU38	Forward and reverse truncated U38 aptamer
FTIR	Fourier transform infrared
FTU38	Forward truncated U38 aptamer

g	Grams
HCP	Hemorrhagic Coli Pilus
HcpA	hemorrhagic coli pilin subunit/monomer
His-HcpA	Histidine tagged hemorrhagic coli pilin subunit/monomer
IPTG	Isopropyl thio β, D-galactoside
Kan	Kanamycin
kDa	Kilodalton
L	Liter
LB	Luria Bertani
mA	milli Ampere
mg	milligram
min	minutes
ml	milliliter
mM	millimolar
Ni-NTA	Nickle Nitrilotriacetic acid
nm	nanometer
nM	nanomolar
O.D	Optical density
PBSNPs	Polymyxin B capped silver nanoparticles
PCR	Polymerase chain reaction
pH	power of hydrogen
PNA	Peptide nucleic acis
RDL	Random DNA library
RNA	Ribonucleic acid
RNA	Ribonucleic acid
ROS	Reactive oxygen species

rpm	rotation per minute
RT	Room temperature
RTU38	Reverse truncated U38 aptamer
s	seconds
SDS	Sodium dodecyl sulphate
SEM	Scanning electron microscopy
SPR	Surface plasmon resonance
ssDNA	single stranded DNA
STEC	Shiga Toxin producing *Escherichia coli*
TAE	Tris Acetate EDTA buffer
TBE	Tris Borate EDTA buffer
TE	Tris EDTA
TEM	Transmission electron microscopy
TEMED	N ,N,N,N – Tetra methyl ethyl diamine
TFP	Type IV pilus
t-RNA	yeast transfer RNA's
U38/FLU38	Full length U38 aptamer
Urea-CMB	Urea coupled carboxyl magnetic beads
UV	ultraviolet
V	Volt
X- Gal	5–Bromo, 4 – chloro, 3 –indolyl β, D-galactoside
µg	microgram
µl	microliter
µM	micromolar
°C	Degree Celsius
A_{620}/A_{520}	Absorbance ratio of 620 and 520 nm

CHAPTER 1
INTRODUCTION

The world population is on the rise and is anticipated to reach 7.6 billion by 2020, with approximately 98% of this population growth taking place in developing countries like India. The population is expected to reach 3.4 billion in urbanized countries across the globe. These exponentially increasing numbers have s*et al.*arm bells for world health and food security. Rising urbanization and changes associated with it has altered the way food is produced and handled, thus lengthening the food chain with chances of introducing or exacerbating foodborne hazards. Outbreak of diseases due to contamination of food by chemicals, microbial pathogens, and toxins represents a serious threat to human health and imposes economic burden on individuals, families, industries and eventually countries [1]. Therefore, food safety is an important public health concern for all countries. Extensive efforts are being made by strategies like Hazard Analysis and Critical Control Point (HACCP) Hurdle technology to prevent, eliminate or reduce the incidences of food borne illnesses by implementing the 'active managerial control' system in food industries [2]. An active managerial control (AMC) system seems to be an attractive ploy for reducing the contamination risk, but this faces challenges of strictly following the critical and rigorous steps involved in AMC. While developed countries seem to have successfully adopted this strategy, it has proven difficult for AMC to establish its roots in developing countries. Consequently, these issues have stressed the need to develop methods to asses and monitor the presence of health hazards to avoid human health problems.

Milk and its related products are highly nutritious and are widely consumed all around the world. Therefore, milk plays an essential role in international market and is given immense economic importance. India is the leading milk producing country on the global map, accounting for 127.9 million tons of milk production [3]. The unorganized, fragmented dairy sector, tropical climate (favoring bacterial growth), laxity in quality control and escalating population with increased demand has made milk vulnerable to different types of adulteration [4]. Adulteration has been defined as deliberately debasing the quality of food either by adding poisonous or deleterious substances, mixing or substituting substances of inferior quality or by removing valuable ingredients from food. Food Safety and Standards Authority of India (FSSAI) reveals that 70% of the milk in India, especially the liquid milk does not conform to the standards [5]. The situation is further deteriorated by the incessant use of synthetic milk in the market. Synthetic milk is a perfect blend of vegetable oil, urea, detergent, powdered sugar/salt and skimmed milk powder in water which imparts it thick and creamy consistency

similar to the natural milk. Urea is one of the key ingredients used to increase the nitrogen content of the synthetic milk, thus mimicking the high protein content of normal milk. Even though urea is secreted in milk as a byproduct of protein metabolism at a harmless concentration (8 – 40 mg/dl) [6], but further addition of urea to milk has adverse effects on human physiology. Addition of urea has been associated with nephritis, renal dysfunctions (acute or chronic), urinary tract obstruction, diabetes and certain extra-renal diseases such as congestive heart failure and liver diseases. Adulteration of milk is mostly restricted to Indian sub-continent. Reports of melamine adulteration in infant milk have emerged recently from China [7]. It becomes imperative to detect urea not only in dairy sector but also in clinical and agricultural industries (environmental analysis). Several extant methods are available for detection of urea which include Van Slyke aeration and titration method [8], gas chromatography [9], calorimetry [10] and fluorimerty [11]. However, these methods have several drawbacks such as use of hazardous chemicals and complicated sample pretreatment which renders the process time consuming and unsuitable for onsite detection. Consequently, these issues have highlighted the need to develop simple, rapid, sensitive and cost effective methods to detect and monitor the presence of undesirable species to avoid human health problems. Biosensors are looked upon as the alternative to the existing method with characteristics to overcome the drawback of the extant detection methods available.

Biosensor is an analytical device which is comprised of a biological molecular recognition element (enzyme, aptamer, antibodies, whole cells, cellular receptors, etc.) and a physico-chemical transducer [12]. Biosensors have been categorized into electrochemical, optical, acoustical, mechanical, calorimetric, or electronic types based on the ability of the transducer to convert the biological response into a measurable signal which usually is proportional to the analytes concentration[13-16]. A range of urease enzyme based biosensors have been developed for detecting urea. These biosensors are based on non-conducting and conducting polymer, sol-gel polymeric matrices, Langmuir-Blodgett films, nanomaterials (based on nanoparticles, quantum dots and nanofibers) and ion-selective field effect transistor [17]. Although these are considered sensors for urea, yet they suffer from complicated sample pretreatment , stability issues with urease enzyme, interference in functionality by ionic strength of the medium, lack of reproducibility, complicated design, long response time and requirement of sophisticated instruments. Therefore, there is a need of a new biological recognition element with greater stability as compared to the enzyme based biosensors.

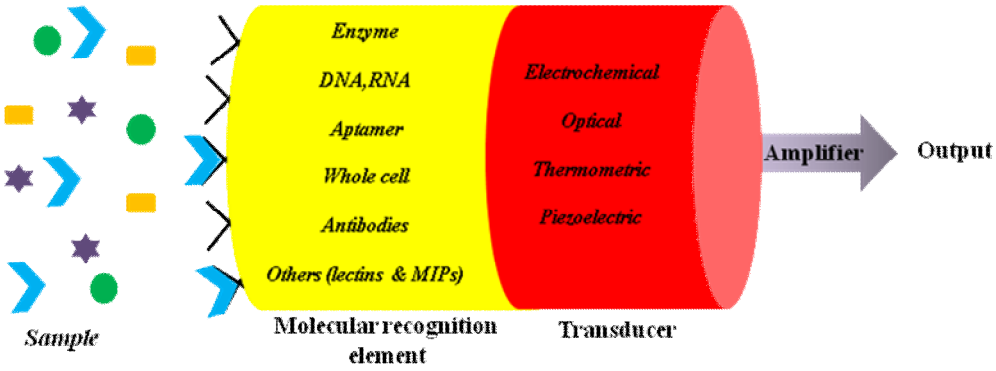

Fig 1.1 Schematic representation of Biosensors

Aptamers are single stranded DNA or RNA biomolecules selected to binding a wide range of targets starting from simple species as ions to complex target such as whole cells [18-36]. Aptamer are generated through an *in-vitro* process known as Systematic Evolution of Ligands by EXponential Enrichment (SELEX) [37, 38]. Aptamers have unprecedented advantages over enzymes or antibodies, as they can be selected for any possible targets in their native conditions, thus extending their use as molecular recognition element (MRE) in detecting analytes in real field samples. Aptamers offer several additional advantages as MRE in biosensors by virtue of stability in different ionic conditions, thermostablity, ability to be synthesized in bulk with high reproducibility and purity. Even though a series of aptamer based biosensors have been developed using different transducers, yet transducers offering "label-free" and "real-time" sensing of target molecule are considered desirable.

With recent advancement in nanotechnology, there has been a surge in development of novel nanaostructures, nanodevices, nanomaterials, and nanoparticles for designing new biosensor with improved properties [39-41]. Metal nanoparticles; especially gold nanoparticles (AuNPs) are being exploited as the transducer elements for developing optical aptasensors. Gold nanoparticles exhibit several exclusive properties such as biocompatibility, chemical stability, strong localized surface plasmon resonance (LSPR), and high extinction coefficient [42]. Gold nanoparticles functionalized with aptamers have been reported for colorimetric detection of several analytes [43-50]. Further, to circumvent functionalization steps which are cumbersome, time consuming and costly; unmodified gold nanoparticles appear to be an excellent choice for developing an aptamer based optical biosensors [51-61]. Aptasensors based on colorimetric detection can be optimized for developing onsite detection methods due

to the specificity, sensitivity, simplicity, and detection of analytes on visual basis or by naked eye.

Apart from adulteration of food, diseases caused by food borne pathogens are a worldwide problem, both in terms of public health and economic cost. Foodborne Disease and Active Surveillance Network (FoodNet) surveyed 15% (an estimated 48 million) of US populations for incidences of infections transmitted by pathogens through food sources. The report confirms 19,056 infections, 4,200 hospitalizations, and 80 deaths in 2013 accounting from *Campylobacter, Cryptosporidium, Cyclospora, Listeria, Salmonella,* Shiga toxin–producing *Escherichia coli (STEC/EHEC)* O157 and non-O157*, Shigella, Vibrio,* and *Yersinia* [62]. Although the rate of incidence of food borne diseases is high, many cases go unnoticed unless and till an outbreak is reported. An estimate from World Health Organization (WHO) testifies that overall only 10% of foodborne infection cases in developed countries and only 1% in developing countries are notified. In India the magnitude of the problem associated with foodborne disease is difficult to estimate as many of them go unreported, unrecognized or un-investigated [63]. In many cases the delay in identifying the etiological agent from the time of exposure, takes several days thus delaying the exact course of treatment for the disease which can prove to be life threatening [64].

Even though *Escherichia coli O157:H7* contributes to only 2% of food borne cases when compared to the *Salmonella* (23.4%), yet the cause to fatality ratio (CRF) are same (0.4) for both the bacteria i:e 0.4, suggesting the importance of *E. coli O157:H7* in terms of food safety for consumers [65]. *E. coli O157:H7* is declared by Centre for Disease Control and Prevention (CDC) amongst the most dreadful foodborne pathogen, causing gastroenteritis diseases in infected individuals. Infection occurs after ingestion of contaminated food such as undercooked beef, raw contaminated milk, unpasteurized apple juice/cider, lettuce, dry cured salami, yogurt, vegetables [66]. Furthermore, transmission has been characterized from sources such as direct contact with cattle and its related environment [66]. *E. coli O157:H7* shows cytopathic effect on different cells causing watery diarrhea which may leads to hemolytic uremic syndrome (HUS) and thrombotic thromobocytopenic purpura (TTP) under severe conditions eventually leading to death [67, 68]. Therefore detection of this dreadful pathogen in clinical and suspected food samples becomes an indispensable step in controlling outbreak of the disease. While traditional culture based methods and some rapid molecular detection techniques (RFLP, PCR, DNA microarray etc), immunological methods, ATP bioluminescence assay and immunomagnetic separation have been developed for *E. coli O157:H7* [69-72]; yet a simple,

rapid, highly sensitive and cost effective approach for bacterial detection is the need of the hour. To fill the void of the conventional and rapid methods, biosensors have emerged as the superior alternative for bacterial detection which will complement the fight to control the further spread of pathogens [73-77]. As chemical biology tools aptamers have evolved as the possible answer to this problem. Infections instigated by *E. coli O157:H7* have been well studied till date and research still continues to decipher various biomolecules involved in its pathogenicity. One of the important factors is Hemorrhagic coli pili (HCP) of *E. coli O157:H7* which is involved in bacterial adhesion whose immunomodulatory role for onset of disease has been well documented [78, 79].

Bacterial infections are not only limited to foodborne diseases, but also have been extensively associated with nosocomial infection due to surgical devices and medical implants. Such infections pose persistent and severe problems that account for high morbidity in hospital settings with significant socio-economic burden on healthcare system worldwide [80-83]. According to Centre for Disease Control and Prevention (CDC), surgical site infections account for ~22% of hospital acquired infections [84]. Bacteria by virtue of its ability to adhere to different surfaces are capable of initiating a process of biofilm formation, which is a key factor for their survival in hostile environment. Biofilm protects bacteria from the assault of antibiotics which otherwise is sufficient enough to kill the planktonic cells [85]. The situation is further deteriorated with pervasive and imprudent use of antibiotics that have contributed immensely to the emergence of multiple drug resistance (MDR) bacteria [86]. Therefore, several prevention strategies are being developed which aims at either inhibiting the adhesion of the planktonic cells or killing the bacterial cells which have adhered. These strategies are based on either modifying the physicochemical properties of the device surface or direct coating of antimicrobial compounds on the surfaces of medical devices [87-90]. Advances in the field of nanotechnology have motivated the scientists to develop innovative strategies to utilize nanomaterials which not only effectively control bacterial infections but can also mitigate their toxins.

One such strategy is the use of silver nanoparticles (SNPs) as antimicrobial coatings on surfaces of medical devices. Since SNPs interact with bacterial surface by random collision, high concentration of SNPs are required to exert antimicrobial effect [91]. Toxicity issues associated with silver demand that silver be used at a concentration as low as possible. To overcome this problem, silver nanoparticles have been synthesized using various biological moieties including antibiotics, enzymes, polysaccharides, and oligopeptides so as to enhance

the antibacterial potential [92-94]. In recent years, antimicrobial peptides (AMPs) have emerged as excellent antimicrobial agents to address multidrug-resistance in bacteria [95, 96]. AMPs act like "molecular knife" and facilitate the damage to bacterial cell membrane even at low concentrations [97]. Additionally, AMPs can stabilize SNPs by exerting polyvalent effect as they form layers on the surface of SNPs and thus prevent agglomeration [98, 99].

This thesis aims at utilizing chemical biology and nanotechnology approach for detection of environmental contaminants and strategy to mitigate nosocomial threat.

Objectives

1. ***Generation of urea specific DNA aptamer and development of an aptasensor for "urea" detection***

This objective deals with generation of urea specific aptamers through Flu-Mag SELEX [110], and initial development of a qualitative aptamer-AuNPs based colorimetric assay *i:e "Presence or Absence"* of urea in real milk samples beyond the natural limit. Further the qualitative approach of the urea specific aptasensor was extended to a quantitative assay, where the limit of detection for the method was determined. The colorimetric assay was further tested for its specificity or selectivity for urea against structurally similar molecules and interfering substances/molecules present in synthetic milk. Eventually the limit of detection for the assay was determined.

2. ***Development of DNA aptamer for Hemorrhagic Coli Pilin (HcpA) of Escherichia coli O157:H7***

This objective deals with development of DNA aptamer against HcpA of *E. coli O157:H7*. In brief the *hcpA* locus of *E. coli O157:H7* encoding for HcpA was cloned and expressed as His-tagged protein. Aptamer selection for recombinant HcpA was performed by SELEX using Ni-NTA bound recombinant HcpA. DNA populations from different rounds of selection for HcpA were tested for its binding towards purified HcpA using electrophoretic mobility shift assay (EMSA). The putative aptamer population of a selected round was amplified and cloned. The clones thus obtained were screened for the best binding aptamer sequence. Development of HcpA specific aptamer further opens up different avenues such as developing an aptasensor for specific detection of *E. coli O157:H7* in buffer as well as different sample matrices.

3.1.2.3. Nanobased strategies for pathogen control

The purpose of this study was to enhance the antibacterial activity and test these preparations for various medical applications. For this (i) we have chosen polymyxin B (antimicrobial peptide) to synthesize bio-functionalized nanoparticles by a simple and efficient method, (ii) We assessed the PBSNPs for their antibacterial and antibiofilm activity against multi drug resistant clinical isolate of *Vibrio fluvialis* and *Pseudomonas aeruginosa* PAO1, (iii) Further, we coated stainless steel surgical blades with PBSNPs and tested their ability to mitigate nosocomial pathogen *Pseudomonas aeruginosa*, (iv) Finally, we tested the ability of PBSNPs to mitigate endotoxins from solution.

CHAPTER 2

REVIEW OF LITERATURE

An anticipated rise in world population to a staggering figure of 7.6 billion in 2020 has aggrandized the already existing and the everlasting problem of global food crisis. This affects the political and economic stability of a country creating social unrest in developed and developing nations. With rapid urbanization across developed countries food handling system has changed to meet the food demand of the population. This magnitude of demand for food has increased the steps in handling the food; extending its storage, processing and distribution further in the food chain, thus increasing the chances of introducing or exacerbating foodborne hazards (Fig.2.1)

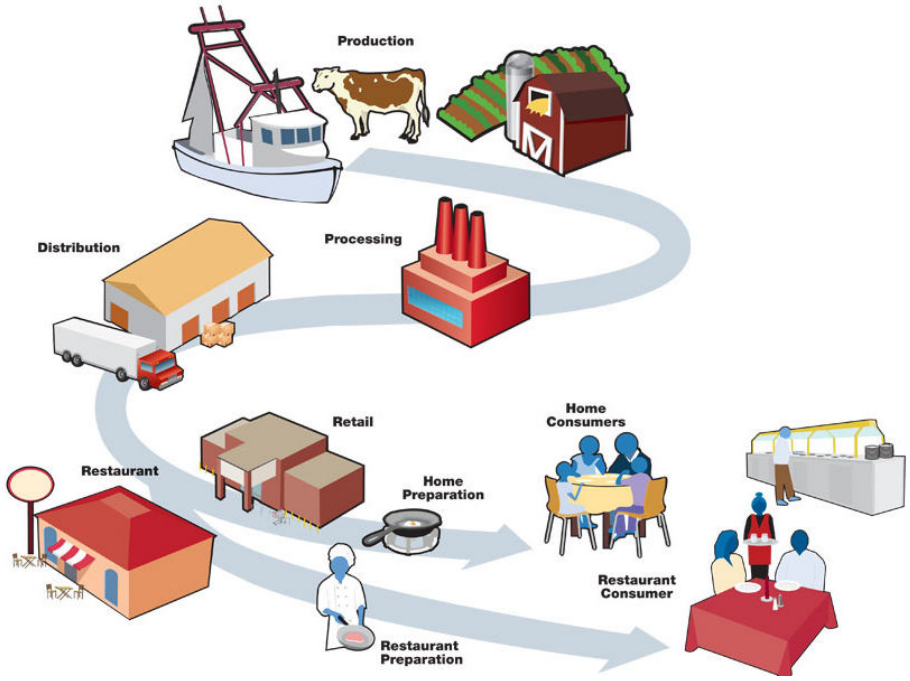

Fig. 2.1 Food production chain: From growth, harvesting, storage, processing to distribution

Since ancient times humans have been dependent on each other for many things, food has been one of the most important thing. Still the scenario remains unchanged in this contemporary world, where food export is an important aspect of trade to meet the demands of the needy. Food in every form is perishable and its consumption has been associated with dreadful diseases. Foodborne disease outbreaks have been linked with either contamination of food by chemicals, microbial pathogens or toxins of microbial origin. These contaminants impose a serious threat to human health and have socio-economic impact on families, directly affecting industries and eventually are a setback to the growth of the country [1]. Therefore,

food safety is a prerequisite for public health worldwide. In recent years the importance of food safety with regards to food borne illness has been addressed by World Health Organization (WHO) by increasing the standards of food safety policies adopted for export. Despite the growing international awareness of foodborne diseases, risk associated with health and socio-economic development, food safety still remains completely unresolved. Although Hazard Analysis and Critical Control Point (HACCP) is a strategy being adopted for food safety, but its rigorous implementation of the active managerial control (AMC) needs to be assessed on a global platform [2]. Apart from this strategy which has contained the situation within limits, there is an ever increasing demand for introducing analytical systems for critically assessing and monitoring the real-time contaminants of the food, further curtailing the incidences of foodborne diseases

2.1. Milk

The history of milk goes way back to 8000 BC and since then it goes hand in hand with the human civilization. Since, its discovery the importance of milk has been summoned in ancient Egyptian, Indian Vedic and ancient Hebrew civilization along with its mention in the Bible [100]. Milk is included in the food pyramid chart prepared by United States Department of Agriculture (USDA) signifying its importance in our day today diet (Fig.2.2).

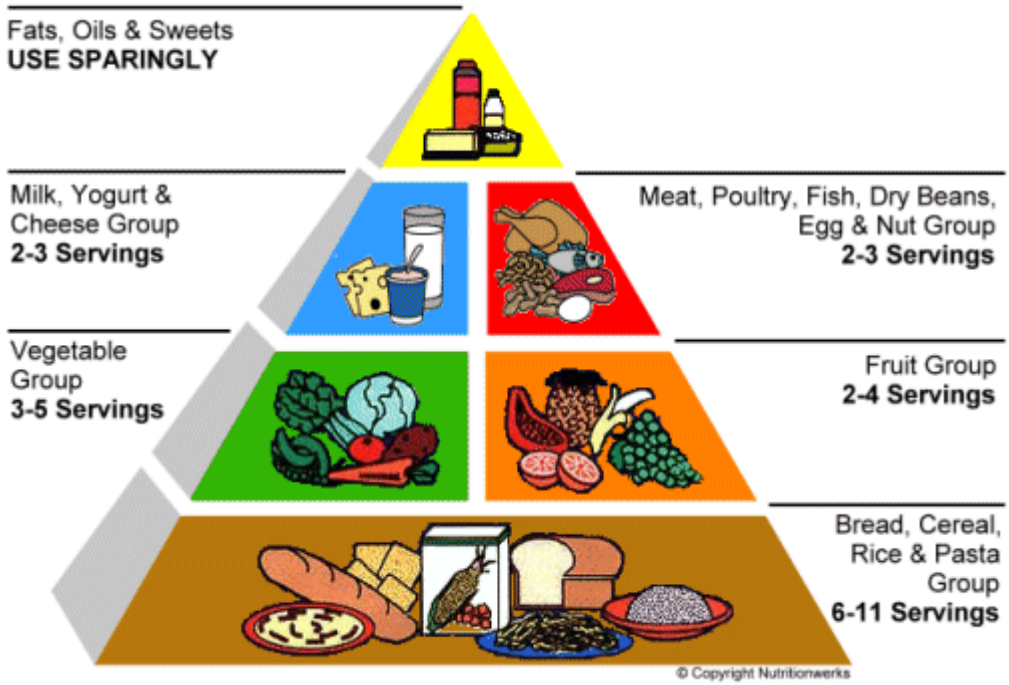

Fig. 2.2: Food pyramid

Milk is considered to be a complete food, supplementing nutrients essential for development and maintenances of the sound physiological status of the body. Therefore, it plays an important role in international market, which gives it immense economic importance. India is the largest milk producing nation on the map, but it fails to meet the increasing demand of the people which are mostly based on the cultural diversity (rituals) and eating habits which greatly involves either milk or milk products in their diets [3]. In India, most of the credit for the failure to meet the demand goes to the unorganized and fragmented dairy sector which is equally supported by the tropical climate providing an ambient temperature for growth of foodborne organisms, thus affecting the quality of milk. Further laxity in quality control and increasing demand has made milk vulnerable to different types of adulteration.

Adulteration is an act of voluntarily deteriorating the quality of the food offered, either by supplementing poisonous or deleterious substance, mixing or substituting inferior quality substances or removal of beneficial substances [101]. Adulteration is not only limited to the intentional act of debasing the quality of food by addition, substitution or removal of essential ingredients of the milk, but also covers the incidental contamination during the food production chain (Fig. 2.1). The most primitive and common act of adulteration is done by increasing the volume of milk adding water, thus decreasing its nutritional value. In China, more than 50,000 infants suffered from renal complications after consumption of milk adulterated with melamine used to increase the nitrogen content of milk, which mimics high protein content [7].

Survey conducted by Food Safety and Standard Authority of India (FSSAI), claims that 70% of the commercially available milk in the market is of inferior quality and is unfit for human consumption [5]. The situation is further deteriorated by the incessant use of synthetic milk in market containing cheaper and highly toxic chemicals for its synthesis. Synthetic milk is a perfect combination of vegetable oil, urea, detergent, powdered sugar/salt and skimmed milk powder in water, imitating the chemical characteristic and composition of natural milk [102, 103]. Role of each ingredient in synthetic milk is listed in the table 2.1.

Table 2.1 Role of synthetic milk components

Synthetic milk components	Purpose/role
Vegetable oil	Represents milk fat
Salt or sugar	Adjustment of lactometer reading
Urea	Increase nitrogen content
Detergent	Emulsifier
Sodium bicarbonate	Adjustment of alkalinity

Synthetic milk can be easily detected based on the differences in it physical and chemical characteristics as compared to the natural milk. But on the contradictory, adulteration of synthetic milk in a defined proportion with natural milk is very difficult to detect as no altercation in the color, taste, odour or consistency of the milk is observed. Prevention of Food Adulteration Act (PFA) system has declared addition of external urea to the milk as illegal and even the Supreme Court of India has stated this act as heinous crime and a punishable offence [104].

Table 2.2 Differences in properties of synthetic and natural milk

Property	**Synthetic milk**	**Natural milk**
Physical		
Colour or appearance	White as natural milk	White
Odour	Saopy smell, once prepared freshly, but disappears when stored overnight at 4 °C	Not distinctive
Taste	Extremely bitter, not palatable at all	Palatable
Density	1.025-1.035	1.025-1.035
Storage	Shows spoilage and appearance of yellow color at room temperature	Curdling but no change in color on storage at room temperature
Texture	Soapy to touch	No soapiness
pH	Highly alkaline,10.5	Slightly acidic, 6.4-6.8
Urea concentration	14mg/ml	0.2-0.7mg/ml
Urea test	Highly positive, intense yellow	Weakly positive, faint yellow color
Fat	4.5%, can be varied easily	4.5%
Sugar test(Resorcinol)	Positive	Negative

Urea is an integral part of synthetic milk production; therefore it becomes impetrative to detect urea, as it imposes severe effect on human health. A brief review of different methods for urea detection is discussed in the following section.

2.2. Urea

Urea [CO $(NH_2)_2$] is an integral part of mammalian physiology (humans and dairy animals), thus signifying its importance in clinical chemistry and dairy industry [105, 106]. Detoxification of ammonia produced as a result of protein metabolism takes place in liver yielding urea as the end product. Urea has been shown to have detrimental effect on human when exceeds its physiological limit. For humans the normal value of blood urea nitrogen (BUN) content ranges from 6-60 mg/dl, whereas in patients suffering from renal inefficiency the value of BUN may vary from 120-300 mg/dl [107]. While, in cattle the normal milk urea

nitrogen (MUN) level is 18-40 mg/dl, with the maximum limit set to be 70 mg/dl [108, 109]. The MUN also acts as the standard for real time monitoring of urea content in dairy industries which is an indicator of protein feeding efficiency [110]. This real time assessment decreases the feed cost, increases the protein content of the milk, and improves the reproductive performance with minimal disposal of urea in environment [111, 112]. Urea is a normal constituent of milk which makes up to 55% of the total non protein milk nitrogen content [113]. MUN of 70 mg/dl in milk is an upper limit and value above this concentration makes milk unfit for human consumption and represents an act of adulteration. Consumption of such milk can lead to severe health problems such as indigestion, acidity, ulcers, impairment of kidney and even cancer. Therefore, it becomes relevant and imperative to detect and monitor urea in environmental and clinical fields, dairy industries and food processing units.

2.3. Urea sensors

Although several different methods have been published and employed for detection of urea especially from the clinical point of view, still there is an increasing demand for simple, sensitive, robust, reliable, cheap and an onsite detection method for sensing urea in other fields such as food science and environmental monitoring.

2.3.1. Colorimetric methods

An extensive literature survey suggests two fundamental colorimetric methods for determination of urea i) direct (non-enzymatic) and ii) indirect (enzymatic) iii) miscellaneous methods.

- The direct method involves the reaction of urea with diacetly-monoxime or similar compounds to give a chromgenic product that can be quantified spectrophotometrically [114, 115].
- The second, indirect method for urea estimation involves the use of urease enzyme to breakdown urea into ammonia which then react's either Nessler's reagent or by Berthelot reaction to forms colored product [116].
- Miscellaneous methods such as Van Slyke aeration, titration and gaseometric, manometric, infrared or UV-visible spectrophotometery measures release of nitrogen after reaction with hypobromite, hypochlorite etc and by combining urease with ammonia ions selective electrode [115, 116].

Various different chemicals have been screened for the direct urea detection methods such as Ehrlich's reagent xanthydrol, o-phthalaldehyde, nioxime, diacetyl-monoxime and benzoylacetyl- monoxime. Among these well studied chemicals, diacetyl- monoxime was

selected as the best candidate offering the least amount of concerns and drawback as compared to the others for its use in different arena of science for estimation for urea. The diacetyl-monoxime method is based on the Fearons reaction to form a yellow colored product [117]. Although this method is the choice for urea estimation over other chemical reagents, it suffers from drawbacks such as instability of the colored formed, interference from polypeptides, amino acids, citrulline, allantoin, semicarbazide, and substituted urea. This method also suffers from drawback of using obnoxious reagents, hazardous chemical with corrosive nature detrimental for equipment in use, heating step adding to the volatile pollution at work place, time consuming and requires pre-treatment of samples. Apart from these disadvantages the method is widely used as it is very specific and avoids ammonia related problem associated with enzymatic based method. Several modifications of Ormsby's *et al.* (1942) diacetyl-monoxime methods have been introduced [118-120] with improvement in stability of the developed color and reduction in assay time. This improved manual method was used to develop automated flow injection analysis by Sullivan, *et al.* 1991 for rapid analysis of different samples ranging from clinical to environmental [121, 122].

These enzymatic methods too are associated with problems of being inaccurate and pose reproducibility issues due to the unavoidable problem with ammonia, giving a false impression of increased nitrogen content in biological fluids such as blood. Also this method is an unattractive ploy for urea estimation in samples which contains either urease inhibitors such as sodium, potassium, fluoride ions and ammonia the product of urease activity [114]. While improvement in the primitive and the development of new chemical methods were in progress, an emerging field of sensor coined as "biosensor" was discovered to tackle all the above issues associated with the chemical method.

2.3.2. Biosensors

Biosensors are looked upon as the alternative method of choice over the traditional chemical methods with advantages of being simple, rapid, sensitive, robust, reliable, and cheap with onsite detection abilities. Owing to their potential advantages biosensors have been applied in environmental monitoring, food safety and field of medical diagnostics [123].

Inspired by the sensing characteristic of biological molecules present in the nature, most of the chemical and physical methods to detect analytes have found an impressive alternative known as the "BIOSENSOR". Biosensors are analytical devices that incorporates molecular recognition element (MRE) linked to a physico-chemical transducer which acts synergistically to sense several different analytes. The MREs of the biosensors are biological molecules such

as enzymes, nucleic acids (DNA, RNA or aptamer), whole cell (bacterial and mammalian), antibodies, cell receptors and other biologically derived or inspired molecules (lectin and molecular imprinted polymers). MRE is the cornerstone of any biosensor as it acts as the probe which recognizes different analytes, while transduction of this biorecognition event into measurable signals is performed by transducer.

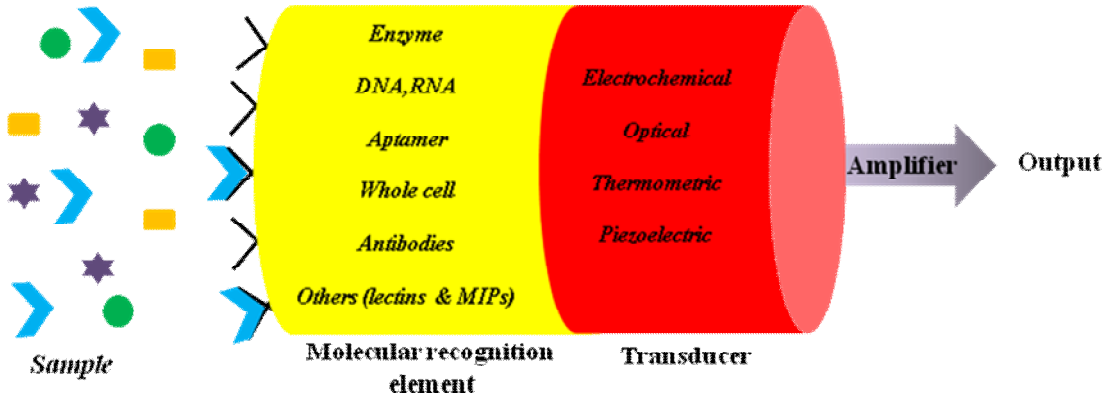

Fig 2.3. Basic design of a biosensor

Biosensors can be divided into different categories based on the physico-chemcial changes that accompanying the recognition event, such as electrochemical (potentiometric, condutometric and amperomteric), optical, thermometeric and piezoelectric. The concept of biosensor came from Professor Leland C. Clark (1962), to sense glucose using glucose oxidase entrapped at the Clarks oxygen electrode. Since then it has acted as the model for rest of the biosensors developed. The first urea sensor was developed by Guilbault and Montalvo employing urease as the biosensing element which degrades urea to ammonium and bicarbonate ions. This biosensor worked on the principle of sensing ammonium ion thus bringing a change in the potential across the cation selective glass electrode.

$$NH_2CONH_2 + 3H_2O \xrightarrow{\text{Urease}} 2NH_4^+ + OH^- + HCO_3^-$$

Different transducing elements such as CO_2 electrode, ammonium gas selective glass electrode, pH electrode, ammonium ion selective electrode and miniaturized urea electrode using ion-selective field effect transistors have been used for sensing urea [108]. Urease based urea biosensors have been developed by using various matrices such as conducting and non-conducting polymers, sol gel, Langumir-Blodget films, nanoparticles and self assembled monolayers (SAMs) [17, 108]. These matrices have played key role in providing urease the support for immobilization, stability in varying temperature, pH and ionic strength, increase in shelf life and thus reducing the cost for developing urea biosensors. Immobilization of urease to different matrices has been achieved either by physical or chemical methods [17].

2.3.2.1. Polymer matrix based urea biosensors

2.3.2.1.1. Non-conducting polymers

Urea biosensors have been fabricated based on wide variety of polymers such as phosphine oxide polyether, polygalacturonate, polyurethane-acrylate, acrylonitrile, hydroxyapatite, alginate, bovine serum albumin, poly (vinyl ferrocenium), polyethylenimine, synthetic latex polymer, activated polyvinyl alcohol (PVA), polyvinyl chloride (PVC) and chitosan [17]. These polymers offer a wide range of characteristics by their ability to be tailored over a range of chemical and physical properties. Apart from providing physical support to the enzyme, mechanical strength and long term stability these polymers presents great flexibility, biocompatibility in designing cost effective biosensors.

Sehitogullari and Uslan's [124] developed a potentiometric biosensor by immobilizing urease on PVA activated with 2-flouro-1-methylpyridiniumtoluene-4-sulfonate (FMP), with detection limit of only 1mM which is lower than the physiological range. Later in 2004, Lakard *et al.* developed a metal electrode potentiometric biosensor using polyethylenimine films [125] The biosensor had quick response time of 15-30 s, detection range $1 \times 10^{-2.5}$ to $1 \times 10^{-1.5}$ M with 4 weeks life time. An increase in the stability of the biosensor developed was linked to the chemical immobilization step, preventing the leaching off of the enzyme from the electrode. Immobilization of urease by electroprecipitating poly (vinyl ferrocium) per-chlorate electrodes was performed by Kuralay *et al.* 2006 biosensor for urea with linear detecting range of 1 to 250 μM and a handsome shelf life of 29 days [126]. Nonetheless, the matrices experience a drawback of releasing toxic degradation products.

Natural polymers such as chitin and chitosan, offers advantages of being biocompatible and non-toxic in nature. Therefore it has been widely used as the immobilization support for urease enzymes for industrial application in detecting urea. The optimized immobilization method was found to be adsorption followed by reticulation of gutaraldehyde solution, with improved response characteristics of 30 s to 2 min, linear detection range of 10^{-4} to 10^{-2} M and 2 months life time [127]. However, further work needs to be carried out for development of natural polymer biosensor with commercial application.

PVC based NH_4^+ ion selective potentiometric biosensors are considered to be the advanced version of the pH electrode [128, 129] and ammonium ion selective electrodes [130, 131] that sense the ammonium ion liberated by enzymatic reaction. These electrodes show strong dependence on buffer capacity with compromised sensitivity and narrow detection limits. PVC membrane glass based electrodes [132, 133] modified with ionophores [134] have

been their possible replacement, with shorter response time, good reproducibility and extended life time of 12 months. The potential use of aminated-PVC membrane electrode has been well discussed [132]. Walcerz *et al.* 1995 developed aminated-PVC pH membrane electrode covalently immobilized with enzyme for estimating urea by quantifying the hydronium ion after enzymatic reaction [135]. Later, in 2002 a miniaturized buffer independent urea sensor was fabricated based on the immobilization of urease on all the solid state, aminated-PVC membrane and NH_4^+ selective electrode [136] with detection range of 5×10^{-2} and 5×10^{-4} M. However, the performance of the sensor was severely affected in presence of sodium and potassium ions. Kovacs *et al.* 2003 developed an optical biosensor in the form of a thin plasticized PVC film comprised of optode-membrane ion selective optical biosensor with ion selective ionophore (nonactin) and ETH 5294 (Chromoionophore). Although the method was sensitive it suffered from the drawback of being influenced by NH_4^+, Na^+, and K^+. The PVC-NH_2 based biosensor was replaced by carboxylated-PVC based biosensors which showed improved performance in response time, sensitivity and durability of the sensors. This developed method also challenges the biosensors based on palmitic acid and non-actin improvised PVC membrane NH_4^+ ion selective electrodes for sensing urea serum concentrations [137].

Regardless of the development in non-conducting polymer based urea biosensors, a lot of them still have to overcome the problems encountered with interfering species. Also the bulky electrodes system needs to be upgraded with miniaturized biosensors, cutting on the cost price for reagents and enzymes used.

2.3.2.1.2. Conducting polymers

Conducting polymers are conjugated polymers synthesized by either chemical or electrochemical methods. These polymers can be synthesized with controlled film thickness, desired conductivity, different functionalization possibilities and using several supporting electrolytes. The conducting polymers have been extensively studied by several researchers for its electrochemical property [138-140], and devices based on these polymers are of increasing clinical importance. A one step process of entrapping enzymes into the polymer during the process of electropolymerization can be achieved, which offers even distribution of polymer films on to the surfaces of electrodes of any shape and size [141].

Among the existing different conducting polymers, polyaniline, polypyrrole and polythiophene has been the choice for designing amperometric based urea biosensors. Out of these three polymers, polypyrrole has been the most widely used fabricating urea biosensors

[142-144]. Polyaniline and polythiophene have not gained the popularity as the polypyrrole has, as they become electro-inactive in neutral pH limiting their use in biosensors. An amperometric flow injection based biosensor was developed by Adeloju *et al.* 1996 [145], with linear detection range of 3-15 mg/l of urea. Rajesh *et al.* 2005 later improved on the sensitivity of the amperometric biosensor by increasing the enzyme concentration while preparing the polypyrrole film with additional use of pulsed amperometric detection [146]. The detection limit achieved was 60 mg/l with linearity in the range of 100-450 mg/l. Apart from advantages this developed biosensor had shelf life of only 2 weeks and requires pre-treatment through anion exchange separators for removing interferants in biological samples before detecting urea [146]. Efforts to improve the sensitivity of biosensor designed using polypyrrole was initiated by Komaba *et al.* 1997 by preparing a composite film with polyion complexes [147]. However, immobilization of urease on to the composite via electropolymerization was exceedingly low. Therefore polyacrylic acids were found to be the replacement of polyions complexes, enhancing the efficiency of immobilization with improved response of 53 mV per decade. Further the sensitivity of 110 mV per decade was achieved by using combination of polyions (polycation polystyrene sulphonate and polyanion polyacrylic acid). The performance of the biosensor was in direct correlation with the amount of enzyme immobilized onto the electrode [148]. Although promising, the shelf-life and the reproducibility of the biosensor have not been reported.

It is well know that the performance of the biosensor strictly depend on the process of immobilization, therefore Adeloju *et al.* 1993 [147] entrapped urease into polypyrrole matrix by electrochemical means with stability of the biosensor of 2 months. However the developed biosensor cannot be reused. Later in the 1997, Adeloju *et al.* fabricated a thin urea biosensor by covalently immobilizing urease onto the copolymer of pyrrole and N-3-aminopropylpyrrole [144]. The biosensor showed stability of 2 months at 4-6 °C, detection range of 6.3×10^{-6} to 4.07×10^{-4} M with electrode sensitivity at 27.5 mV/dl. The use of polypyrrole offer an advantage of being a pH sensitive indicator at near –IR range, therefore acting as an optical indicator, with detection limit for urea in linear range of 0.06–1 M [142].

A phenylyaniline-poly(n-butyl-methacrylate) (Pn-PBMA) composite film with a homogenous combination of poly(vinyl methyl ether) (PVME) and poly(vinyl ethyl ether) (PVEE) as dispersants, has been adapted for the fabrication of urea and uric acid biosensors. Further a composite of polyaniline-Nafion based amperometric biosensor was developed using casting and electrochemical immobilization methods. It was found that casting method based

biosensor was better in it detection ability, with sensitivity of 6 mg/dl. However these methods still have to find their grounds in detecting urea in real time clinical samples. A multifunctional biopolymer layer based amperometric biosensor was developed using poly(pyrrole) and poly(5-amino-1-naphthol) [149]. Poly(5-amino-1-naphthol) playing a role of reducing interferences signal of ascorbic and uric acids, while the poly(pyrrole) acts as the electrochemical transducer. The developed method showed chemical immobilization to be the best for the performance of the urea biosensor developed, with better sensitivity, stability and shelf life compared to the other immobilizations methods. The sensor was sensitive upto 100 mM concentrations in a linear range with its possible use in clinical samples. Chirizzi *et al.* 2011[150] developed electrosynthesized poly(o-phenylenediamine) (PPD) film potentiometric biosensor with buffering capability. Urease was immobilized onto the galssy carbon electrode using PPD film, with limit of detection in the range 10 µM to 1 mM exhibiting sufficient sensitivity for practical urea estimation. Later in the same year, Lakard *et al.* 2011 [151] came up with a potentiometric urea biosensor based on urease either by layer by layer physisorbtions or by covalent immobilization on to the charged polysaccharides electrodeposited polyaniline. A better stability of the biosensor was due to the protecting role played by the polysaccharide and the sensitivity achieved was 1 µM to 0.1 mM.

In recent years, progress in the development of new conducting polymer and molecular imprinted polymers (MIPs) holds promise for the development of urea biosensors with better stability and improved reproducibility. MIPs are polymers tailored with predefined specific recognition site for the interaction of the target molecule, thus acting as the new generation of recognition elements. Huanga *et al.* 2009 [152] developed a biosensor with the aid of MIPs specific for urea on the gold electrode surface. However, the method suffers from the instability of the MIPs. Therefore, Alizadeh *et al.* 2013 [153] used cross-linked imprinted polymers offering a better stability and selectivity to the MIPs. A capacitive biosensor for urea with nanosized urea imprinted polymer receptors on graphite electrode surface was fabricated. Although, the biosensor showed dynamic linear range of detection of 0.1 picomolar to 0.1 mM, but suffers from drawback of being pH sensitive, with loss of activity in pH above 5. Also removal of interfering Ca^{+2} and Mg^{+2} by cation exchange resins was mandatory before samples are analysed for the urea estimation.

2.3.2.1.3. *Sol-gel based urea biosensors*

Sol-gel matrices are known to inherit different physical (rigidness, thermal and tunable porosity) and chemical (inertness and photostability) properties, therefore widely used for

fabricating several opto-electronic based biosensors. Immobilization of urease in tetramethyl orthosilicate sol-gel was used for coating on to a screen-printed inter-digitated array electrode for developing a conductometric urea biosesnor. The method showed detection in a linear range of 0.03–2.5 mM[154]. Even though the biosensor offers good reproducibility, denaturation of urease during encapsulation steps limits its shelf life only to 25 days. Tetra ethoxy orthosilicate (TEOS) sol-gel based embedded with urease, acetyl choline esterase with FITC dextran optical sensors have been developed as the optical biosensor for detection of multiple analytes such as urea. The sensor detects urea in 2.5 to 50 M range, but displays poor stability and with 45% drop in the sensitivity within 4 weeks [155]. Tetramethy-lorthosilicate (TMOS) derived sol–gel urease microencapsulated biosensors offer greater stability and sensitivity with detection limit of (0.01–30 mM) [156]. Although the method is suitable for estimating urea in serum samples, the results are highly variable in presence of interfering analytes (glucose, ferrous sulphate, thiourea and mercury chloride) and suffers from longer response time with stability of just 2 weeks. Sol-gel based urea biosensors suffers from drawback of lack of reproducibility, sensitivity and unknown catalyst matrix interaction probing researcher to find solutions to the existing problems or come up with a better alternative material.

2.3.2.2. Langmuir-Blodgett film

The Langmuir-Blodgett (LB) film technology preserves the biological activity of the enzymes which has been extensively used for sensing cholesterol, glucose and urea [157]. An ion selective field effective transistor (ISFET) functionalized with octadecylamine embedded urease enzyme films have been used for detecting urea in linear range of 0.2-20 mM. This developed sensor displayed a quick response time of 15 s and better stability was achieved using gutaraldehyde as the stabilizing agent [158]. LB films have been used for stably immobilizing urease monolayers onto octadecyl silane-modified SiO_2/Si substrates. A potentiometric urea biosensor based on mixed monolayer of poly(N-vinyl carbazole) and stearic acid of LB onto the electrode demonstrated sensitivity of 5mM, with shelf life of 5 weeks [157]. The notable fact of the LB film based biosensors is that most of them are not tested for urea detection in clinical samples and effect of interfering analytes has not been reported. A detailed study of the LB film based biosensor would give a better perspective of the promises the methods shows in developing urea biosensors.

2.3.2.3. Nanomaterials

Several nanomaterials with dimensions ranging from 1 to 100 nm are the products of nanotechnology, aiming at controlling the matter at its atomic level. These nanomaterials

exhibits distinct chemical and physical properties from there bulk matter counterparts such as enhanced plasticity [159], reactivity and catalytic activities [160], improved thermal and optical properties [161, 162], better electron transport and quantum mechanical properties [163, 164]. Apart from these properties, they also exhibit unique surface chemistry, biocompatibility and high surface area and large pore volume ratio. These novel properties have approved there uses in fabricating different promising biosensing platforms for chemical, biomedical and environmental sensing of several analytes [165]. Different nanomaterials such as metal nanoparticles (gold and silver), quantum dots and rods, magnetic nanoparticles, nanowires, nanofibers and nanotubes have been profoundly used in developing numerous biosensors for different applications.

Rapid progress in the field of nanotechnology has seen surge in the growth of nanomaterials with new properties. Functionalization of nanomaterials with natural biomolecules (enzymes, DNA, RNA and antibodies), ligands and bioactive groups; have been adapted to produce sensitive and selective biosensor for detection of a particular analyte [166]. Immobilization of enzymes on to different nanomaterials such as nanoparticles, quantum dots and nanofibers for selective sensing of urea is discussed in brief.

2.3.2.3.1. Nanoparticles

Gold nanoparticles (AuNPs) have been utilized for immobilization of enzymes onto the self assembled monolayers via chemical adsorption with retention of enzymatic activity [167, 168]. Yang *et al.* 2006 [167], developed a renewable potentiometric mercury sensor based on urease immobilized self assembled gold nanoparticles. Tiwari *et al.* 2009 [169], fabricated a urea sensor using a pH sensitive natural dye; heamtein. AuNPs electrode was functionalized with hyperbranched polyester-Boltron ® H40 (H40–Au) coated indium-tin oxide and further immobilized with urease to develop an amperometric based urea biosensor. The developed sensor demonstrated higher sensitivity in range of 0.01- 35 mM owing to efficient immobilization and showed enhanced shelf life with response time of 3 s. Tyagi *et al.* 2013 [170], deposited nickel oxide (NiO) nanoparticle film onto the idium tin oxide (ITO) coated glass substrate. This NiO-ITO-glass substrate acted as an efficient matrix for immobilization of urease for developing a urea biosensor. This method showed faster response time of 5s with urea detection in linear range from 0.83–16.65 mM. Most recent development in the field of nanoparticle came from Tyagi *et al.* 2014 [171], with development of NiO nanorod urea biosensor. The NiO nanorod biosesnor showed exact same range of detection and response time as NiO nanoparticles.

2.3.2.3.2. Quantum dots

Quantum dots are semi-conductors fluorophores with higher luminescent and photostable properties. A slightest change in the surface property of QDs results in a dramatic change in its optical property. This property has been exploited for fabricating biosensors for detection of specific analytes by coupling QDs with several biomolecules. A urea biosensor was developed by Haung *et al.* 2007 using a CdSe/ZnS QDs as an indicator with urease as the catalyst [172]. The urea detection system was based on the enhancement of the QDs luminescent intensity, which was in correlation to the enzymatic degradation product of urea. The detection limit of sensor was 0.01-100 mM with optimization of buffer conditions (pH and concentration). Later in 2008, Duong and Rhee developed urea biosensor using CdSe/ZnS QDs entrapped in sol-gel matrix [173]. The sensitivity of the sensor for urea was linear in range of 0-10 mM. The entrapped enzyme showed higher enzyme activity as compared to membrane immobilized urease and 12 fold better than urease immobilized on double layer. The sensor was stable for 2 months and is claimed to be suitable for biomedical and environmental applications.

Molecular imprinted chitosan film doped with CdS quantum dot was utilized for developing a voltametric based urea biosensor [174]. The QDs-CdS-MIP displayed quicker adsorption time, linear range of detection 5 picomolar to 100 nM, with lower detection limit of 1 picomolar. The feasibility of practical application for the developed methods was tested by estimating urea in blood. The method was found to be stable with good reproducibility. Azadbakht and Gholivand, used penicillamine-CdS quantum dot modified AuNPs electrode for the covalent attachment of Ni-2,3-pyrazine dicarboxylic acid (Ni-PDA) film for developing a QDs based urea biosensor [175]. The biosensor displayed excellent electrochemical catalytic activity towards urea oxidation. The method displayed quicker response time with good reproducibility, while the applicability of the method in real field samples still remains unexplored. Nonetheless the field needs further development with challenges of scientific queries to be answered.

2.3.2.3.3. Nanofibers and nanoporus membranes

Nanofibers synthesized by electro-spinning technique have been used for fabricating urea biosensor. A biosensor based on nanocomposite of urease and PVP showed faster response time with higher sensitivity [176]. Silicon wafer based amperometric urea biosensor was developed by immobilizing urease onto the organic polymeric conductor [177]. In another method the urease coupled SAM was chemisorbed onto the gold electrode by EDC coupling which showed three fold better sensitivity as compared to the previous reported method [178].

Also recently different nanomaterials based urea biosensor have been developed using zinc oxide, irconium oxide, iron oxide, tin oxide, titanium oxide nanoparticles, double layered hydroxides etc [179].

2.3.2.4. Miscellaneous

Some of the latest urea detection methods are summarized in the following section. Gabrovska *et al.*. discovered a new matrix for urease immobilization composed of rhodium nanoparticles embedded in a coploymer of chitosan with chemically modified aniline polymer [180]. The membrane thus developed was able to sense urea linearly from 1.6-8.2 mM with lower detection limit of 0.5 mM. The membrane thus developed was only stable for 10 days with performance of 86.8 % on the last date. An optical sensor for urea based on surface plasmon resonance was fabricated for biomedical applications by Bhatia and Gupta [181]. The optical probe of the biosensor is layered with silicon, silver and urease enzyme which shows a decrease in resonance wavelength proportional to the increasing urea concentration. The sensor was able to sense urea in the range of 0-160 mM, close to the range of physiological serum. It was observed that the sensitivity of the sensor decreases with the increase in the urea concentration with no effect on the accuracy of the developed method was seen. A novel piezoelectric biosensor was developed by immobilizing single enzyme nanoparticles on to the nanoporus alumina membrane for sensing urea in liquid and urine samples [182]. The method demonstrated great stability with quick response time of 12 s and linear detection range of 0.08 µM to 1mM with lower detection limit of 0.05 µM. The feasibility of the method was confirmed by testing its use in biological sample such as urine.

Even though there are number of biosensors developed so far, a lot of ongoing research is still in the wake of finding one simple, reliable, sensitivity, accurate yet robust method applicable for different types of samples at once. Commercially available methods are all enzyme based methods which suffer from drawback of high cost, complicated construction and requirement of reference electrode. The urease based methods have been shown to be nonspecific and catalyze the hydrolisis of other biomolecules such as formamide, acetamide and N-hydroxy urea. Also the presence of ions such as sodium, potassium and fluoride have shown to have inhibitory affect on the urease enzyme thus hampering the performance of the urease based biosensor. Apart from the search of advanced material with better signal transducing abilities, there is a need for seeking new biological recognition elements which can substitute or fulfill the shortcomings of the enzyme based biosensors. Nucleic acids aptamers can act as the protagonist of the forthcoming enzyme free biosensors.

2.4. Aptamer-gold nanoparticle based optical biosensors for small molecules

2.4.1. Systematic Evolution of Ligands by EXponential Enrichment (SELEX) process

Since the discovery of nucleic acids, they have been admired as the genetic material inheriting the role of carrying information that encodes for protein. Later as the time travelled through the phase of pioneering research in molecular mechanism of genetics, additional functions of nucleic acids were explored. In 1990's two independent research groups working separately came up with the revelation of identifying RNA sequences capable of binding a particular ligand in a specific manner, which were selected through an *in vitro* process called Systematic Evolution of Ligands by EXponential Enrichment (SELEX) [37, 38]. This functional nucleic acid were called aptamers, derived from the Latin aptus, meaning "to fit" and mers standing for "oligomer". Later, just preceding the discovery of RNA aptamer, DNA aptamer was also discovered by one of the same pioneering group.

A typical process of SELEX as shown in fig. begins with random DNA or RNA library pool of sequences, ideally containing 30-80 random nucleotide sequence flanked by two fixed primer domains. This pool of DNA is initially incubated with the target of interest which in case of small molecules, are immobilized to solid support matrix. Binding step is followed by separation step which involves washing off the unbound or non-functional sequences from the biding sequences. Bound sequences are eluted from the target by means of change in conditions such as temperature, pH, ionic change or use of chaotropic agent depending on the strength of molecular interaction between the target and the bound sequences. The separated sequences are than amplified to generate enough products to start up the selection process once again. As the PCR products are double stranded, they are rendered single stranded either by bead based method or by gel electrophoresis. Whereas RNA is transcribed from the PCR product by *in vitro* transcription and the pooled is RNA directly used of next round of SELEX.

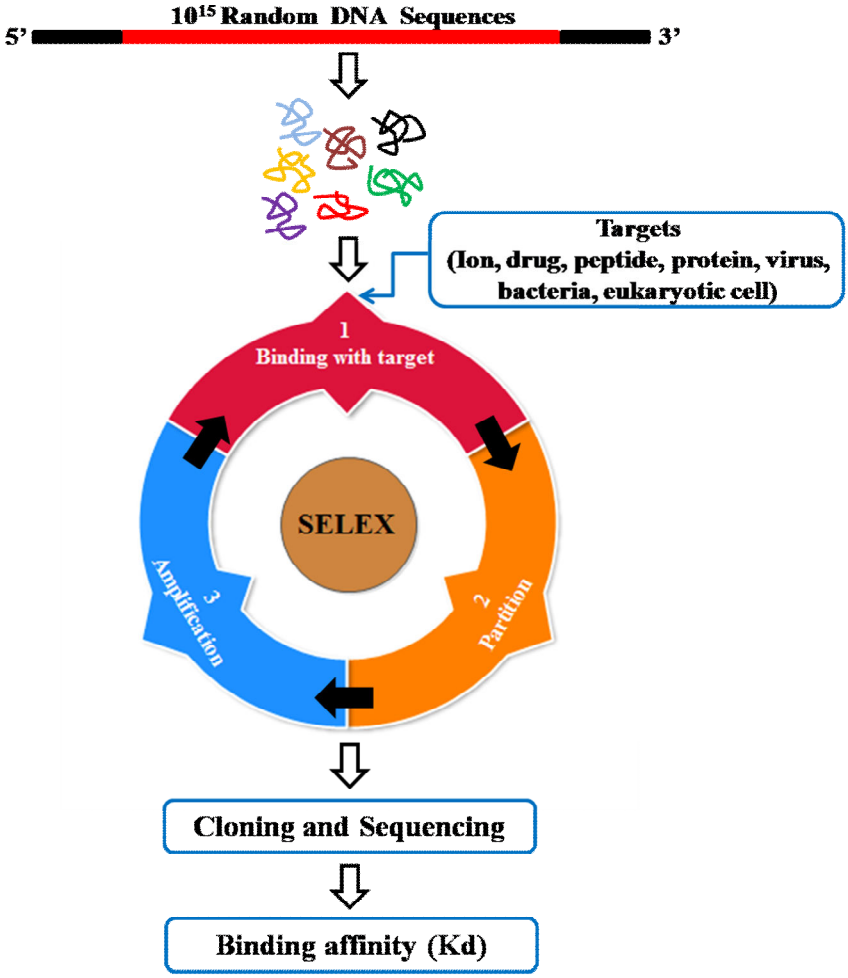

Fig 2.4 Schematic representation of SELEX process

2.4.2. Aptamers

Aptamers are single stranded oligonucleotide of RNA, DNA or PNA (peptide nucleic acids), which folds into intricate three-dimensional structure with help of Watson-Crick base pairing of the nucleotide, favoring formation of different functional nucleic acid domain enabling them to carry out functions such as gene regulation (Riboswitches), catalytic activity (DNAzymes) and ligand-binding. Since its discovery, different aptamer with high binding affinity and specificity has been developed for targets ranging from small molecules (organic dye, pesticides, drugs and chemical additives), metal ions, amino acids, peptide, proteins, to whole cells [18-35, 183-188]. Owing to the ligand binding property, aptamers plays an important role in diagnosis, by being an integral part of the biosensor and in therapeutics by inhibiting functions of certain biological molecules [189, 190]. Aptamers are also called as the "chemical antibodies" due to their synthetic nature and is considered to be an archrival of antibody when it comes to their potential use in different biosensors as the MRE [191].

2.4.3. Aptamer v/s Antibody/Enzymes

Antibodies have always fascinated the field of biosensors by acting as the formidable sensing element since its days of discovery. Along with enzymes the antibodies dominated the field of biosensor and were considered as the gold standard recognition element, until the discovery of aptamer which offers unprecedented advantages over these conventional natural sensing elements. First, aptamers can be selected in conditions mimicking the target's natural environment (pH, temperature and salt concentration). Second, aptamers in principle can be generated against any possible target, even for small molecules (metal ions, organic dyes, drugs, pollutants and chemical adulterants) for which antibodies are almost impossible to develop. Third, aptamers are also called as chemical antibodies as they are selected by *in vitro* process, once selected they can be generated in bulk via chemical synthesis with high accuracy and reproducibility with minimum batch to batch variation in their performance. Whereas, antibody generation uses animal or cell culture facility, which increases the chance of batch variation and finally may affect the performance of the biosensor. Fourth, the phophodiester bond of the nucleotides imparts aptamer greater stability to thermal and chemical changes. In changing conditions of pH, ionic strength or temperature, as antibodies tends to get denatured irreversibly whereas aptamers denature reversibly and can regain their functionality when conditions become favorable. Therefore, antibodies have limited use in onsite detection of analytes. Four, aptamers can be easily modified with different fluorescence tag, electrochemical indicators and nanoparticles. Apart from the advantages mentioned aptamers ability to undergo conformational changes upon target binding, this has introduced a new strategy in developing biosensor.

Owing to these advantages, aptamers have become an integral part of upcoming biosensors for environmental monitoring, food sector and in the field of medical diagnostics. Numerous aptamers have been generated till date for a wide variety of target namely cells, small molecules, proteins and virus (Fig.2.5).

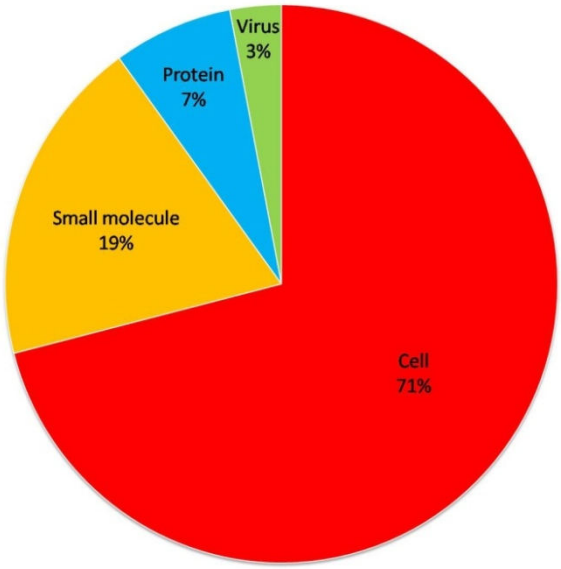

©Challenges and Opportunities for Small Molecule Aptamer Development

Fig 2.5 Data for aptamer generated against different target from 1990-2011.

2.4.4. Small molecule aptamers

Although selection of aptamer started with the small molecule in 1990 [37, 38], but they make up only 19% among all the aptamers discovered till 2011. The decrease in the number of small molecule aptamer attributes to the fact that it is relatively easy to select aptamers against larger targets as they offer more functional groups and structural motifs, creating a possibility of fishing out sequences interacting with the target via hydrogen bond, hydrophobic or electrostatic interactions [189]. Regardless of the situation, small molecules play important role in biological process, as they can easily diffuse across the cell membrane [192]. Small molecules such as toxins, carcinogens, toxic adulterants and pesticides in food, organic dye and toxic chemicals released in water bodies are harmful in nature, while molecules involved in cell signaling, pigments in plants, defense molecules and antibiotics are the better side of it [193, 194]. Therefore sensing of the hazardous small molecules becomes an imperative task in agriculture, medicine and environmental analysis.

Although aptamers developed for small molecules are meager in number, they are among the most widely studied aptamers in the literature. The aptamer against ATP is second most studied aptamer in terms of the publication, just preceding the thrombin aptamer and has been extensively used for developing various aptamer based assays and biosensors. Cocaine and theophylline aptamers are among the top ten most frequently used aptamer for biosensing purpose [195]. Small molecule aptamers have shown extraordinary selectivity, even able to discriminate structural analogs of target molecules differing by a single residue. Theophylline

RNA aptamer has shown such remarkable specificity of 10,000 times weaker binding affinity for caffine a structural homolog, differing by a single methyl group. Theophylline aptamers selectivity was 10 fold higher than the antibody counterpart [196]. The selectivity of aptamer was further extended to differentiate between the entaniomers of small molecules [197]. Initial aptamer development showed partially distinguishing characteristic between L and D amino acid, but later a RNA aptamer was developed by Geiger *et al.* 1996, displayed high affinity and complete enantio-selectivity [198-200]. Recently, DNA aptamers with entiaoselectivity was developed for small molecules like (R)-thalidomide and for (S) and (R) - ibuprofen [201, 202].

More recently, Carother *et al.* 2010 gave possible explanation or reasons on the scarcity of high affinity small molecule aptamer for sensing purpose by demonstrating a linear relationship of affinity (kD) with the molecular size of the target molecules. These predictions came on the basis of 8 aptamer selected for the study and was consistent with the other studies showing a direct proportionality of kD with targets molecular weight [203]. However, this theory does have exception of high affinity aptamer against theophylline (180 g/mol). Many such aptamers have been developed with affinity from low to mid micromolar to nanomolar range such as Bisphenol-A [20] and oxytetracycline [56] aptamer. Whereas, natural aptamers such as thiamine, guanine and glycine riboswitches; show remarkable binding affinity for their target small molecules [204-206]. Altogether, this indicates that an artificial SELEX process do have potential to select aptamers with high affinity and specificity similar to the naturally existing ones. A comprehensive list of small molecule aptamers developed so far is enlisted in the table below.

Table 2.3 List of aptamers for small molecules with its chemical nature and binding affinity (Kd)

Target	DNA/RNA	Binding affinity (Kd)	Reference
Organic dye	RNA	100-600 µM	[37]
Reactive green19	DNA	33 µM	[24]
D-tryptophan	RNA	18 µM	[198]
Theophylline	RNA	100 nM	[196]
L- citrulline	RNA	62–68 µM	[199]
Flavin mononucleotide	RNA	0.5 µM	[207]
Kanamycin A	RNA	≤ 300 nM	[208]
Nictoinamide adenine dinucleotide	RNA	2.5 µM	[209]
Adenosine monophosphate and adenosine triphosphate	DNA	6 µM	[210]
L- arginine	DNA	2.5 mM	[211]
L- argininamide	DNA	0.25 mM	[211]
L- arginine	RNA	300 nM	[200]
Dopamine	RNA	2.8 µM	[212]

Sulforhodamine B	DNA	190 nM	[213]
Streptomycin	RNA	1-10 μM	[214]
L-isoleucine	RNA	200-500 μM	[215]
Malachite green	RNA	≤1 μM	[216]
Cyclic adenosine monophosphate	RNA	10 μM	[217]
Adenosine triphosphate	RNA	127-223 μM	[218]
L-tyrosine	RNA	35 μM	[219]
S-adenosyl homocysteine	RNA	0.2-0.8 μM	[220]
Neomycin	RNA	1.8 μM	[221]
L-tyrosinamide	DNA	4.5 μM	[222]
Tetracycline	RNA	1 μM	[183]
Kanamycin B	RNA	180 nM	[28]
Adenine	RNA	10 μM	[18]
Flavin adenine dinucleotide	RNA	50 μM	[223]
L-isoleucine	RNA	1-7 mM	[29]
Adenosine triphosphate	RNA	2 μM	[224]
Tobramycin	RNA	30–100 nM	[225]
Kanamycin	RNA	10–30 nM	[225]
Adenosine triphosphate	RNA	5 μM	[226]
Ethanolamine	DNA	6–19 nM	[21]
Codeine	RNA	2.5–4 μM	[227]
(R)-thalidomide	DNA	1 μM	[201]
Oxytetracycline	DNA	10 nM	[228]
Ochratoxin A	DNA	200 nM	[229]
Dopamine	DNA	700 nM	[230]
Diclofenac	DNA	2.7–166.34 nM	[231]
(S) and (R)-ibuprofen	DNA	1.5–5.2 μM	[202]
Kanamycin	DNA	78.8 nM	[57]
L-tryptophan	DNA	1.757 μM	[232]
Bisphenol A	DNA	8.3 nM	[20]
Ochratoxin A	DNA	96–293 nM	[233]
Polychlorinated biphenyls (PCB77)	DNA	4.02, 8.32 μM	[25]
fchlorinated biphenyls (PCB72 and PCB106)	DNA	60–100 nM	[234]
Ampicillin	DNA	9.4–13.4 nM	[58]

There are certain technical challenges associated with development of aptamers against small molecules. Immobilization of these small molecules is a must for carrying out SELEX for the small molecules and has been achieved by using solid support such as magnetic, acrylic and agarose and sepahrose beads. While not all of the small molecules can be directly immobilized on beads, therefore modifications of either small molecules or the surface matrix becomes mandatory for its immobilization, which may alter the natural chemical nature of molecules by eclipsing some functional groups. For example, aptamer developed against

immobilized rhodamine demonstrates weaker biding affinity for rhodamine in solution [235]. Other technicality issue with small molecule aptamer is quantifying its binding affinity for the target molecules. Different methods have been employed for this such as separation, fluorescence; mass sensitive based (QCM and SPR) methods [236] do face challenges due to the nature of small molecular size, mass, many time no intrinsic fluorescence and problems associated with labeling which alters its chemical nature etc. Due to this issues, contemporary methods such as microchip electrophoresis and atomic force spectroscopy has been adapted, but yet no single techniques can be generalized for estimating the binding affinity in terms of dissociation constant (Kd) of small molecules [237, 238].

While the aptamer technology is more than two decade old, still challenges are imposed on its integrity over its practical application of developing novel aptamers for small molecules which are relevant from industrial, environmental and medical point of view. Nonetheless, with advancement in science and the impact that small molecules are having on day today's life, this will surely boost the development of aptamer field against new small molecules and their applicability in biosensing field. The molecular recognition element is known as the corner stone of the biosensor and aptamer clearly has the edge over the other MRE's available in market. However, transducer of the biosensor plays an indispensible part and has been categorised into electrochemical (amperometric, conductometric and potentiometric), optical (SPR, fiber optics, nanoparticles, Raman and FTIR) and mass (piezoelectric and magnetoelastic) based on the type of signal they generate.

2.4.5. Gold nanoparticles (AuNPs)

Recent advancement in nanotechnology has seen a surge in development of novel nanaostructures, nanodevices, nanomaterials, and nanoparticles which are currently used as the transducer in different biosensors [39, 41]. Nanomaterials are structures ranging from 1-100 nm in size with large surface are to volume ratio and exhibiting unique physical, chemical, structural, mechanical, electrical, optical, magnetic and catalytic characteristic surfacing from its quantum effect [239]. Different nanomaterials such as silica, gold nanoparticles, carbon nanotubes and gold nanorods have been adopted as the platform for fabricating biosensors. Among all these nanomaterials, gold nanoparticles (AuNPs) are being exploited as the transducer element in developing optical aptasensor as they exhibit several exclusive properties such as biocompatibility, chemical stability, strong localized surface plasmon resonance (LSPR), and high extinction coefficient [42]. To date, gold nanoparticles have been synthesized by physical, chemical and green chemistry methods. Moreover, introduction of new techniques

for synthesis are continuously evolving to control the size and shape, so as to improve its sensing, photothermal, diagnostics and drug delivery properties [240-248]. Gold nanoparticles synthesized by Turkevich *et al.* which was later slightly modified by Ferns *et al.* 1970 [165, 247-250] is the most widely used method for obtaining 10-20 nm citrate capped nanoparticles. In addition to sodium citrate, different reducing agents such as hydroquinone have been used for synthesizing 50-200 nm monodispersed AuNPs [251]. Besides using aqueous phase for synthesis, organic phase has been used for preparation of 2-5 nm AuNPs, reducing the gold salt by sodium borohydride in presence of alkenethiol [252]. Various organic phases like toluene, chloroform, and hexane have been used for carrying out synthesis of AuNPs. Later, an era of monolayer protected clusters of AuNPs synthesis began by functionalizing the surface of AuNPs with thiol, DNA, RNA, proteins and many amphiphilic polymers, which came into the field of biosensing [49, 253-256].

2.4.6. Aptasensors

The combination of gold nanoparticles with DNA offers greater flexibility towards developing new biosensors based on optical (colorimetric and fluorescence), electrochemical, surface-enhanced Raman scattering (SERS), SPR and mass spectroscopy [41]. The aptamer coupled gold nanoparticle sensors demonstrated higher specificity and selectivity in sensing DNA, protein, heavy metals, small molecules and other biological relevant molecules in health, food safety and biomedical fields [239, 242, 253, 256]. Optical sensors, in particularly the colorimetric based biosensor have utilized gold nanoparticles LSPR and distance dependent optical property [42][46]. A large number of aptamer functionalized-AuNPs colorimetric aptasensor have been reported for detection of several different analytes [43-50, 257-261]. Aptamer functionalization process involves a number of cumbersome steps, are time consuming and costly method. Further to overcome these disadvantages of functionalized-AuNPs, Rothberg *et al.* 2004 [60] discovered an alternative method of detecting specific DNA sequences of genomic DNA using label free gold nanoparticles. The method is based on the principle of that short ssDNA sequences adsorb preferably on the surface of AuNPs than the dsDNA, protecting them from the assault of change of pH or ionic strength. This interaction is possible as the ssDNA is sufficiently flexible to uncoil the bases, which interacts with the gold nanoparticle with attractive Van der Walls force. On introduction of target, aptamer binds the target rendering AuNPs susceptible to the pH or ionic change which neutralizes the negative charge of the AuNPs causing them to aggregate with a visual color change from red-purple.

This pioneering research of employing unmodified AuNPs has brought revolution in the colorimetric based methods, with a possible naked eye read out eliminating the need of sophisticated instrument used in other methods. Aptamers conformational change accompanied by target binding has been employed in large number of aptamer based colorimetric assay for different small molecules.

2.4.7. Colorimetric aptasensor for small molecules using unmodified AuNPs

Despite the fact, a large number of aptamers have been discovered till date; only limited aptamer-AuNPs colorimetric assays utilizing unmodified AuNPs have been developed so far. The possible limiting factor is that not all the aptamer embrace structural changes on target binding which is the principle of the assay.

Wang *et al.* 2007, group was the first to have taken advantage of Rothberg *et al.* 2004 [51] discovery and developed a colorimetric assay for sensing ATP molecule [55]. The assay was named as ATBR (aptamer target binding readout), with slightly modified version of the assay described by Rothberg. The novel strategy translated the ATP binding event to the dehybridization of an ATP aptamer-anti ATP aptamer hybridized duplex, resulting in aptamer-ATP complex with subsequent release of the anti-ATP aptamer oligo. AuNPs are protected by the liberated ssDNA, showing resistance to higher salt concentration still remaining red, while AuNPs get aggregated in absence of ATP. This sensitivity of the assay was 0.6 µM and 2 µM by UV-visible spectroscopy and visual basis respectively. Apart from being sensitive this method displayed high selectivity against other structural analog molecules like CTP, GTP and UTP.

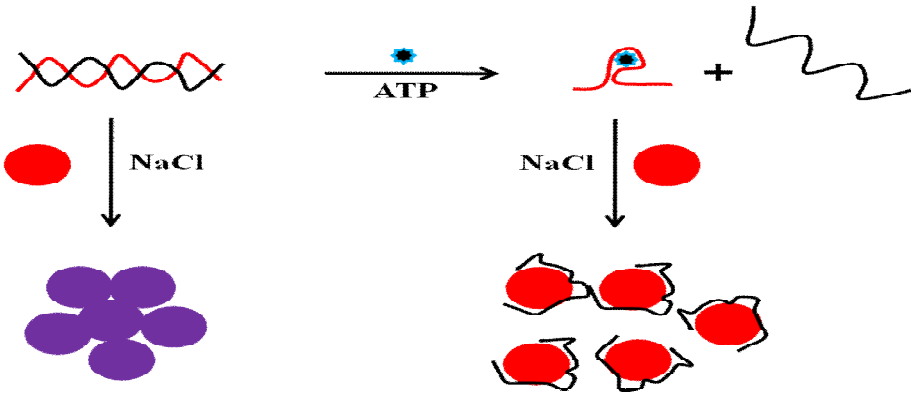

Fig 2.6 AuNPs based ATBR colorimetric assay for ATP molecule: In absence of ATP the AuNPs are not protected by the ATP aptamer-anti ATP aptamer complex, therefore are readily aggregated under high salt conditions; in the presence of ATP, a binding event of ATP with ATP aptamer releases the anti-ATP aptamer, thus protecting the AuNPs from aggregating in presence of salt.

Almost a year later, Zhang *et al.* 2008 came up with a novel strategy of visually detection cocaine using a rationally engineered aptamer structure [54]. The initial attempt of the group to detect cocaine was based on the strategy adopted by Wang *et al.* 2007. Although this displacement strategy is generic, it suffers from drawback of displaying slow kinetics, which reduces the performance of the assay. Therefore in the wake of overcoming this shortcoming a new approach was pursued, which is universal, rapid and sensitive. This group demonstrated that aptamer can be rationally engineered by deleting, adding or modifying the nucleotides in the non conserved region without perturbing their ligand binding site. The cocaine aptamer was sliced into two parts ACA1 and ACA2 with modification to prevent inter-strand binding. Interestingly, in case of cocaine free sample both the part of the cocaine aptamer remained free, thus protecting the AuNPs from aggregating in presence of salt. Whereas, in presence of cocaine the two parts of cocaine aptamer transformed into a cocaine binding structure by interacting with each other. This method was sensitive enough to detect cocaine at concentration as low as 20 µM with higher limit of 200 µM. Also the assay is specific over two structural analogs ecgonine methyl ester and benzoyl ecgonine.

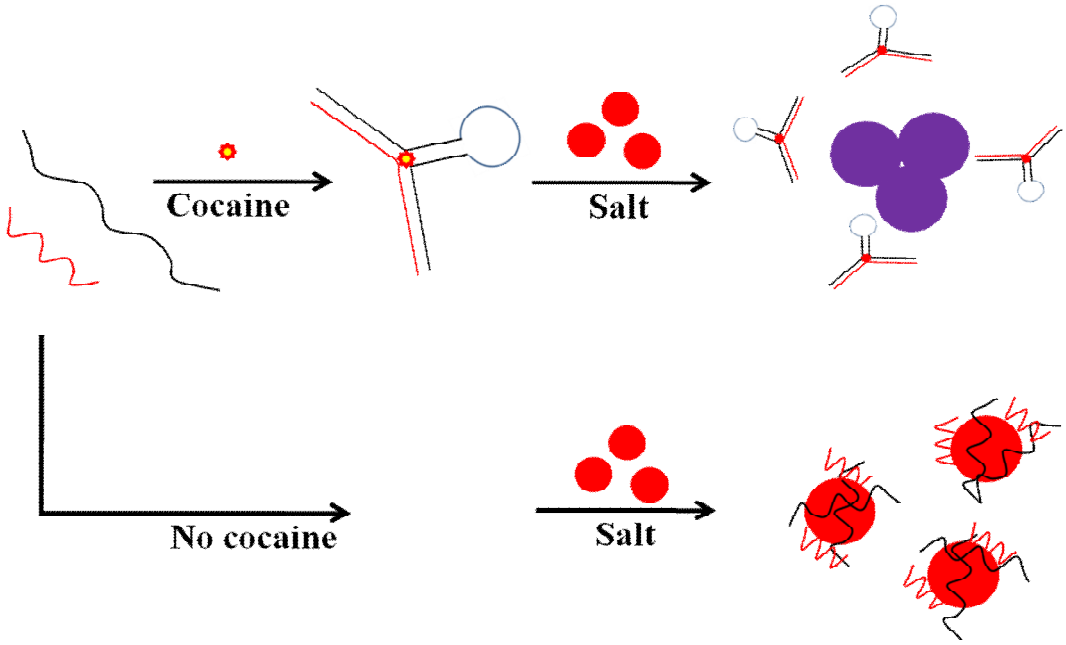

Fig 2.7 A schematic representation of a rationally engineered cocaine aptamer based colorimetric assay for cocaine detection by visual observation.

Kim and co-workers have successfully developed a colorimetric aptasensor for detection of oxytetracycline (OTC), which is a nuisance in many dairy and other food products and pose a serious threat to human health [56]. In their study, initial experimental setup resulted in a higher detection limit, forcing them to optimize the conditions to achieve better sensitivity.

After optimizing several parameters such as salt concentration, aptamer molar ratio to AuNPs and AuNPs concentration; they were able to detect OTC with higher sensitivity in a linear dynamic range of 25 nM to 1 µM, which meets the USA-FDA regulation limits. A greater sensitivity was only achievable by using UV-visible spectrophotometer.

Song *et al.* 2011 became the first group to have developed a DNA aptamer against kanamycin and showed its applicability in developing AuNPs-based aptasensors [57]. The detection limit for the colorimetric assay was found to be above 10 nM with best results seen at 25 nM concentration. The developed assay was specific and showed no cross reactivity with streptomycin, sulpfadimethoxin and ampicillin.

The arsenal of the aptamer-AuNPs assay was further raised to a new level by Yang *et al.* 2011 by detecting ochratoxin A (OTA), a class of mycotoxin found in food commodities [262]. Binding of OTA aptamer to ochratoxin A induced a structural change from random coil to a rigid antiparallel G-quadraplex structure, which was demonstrated for the first time with circular dichroism study. The developed assay was sensitive to detect from 20-625 nM in a rapid span of 5 min. the specificity of the assay was tested with warfarin and showed no change in color at 5 and 10 µM concentrations.

The functionality of the aptamer-AuNPs aptasensor was further extended by Zheng *et al.* 2011 by detecting a neurotransmitter (dopamine), marker for neurological disorder such as Alzhiemers and Parkinson's diseases [60]. The limit of detection for the assay was 5.4-54 µM, and was specific against the other interfering molecules such as dihydroxyphenylalanine, catechol, epinephrine, 3, 4- dihydroxyphenyl acetic acid, homovanillic acid and ascorbic acid.

Song *et al.* 2012 developed an ampicillin specific aptamer and consequently used it for the development of AuNPs-aptasensor assay based on dual fluorescence–colorimetric method to detect ampicillin [58]. This method was used for detecting ampicillin in water and field samples of milk and the limit of detection was 10 ng/ml.

Later in the year Mie *et al.* 2013 developed a label free aptasensor for detection an endocrine disrupter bisphenol A [263]; using anti bisphenol aptamer developed by Jo *et al.* 2011 [20]. The limit of visual detection for this method was 0.1 ng/ml.

The aptamer-AuNPs aptasensors offers several advantages of being simple, rapid, and in many cases provides a naked eye detection of the desired target analyte without the need of sophisticated instrument. Thus, aptasensor has emerged as a new field of interest for small molecule detection. Based on the principle of these assay, a method for detection of urea in adulterated milk samples can be developed.

Apart from adulteration of food, diseases caused by food borne pathogens are a worldwide problem, both in terms of public health and economic cost. Foodborne Disease and Active Surveillance Network (FoodNet) surveyed 15% (an estimated 48 million) of US populations for incidences of infections transmitted by pathogens through food sources. The report confirms 19,056 infections, 4,200 hospitalizations, and 80 deaths in 2013 accounting from *Campylobacter, Cryptosporidium, Cyclospora, Listeria, Salmonella,* Shiga toxin–producing *Escherichia. coli (STEC/EHEC)* O157 and non-O157*, Shigella, Vibrio,* and *Yersinia* [62]. Although, over the last few years the rate of foodborne diseases have remained constant a large number of cases have been associated either with commercially available foods or outbreaks span between states or even countries.

2.5. Escherichia coli O157:H7

Escherichia. coli O157:H7 is a gram negative facultative anaerobic bacillus, colonizing the intestinal tract of humans and other animals. Since its discovery, by Theodor Escherich in 1885; these commensal have been the causative agents of gastro-intestinal complications in humans. In 1982, a diarrheal outbreak was associated with identification of different pathogenic strains of *E .coli.* Later these strains were designated as enteropathogenic *E. coli* (EPEC), enteroinvasive *E. coli* (EIEC) and enterotoxigenic *E. coli* (ETEC) [72]. Later in the same year a new strain referred as *E. coli O157:H7* was implicated in outbreaks associated with hemorrhagic colitis (HC) and hemolytic uremic syndrome (HUS) and have been designated as enterohemorrahgic *E. coli* (EHEC). Of all the *E. coli* strains, Centre for Disease Control (CDC) has declared O157:H7 serotype as the most dreadful food-borne pathogen as it causes life threatening diseases. Infection occurs after ingestion of contaminated food such as undercooked beef, raw contaminated milk, unpasteurized apple juice/cider, lettuce, dry cured salami, yogurt, vegetables [66]. Furthermore, transmission has been characterized from sources such as direct contact with cattle and its related environment. Fig 2.8 shows the pathogenesis of *E. coli O157:H7*, with initial adherence to the microvilli cells, production of toxins followed by ischemic damage to the colon cells resulting in hemorrhagic condition [264].

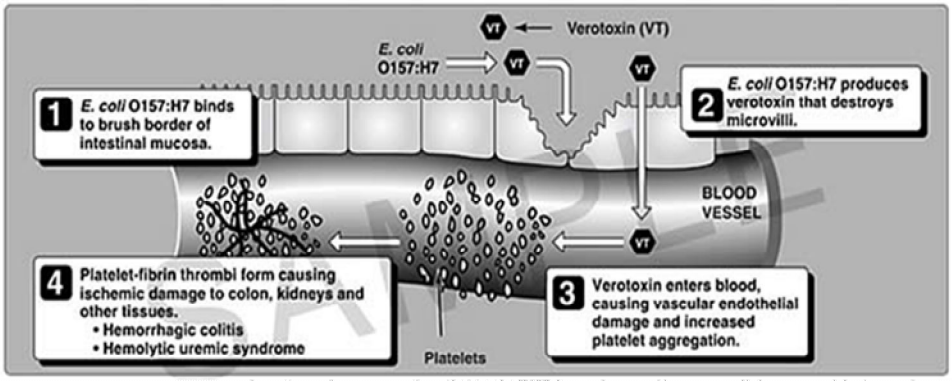

Fig 2.8 Pathogenesis of *E. coli O157:H7* infection

Pathogenicity of *E. coli O157:H7* has been generally associated with two major factors such, Shiga toxin 1, 2 and locus for enterocyte effacing islands (LEE). *E. coli O157:H7* cells gets attached to the intestinal cells via development of attaching and effacing (AE) lesions thus causing gastroenteritis and HUS infections [265, 266]. Colonization of the intestinal mucosa has known to be the primary step towards establishing EHEC infections in humans. The role of intimin and Tir protein mediated bacterial attachment has been well documented [267], but it was found that he mutants of itimin were still able to colonize the epithelial cells, thus indicating the role of unidentified adhesions [268]. While, certain less characterized adhesins are proposed to be associated with bacterial adhesion, but they are only present in certain EHEC strains.

Other than LEE, *E. coli O157:H7* encodes for a large number of putative genes involved in fimbriae and pilin biosynthesis [269, 270]. Several adhesins have been associated with different EHEC strains such as SFP of sorbitol fermenting EHEC O157, long polar fimbriae, curli, type I pilus, type IV pilus (TFP) [271]. Most of them are yet to be explored for their possible role in pathogenesis [79]. Recently it has been reported that a EHEC strain produces an adhesion appendage called *E. coli* common pilus (ECP) which are produced in other pathogenic and non pathogenic strains of *E. coli* [272]. Later it was characterized that either strains lacking ECP were unable to adhere to the cultured epithelial cells. Therefore, studies need to be done to elucidate the role of the pili proteins in pathogenesis. Therefore, a series of research by Giro.J.A group deciphered the role of TFP present in *E. coli O157:H7* and named it as hemorrhagic coli pilus (HCP). The HCP is composed of 19 kDa pilin subunits encoded by the hcpA locus of *E. coli O157:H7* genome. The TFP are produced in many gram negative bacteria and plays an important role in pathogenesis by acting as a potent virulence factor, adding to the survivability and aiding in transmission [273]. TFP has been associated with different functions such as attachment to the eukaryotic cells, twitching motility, biofilm

formation, DNA uptake and bacterial aggregation [79]. It has been reported that HCP is specifically expressed in *E. coli O157:H7* [273], thus it can be an attractive target molecule for the specific bacterial detection.

As *E. coli O157:H7* is an acclaimed life threatening pathogenic bacterial species, therefore its detection in different food matrices and clinical samples becomes imperative for the further containment of the spread of disease. This review aims at briefly summarizing different methods for the *E. coli O157:H7* detection.

2.6. Different methods for bacterial detection

The review gives a brief introduction of different methods ranging from the traditional culture based method to some rapid molecular detection techniques (PCR, DNA microarray etc), immunological methods and immunomagnetic separation have been developed for *E. coli O157:H7*. Different biosensors and introduction of nanotechnology based methods for rapid, sensitive and specific detection of *E. coli O157:H7* has been briefly discussed.

2.6.1. Culture based methods

A conventional bacterial detection method involves typical steps of a pre-enrichment, selective enrichment, selective plating, biochemical tests and seriological confirmation. Development of bacterial specific media for direct identification has been attained, but are only restricted to genera levels for almost all bacterial species. For specific detection of *E. coli O157:H7* the biochemical characteristic of O157:H7 is exploited, as they usually do not ferment β- glucuronidase. Thus, sorbitol MacConkey agar (SMAC) is used as the specific media for *E. coli O157:H7*, which allows differentiation from the rest of the *E. coli* species bases on the color of the colonies [274]. Further modification of the media with trypticase soya agar enabled detection of *E. coli O157:H7* from acidic apple cider [275]. The culturing methods is always performed in combination specifically with the IMViC test for differentiating the *E. coli* from the rest of the Enterobacteriaceae family [276]. Although the conventional method are considered as the gold standard method for bacterial detection and identification, they suffer from drawback of being time consuming, labor intensive, less sensitive and interferes with selective identification of bacterial due to the presence of microbial flora. Combination of other methods has been adopted to reduce on the time taken by the conventional method. The combination of commercially available rainbow agar with PCR showed a reduced time of detection to 30 h [72].

2.6.2. Rapid methods

Rapid methods have been looked upon as the alternative to the conventional culture based method for faster, sensitive and specific bacterial detection and identification. Some of the rapid methods are discussed in brief such as PCR, ELISA, real time PCR and immunomagnetic separation

2.6.2.1. PCR and Real-time PCR

To achieve rapid and accurate epidemiological investigation of the outbreak, it becomes mandatory for any method to be able to differentiate the target bacterial species from the other similar bacterial serogroup which are non pathogenic. DNA amplification technology offers with the advantages of being highly specific and sensitive method for bacterial detection aiding in the conformation of the infectious agents in a rapid manner. As the process requires very minute amount of DNA, very few number of bacteria can be detected using this technique.

A number of PCR based methods have been developed for *E. coli O157:H7* detection which generally involves a multiplex PCR, targeting non-specific genes of *E. coli O157:H7* [277-279]. This method is suitable only for isolated strains of bacteria, thus limiting its use in samples containing mixture of different strains of *E. coli O157:H7*. Therefore, this method needs to be improved with detection of gene only specific for pathogenic strain of *E. coli O157:H7*. Moreover, an internal amplification control needs to be included in the PCR based techniques, so as to eliminate the false negative results which may be the due to the presence of PCR inhibitors in the sample.

Traditional PCR based methods are based on end point assay and the results have to be visualized by gel electrophoresis method. However, a real-time assessment of PCR products of the target genes can be achieved using real-time PCR protocol [74]. Real-time either uses fluorescent dye intercalation or fluorescent tagged gene specific primers for detection of the PCR product in an online manner. Extensive research has been conducted utilizing real-time PCR for specific detection of *E. coli O157:H7* [280]. Rapid detection of *E. coli* O157:H7 multiplex real-time was performed by Jothikumar. N and Griffiths. M.W., 2002 [74], by amplifying *stx1* and *stx2* gene by real-time SYBR Green fluorescent PCR assay. Multiplex PCR has been also adapted for detection of several microbes at a time, targeting different individual specific genes. Kim *et al.* 2007 has reported detection of different microbes such as *E. coli O157:H7*, *Salmonella typhimurium*, *Staphylococcus aureus*, *Listeria monocytogenes,* and *Vibrio parahaemolyticus* using a single PCR [281]. Real-time PCR, despite being rapid

suffers from drawback of being costly, requires sophisticated instruments, laborious and need skilled personnel's for its operation.

2.6.2.2. Immunological assays

Immunological based methods for detection of different targets ranging from bacterial cells, spores, viruses and toxins have been developed so far [282]. These assays are based on the specific interaction of antibodies with its target antigen. Various immunological assays have been developed for detection of different pathogenic microbes which includes *E. coli*, *L. monocytogenes*, *Salmonella spp* and others [283-285]. At present different immunoassays have been developed such as enzyme immunoassay, enzyme linked immunosorbent assay (ELISA), enzyme linked fluorescent assay (ELFA), immune-precciptation ,agglutinin and radio immuno assays [286]. *E. coli O157:H7* was detected using polyclonal IgG antibodies from chicken by sandwich ELISA method; the assay utilized a secondary antibody specific to the primary IgG immunoglobulins. The method was able to detect up to 40 CFU/ml [74]. A rapid and sensitive chemiluminescence immunoassay for *E. coli O157:H7* detection with signal dual-amplification using glucose oxidase and laccase were developed by Zang *et al.* 2014 [287]. The developed method was based on luminol-H2O2-laccase reaction which demonstrated a linear range of detection from 10^3-10^5 CFU/ml in total time of <2.0 h.

Antibodies have been widely used for detection purpose; therefore it has found commercial importance in the field of biological sensors. A combination of PCR and ELISA (VIDAS ECO O157®) was adopted for detection of *E. coli O157:H7* in cheese samples [288]. Another example of commercially available *E. coli* O157H7 kit is ABNOVA's ELISA kit, which utilizes Horseradish peroxidase conjugated anti-*E. coli* antibodies which gives a colored product in presence of TMB; a chromogenic substrate for detection and quantification. In addition to the spectrometric detection, electrochemical detection by voltammetry changes with use of an electroactive enzyme have been reported [289]. This method was sensitive to detect, 10^3 -10^5 CFU/ml have with limit of detection as low as 1 CFU/ml after enrichment process.

Different methods have been reported for bacterial detection using antibodies in combination with other detection methods, to complement and improve the sensitivity and specificity of the developed method.

2.6.2.3. Immunomagnetic separation

Isolating desired bacterial species from food and water samples have been a daunting task, because of low bacterial count, interference from sample matrix and presence of inherent

microbes. Therefore immunomagnetic separation (IMS) techniques have been used for concentrating the desired bacterial species from the sample matrix and separating them from the background microbial flora and complex sample matrix. The IMS method was developed as an alternative to the primitive methods such as use of filter and immunoaffinity beads. While these primary methods suffered from drawback of clogging, because of particles present in the sample matrix, limiting their further use.

Infectious dose of *E. coli O157:H7* has been reported to be as low as a single cell to 100 CFU/ml [67], therefore the detection method need to be sensitive to be able to detect such low number of bacteria. Along with the low number the interference from nonspecific group of bacteria are the obstacles for accurate identification of the infectious agent. Thus to overcome this drawback, immunomagnetic separation technique (IMS) was developed. As shown in the Fig. 2.9, the method utilizes *E. coli O157:H7* specific polyclonal or monoclonal immunoglobulin immobilized to Fe-magnetic nanoparticles (shown as small red circle) for entrapment and enrichment of the specific bacterial cells (blue cells represent *E. coli O157:H7*) from the other background flora. This method has been widely used for extracting *E. coli O157:H7* from different samples matrices [290].

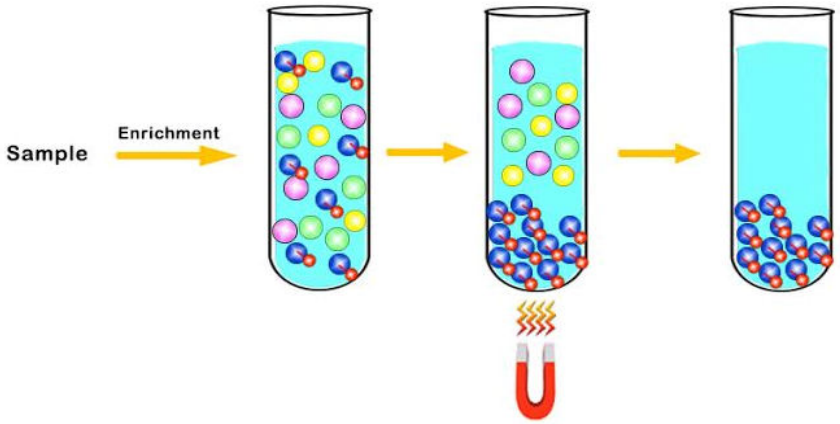

Fig 2.9 Schematic representation of immunomagnetic separation method

A comparison study of commercially available standard ELISA technique (Tecra) was performed with IMS-ELISA to investigate the performance of the assays in terms of *E. coli O157:H7* detection in mince beef samples. The IMS-ELISA methods was found to be more sensitive than the commercial ELISA kit, as the IMS technique was able to concentrate the bacterial ells from the background of the sample matrix.

IMS coupled with real-time PCR method have been used to increase the sensitivity of the PCR method. Fedio *et al.* 2011 utilized Pathatrix™ IMS beads for the enrichment of *E. coli*

O157:H7 from the artificially contaminated raw ground beef samples. Further, IMS has been used in combination with fluorescence immunoassay by Zhu *et al.* 2011 [291], with high capture efficiency with detection limit of ass low as 10 CFU/ml.

The use of immunomagnetic separation (IMS) for capturing and detecting foodborne pathogens has gained popularity, partially due to the introduction of automated and high throughput IMS instrumentation. Although IMS methods have reduced the time span for the specific detection of bacterial species, an enrichment step is mandatory for the sensitivity of the method. Nevertheless it has been the method of choice for most of the bacterial detection in recent times.

Recent development in the field of biotechnology have opened new avenues for the development of novel and advanced microbial detection systems. These methods promise greater degree of specificity, sensitivity and lower detection range. In addition, micro and nano fabrication technology has made it possible to integrate multiple processes in form of microarrays in a sequence for high throughput screening.

2.6.3. Microarrays

Microarrays consist of an orderly arrangement of probes (oligonucleotides, DNA fragments, proteins, sugars, or lectins) attached to a solid surface [64]. It is like a miniature laboratory, and often referred to as a "lab-on-a–chip" device. Microarrays are fabricated with different technologies for example, photolithography, inkjet printing, and electrochemistry. This technology has been widely used for identification of microbial virulence factors, antimicrobial resistance, and bacterial detection etc. The major strength of microarrays is its ability to be used as a miniaturized device for the development of high throughput detection system.

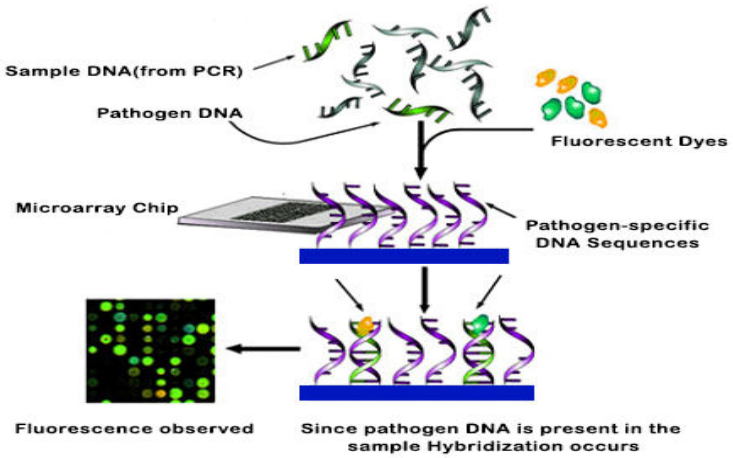

Fig 2.10 Schematic representation of DNA microarray based bacterial detection assay

Gehring *et al.*. developed a sandwich protein based microarray for detection of *E. coli O157:H7*. Biotinylated capture antibodies were immobilized onto streptavidin-modified gold slides to analysis the bacterial load. The method was sensitive and detected 3×10^6 CFU/ml of *E. coli O157:H7* [292]. Furthermore, the method was slightly modified with carbohydrate as the recognition molecules for specific detection of *E. coli O157:H7* [293].

As shown in Fig 2.10, a DNA microarray has the potential to hybridize hundreds to thousands of genomic targets simultaneously. Further, this method eliminates the expression dependent identification of bacterial pathogens, as is the case with other microarrays (protein or lectin based). The method provides an inexpensive, flexible and strain-specific detection and identification of pathogens [294]. The microarray method has limited use in bacterial detection assay as it suffers from the drawback of not being able to discriminate between the dead and live cells.

2.6.4. Biosensors

Biosensors are analytical devices that incorporates molecular recognition element (MRE) linked to a physico-chemical transducer which acts synergistically to sense several different analytes. The MREs of the biosensors are biological molecules such as enzymes, nucleic acids (DNA, RNA or aptamer), whole cell (bacterial and mammalian), antibodies, cell receptors and other biologically derived or inspired molecules (lectin and molecular imprinted polymers). Antibodies have been the primary choice as the molecular recognition element for bacterial detection in different sample matrices. This section briefly gives a review of different bacterial biosensors developed for specific bacterial detection.

2.6.4.1. Surface plasmon resonance (SPR) biosensors

SPR biosensors are based on the principle of biomolecular interaction between the immobilized recognition molecule with the target analyte Fig. 2.10 [295]. This interaction leads to a change in the refractive index of the sensor, which is linearly proportional to the number of target molecule present in the sample. Based on this principle different SPR immunosensors have been fabricated with an aim for specific bacterial detection. A SPR sensor specific for *E. coli O157:H7* was developed by Fratamico *et al.* using a monoclonal antibody immobilized to the gold surface with further detection of *E. coli* cells with a polyclonal antibody. The developed method detected $5\text{-}7\times10^7$ number of cells [296].

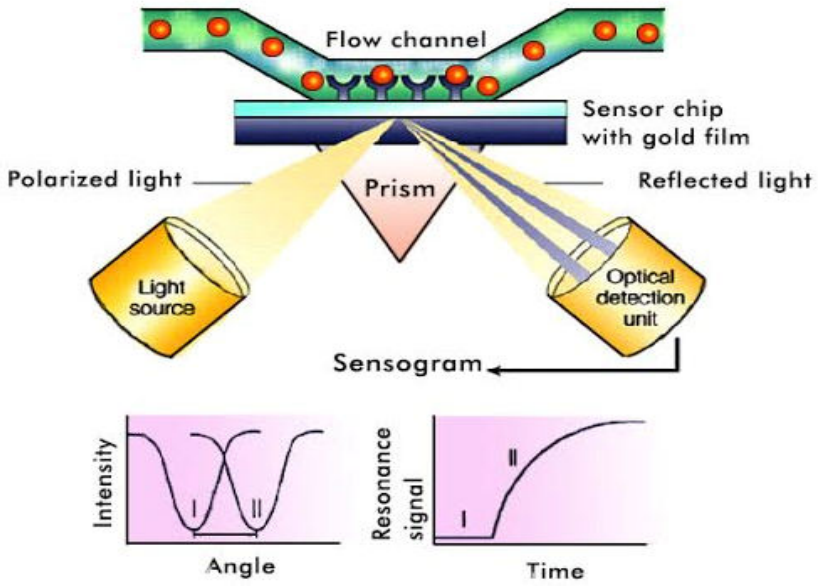

Fig 2.11 Schematic representation of surface plasmon resonance based biosensor

SPR being a heterogeneous method requires complicated surface chemistry and immobilization of different molecular recognition species onto a relatively expensive gold-plate slides or nanoparticles. Also this method requires sophisticated instrument and skilled personnel's for its handling, extensive optimization steps which may differ from sample to sample limits its use as the bacterial detection strategy.

2.6.4.2. Fiber optic biosensors (FOBs)

FOBs have developed into highly specific and sensitive tools for rapid detection of bacteria. They are based on immunoassays and nucleic acid hybridization and available in a number of assay formats. The recognition elements are immobilized on the core of optical fibers which are constructed of silica glass, with modified optical properties. When the excitation light from a laser or white light travels through the waveguide via total internal reflection, the transitory wave produced at the surface of the fiber core excites the fluorophore and they emit light of higher wavelength which is captured. The exhibit several advantages including speed of detection, sensitivity, specificity and portability. These benefits of FOBs make them promising alternatives for the detection of bacteria. Ferreira *et al.* demonstrated one of the first applications of FOBs for the detection of aerosolized bacteria responsible for nosocomial infections and found applicability in the critical-care units of hospitals [297]. At present, wide spread applications of these sensors is limited by their cost and complexity in design.

2.6.4.3. Cantilever biosensors

Due to their high sensitivity, cantilevers can be used for the detection of molecular targets. These cantilevers resemble atomic force microscopy (AFM) tips and can be attached with MRE. Upon binding of a target, the cantilever deflects a couple of nanometers, thereby facilitating its detection. Since the deflection is proportional to the amount of target binding, cantilever biosensors are quantitative [298]. Figure 2.12 shows schematic representation of the cantilever biosensor based bacterial detection. A cantilever biosensor was constructed by Iic *et al.* for the detection of *E. coli O157:H7*. It could detect up to 10^6-10^9 CFU/ml [299]. The advantages of these biosensors include the absence of any enzymatic amplification steps such as PCR and the need of labels (*i.e.* fluorophore). However, developing these sensors into a simple and user friendly sensor would require significant

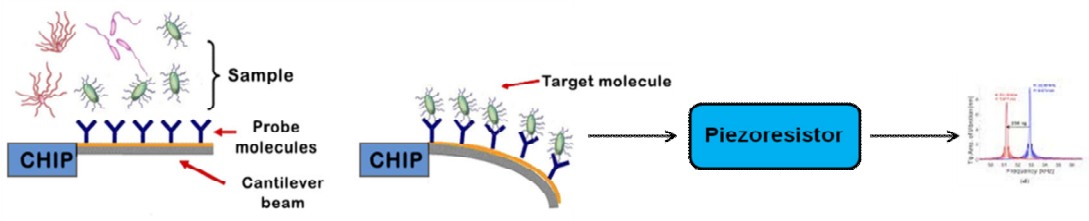

Fig 2.12 Schematic representation of cantilever based bacterial detection system

2.6.4.4. Electrochemical biosensors

Electrochemical based biosensors are classified into amperometric, potentiometric, conductometric and impedimetric based on the different signals these transducing elements can sense. Amperometric biosensors are the most adopted method of choice among the other electrochemical biosensor, as they are superiorly sensitive and have better linear range of detection. Amperometric biosensors have been widely accepted and at present there are numerous commercially successful devices available in the market [300].a rapid and sensitive detection method was developed by Setterington *et al.* 2012, which is based on magnetic extraction of bacterial cells using immunofunctionalized magnetic plyalinine core shell nanoparticle. The method was able to detect bacteria ranging from 6-40 CFU/ml.

Apart from the amperometric based detection of *E. coli* O157:H7, screen printed integrated microsystem based on electrochemical impedance and by amperometric signals have show to detect 10^2 and 10^8 CFU/ml respectively in less than 30 min with optimized sample volume of 10 µl [301].

An impedimetric label free immunosensor was developed for detection of *E. coli* O157:H7 by Barreiros *et al.* 2013[302]. This method was based on the covalent immobilization of anti *E .coli* antibodies with the aid of self assembled monolayer of mercaptohexadecanoic acid onto the gold electrode. The developed immunosensor was able to detect *E. coli* O157:H7 with a linear range of 10^3-10^4 CFU/ml. The lower detection limit by electrochemical impedance spectroscopy was found to be 2 CFU/ml and the method demonstrated specificity with no significant adsorption of *Salmonella typhimurium*.

2.6.5. Nanotechnology based biosensors

Identification of pathogenic agents by different conventional molecular methods have been widely accepted and used in different laboratories across the world. Although being highly specific, sensitive and reproducible, these methods are not feasible to be adopted for onsite detection purpose as they require sophisticated, expensive instruments which are operate by trained personnel and are time consuming. Biosensors have been developed as an alternative method with rapid, specific and sensitive detection of different analytes. Despite promises shown by these methods of being rapid and sensitive, only few methods have been developed for onsite detection owing to the bulky nature of the developed biosensors. With introduction of nanotechnology different nanomaterials have been developed to achieve faster, sensitive and more economical diagnostic assays.

Nanotechnology combined with material science has revolutionized the field of biosensing. Functionalized nanomaterials have been used as catalytic agents, for immobilization of diverse organic and inorganic molecules, as optical or electroactive labels to improve the biosensing ability by demonstrating higher stability, specificity and sensitivity. Different nanomaterials such as metal nanoparticles, nanowires, carbon nanotubes, nanocomposite and nanostructured materials are used as the biosensing platform for environmental, medical and food related industries [303].

A nanobiosensor is composed of a molecular recognition element (MRE) and a signal transducing element. In a typical nanobiosensor, nanomaterials act as the signal transducer which is coupled to different molecular recognition elements such as, antibodies, aptamers, peptides and carbohydrate moieties [74] for target recognition. Apart from the highly adopted nanomaterials-antibody based bacterial detection methods, aptamers have emerged as the rivals of antibodies. Nonmaterial coupled aptamer biosensors are called as aptasensors and they have been adapted for detecting several different analytes which are of significant importance in medical, environmental and food industries.

2.6.6. Aptamer based biosensors

Aptamers are single stranded oligonucleotide of RNA, DNA or PNA (peptide nucleic acids), which folds into intricate three-dimensional structure with help of Watson-Crick base pairing of the nucleotide, favoring formation of different functional nucleic acid domain enabling them to carry out functions such as gene regulation (Riboswitches), catalytic activity (DNAzymes) and ligand-binding. Owing to the ligand binding property, aptamers plays an important role in diagnosis, by being an integral part of the biosensor and in therapeutics by inhibiting functions of certain biological molecules [189, 190]. Aptamers are also called as the "chemical antibodies" due to their synthetic nature and is considered to be an archrival of antibody when it comes to their potential use in different biosensors as the MRE [191].

	APTAMER	**ANTIBODY**
Production	*In vitro* process of generation (Chemical synthesis)	Invivo process (Biological synthesis i:e animals are required)
Target	Developed virtually against any target	Limited targets (can't be generated against small molecules and toxins)
Specificity	Able to differentiate isomers of amino acids	Cannot clearly differentiate between similar target
Stability	Thermostable, can be renatured after thermal denaturation	Temperature sensitive, irreversible damage after denaturation
Batch variations	Little or No	Significant
Cost	Relatively economic once generated against a target	Expensive due to down-streaming processes involved in purification
Chemical modification	Ease of synthesis and open to wide range of modifications	Hard to manipulate through modifications

Owing to these advantages and their ability to be selected against a myriad target analytes; aptamers have tremendous potential in diverse field of biosensing as shown in fig

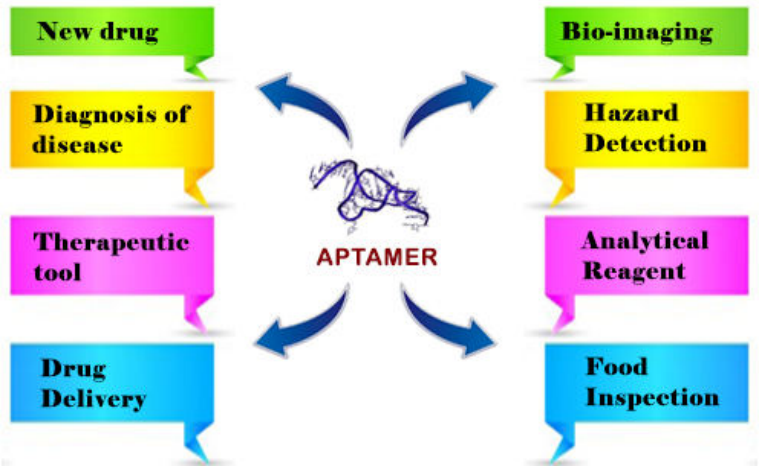

Fig 2.13 Schematic representation of various application fields of aptamers

Aptamer technology offers development of an inexpensive, rapid, sensitive detection system for microbial pathogens [304-306]. Aptamers have been selected for different microbes such as *Lactobacillus acidophilus* [26], *Salmonella enterica* serovars [307], *Salmonella typhimurium* [308], *Listeria monocytogenes* [309], *Staphylococus aureus* [310], *Shigella dysenteriae* [184], *E. coli* NSM59 [311], *Campylobacter jejuni[312] , Mycobacterial tuberclosis[313, 314]* etc. Several research groups have used these aptamers in conjugation with different nanomaterials for their specific detection. The major advantage of aptamers in the area of cellular detection is their ability to target and specifically differentiate microbial strains without the need of any previous knowledge of the membrane or structural changes present in a particular microorganism.

Stratis-Cullum and coworkers reported a qualitative capillary electrophoresis immunoassay method for specific detection of *Campylobacter jejuni [315].*This methods was highly specific even in presence of *E. coli* O157:H7 and *Salmonella typhimurium*. Another report by So *et al.* for specific detection of *E. coli* was developed by functionalizing *E. coli* aptamer onto the single walled carbon nanotubes using field effective transistor as the signal transducer [316]. The sensitivity of the method was found to be between 10^5 -10^7 CFU/ml. Further, Vivekananda and Kiel utilized biotin labeled aptamer and coupled it to the streptavidin-conjugated alkaline phosphatase for developing a dot blot assay specific for *Francisella tularensis* detection [317]. Queirós *et al.*. developed a label-free DNA aptamer-based impedance biosensor for the detection of *E. coli* outer membrane proteins (OMPs) [318]. Gold electrode was immobilized with 6-mercapto-1-hexanol(MCH) labeled *E. coli* specific aptamer for OMPs which detected *E. coli* OMPs in linear dynamic range of $1 \times 10^{-7} – 2 \times 10^{-6}$ M.

Aptamer mediated assays are mostly based on fluorescence and colorimetric techniques. Fluorescent detection is widely employed due to the availability of many different fluorophore and quenchers. The ease of labeling aptamers with fluorescent dyes, have shown to inherit capability for real-time detection of variety of analytes. Such modified aptamers are known as signaling aptamers. Nanotechnology has introduced nanomaterials such as Quantum dots (QDs) which are seen as the replacement of other organic and synthetic fluorescent dyes used in developing biosensors. Owing to a high photostability and better fluorescence quantum yield they have been accepted widely and are used in arrays of biosensors.

Bruno *et al.* [312] utilized an aptamer selected against membrane protein of *Campylobacter jejuni* to develop a detection method based on sandwich assay using magnetic

bead and red quantum dot. This method was tested for specific bacterial detection in various food matrices and showed no cross reactivity with other bacterial species but exhibited some cross reactivity with *Campylobacter coli* and *Campylobacter lari.*

Different nanomaterials such as silica, gold nanoparticles, carbon nanotubes and gold nanorods have been adopted as the platform for fabricating biosensors. Among all these nanomaterials, gold nanoparticles (AuNPs) are being exploited as the transducer element in developing optical aptasensor as they exhibit several exclusive properties such as biocompatibility, chemical stability, strong localized surface plasmon resonance (LSPR), and high extinction coefficient [42]. An aptamer coupled gold nanoparticle sensors have demonstrated higher specificity and selectivity in sensing DNA, protein, heavy metals, small molecules and other biological relevant molecules in health, food safety and biomedical fields [239, 242, 253, 256]. A large number of aptamer functionalized-AuNPs colorimetric aptasensor have been reported for detection of several different analytes [43-50, 257-261].

Thereby, influenced by these properties of gold nanoaprtilces, Wu *et al.* [319] developed a label free colorimetric based aptamer-gold nanoparticles assay for specific detection of *E. coli* O157:H7 and *Salmonella typhimurium.* A truncated version of LPS specific aptamer on to the surface of polydiacetylene PDA modified gold nanoparticles. The aptasensor thus developed was based on the principle of aggregation of aptamer adsorbed gold nanoparticle in presence of specific bacterial cell, leading to a color change from red to purple upon addition of high salt. A rapid and cheap method was developed with no need of sophisticated instrument and even circumventing the process of cell lysis which seems to be a necessary step in many bacterial detection methods. The limit of detection for the method was determined to be 10^4-10^8 colony-forming units CFU/ml in a span of 2 h.

Bacterial infections are not only limited to foodborne diseases, but also have been extensively associated with nosocomial infection due to surgical devices and medical implants. Such infections pose persistent and severe problems that account for high morbidity in hospital settings with significant socio-economic burden on healthcare system worldwide [80-83]. According to Centre for Disease Control and Prevention (CDC), surgical site infections account for ~22% of hospital acquired infections [84]. Although the risk of infection after surgical implantations is low, they have been associated with substantial morbidity, repeated surgeries and prolonged therapy [320]. This increases the burden on the healthcares system and economic burden on individual's family and insurance companies [320-322].

Pseudomonas infection is generally associated with hospital acquired infection, which tends to infect immunocompromised individuals and is responsible for 10% of the nosocomial infections [323]. *Pseudomonas aeruginosa* is the most common infectious agent for causing *Pseudomonas* infection. *Pseudomonas* causes infections like pneumonia, blood related infections and surgical site infections. Risk of infection is augmented in individuals who are on ventilators or intravascular devices such as catheters, patients with burn injuries and wounds caused by surgery [324]. Among all the type of infections the surgical site infection is the most tormenting issue causing severe illness and deaths in infected individuals. Infection caused by *P. aeruginosa* has become difficult to treat, due to the intrinsic ability of *Pseudomonas* to form biofilms which show limited susceptibility to the antimicrobial treatments [325, 326]. Biofilms are surface attached microbial communities with architectural characteristics, phenotypic and biochemical properties different from their free swimming, planktonic counterparts [327] Biofilm formation begins with attachment of bacterial cells with the surface, followed by growth an aggregation to form a bacterial community and secretion of exopolysaccharide leading to the formation of an extracellular matrix around the bacterial community [328] (Fig. 2.14). This extracellular layer along with the distinct mechanism exhibited by the microbial communities acts as the barrier for antimicrobials agents and plays a key role in increasing the antibiotics resistance to 1000 fold greater than the planktonic counterparts [329].

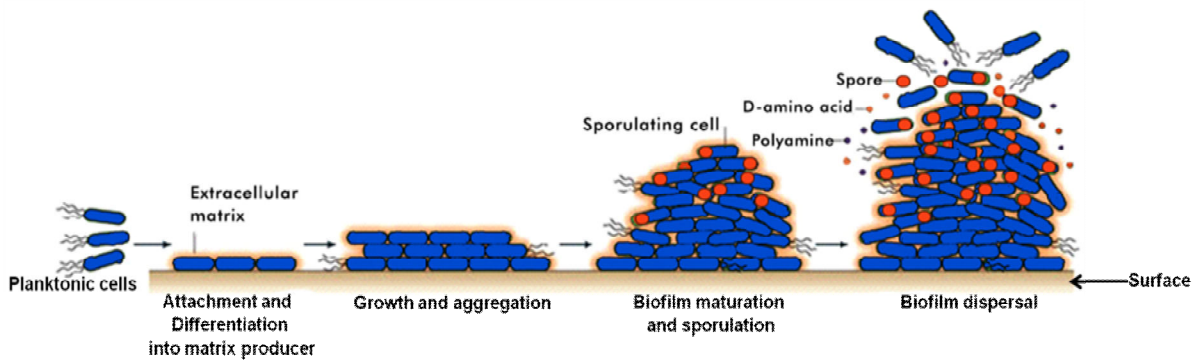

Fig 2.14 Steps involved in biofilm formation

Apart from this *P. aeruginosa* has evolved over the time to develop antibiotic resistance towards different antimicrobials used during the course of therapeutic treatment [330]. Also, antibiotic resistance have emerged from the exchange of antimicrobial resistances gene among different strains from patients to patients [331]. The ability to tolerate antibiotics and allelic exchange of antibiotic resistance gene has resulted in emergence of multi drug resistant (MDR) *P. aeruginosa*.

The conventional antimicrobial drugs have failed to control the infectious diseases caused by the MDR strains, therefore there is dire need of novel antimicrobial agent to confront the challenges imposed by these superbugs. With an aim to deal with the problems associated with bacterial biofilm and the MDR strains, several different counter measures have been adopted [332, 333]. The following section gives a brief review of different antimicrobial strategies implemented for curtailing the health hazards caused by these persistent microbial communities.

2.7. Antimicrobial coatings

The phenomena of bacterial adherence and their ability to grow onto the surfaces were first recognized by Zobell *et al* [334]. It was established that bacteria prefer to colonize a solid surface rather than free dwelling in their planktonic state [335]. Extensive studies on the mechanism of the biofilm formation have been done over the past decades, thus different attempts have been made by modifying surfaces to inhibit bacterial adhesion and are called as antifouling surfaces. In many cases the surfaces are impregnated or coated with bactericidal agents such as antibiotics, antimicrobial peptides etc, thus acting as the biocidal surfaces [336-338].

2.7.1. Surface modifications

Surface modification is an antifouling strategy which may resist or prevent bacterial adhesion due to unsuitable surface topography or surface chemistry with respect to the different bacterial cells [339, 340]. Based on the topological characteristics rough surfaces are likely to adhere more bacterial cells as compared to the smoother surface, owing to the adhesive forces and larges surface area offered by the rough surface. Further, this study has been contradicted by Whitehead *et al.* bacterial colonization can occur on the surfaces with an average roughness (Ra) of the order of only a few nanometres or sub-nanometres [341]. Additionally role of hydrophobicity and surface charges have been studied for its antifouling role and it was found that hydrophobic surfaces are more prone to bacterial adherence because of stronger interaction [342]. On the other hand hydrophilic surfaces were comparatively resistant to bacterial attachment [342].

One of the key strategies for imparting adhesion resistance involves the functionalization of surfaces with poly(ethylene glycol) (PEG) or oligo(ethylene glycol). Several alternatives to PEG-based coatings have also been designed over the past decade. While protein-resistant coatings may also resist bacterial attachment and subsequent biofilm formation, in order to overcome the fouling-mediated risk of bacterial infection it is highly desirable to design coatings that are bactericidal.

Quaternary ammonium compounds (QAC) are positively charge molecules which have shown to have bactericidal activity. The antibacterial activity is due to the cationic surfactant like properties. These compounds have limited used in operation theaters, ceiling fans, floors of hospital environment. QAC have has not being applied to the surgical devices or implants as they are cytotoxic in nature. Moreover, studies have found bacterial resistance has developed towards it, owing its extensive use.

2.7.2. Antibiotic coatings

Bacterial biofilm is known to be refractory to most of the antibiotics, as the microbial community is protected by the extracellular polysaccharide matrix. As a consequence only sub-inhibitory concentrations of antibiotics reach the bacterial cells in the biofilm, leading to the development of antibiotic resistance. Bacterial adherence to medical device leads to severe complications and in worst case leads to removal of implant. Therefore antibiotic coatings are seen as the remedy for this problem. Reports of the use of gentamycin mixed in cements of

orthopedic or orthodontic implants have shown to slow release of antibiotic in local areas preventing the bacterial adhesion.

Antibiotics have been applied with biodegradable a surface coating, which leads to the slow release of antibiotics at the surface-tissue interface. Poly(D.L-lactide) containing gentamycin drastically reduced the infection by locally releasing the antibiotics as compared to the systemic gentamycin treatment.

2.7.3. Silver nanoparticle (AgNPs)

Since its emergence, nanotechnology has revolutionized the scientific world. There are hardly any branches of science and technology where it does not put its impression. The magical touch of nanotechnology not only enriches the field of modern medicine and cosmetics but also establish its presence in environmental remediation, conserving renewable energies, protecting medical devices from the pathogenic microorganisms [343, 344]. Because of its unique physical properties, nanoparticles have been utilized for diverse applications which are important to improve the quality of human life. Silver based nanoparticles (AgNPs) have gained an increasing attention now a day because of its extraordinary physicochemical and biological properties. In addition to its excellent electrical and thermal conductivity, it has good chemical stability and catalytic potential. In terms of biological effect, silver based nanoparticles have broad spectrum antimicrobial potency. Because of this quality, AgNPs are extensively used in various consumer products of daily use, including plastics, soaps, pastes, food and textiles. Various databases indicate that the research interest on AgNPs is escalating rapidly since last 10 years. China tops the list of the countries publishing maximum number of research papers on silver based nanoparticles. USA and India are also contributing a lot on research of AgNPs and publishing a good number of research articles on this topic.

Ag-NPs have some big role to play in these circumstances because of its broad spectrum antimicrobial activity as and low toxicity. Various research article shows that Ag-NPs are effective against a wide variety of microorganisms. The efficiency of the nanoparticle depends on its quality, in particular its size and physicochemical properties [345, 346]. Therefore, an efficient and economically feasible method of synthesis is the key to success of silver based nano-biotechnology research. There are multiple approaches have been developed and followed by various research group worldwide. The most frequently used methodology of synthesizing Ag-NPs includes chemical synthesis, physical synthesis, photochemical synthesis and biological synthesis [347-354].

Studies have concluded that silver nanoparticles offer better antibacterial activity as they allow more effective contact with bacteria due to their large surface area property. The possible ways silver nanoparticles exert their antimicrobial activity after interacting with bacterial cells is by (a) release of silver ions and generation of reactive oxygen species (ROS); (b) interaction with membrane protein and disrupting its function; (c) disturbing the cell membrane permeability by accumulation; (d) entering into the cells, releasing the silver ions and generating ROS thus causing DNA damage [355, 356]. Because of these distinct antibacterial properties, several rapid and efficient methods for silver nanoparticle synthesis have emerged as a research area of interest for biomedical applications. [346, 357, 358]. Several reports of biological synthesis using bacterial cells, fungi and plant extracts have shown to mediate the silver nanoparticle formation [359]. On the basis of these biosynthetic mechanism, different biological molecules such as proteins [360],peptide [361, 362], antimicrobial peptide [363] [364], carbohydrates, antibiotics [364, 365], antibiotics [366] have been explored to direct the molecular control of silver nanoparticles. Additionally, a combination of biomolecules with inorganic compounds; have led to the development of novel particles with merged functional properties of both the compounds.

A hybrid antimicrobial enzyme and silver nanoparticles coating for medical device was developed by Eby *et al.* [360]. In this method silver nanoparticle was synthesized using Lyzozyme as the reducing and capping agent, which was electrophoretically deposited on surgical blades. The antimicrobial effect on these surgical blades were tested against *Klebsiella pneumoniae*, *Bacillus anthracis*, *Bacillus subtilis*, *Staphylococcus aureus* and *Acinetobacter baylyi* for their antimicrobial, demonstrated a 3 log reduction of bacterial growth.

A sodium borohydrate reduction method was used for preparing β-cyclodextrin capped silver nanoparticles [365]. The antimicrobial activity of the nanoparticle was studied against *Escherichia coli*, *Pseudomonas aeruginosa* and *Staphylococcus aureus* showed 90- 92 %, 97% and 97% inhibitory activity against respective bacteria.

Antimicrobial peptides (AMPs) are well-known components of the innate immune system and also produced by many microbes to eliminate other microbial community present in the niche. These AMPS can be applied to overcome biofilm-associated infections. Their relevance has been increasing as a practical alternative to conventional antibiotics, which are declining in effectiveness. The recent interest focused on these peptides can be explained by a group of special features, including a wide spectrum of activity, high efficacy at very low concentrations, target specificity, anti-endotoxin activity, synergistic action with classical

antibiotics, and low propensity for developing resistance. Therefore, the development of an antimicrobial coating with such properties would be worthwhile. The immobilization of AMPs onto a biomaterial surface has further advantages as it also helps to circumvent AMPs potential limitations, such as short half life and cytotoxicity associated with higher concentrations of soluble peptides.

A novel bio-conjugate of silver nanoparticle with antimicrobial peptide G-Bac3.4 exhibited antimicrobial activity against *P. aeruginosa* resistant to traditional antibiotics and the strain *S. aureus* (MRSA ATCC 33591) resistant to methicillin [364]. The developed method showed increased antibacterial activity even in presence of low concentration of antimicrobial peptide concentration.

Another promising approach of conjugating two different antimicrobial peptides onto the silver nanoparticle was reported by Mei *et al.* [363]. The surface immobilized bacitracin and polymyxin-E conjugate showed antibacterial activity against *E. coli* and *S. aureus.*

CHAPTER 3

MATERIALS AND METHODS

3.1. MATERIALS

3.1.1. Media

3.1.1.1. Luria Bertani (LB) Broth

25g of LB-broth powder (Merck, India) was dissolved in 100 ml of distilled water. Finally the volume was made up to 1000 m. with distilled water and was autoclaved for 15 min at 121 °C (15 lb/in^2).

3.1.1.2. LB Agar

25 g of LB-broth powder (Merck, India) and 2g of bacteriological grade agar (Merck, India) were dissolved in 100 ml of distilled water. Finally the volume was made up to 1000 ml with distilled water and was autoclaved for min at 121 °C (15 lb/in^2).

3.1.1.3. M63 minimal media

3.1.1.3.1. Composition of for 5X stock media

$(NH_4)_2 SO_4$	1 g
KH_2PO_4	6.8 g
$FeSO_4$	0.25 mg

The pH was adjusted to 7 with KOH and the volume was made up to 100 ml.

It was autoclaved at 121 °C for 15 min (15 Ib/in^2).

3.1.1.3.2. 1X minimal medium

5X M 63 media	20 ml
1M $MgSO_4.7H_2O$ [a]	100 ul
20 % Glucose [b]	2 ml
0.5% thiamine [b] (vitamin B1)	1 ml
20% casamino acid [b]	1 ml

All the above components were transferred aseptically into an autoclaved flask and the volume of the media was made up to 100 ml with autoclaved distilled water.

a - filter sterilized and stored at 4 °C.

b- autoclaved and to be stored at room temperature

3.1.1.4. Muller Hinton Broth (MH broth)

Beef extract	2.0 g
Casein digest	17.5 g
Starch	1.5 g

All the above components were dissolved in 1000 ml of distilled water and autoclaved for 15 min at 121 °C (15 lb/in^2).

3.1.2. Reagents and buffers

3.1.2.1. Generation of urea specific DNA aptamer and development of an aptasensor for "urea" detection

3.1.2.1.1. Bio-Mag®Plus Carboxyl Protein Coupling Kit

a) 1-Ethyl-3-(3-dimethylaminopropyl) carbodiimide (EDC) is a carboxyl activating agent supplied in powdered form and used as per manufacturer's instruction for coupling molecules through amide bond.

b) BioMagPlus Carboxyl magnetic beads

3.1.2.1.2. 1M NaCl

5.85 g of sodium chloride (Merck, India) salt was dissolved in 50 ml of distilled water and final volume was made up to 1000 ml. It was autoclaved for 15 min at 121 °C (15 lb/in2) and stored at RT

3.1.2.1.3. 1M Tris-HCl (pH 7.5)

12.114 g of Tris base (Merck, India) was dissolved in 50 ml of distilled water and its pH was adjusted to 7.5 by adding conc. HCl. After pH adjustment, the volume was made up to 100 ml with distilled water. It was autoclaved for 15 min at 121 °C (15 lb/in^2) and stored at RT.

3.1.2.1.4. 1M $MgCl_2$

9.5211 g of magnesium chloride salt (Merck, India) was dissolved in 50 ml of distilled water and finally the volume was made up to 100 ml. It was autoclaved for 15 min at 121 °C (15 lb/in^2) and stored at RT

3.1.2.1.5. 1M KCl

7.455 g of potassium chloride salt (Merck, India) was dissolved in 50 ml distilled water and finally the volume was made up to 100 ml. It was autoclaved for 15 min at 121 °C (15 lb/in^2) and stored at RT.

3.1.2.1.6. Yeast t-RNA (20mg/ ml)

20 mg of the yeast t-RNA (Sigma Aldrich, USA) lyophilized powder (Sigma Aldrich, USA) was dissolved in 1 ml of DNase and RNase free molecular grade water (HiMedia, India). Aliquots of 1 mg/ml were prepared from the stock and kept in deep freezer until use.

3.1.2.1.7. BSA (2mg/ml)

2 mg of Bovine Serum Fraction V (Sigma Aldrich, USA) was dissolved in 1 ml of DNase and RNase free water and stored at – 20 °C until use.

3.1.2.1.8. 1M Urea

6.006 g of urea (Himedia, India) was dissolved in 50 ml of autoclaved distilled water; finally the volume was made up to 100 ml. It was prepared freshly prior to use.

3.1.2.1.9. 3M Sodium acetate (pH 5.2)

40.81 g of sodium acetate (Merck, India) was dissolved in 80 ml of distilled water. The pH was adjusted to 5.2 with glacial acetic acid. Final volume was adjusted to 100ml and sterilized by autoclaving and stored at RT.

3.1.2.1.10. 0.5M EDTA

18.61 g of Disodium Ethylene Diamino Tetra Acetate.2H2O (Merck, India) was dissolved in 80 ml of double distilled water and the pH was raised to 8 using sodium hydroxide pellets. The volume was adjusted to 100 ml with double distilled water, sterilized by autoclaving and stored at RT.

3.1.2.1.11. 10% (w/v)Ammonium per sulphate (APS)

10 mg of APS (Merck, India) was dissolved in 1 ml of distilled water. It was stored at 4°C.

3.1.2.1.12. 50X TAE Buffer

Tris-base	242 g
Glacial acetic acid	57.1 ml
EDTA (0.5M, pH8.0)	20 ml

The volume was made up to 1000ml with milliQ water, autoclaved for 15 min at 121 °C (15 lb/in^2) and stored at RT.

3.1.2.1.13. 6X Gel loading Buffer

Bromophenol blue (w/v)	0.25%
Glycerol	30.0%
Xylene cyanol FF (w/v)	0.25%

Autoclaved water was used for preparation and stored at 4°C.

3.1.2.1.14. 10X TBE buffer

Tris base	54 g
Boric acid	27.5 g
EDTA (0.5M, pH8)	20 ml

The volume was made up to 500ml with milliQ water, autoclaved for 15 min at 121 °C (15 lb/in^2) and stored at RT.

3.1.2.1.15. 40% acrylamide mix (29:1)

47.5 gm of acrylamide (Himedia, India) and 2.5 gm of bisacryl amide (Himedia, India) were dissolved in 125 ml of DEPC treated water in an amber color bottle.

3.1.2.1.16. 10% Urea denaturing PAGE

Urea (Himedia, India)	210 gm
10X TBE	50 ml
40% Acryl amide/Bis acrylamide (29:1)	125 ml

The volume was made to 500 ml with autoclaved distilled water.

3.1.2.1.17. 2X Urea gel loading buffer

Sucrose (USB, Molecular biology grade)	8g
Bromophenol blue (Himedia, Molecular biology grade)	10 mg
Xylene cyanol FF (Himedia, Molecular biology grade)	10 mg
10% Sodium dodecyl sulfate (USB, electrophoresis grade)	400µl
10X TBE	4ml

3.1.2.1.18. Selection buffer pH 7.5

NaCl	250 mM
Tris–HCl (pH 7.5)	100 mM
$MgCl_2$	25 mM
KCl	5 mM
Tween 20	0.02%

All of the above reagents at respective concentration were used and transferred aseptically to an autoclaved reagent bottle. Volume makeup was done with autoclaved milliQ water. Aliquots were made in 1.5 ml micro-centrifuge tubes and stored at 4 °C until use.

3.1.2.1.19. Binding buffer pH 7.5

NaCl	250 mM
Tris–HCl (pH 7.5)	100 mM
$MgCl_2$	25 mM
KCl	5 mM
Tween 20	0.02%
Yeast t-RNA	0.1 µg/ml
BSA	20 µg/ml

All of the above reagents at respective concentration were used and transferred aseptically to an autoclaved reagent bottle. Volume makeup was done with autoclaved milliQ water. Aliquots were made in 1.5 ml micro-centrifuge tubes and stored at 4 °C until use.

3.1.2.1.20. Elution buffer pH 7.5

NaCl	250 mM
Tris–HCl (pH 7.5)	100 mM
$MgCl_2$	25 mM
KCl	5 mM
Tween 20	0.02%
Urea	6 mM

All of the above reagents at respective concentrations were used and transferred aseptically to an autoclaved reagent bottle. Volume makeup was done with autoclaved milliQ water. Aliquots were made in 1.5 ml micro-centrifuge tubes and stored at 4 °C until use.

3.1.2.1.21. X-Gal (5-bromo-4-chloro-3indolyl-β-D-galactopyranoside)

20 mg of X-Gal (Merck, India) was dissolved in 1ml of dimethyl form amide and stored in a glass tube wrapped in aluminium foil and kept at 4°C.

3.1.2.1.22. IPTG (Isopropyl-thio-β-D-galactoside) (100 mM)

238 mg of IPTG (Merck, India) was dissolved in 8 ml of double distilled water. Final volume was adjusted to 10 ml with distilled water and sterilized by filtration through a 0.22 µm millipore filter. The solution was stored at -20 °C.

3.1.2.1.23. Gold chloride ($HAuCl4.X\ H_2O$) solution (50mM)#

1.6 g of hydrated HAuCl4 salt (Sigma Aldrich, USA) was dissolved in 100 ml of milliQ water. The solution was filtered through 0.2 micron PVDF membrane syringe filter and stored at 4 °C until use.

The solution was prepared in aqua-regia treated, hot air oven dried glassware.

3.1.2.1.24. L-glycine (1M)

750 mg (Merck, India) of L-glycine was dissolved in 10 ml of milliQ water. It was prepared freshly prior to its use.

3.1.2.1.25. L-tyrosine (1M)

1.811 g (Merck, India) of L-tyrosine was dissolved in 10 ml of milliQ water. It was prepared freshly prior to its use.

3.1.2.1.26. L- phenyl alanine (1M)

2.156 g (Merck, India) of L-tyrosine was dissolved in 10 ml of milliQ water. It was prepared freshly prior to its use.

3.1.2.1.27. L-Glutamate (100 mM)

1.471 g (Merck, India) of L-glutamate was dissolved in 10 ml of milliQ water. It was prepared freshly prior to its use.

3.1.2.1.28. Sodium chloride (1M)

5.8 g (Merck, India) of Sodium chloride was dissolved in 10 ml of milliQ water. It was prepared freshly prior to its use.

3.1.2.1.29. Glucose (1M)

1.8 g of glucose (Merck, India) was dissolved in 10 ml of milliQ water. It was prepared freshly prior to its use.

3.1.2.1.30. Sodium bicarbonate (1M)

800 mg of sodium bicarbonate (Merck, India) was dissolved in 10 ml of milliQ water. It was prepared freshly prior to its use.

3.1.2.2. Development of DNA aptamer for Hemorrhagic Coli Pilin (HcpA) of *Escherichia coli* O157:H7

3.1.2.2.1. 10mM ATP

100 mM stock solution of ATP (Fermentas, USA) provided by fermentas was diluted 10 times with nuclease free water.

3.1.2.2.2. 0.5M EDTA

As mentioned in section 3.1.2.1.10.

3.1.2.2.3. Ethidium bromide (10 mg/ml)

10 mg of ethidium bromide (Merck, India) was dissolved in 1 ml of distilled water. The solution was stored in a dark bottle at room temperature.

3.1.2.2.4. 15% SDS PAGE composition

Resolving Gel (pH 8.8, 10 ml)

30% Acrylammide mix (29:1; Acrylamide:Bisacrylamide)	5 ml
1.5 M Tris-Cl (Himedia, India; pH 8.8)	2.5 ml
10% (w/v) SDS (Himedia, India)	100 µl
10% (w/v) APS (Himedia, India)	100 µl
TEMED (Himedia, India)	5 µl
Autoclaved water	2.3 ml

Stacking Gel (pH 6.8, 5ml)

30% Acrylamide mix (29:1; Acrylamide: Bisacrylamide)	830 µl
1 M Tris-Cl (Himedia, India; pH 6.8)	630 µl
10% (w/v) SDS (Himedia, India)	50 µl
10% (w/v) APS (Himedia, India)	50 µl
TEMED (Himedia, India)	5 µl

Autoclaved water	3.4 ml

3.1.2.2.5. 10X SDS buffer

Tris base	30.0 g
Glycine	144.0 g
SDS	10.0 g

These components were dissolved in 1000 ml of distilled water. Stock solution was stored at room temperature and diluted to 1X with distilled water before use.

3.1.2.2.6. IPTG (Isopropyl-thio-β-D-galactoside) (100 mM)

As mentioned in section 3.2.1.23

3.1.2.2.7. X-Gal(5-bromo-4-chloro-3indolyl-β-D-galactopyranoside)

As mentioned in section 3.2.1.24

3.1.2.2.8. 3M Sodium acetate (pH 5.2)

As mentioned in section 3.1.2.1.19

3.1.2.2.9. 1M Tris (pH 7.5)

121.1 g of tris base (Merck, India) was dissolved in 80 ml of distilled water, pH was adjusted to 7.5 by adding concentrated HCl. Final volume was made upto 1 liter using distilled water and sterilized by autoclaving.

3.1.2.2.10. 10% Glycerol

50 ml of glycerol was mixed with 450 ml of water and sterilized by autoclaving

3.1.2.2.11. TE (pH-8)

10mM Tris .Cl (pH-8)

1mM EDTA (pH-8)

The volume was adjusted with distilled water to pH 8 and sterilized by autoclaving and stored at 4 ° C.

3.1.2.2.12. 50X TAE BUFFER

As mentioned in section 3.1.2.1.13.

3.1.2.2.13. 10X TBE BUFFER

As mentioned in section 3.1.2.1.14.

3.1.2.2.14. 6X Gel loading Buffers

As mentioned in section 3.1.2.1.14

3.1.2.2.15. 1 M Dibasic sodium phosphate anhydrous

14.19 g of Disodium phosphate salt (Merck, India) was dissolved in 90 ml of water and the final volume was made up to 100 ml with water.

3.1.2.2.16. 1 M Monobasic sodium phosphate

15.6 g of monobasic sodium phosphate salt (Merck, India) was dissolved in 90 ml of water and the final volume was made upto 100 ml with water

3.1.2.2.17. 1 M Sodium phosphate Buffer (pH-7.4)

50 ml of 1M Dibasic sodium phosphate solution was added in a beaker and slowly 1M monobasic sodium phosphate solution was added with constant stirring until the pH of the solution reaches 7.4

3.1.2.2.18. 50% glycerol

50 ml of glycerol (Merck, India) was added in a 100 ml measuring cylinder and the final volume was made up to 100 ml with milliQ water.

3.1.2.2.19. 3M NaCl

8.76 g of NaCl (Merck, India) was dissolved in 40 ml milliQ water and the final volume was made up to 50 ml with milliQ water.

3.1.2.2.20. 3M Imidazole

6.08 g imidazole (Merck, India) was dissolved in 20 ml milliQ water and the pH of solution was adjusted to 7.4 and the solution was made up to 30ml with milliQ water.

3.1.2.2.21. Lysis buffer

Sodium Phosphate buffer (pH 7.4)	20 mM
Glycerol	10%
NaCl	500 mM
Imidazole	5 mM
Lysozyme	200 µg/ml
RNase	5 µg/ml
DNase	10 µg/ml

3.1.2.2.22. Equilibration buffer (pH 7.4)

Sodium Phosphate buffer (pH 7.4)	20 mM
Glycerol	10%
NaCl	500 mM
Imidazole	10 mM

3.1.2.2.23. Wash Buffer 1 (pH 7.4)

Sodium Phosphate buffer (pH 7.4)	20 mM
Glycerol	10%
NaCl	500 mM
Imidazole	20 mM

3.1.2.2.24. Wash Buffer 2 (pH 7.4)

Sodium Phosphate buffer (pH 7.4)	20 mM
Glycerol	10%
NaCl	500 mM
Imidazole	50 mM

3.1.2.2.25. Elution Buffer (pH 7.4)

Sodium Phosphate buffer (pH 7.4)	20 mM
Glycerol	10%
NaCl	500 mM
Imidazole	50 mM

3.1.2.2.26. 30% Acrylamide mix (29:1; Acrylamide: Bisacrylamide) – Himedia

3.1.2.2.27. 1.5 M Tris-Cl (pH 8.8)

12.114 g of Tris base (Merck, India) was dissolved in 50 ml of distilled water and its pH was adjusted to 8.8 by adding conc. HCl. After pH adjustment, the volume was made up to 100 ml with distilled water.

3.1.2.2.28. 1 M Tris-Cl (pH 6.8)

12.114 g of Tris base (Merck, India) was dissolved in 50 ml of distilled water and its pH was adjusted to 6.8 by adding conc. HCl. After pH adjustment, the volume was made up to 100 ml with distilled water

***3.1.2.2.29.* 10% (w/v) SDS**

1 g of SDS (Merck, India) was dissolved in 10 ml of distilled water.

3.1.2.2.30. 10% (w/v) APS

10 mg of APS (Merck, India) was dissolved in 1 ml of distilled water.

3.1.2.2.31. Selection buffer pH 7.5

NaCl	250 mM
Tris–HCl (pH 7.5)	100 mM
$MgCl_2$	25 mM
KCl	5 mM
Tween 20	0.02%

All of the above reagents at respective concentration were used and transferred aseptically to an autoclaved reagent bottle. Volume makeup was done with autoclaved milliQ water. Aliquots were made in 1.5 ml micro-centrifuge tubes and stored at 4 °C until use.

3.1.2.2.32. Binding buffer pH 7.5

NaCl	250 mM
Tris–HCl	100 mM
$MgCl_2$	25 mM
KCl	5 mM
Tween 20	0.02%
Yeast t-RNA	0.1 µg/ml
BSA	20 µg/ml

All of the above reagents at respective concentration were used and transferred aseptically to an autoclaved reagent bottle. Volume makeup was done with autoclaved milliQ water. Aliquots were made in 1.5 ml micro-centrifuge tubes and stored at 4 °C until use.

3.1.2.2.33. 30% Acrylamide mix (19:1; Acrylamide:bisacrylamide) – Himedia, India

3.1.2.2.34. 8% Native PAGE Mix

25 ml of 1X TBE (diluted from 10 TBE stock), 2.5 ml of 1M $MgCl_2$,7.5 ml of 100% glycerol was added to 10 ml of 40% Acrylamide/bis-acrylamide (19:1) Himedia, India; and the total volume was made up to 50 ml with Milli-Q water. It was stored in an amber-coloured bottle.

3.1.2.2.35. 4X Gel-shift Buffer

2 mg of yeast tRNA and 3mg of BSA were dissolved in 4X selection buffer supplemented with 10% glycerol in total volume of 10 ml. Aliquots of the buffer were made in 1.5 ml micro-centrifuge tubes and stored at -20° C.

3.1.2.2.36. Native gel running buffer for EMSA

TBE	0.5X
$MgCl_2$	5mM
Glycerol	1.5%

3.1.2.3. Nanobased strategies for pathogen control

3.1.2.3.1. Polymyxin B sulphate (1 mg/ml)

10 mg of polymyxin B sulphate salt (Sigma Aldrich, USA) was dissolved in 100% methanol (Merck, India).

3.1.2.3.2. Sodium borohydrate (100 mM)

37.8 mg of sodium borohydrate salt (Merck, India) was dissolved in 10 ml of milliQ water. This solution was prepared freshly.

3.1.2.3.3. Proteinase K storage buffer

Glycerol	50 ml
1M Tris-HCl pH 7.5	1 ml
CaCl2	0.29 g

Make up the volume to 100 ml with autoclaved distilled water.

3.1.2.3.4. Proteinase K (10 mg/ml)

100 mg of proteinase K powder (Sigma Aldrich, USA) was dissolved it in 10 ml of proteinase K storage buffer. Aliquots were made into 1.5 ml of microcentrifuge tubes and stored at -20 °C

***3.1.2.3.5.* Live/Dead BacLight Bacterial staining kit (Invitrogen, USA)**

Prepare 1:1 mixture of solution A and solution B in milliQ water.

Table 3.1 Bacterial strain used in this study

Serial No.	Name of strain	Antibiotic resistance
1	*Escherichia coli* O157:H7	NE
2	*Pseudomonas aeruginosa* PAO1	gentamycin, ciprofloxacin, tobramycin, oflaxacin, nalidixic acid, kanamycin, tetracycline, novobiocin and vancomycin
3	*Vibrio fluvialis* L-15318	ampicillin, kanamycin, rifampicin, norfloxacin, cephalothin, oxacillin and vancomycin

NE- not evaluated

Table 3.1 Oigonucleotides used in this study

Name of oligo's	Sequence 5'-3'
Random DNA library	GTCTTGACTAGTTACGCC-N_{40}-TCATTCAGTTGGCGCCTC
FITC labeled Forward Primer (DrF) for SELEX	*FITC*- GTCTTGACTAGTTACGCC
Reverse Primer (DrRA) for SELEX	GAGGCGCCAACTGAATGrA
U38/FL38	GTC TTG ACT AGT TAC GCC CAA CAC AAG GCA CAG ATA GCA GCC TGT TAC CAT CAT CCC CTC CTC ATT CAG TTG GCG CCT C
U2	GTC TTG ACT AGT TAC GCC CAA ACC ACG GAG TAG AAT CGT TAT CAT GCA TAT TGG CCC CCT CCT CAT TCA GTT GGC GCC TC
U7	GTC TTG ACT AGT TAC GCC CAA AGA CCA CAC GAC ACA AAG TAT GTA ATT AAT GTC CGA ATG CCT CAT TCA GTT GGC GCC TC
U10	GTC TTG ACT AGT TAC GCC CAC ATT AGG TTG GAT AGG TTG GTA TGT GTA TGC GTT GT GTC CTC ATT CAG TTG GCG CCT C
U13	GTC TTG ACT AGT TAC GCC CAA GGA GGA AGG GAT AAG ACG TGG AGT GTA GTA GCT ACC GGT CCT CAT TCA GTT GGC GCC TC
U17	TTG ACT AGT TAC GCC CAC CAA CCC AGT GCA CAA ACC CAA GTA TTC TCT CGT CGC CGT CCT CAT TCA GTT GGC GCC TC
U34	GTC TTG ACT AGT TAC GCC GAC CGG GAG GGA
FTU38	CAA CAC AAG GCA CAG ATA GCA GCC TGT TAC CAT CAT CCC CTC CTC ATT CAG TTG GCG CCT C
RTU38	GTC TTG ACT AGT TAC GCC CAA CAC AAG GCA CAG ATA GCA GCC TGT TAC CAT CAT CCC CTC C
FRTU38	CAA CAC AAG GCA CAG ATA GCA GCC TGT TAC CAT CAT CCC CTC C
Forward primer for HcpA (hcpA-F)	ATCCGGGATCCTTTACACTTATCGAACTGAT
Reverse primer for HcpA (hcpA-R)	ATGCCAAGCTTTTAGTTGGCGTCATCAAA
Random DNA sequence	CTC CGC GGT TGA CTT ACT CCG GGT GGG TGG TGG TGG GCA CTT CCG GGT GGG TTA GGG AGG CCG CAT TGA TCA GTT CTA

3.2. METHODS

3.2.1. Immobilization of urea on carboxyl magnetic beads

BioMag®Plus carboxyl beads were used as immobilization supports and used according to manufacturer's instructions. Aliquots of 20 mg/ml carboxyl magnetic beads were taken in 15 ml conical centrifuge tubes and washed twice with 5 ml of 2(N-Morpholino) ethanesulfonic acid (MES) buffer (pH 5.2). After subsequent washing steps, the supernatant was discarded after magnetically separating out the beads. Finally, the beads were resupended in 5 ml of MES buffer and were activated using 1.6 mg of N-(3-dimethylaminopropyl)-N-ethylcarbodiimide (EDC) per mg of BioMag®Plus carboxyl beads. The mixture of beads and EDC were incubated for 1 h with gentle shaking at RT and washed twice with 5 ml of MES buffer. Finally the carboxyl activated beads were mixed with 1 ml of 100 mg/ml of urea prepared in MES buffer (pH-5.2) and incubated overnight at RT with gentle mixing. After incubation, the reaction tube was placed in a magnetic stand for 5 min to separate the urea bound beads from the unbound urea present in the supernatant. The concentration of unbound urea in supernatant was estimated using diacetyl-monoxime standard curve plot for urea (50-3000 µg/ml).

After immobilization, urea coupled magnetic beads (urea-CMB) were resuspended and stored in selection buffer; SB (section 3.1.2.1.18). EDC activated magnetic beads without urea (naked CMB) was used for negative selection.

3.2.2. Systematic evolution of ligands by exponential enrichment (SELEX) for urea selection

Urea aptamers were selected from a random pool of ssDNA (N_{44}) molecules using the principle of Flu-Mag SELEX [367]. For the first round, 2 nmoles (10^{15} ssDNA) oligos were heated in 650 µl of selection buffer (section 3.1.2.1.18) at 92 °C for 10 min. The denatured oligos were then allowed to cool down at RT for 15 min. The annealed ssDNA molecules were mixed with 100 µl of urea-CMB (20 mg/ml) resuspended in binding buffer (Section 3.1.2.1.19) and incubated for 45 min at RT with gentle mixing by placing it on Labnet gyromini nutamixer. After incubation, the beads were separated from the unbound ssDNA molecules with the help of a magnetic stand. The urea-CMB were then washed twice 500 µl of selection buffer to remove off the loosely bound ssDNA molecules. Elution of the bound ssDNA molecules was performed by incubating the beads with 100 µl of elution buffer containing free urea (selection buffer with 6mM urea, pH 7.5). After elution, PCR was performed using specific sets of primer (FITC labeled forward and ribolinked reverse primers) as mentioned in table 3.2 to enrich the population of the selected molecules.

PCR mixture:

Reagents	Volume (µl)
10X reaction buffer	10 µl
2mM dNTPs	10 µl
10 µM DrF	3 µl
10 µM DrRA	3 µl
Biotool Taq-DNA polymerase (1 U/ µl)	1 µl
Nuclease free water	10 µl
Template	1picomole
Total	100 µl

PCR program:

Steps	Temperature (°C)	Time (min)
1	95	5
2	95	1
3	55	0.30
4	72	0.30
Repeat step 2-4 for 30 times		
6	72	10
7	4	Hold

The double stranded PCR product was rendered single stranded by performing 10% urea-denaturing polyacrylamide gel electrophoresis (PAGE) [36]. The PCR product was precipitated using 2.5 volumes of chilled ethanol (Merck, molecular grade, India) and kept at -20 °C for 2 h. After incubation, the samples were centrifuged at 13000 rpm for 30 min at 4 °C. Ethanol was gently removed with a pipette without touching the pellet, and the pellet was gently washed twice with 70% ethanol by inverting the tube 3-4 times. The samples were centrifuged at 13000 rpm for 30 min at 4 °C, subsequently ethanol was drained and the pellet was air dried. For every 100 µl of PCR product, the dried pellet was resuspended in 250 µl of 0.25 N NaOH and samples were placed in heating block maintained at 92 °C for 10 min. After heating the samples were snap chilled on ice for 5 min, followed by addition of 25 µl of 3M sodium acetate pH 5.2 and precipitated with 2.5 volume of absolute ethanol by placing the samples at -20 °C for 2 h. DNA was recovered by centrifugation at 13000 rpm for 30 min at 4 °C, followed by two 70% washes as mentioned earlier. The pellet was dried and resuspended in 20 µl of nuclease free water. The samples were loaded in already casted and pre-run 10% urea

denaturing PAGE. The gel was run at 300-400 V till the tracking dye (bromohenol blue) has migrated ¾th of the gel length. The power supply was turned off and the gel was carefully wrapped in cling film. The gel was visualized under UV in gel doc (BioRad, USA) and the fluorescent band of DNA visible at xylene cyanol tracking dye (migrates at 55 nucleotide in 10% denaturing PAGE) was excised.

The excised gel was collected in 1.5 ml of micro-centrifuge tube and finely minced with 1 ml autoclaved tip. 700 µl of elution buffer (section 3.1.2.1.20) was added and the tube was placed at 40 °C incubator with overnight shaking at 250 rpm. The samples were centrifuged at 13000 rpm to spin down the debris of the gel, and remove the supernatant gently with a pipette into a new micro-centrifuge tube while taking care not to carry any gel pieces. The precipitation step was done as mentioned earlier with sodium acetate and absolute ethanol. The DNA pellet was resuspended in 50 µl of nuclease free water. These selected ssDNAs were further used as the starting material for next round of selection. First four rounds of SELEX were performed against urea-CMB and a step of counter selection using EDC activated carboxyl magnetic beads was introduced to eliminate the ssDNA molecules binding nonspecifically to the beads. These iterative selection steps were carried out for 10 rounds.

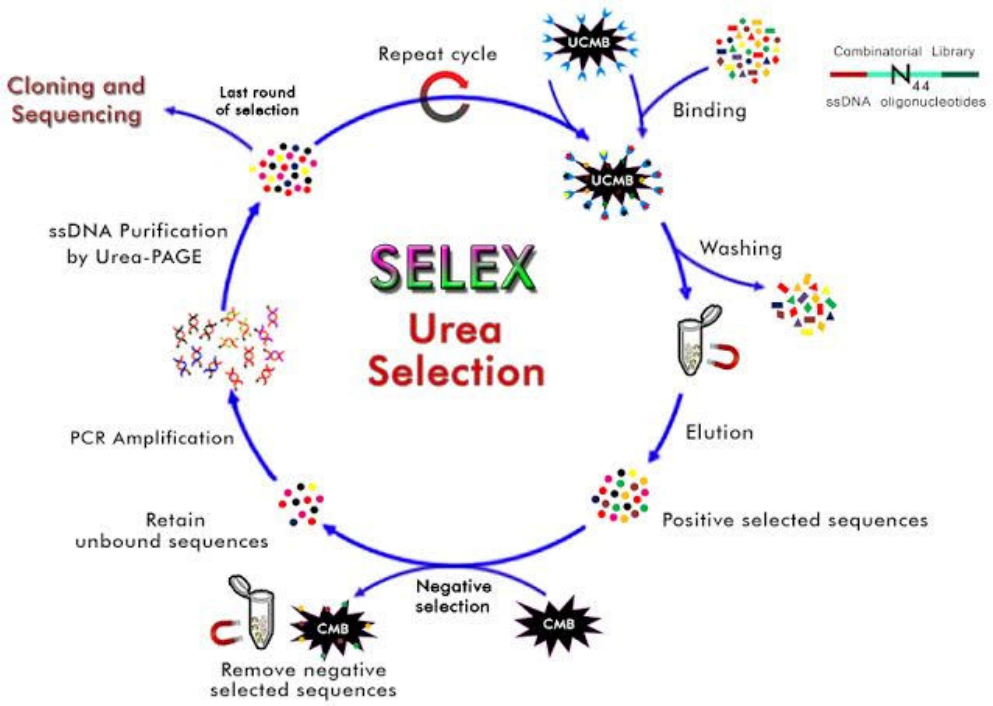

Figure 3.1 Schematic representation of Flu-Mag SELEX for urea

Table 3.3 Design for Flu-Mag selection strategy for urea

Round	Volume of beads for negative selection	Volume of beads for selection	Amount of t-RNA	Amount of BSA	Time of incubation with conjugated beads	No. of washes given
1	-	250 µl	2 µg	120 µg	45 min	1
2	-	250 µl	4 µg	140 µg	45 min	2
3	-	200 µl	5 µg	140 µg	30 min	2
4	-	200 µl	5 µg	140 µg	20 min	3
5	300 µl	200 µl	10 µg	140 µg	20 min	4
6	300 µl	200 µl	10 µg	140 µg	20 min	6
7	350 µl	100 µl	10 µg	140 µg	15 min	6
8	350 µl	100 µl	10 µg	140 µg	15 min	8
9	400 µl	100 µl	30 µg	140 µg	10 min	10
10	400 µl	100 µl	30 µg	140 µg	10 min	10

3.2.3. Enrichment of selected population from alternate round of selection, for preliminary binding studies using fluorescence spectrophotometer

After 10 rounds of selection, populations of selected rounds (4, 7, 8, 10) along with the RDL (random DNA library) were enriched by using PCR. The dsDNA was rendered single stranded using 8M urea denaturing PAGE. The FITC labeled population of different rounds was appraised for their binding affinity towards urea by measuring the fluorescence intensity as compared to the naïve RDL. The fluorescence based assay was performed by incubating 125 nM of annealed FITC labeled population of different rounds with 100 µl of urea-CMB (20 mg/ml) and incubating it for 45 min at RT on Labnet gyromini nutamixer with constant shaking. After incubation, the beads were magnetically separated and unbound ssDNA molecules were removed by two washing steps. The bound FITC labeled ssDNA molecules were eluted using 750 µl of elution buffer supplemented by 6 mM urea. The amount of eluted ssDNA molecules were determined by measuring the fluorescence intensity at 525 nm with an excitation of 490 nm.

3.2.4. Cloning, sequencing and sequence alingment of selected aptamer pools

Based on the preliminary fluorescence binding study, the population displaying best binding was PCR amplified and cloned in pTZ57R vector (InsT/A Cloning *kit;* Fermentas, USA) as per manufacturer's instruction. The clones thus obtained were picked randomly based on the blue white screening [368] and sequenced (Eurofins, USA). The sequences obtained were aligned based on sequence homology using Bio Edit software and divided into categories.

3.2.5. Screenig of best urea binding aptamer by fluorescence based assay

Different representative sequences from each category were chossen as potential aptamer candidates for urea as target molecule. By performimg fluoresccence based assay as mentioned in 3.2.3 section the binding ability of aptamer canditates were determined as compared to RDL

3.2.6. Determination of dissociation constant (K_d) of urea aptamer

In order to determine the binding affinity of the selected aptamer (U38), varying concentration of aptamer (0-350 nM) annealed in 250 µl selection buffer was incubated with fixed concentration of urea-CMB (2 mg) in 750 µl of binding buffer. After 45 min of incubation at RT under mild shaking condition, two gentle washes with 750 µl of binding buffer were given prior to elution of bound aptamer with 1000 µl of elution buffer. The concentration of the eluted aptamer was estimated by measuring the fluorescence intensity, saturation curve was plotted and the Kd value was calculated by employing the non-linear regression analysis using GraphPad Prism software (version 6.0, San Diego, CA, USA).

3.2.7. Circular dichroism measurement (CD)

The CD spectra of free U38 aptamer, U38 aptamer with 100 mM urea and U38 aptamer with non-target molecule (100 mM glycine as a control) at a final concentration of 5 µM in a selection buffer were recorded on Applied Photophysics spectropolarimeter interfaced with a computer and equipped with a Peltier temperature device. The spectra were recorded in wavelength range of 200–320 nm; the data gathered were the average of three scans. The scan of the selection buffer alone recorded at room temperature was subtracted from the spectra of above test samples. Melting curve from 20 to 100 °C was monitored by CD signals at 276 nm for U38 aptamer alone and in presence of urea and glycine separately and the graph was plotted for changes in ellipticity versus temperature.

3.2.8. Preparation and characterization of gold nanoparticles (AuNPs)

Gold nanoparticles (AuNPs) were prepared by citrate reduction method as previously described in literature [369]. Before starting with the preparation of gold nanoparticles, the glass material required (two neck round bottom flask, magnetic pellet, measuring cyclinder and

spatula) for preparations were treated with freshly prepared aqua regia (3HCl:1HNO_3) for 1 h. After aqua regia treatment, the glassware's were thoroughly rinsed with milliQ water and then oven dried for 2-3 h to remove any traces of acids that can interfere with the preparation of AuNPs. For preparation of AuNPs, 50 ml of 1 mM $HAuCl_4.H_2O$ was heated in a two neck flask under constant stirring condition till condensation appeared on the neck of the flask. To the boiling solution of gold salt, 5 ml of 38.8 mM of sodium tri-citrate was added drop wise. A gradual color change from yellow-colorless-purple-wine red was seen in 5 min which indicated the formation of AuNPs After attaining wine red color the flask was removed from the hot plate and kept on to other magnetic stirrer maintained at RT and stirred continuously in order to bring down the temperature of the solution to RT. The AuNPs thus prepared were characterized by UV-visible spectroscopy, dynamic light scattering (DLS) and Transmission electron microscopy (TEM).

3.2.9. Preparation of milk samples for urea testing

Milk samples (200 µl) were spiked with different concentrations of urea (20-250 mM) and precipitated using 4 volume of chilled methanol for 5 min to eliminate the interfering proteins. Subsequently, these samples were centrifuged at 12000 rpm for 15 min at 4 °C. The supernatants of respective samples were collected in fresh tubes, labeled as processed milk samples and further used for urea detection. A control sample of milk without urea was prepared as mentioned above. All the samples were freshly prepared prior to its use.

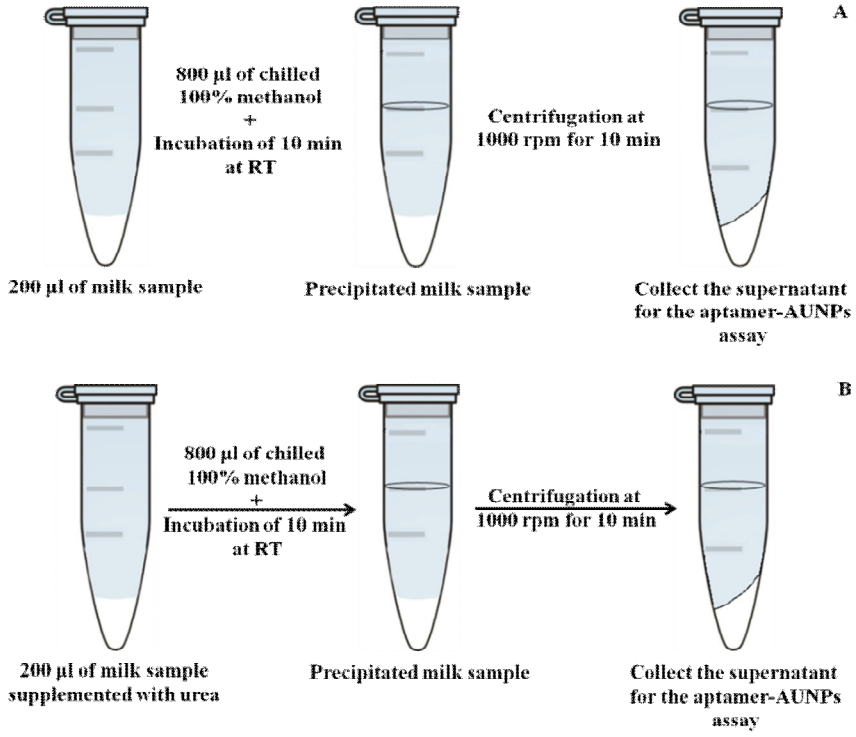

Fig 3.2 Preparation of milk sample for urea detection by aptamer-AuNPs assay: (A) Control and (B) Test sample with varying concentration of urea

3.2.10. Visual detection assay for urea based on aptamer-AuNPs aptasensor

For developing an aptamer-AuNPs based aptasensor, three different aptamer candidates (U7, U34 and U38) were selected along with a random sequence acting as a control for further experiments. HPLC purified candidate sequences and a random sequence as control was purchased from Eurofins, USA. Aptamer candidates and a random sequence at 250 nM concentration were incubated with AuNPs (2.75 nM) for 2 min at RT. Subsequently, 50 µl of processed milk samples spiked with 100 mM urea was added to each test samples and further incubated for 2 min at RT. After incubation, 1.5 µl of 5 M NaCl (250 mM) was added to each sample and absorbance spectra of samples were measured by scanning from 350 nm to 750 nm

3.2.11. Truncation study of U38 aptamer and secondary structural analysis by Mfold software

Urea specific full length U38 (U38) aptamer (80bp) was shortened by truncating either forward (FT-U38) or reverse (RT-U38) or both the primer (FRT-U38) domains of the aptamer sequence. The truncated sequences were commercially synthesized with HPLC purification and assessed for their performance to detect 100 mM urea in milk sample using same principle as mentioned for full length U38 (U38) of aptamer-AuNPs aptasensor in section 3.2.10, with appropriate control for each oligo. Secondary structural analysis of all oligos (U38, FTU38, RTU38 and FRTU38) was performed using Mfold software [370] with default settings and predefined salt conditions used in selection (section 3.2.2)

3.2.12. Specificty and interference test of the assay

In order to evaluate the specificity of the U38 aptamer towards urea, different structurally related small molecules such as glycine, alanine, serine and tyrosine were individually examined for its ability to bind the aptamer. Milk samples spiked with 100 mM of each of the above small molecule were processed as aforementioned. From each sample 50 µl volume was added to already adsorbed U-38 aptamer (250 nM)-AuNPs (2.75 nM) with subsequent addition of salt and observed for color change as mentioned earlier.

Similarly interfering components of synthetic milk such as sodium chloride (500 µM); glucose (600 µM); Sodium bicarbonate (20 mM) and Tween-20 (1%; v/v) were spiked in milk along with 100 mM urea and tested for interference for the developed assay. Normal milk sample and urea (100 mM) spiked milk samples were considered as negative and positive controls respectively.

3.2.13. Fluorescence recovery assay

The FITC labeled U38 aptamer at 250 nM concentration was mixed with 300 µl AuNPs (2.75 nM) and incubated for 2 min. Later, 50 µl of the processed spiked milk sample with urea

(100 mM) was added to the above solution. A recovered fluorescence reading was measured at 0 and 10 min time intervals, with excitation at 490 nm and emission collected at 525 nm. The fluorescence intensity of the FITC aptamer alone and FITC aptamer with AuNPs without any addition of processed milk sample were used as the standard for maximum and minimum fluorescence value, respectively. Milk samples spiked with 100 mM glycine instead of urea was used as control. In another set of control experiment, 100 mM urea-spiked milk sample was treated with 100 unit of Jack bean urease (Sigma Aldrich, USA) and its effect on fluorescence recovery was studied.

3.2.14. Limit of detection for the aptamer-AuNPs based aptasensor

To evaluate the detection limit of aptamer-AuNPs based sensor, U38 urea specific aptamer (250 nM) was incubated with AuNPs (2.75 nM) for 2 min at RT. Subsequently, 50 µl of processed milk samples spiked with different concentration of urea (0-200 mM) were added separately and further incubated for 3 min at RT. After incubation, addition of 250 mM NaCl was followed by visual observation, UV-visible (400-750 nm) and fluorescence emission spectra of AuNPs were recorded immediately at λ_{exi}=350 nm and scanned up to 700 nm.

3.2.15. PCR amplification and cloning of *hcpA* locus from *E. coli* O157:H7

The genetic locus encoding for HcpA pilin was amplified from the genomic DNA of *Escherichia coli* O157:H7, using specific primer for the gene by polymerase chain reaction (PCR) using PCR program as mentioned below.

PCR mixture:

Reagents	**Volume (µl)**
10X reaction buffer	10 µl
2 mM dNTPs	10 µl
10 µM hcpA-R	3 µl
10 µM hcpA-F	3 µl
Pfu DNA polymerase (10 U/ µl)	0.5 µl
Nuclease free water	73 µl
E. coli O157:H7 genomic DNA	0.5 µl
Total	**100 µl**

PCR program:

Steps	Temperature (°C)	Time (min)
1	95	5
2	95	1
3	52	0.30
4	72	0.45
*Repeat step 2-4 for **5** times*		
6	95	1
7	55	0.30
8	72	0.45
*Repeat steps 6-8 for **25** times*		
9	72	10
10	4	HOLD

The PCR product was checked for the desired amplification by performing gel electrophoresis in 1% agarose gel using standard DNA marker as the reference. The PCR product along with pET28(a) (Novagen) were digested with restriction enzyme *BamH*I and *Hind*III (Fermentas, USA) by incubating at 37 °C for 2-3 h. Digestion reaction was stopped by heat inactivating the enzyme at 70 °C for 10 min. Dephosporylation of vector was performed by adding FastAP (Fast Alkaline phosphatase; Fermenats; USA) according to manufacturer's instructions. Reaction was stopped by heat inactivating at 70 °C for 10 min. Restriction digested PCR product and pET28 (a) vector were gel purified using Qiagen gel extraction kit as per manufacturer's instructions. Ligation reaction was setup as mentioned in the following table.

Reagents	Final Conc. (In 10µl)	Volume (In 10 µl)
10X T4 ligase buffer(Fermentas, USA)	1X	1 µl
T4 DNA ligase (10 U/µl)	5 U	0.5 µl
ATP (10mM)	0.5 mM	0.5 µl
pET28a	100 ng	2 µl
Amplified *hcpA* gene	300 ng	6 µl

Ligation reaction was carried out by incubating the reaction mixture at 16 °C overnight. Further the reaction mixture was heat inactivated at 70 °C for 10 min and stored at -20 °C until use. The ligated vector thus prepared was transformed by electroporation into *E. coli* DH5α

electrocompetent cells and plated on LB-Kan plates (LB agar plates supplemented by 50 µg/ml of kanamycin). The plasmids from the transformants were confirmed for insert (*hcpA*) by performing double digestion using *BamH*I and *Hind*III restriction enzyme.

Reagents	**Final Conc. (In 20 µl)**	**Amount (In 20 µl)**
10X R buffer*	1X	2 µl
*BamH*I (10 U μl^{-1})	10 U	1 µl
*Hind*III (10 U μl^{-1})	5 U	0.5 µl
Recombinant plasmid	500 ng	10 µl
Nuclease free water		6.5 µl

Once the hcpA gene was confirmed, the vector was transformed into *E. coli* BL21 (DE3) strain for HcpA expression. The *E. coli* BL21 (DE3) transformed with *hcpA*-pET28(a) recombinant vector for overexpression of HcpA pilin subunit.

3.2.16. Overexpression study of recombinant-HcpA

With an aim to check the HcpA expression, a pilot scale experiment for HcpA production was performed using IPTG inducible T7 promoter of pET28a expression vector and *E. coli* BL21 (DE3) cells as host. For induction, *E. coli* BL21 (DE3) cells harbouring *hcpA*-pET28(a) recombinant vector were grown to ~0.8 $O.D_{600}$ and induced with 0.7 mM IPTG (Himedia, India). Further, cells were incubated at 250 rpm shaking condition for 6 h at 20°C (Kuhner incubator). In order to confirm the expression of HcpA, 1 ml cell culture was withdrawn from the induced and uniduced samples (without IPTG induction) in 1.5 ml micro-centrifuge tubes (Tarson, India) and centrifuged at 12,000 rpm for 10 min to pellet down the cells. In order to check the expression, samples were prepared by boil-prep method, wherein respective cell pellets were resuspended in 1 X SDS gel loading buffer and heated at 92°C for 5 min (Dry bath; GeneI, Bangalore). The expression of recombinant Histidine tagged HcpA (His-HcpA) was analyzed on 15% SDS-PAGE (Bio-RAD mini gel assembly).

3.2.17. Purification and quantification of overexpressed protein

E. coli BL21 (DE3) cells harboring recombinant plasmid *hcpA*-pET28(a) was induced under optimized conditions for large scale purification of His-HcpA. Further, the induced culture was centrifuged at 10000 rpm at 4 °C to pellet down the cells. The cells were resuspended in 10 ml of lysis buffer (section 3.1.2.2.21) and lysed using French press at 20000 psi. The cellular debris was settled down by centrifugation at 20000 rpm for 20 min at 4 °C. Carefully the supernatant (crude extract) was transferred in an autoclaved 15 ml centrifuge

tube. Briefly, Ni-NTA column was prepared by loading 4 ml of Ni-NTA resin (Qiagen, USA) on to a bed of glass wool in 10 ml of syringe column. The column was equilibrated with 40 ml (10 bead volume of Ni-NTA beads) of equilibration buffer (section 3.1.2.2.22) prior to loading the supernatant. The protein lysate was loaded to the equilibrated Ni-NTA column and incubated for 30 min at 4 °C. After incubation, the flow through was collected and the column was washed with 40 ml of wash buffer 1 (section 3.1.2.2.23) and subsequently with 40 ml of wash buffer 2 (section 3.1.2.2.24). Elution of protein was done with 15 ml of elution buffer in aliquots of 1.5 ml (section 3.1.2.2.25). Eluted fractions were analyzed on 15% SDS-PAGE to check the purity of protein. After analysis the eluted fractions containing the HCP protein were pooled and imidazole was removed by passing it through the 3 kDa centrifugal devices according to the manufactures protocol. Buffer exchange was performed twice with 50 ml of 20 mM sodium phosphate buffer and the protein sample was concentrated to 1 ml. The concentration of the dialyzed protein samples were estimated using Micro BCA™ Protein Assay Kit (Thermo Scientific, Pierce, USA), as per manufacturers instruction.

3.2.18. SELEX for HcpA using Ni-NTA bound His-HcpA

The purified, concentrated and dialyzed His-HcpA (30 mg/ml) was incubated with 1ml of Ni-NTA beads at 4 °C for 60 min. HcpA immobilized Ni-NTA beads were packed in 1 ml sintered column (BioRad) and equilibrated as described in section 3.2.16 with binding buffer. For the first round of selection, 10^{15} molecules of annealed ssDNA oligos were resuspended in 250 µl of selection buffer was added to HcpA immobilized Ni-NTA beads and incubated for 60 min with gentle intermittent mixing. The column was then washed twice with 1 ml of selection buffer and ssDNA molecules were eluted with elution buffer. The course of selection is described in the table 3.4, with the introduction of counter selection with naked Ni-NTA beads after 3 rd round of SELEX.

Table: 3.4 SELEX strategies for selection of aptamer for HcpA pilin

Rounds	Volume of Ni-NTA beads with bound HcpA taken for selection	Volume of Ni-NTA beads taken for counter selection	Amount of t-RNA (µg)	Amount of BSA (µg)	Time of incubation for selection (min)	Time of incubation for counter selection	Number of washes
1	100 µl + 650 µl SB	-	2	125	60	-	2
2	100 µl + 650 µl SB	-	2	125	60	-	2
3	50 µl + 700 µl SB	-	5	140	30	-	3
4	50 µl + 700 µl SB	50	5	140	30	30	3
5	50 µl + 700 µl SB	50	10	150	20	30	4
6	20 µl + 730 µl SB	50	10	150	20	30	4
7	20 µl + 730 µl SB	50	20	160	20	30	6
8	20 µl + 730 µl SB	50	20	160	15	40	6
9	10 µl + 740 µl SB	50	20	160	15	40	8
10	10 µl + 740 µl SB	50	20	160	15	40	8

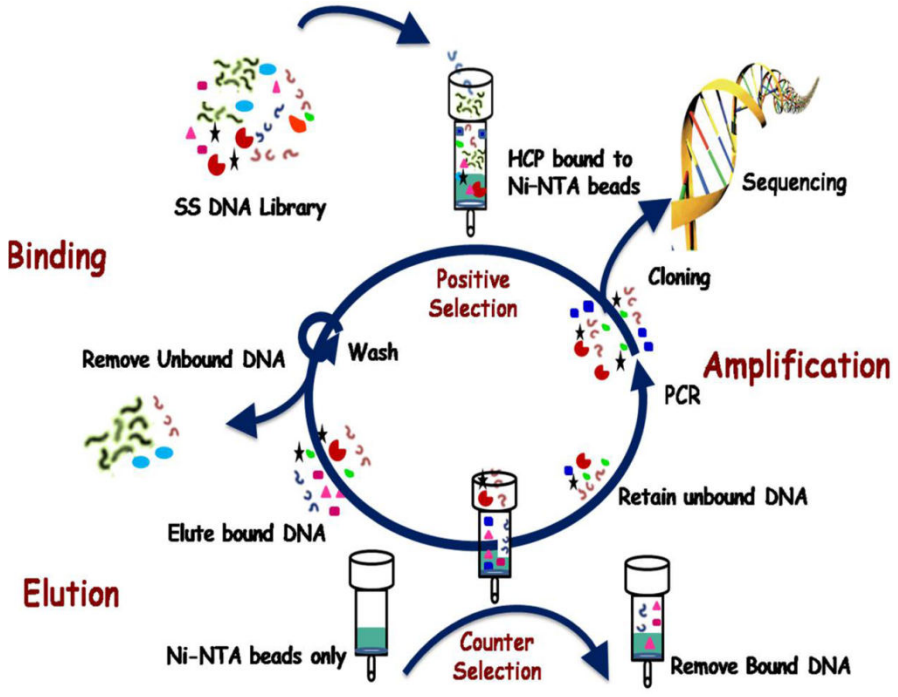

Fig. 3.3 Schematic representation of SELEX process for HCP specific aptamer generation

3.2.19. Enrichment of selected population from alternate round of selection, for preliminary binding studies by Electrophoretic Mobility Shift Assay (EMSA)

After 10 rounds of selection, populations of selected rounds (8 and 10) along with the RDL (random DNA library) were enriched by using PCR. The dsDNA were rendered single stranded using 10% urea denaturing PAGE (section 3.2.2). The FITC labeled population of different rounds were appraised for their binding affinity towards HcpA by performing EMSA. For EMSA, gel was casted by cleaning the plates of mini PAGE apparatus (BioRad, USA), and pouring 10 ml of 8% native PAGE mix supplemented with 100 µl of 10% APS and 10 µl of TEMED (Himedia, India). The gel was given a pre-run at 100V in a 4 °C chamber using 0.5 X TBE as the running buffer till an effective current in gel drops to 10 (it takes generally an hour). Meanwhile, the binding reaction was set with fixed concentration of HcpA (0.01 µM) and 100 nM annealed FITC labeled DNA (round 8, 10 and RDL), 1X concentration of 4X gel shift buffer and finally making the volume to 20 µl by adding selection buffer. The reaction mixture was incubated at RT for 30 min with intermittent gentle tapping after every 5 min. After incubation, the samples were loaded in the gel with proper control of only DNA and RDL for each round. The unused well of the gel were loaded with 1X gel loading dye, to track down the migration of the samples and were allowed to migrate till 3/4th of the length of the gel. Carefully remove the gel plate and scan the gel by exciting the FITC labeled DNA with blue laser (490 nm) using Typhoon scanner (Typhoon FLA 9500, GE healthcare, USA).

3.2.20. Facile synthesis and characterization of polymyxin B capped silver nanoparticles

Synthesis of polymyxin B capped silver nanoparticles (PBSNPs) was based on a method described earlier with some modifications [371]. Briefly, silver nanoparticles were prepared by addition of freshly prepared silver nitrate (2 mM) and $NaBH_4$ (0.6 mM) to a polymyxin B solution in methanol. The resultant mixture was incubated for different time periods at 30 °C under illumination at 40W yellow light (141.3 lux). The optimum polymyxin B concentration for this reaction was determined by a set of batch experiments where the concentration of the peptide was varied between 0-100 µg/ml. The prepared PBSNPs were dialyzed against miliQ water for 12 h using a 10 kDa cut-off membrane to remove unbound polymyxin B and free silver ions. Citrate capped silver nanoparticles (CSNPs) were synthesized using previously published method and were used as control in the experiments [372]. PBSNPs and CSNPs were characterized by using UV-visible spectroscopy, transmission electron microscopy (TEM), zeta potential, dynamic light scattering (DLS), Fourier transform infrared (FTIR), and circular dichroism (CD) spectroscopy. Surface Plasmon resonance (SPR) spectra of PBSNPs and CSNPs were recorded using the UV-visible

absorbance spectrometer (SpectraMax Plus spectrophotometer, Molecular Devices LLC, USA). The stability of nanoparticles was determined by measuring zeta potential using a Zetasizer (Malvern, UK). The morphology and size of nanoparticles were observed using TEM (JEOL JEM-2100F, JEOL, Japan). For TEM analysis, samples were prepared on carbon coated copper grids and examined with an accelerating voltage of 200 keV. Concentration of silver ions (Ag^+) in CSNPs and PBSNPs were determined by Atomic Absorption Spectrophotometer (AAS, GBC Avanta, USA) using silver nitrate ($AgNO_3$) standards. Presence of polymyxin B on the surface of silver nanoparticles and the effect of attachment on the secondary structure of peptide were measured with FTIR (Thermo Nicolet Nexus 670, USA) and CD spectroscopy (Applied Photophysics Chirascan^{TM} CD-spectrometer, Surrey, UK), respectively. CD measurements were carried out at 25 °C using a cylindrical fused quartz cell of 0.2 mm path length. Free polymyxin B and citrate capped nanoparticles were used as control.

3.2.21. Determination of minimum inhibitory concentration (MIC) and characterization of bacterial morphology by scanning electron microscopy (SEM)

The susceptibility of the microbial cells to CSNPs and PBSNPs were determined by microbroth dilution assays of clinical and laboratory standards institute (CLSI) in MH broth for both Gram-negative bacterial strains [373, 374].The cellular growth was observed at $O.D_{600}$ after 10 h. Growth above 10% of the O.D at 600 nm ($O.D_{600}$) of the positive control (lacking any antimicrobial agent) was considered as uninhibited growth. MIC is the lowest concentration of PBSNPs that inhibited the visible growth of microorganisms. CSNPs with same concentration were taken as a control. The assays were repeated three times with two replicates in each plate.

For SEM analysis, bacterial cells treated with MIC concentration of CSNPs and PBSNPs were collected by centrifugation at 10000 rpm for 10 min. The cells were primarily fixed with 2% gutaraldehyde followed by gradual dehydration with ethanol gradient (25, 50, 70, 80, 90 and 100%). The prepared samples were coated with a layer of gold and observed under SEM (Ultra Plus Field Emission, Carl Zeiss, Germany)

3.2.22. Biofilm inhibition assay

P. aeruginosa PAO1 biofilm formation was achieved by modifying the previously described assays [375, 376]. Briefly, *P. aeruginosa* PAO1 was grown overnight in LB medium at 37 °C with shaking at 250 rpm. Fresh LB medium was seeded with 1% of overnight culture and incubated at 37°C till an $O.D_{600}$ of 1.0 was attained. To investigate the bactericidal effect of CSNPs and PBSNPs on planktonic cells of *P. aeruginosa* PAO1, different concentrations of CSNPs (2.4- 25000 Ag^0 ng/ml) and PBSNPs (4.3 - 4500 Ag^0 ng/ml) were suspended in M63

minimal medium in a 96 well plate. The above culture was diluted 1: 100 in M63 minimal medium and added to varying concentrations of CSNPs and PBSNPs to reach a concentration of 10^8 CFU/ml. Media subcultured with diluted cells without SNPs was taken as positive control and the plate was incubated at 37 °C for 6, 12 and 24 h under static condition. M63 minimal medium alone was used as the negative control. After incubation, the planktonic cells were removed and the wells were gently washed 3 times with 300 µl of sterile 0.9% saline. The biofilm was stained with 300 µl of 0.1% aqueous CV solution for 15 min at RT. The stained film was washed thrice with 0.9% saline, air dried and solubilized with 300 µl of 30% acetic acid. The solubilized CV from each well was transferred to a new 96 well plate and the inhibition of biofilm was quantified by measuring the $O.D_{550}$ [377]. The above experiments were conducted in triplicates and the results were represented using two-way ANOVA statistics of GraphPad Prism for variation in independent experiments.

3.2.23. Live/Dead staining of the bacteria in the biofilm

To study the effect of PBSNPs on biofilm formation, *P. aeruginosa* PAO1 was grown to an $O.D_{600}$ of 1.0 and diluted 1:100 in M63 minimal medium. Aliquots of 1 ml (10^8 CFU/ml) of diluted culture were transferred to a 6 well plate with a sterile 13 mm coverslip along with MIC and sub-MIC of PBSNPs in a final volume of 2 ml. Control samples were prepared on a sterile glass coverslip with *P. aeruginosa* PAO1 cells (positive) and M63 minimal media (negative) without any SNPs [378, 379]. The wells were washed twice with 3 ml of sterile 0.9% saline. The coverslips were stained with 1.5 ml mixture of 0.8 µM SYTO9 green fluorescent dye and 10 µM propidium iodide (PI) red fluorescent dye of Live/Dead staining kit (LIVE/DEAD® *Bac*Light™ Bacterial Viability Kit, Invitrogen Molecular Probes, USA) and observed under fluorescence microscope (Carl Zeiss, Axio Scope A1, Germany) at 1000X magnification.

3.2.24. Viability analysis of PBSNPs treated *P. aeruginosa* PAO1

To examine the bactericidal effect of PBSNPs on planktonic cells, *P. aeruginosa* PAO1was subcultured in fresh LB broth and incubated at 37 °C. After an $O.D_{600}$ of 0.4 was attained, 2 ml of culture was centrifuged at 6000 rpm for 5 min. The cells were washed twice with sterile 0.9% saline and finally resuspended in 2 ml of sterile 0.9% saline. To carry out the Live/Dead staining of strain PAO1, 100 µl (10^8 CFU/ml) of resuspended cells were treated with MIC (4.5 Ag^0 µg/ml) of sonicated PBSNPs, whereas untreated cells were taken as control. Three different samples, untreated (stained and unstained) and MIC treated (stained) PAO1 cells were prepared. After incubation of 2 h, samples were centrifuged at 10000 rpm for 10 min at 4 °C, supernatant was discarded and the cell pellet was resupended in 100 µl of 0.9% saline.

Untreated and MIC treated samples were stained with 1 µl of 1:1 mixture of solution A and B of LIVE/Dead staining kit. Untreated-unstained sample was used as the control. The samples were analyzed on flow cytometer (BD FACS Verse™ BD Biosciences, USA) to discriminate between live and dead cells [380, 381]. All the data obtained were plotted on log scale for PI-PE A representing the red fluorescence against the syto-FITC A .The above stained samples were also visualized using fluorescent microscopy at 1000X magnification.

3.2.25. Electrophoretic deposition of polymyxin B and citrate capped silver nanoparticles

Electrophoretic deposition of PBSNPs and CSNPs was performed on stainless steel surgical blades (No.15 Glassvan, India) using procedure described earlier [360]. To observe the PBSNP coating on surgical blades, atomic force microscopy (NTEGRA, NT-MDT, Russia) was performed. Antibacterial activity of PBSNPs, CSNPs and uncoated surgical blades (negative control) were tested on MH agar plate spread with 100 µl of 0.2 $O.D_{600}$ *P. aeruginosa* PAO1 cells and incubated overnight at 37 °C. To ascertain the contribution of polymyxin B towards antibacterial activity, PBSNPs coated surgical blade was treated with proteinase K (5 mg/ml) for 1 h at 37 °C followed by incubation with *P. aeruginosa* cells on agar assay as mentioned above

3.2.26. Removal of Endotoxin by PBSNPs

Endotoxin removal efficiency of PBSNPs was assessed using endpoint endotoxin assay kit (ToxinSensor™ Chromogenic Limulus Amebocyte Lysate Endotoxin Assay Kit, GenScript, USA). The lysate (0.05 EU/ml) was incubated with 100 µl of PBSNPs and CSNPs separately for 30 min at 37 °C followed by centrifugation at 14000 rpm for 15 min. The presence of endotoxin was determined in the supernatant as per manufacturer's instructions. CSNPs and standard endotoxin provided with the kit were taken as controls. Endotoxin removal ability of PBSNPs and CSNPs was compared by measuring the absorbance at $O.D_{545}$. Concentration of the remaining endotoxin in the supernatant was estimated from the standard curve.

CHAPTER 4

GENERATION OF UREA SPECIFIC DNA APTAMER AND DEVELOPMENT OF AN APTASENSOR FOR "UREA" DETECTION

4.1. Immobilization of urea on carboxyl magnetic beads

Urea was immobilized with BioMag®Plus carboxyl beads as described in the section 3.2.1. The carboxyl terminated beads were activated by EDC to form an intermediate complex of acylisourea activated microparticles which further reacts with the free amine group of urea to form amide bond. This chemistry thus gives us an opportunity of developing aptamer against the immobilized urea. .

Fig 4.1A Urea immobilization: EDC assisted coupling of urea to carboxylic magnetic beads.

Coupling efficiency of the EDC chemistry was calculated by determining the concentration of immobilized urea on the carboxyl beads. For this, a standard curve for urea was plotted by diacetyl-monoxime method (R^2 value of 0.9981, Fig. 4.1B). The coupling efficiency of the EDC chemistry was derived using the formula mentioned below.

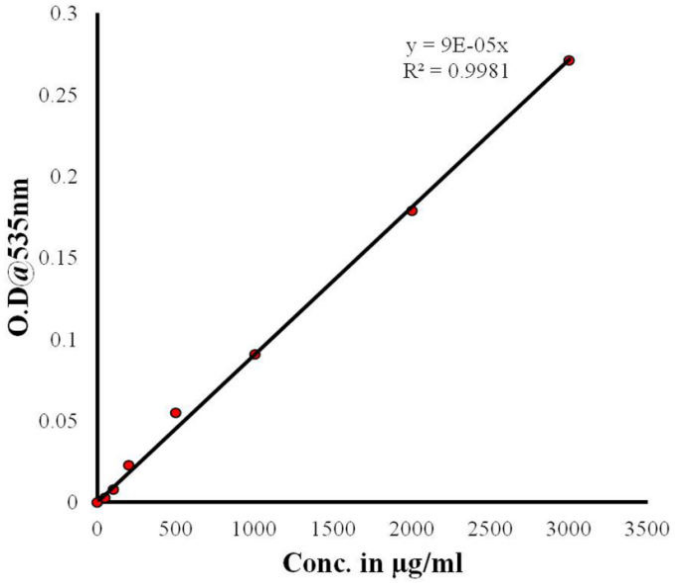

Fig 4.1B Standard curve of urea: Coupling efficiency of magnetic beads calculated on the basis of standard curve for urea by diacetyl-monoxime method.

$$\text{Coupling Efficiency} = \left[\frac{A \times \text{Dilution factor} - B \times \text{Dilution Factor}}{A \times \text{Dilution Factor}}\right] \times 100 \qquad \text{——Equation 1}$$

A – O.D at 535nm of pre-coupling solution, **B**- O.D at 535nm of post-coupling solution

From above equation (1) the coupling efficiency was calculated to be 61%.

4.2. Systematic Evolution of Ligands by EXponential Enrichment (SELEX) for generation of urea specific DNA aptamers

A Flu-Mag based *in-vitro* selection was performed by using carboxyl magnetic beads as immobilization support for urea (Fig. 4.1A). After first round of SELEX, labelling of selected DNA population was labelled during PCR (Fig.4.2.1) using 5' FITC-DrF forward primer for ease of visualization of DNA molecules on denaturing PAGE (Fig.4.2.1B) as mentioned in section 3.2.2. Initial three rounds of positive selection were carried out by incubating the random DNA library (RDL) with urea coupled carboxyl magnetic beads (urea-CMB). A negative selection step with unconjugated carboxyl magnetic beads was introduced after third round of selection to eliminate the DNA sequences binding non-specifically to the beads. Subsequently, DNA sequences bound to the carboxylated magnetic beads were separated from the unbound sequences; which were further incubated with urea-CMB for positive selection. Selection pressure in terms of decreased time of incubation with urea-CMB, increased time of incubation with naked beads, increased concentration of BSA, tRNA (blocking agent) and increased number of washing steps were progressively introduced during the entire selection process. This eliminates weak and nonspecific binding sequences with subsequent enrichment of target specific sequences.

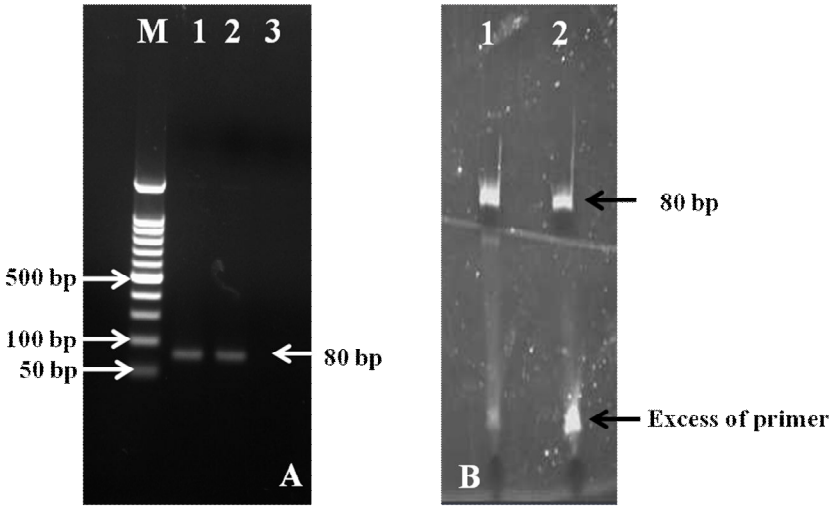

Fig 4.2.1 A) 2.5% agarose gel (lane M-standard 50bp marker, lane 1 and 2-PCR amplified product after initial steps of selection, lane 3- negative control), **B)** 10% urea denaturing PAGE (Lane 1 and 2- 80bp of ssDNA product).

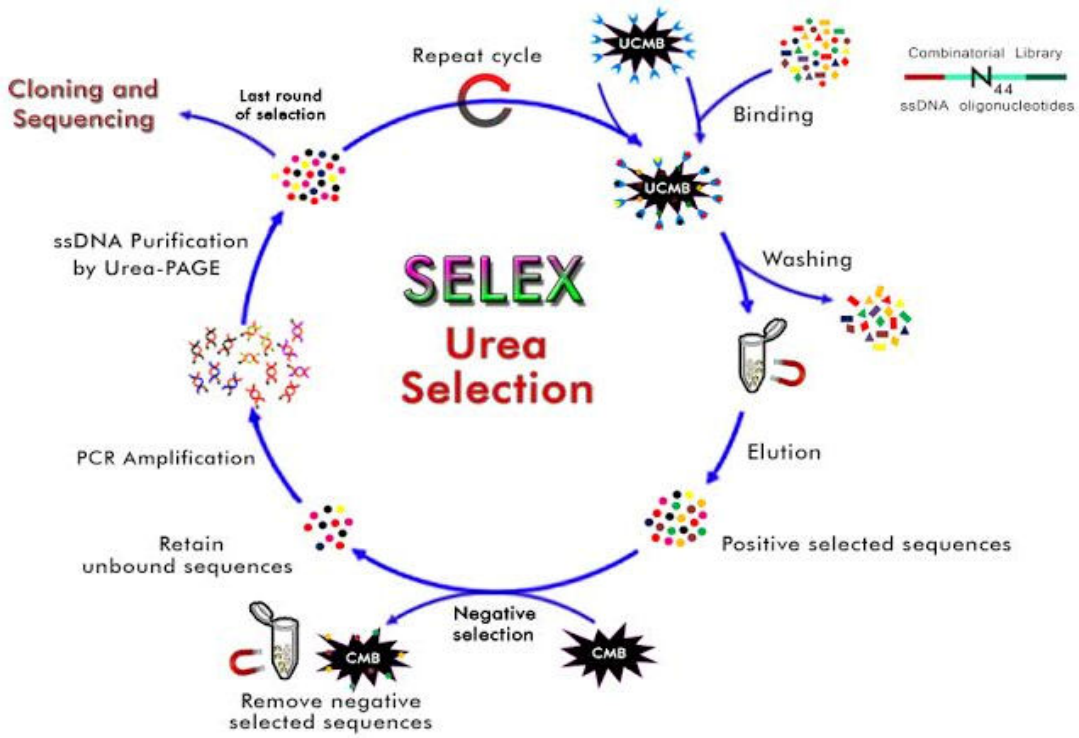

Fig 4.2.2. Schematic representation of Flu-Mag SELEX for urea.

After ten rounds of selection, enriched population of rounds 4, 7, 8 and 10 were examined for their binding affinity to urea as compared to the RDL by performing fluorescence assay as described in section 3.1.3. Figure 4.2 shows the fluorescence data of rounds 4, 7 and 8 which indicates that there is a progressive enrichment of pool of DNA sequences specific for urea starting from 4^{th} to 8^{th} round of selection.

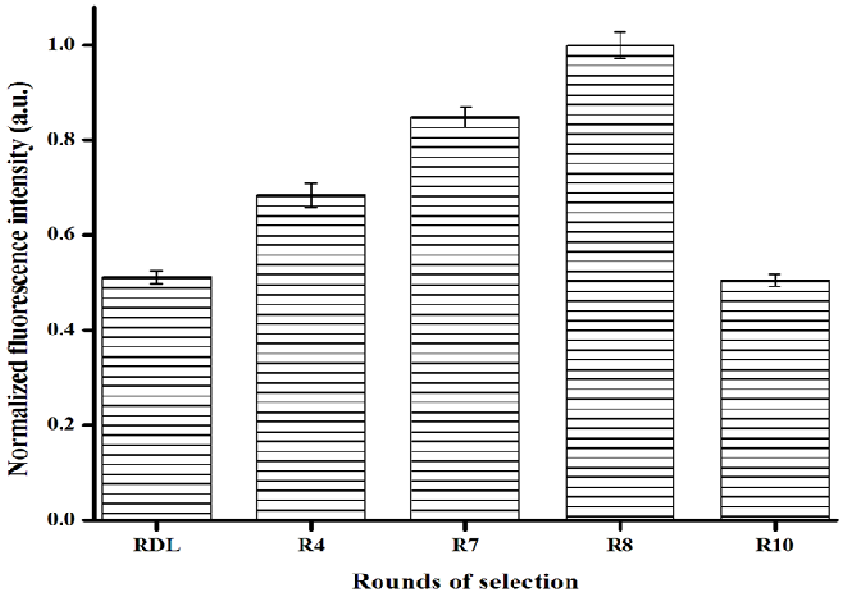

Fig 4.2.3 Enrichment of urea specific sequences during Flu-Mag SELEX: Evaluation of the affinity for enriched DNA pool of different rounds against the RDL for urea-CMB by Flu-Mag selection based fluorescence assay

However, after eighth round of SELEX, a decline in the fluorescence was observed, suggesting that no further enrichment of aptamers occurred [25]. This difference in fluorescence intensities indicated that DNA sequences binding specifically to urea have been enriched. Based on the above data it was decided to clone 8th round of population.

4.3. Cloning, sequencing alignment of 8th round of population and folding pattern of representative putative aptamers of each category

The 8th round selected pool of DNA were PCR amplified and cloned into T/A cloning vector as mentioned in section 3.1.4. Forty white colonies were picked from the IPTG-XGal plates based on blue/white selection screening and sequenced. The sequences thus obtained were grouped in 7 different categories based on sequence similarity. There were 9 orphan sequences which could not be placed into any group (Fig 4.3.1).

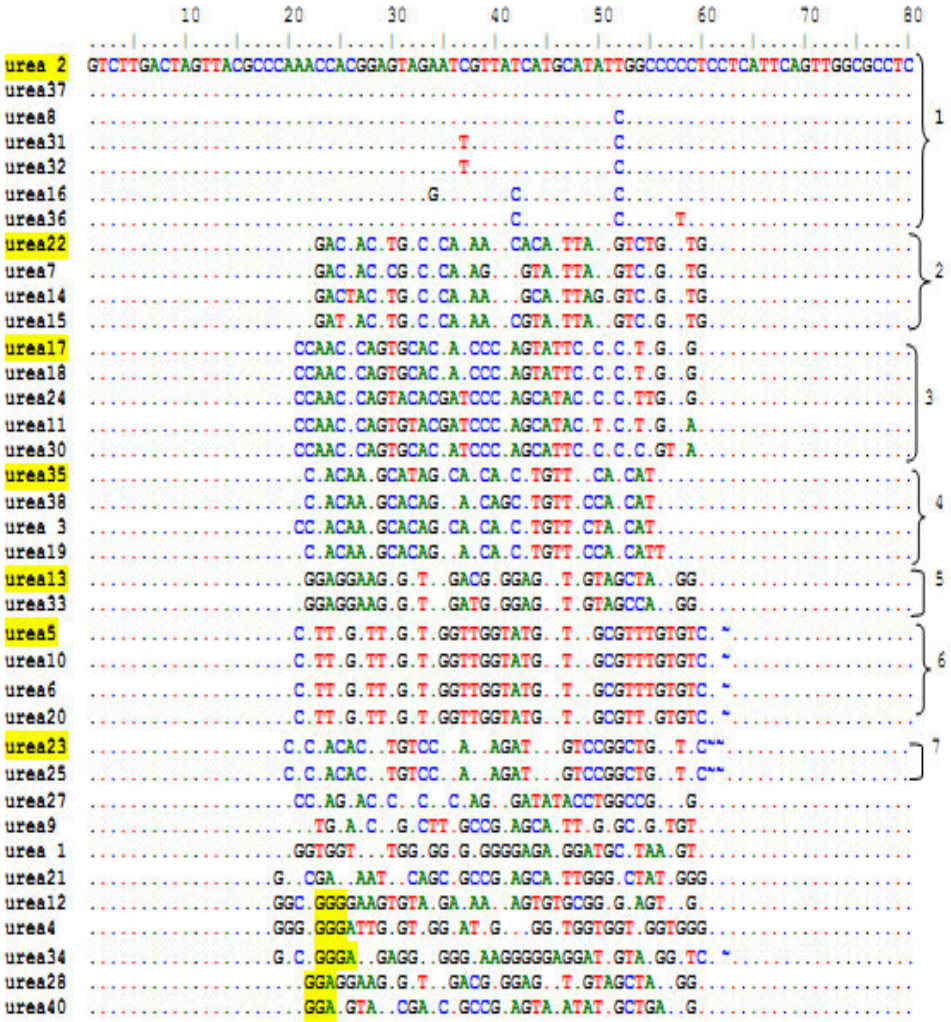

Fig 4.3.1 Sequence alignment by BioEdit software: DNA population of 8th round of urea selection was cloned and categorized based on sequence similarities obtained from BioEdit software.

Selected aptamers are single stranded DNA species which tend to fold into a three dimmensional structure which are characteristic of their sequences. The secondary structure of one representative aptamer candidate from each catergory (U2, U10, U13, U17, U34 and U38) was analyzed by Mfold software [370] (Fig. 4.3.2). Sequences were analyzed for their possible folding using predefined salt conditions as per the selection protocol (section 3.2.2), while other parameters were set at default.

U2- GTC TTG ACT AGT TAC GCC CAA ACC ACG GAG TAG AAT CGT TAT CAT GCA TAT TGG CCC CCT CCT CAT TCA GTT GGC GCC TC

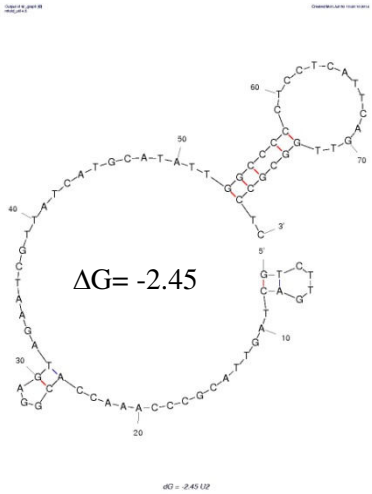

U7- GTC TTG ACT AGT TAC GCC CAA AGA CCA CAC GAC ACA AAG TAT GTA ATT AAT GTC CGA ATG CCT CAT TCA GTT GGC GCC TC

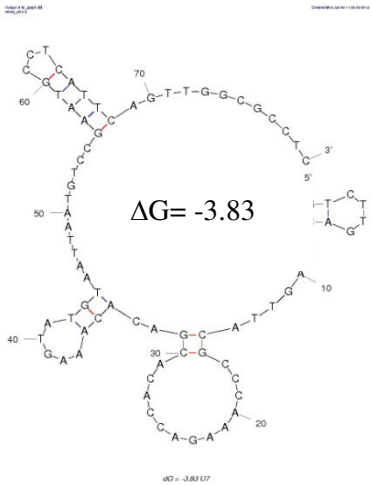

U10- GTC TTG ACT AGT TAC GCC CAC ATT AGG TTG GAT AGG TTG GTA TGT GTA TGC GTT GT GTC CTC ATT CAG TTG GCG CCT C

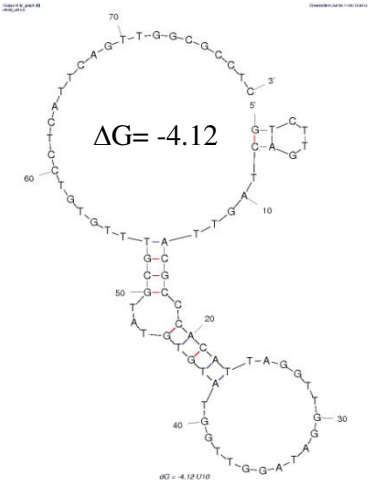

U13- GTC TTG ACT AGT TAC GCC CAA GGA GGA AGG GAT AAG ACG TGG AGT GTA GTA GCT ACC GGT CCT CAT TCA GTT GGC GCC TC

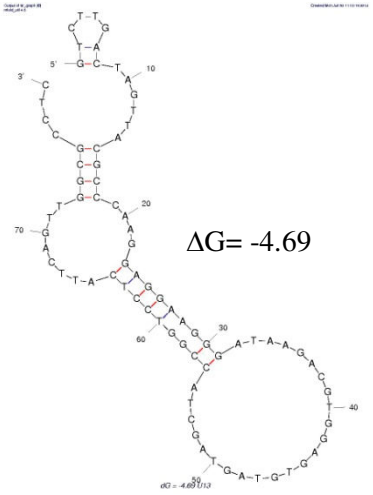

U17- GTC TTG ACT AGT TAC GCC CAC CAA CCC AGT GCA CAA ACC CAA GTA TTC TCT CGT CGC CGT CCT CAT TCA GTT GGC GCC TC

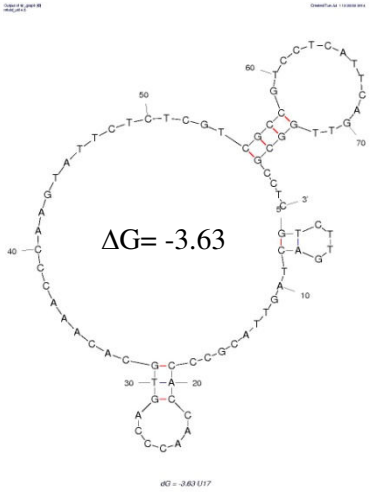

U34- GTC TTG ACT AGT TAC GCC GAC CGG GAG GGA GGG AGG GGA AGG GGG AGG ATG TAA GGA TCC TCA TTC AGT TGG CGC CTC

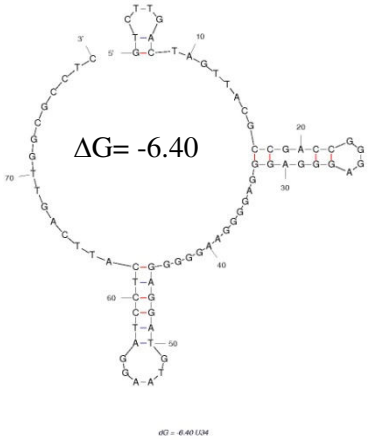

U38- GTC TTG ACT AGT TAC GCC CAA CAC AAG GCA CAG ATA GCA GCC TGT TAC CAT CAT CCC CTC CTC ATT CAG TTG GCG CCT C

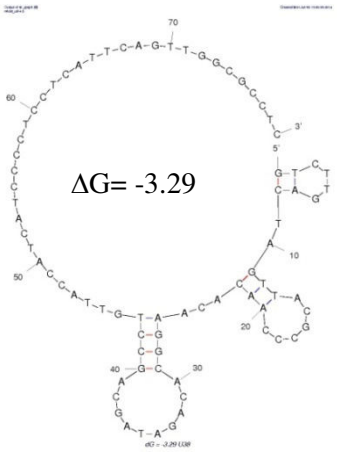

Fig 4.3.2 Secondary structure folding of putative aptamer candidature sequences (U2, U7, U10, U13, U17, U34 and U38). Free energy is shown in kcal/mol as ΔG .

4.4. Screening of aptamers by fluorescence based assay

In the quest of identifying the sequences with the highest binding affinity for urea, a fluorescence based assay was performed with individual putative aptamer sequence of each category. As control, FITC labelled RDL (FITC-RDL) was taken. Following binding of FITC-RDL and FITC labelled representative selected sequences with urea-CMB, the bound DNA was eluted using free urea (as in section 3.2.2). Fluorescence signal of the eluted sequences were measured and normalized with buffer used for binding study. The normalized fluorescence signal thus obtained is in direct correlation to the binding affinity of sequences. For example, the sequence with high affinity for urea will bind strongly as compared to the one with low or negligible affinity. The result in Fig. 4.4 shows normalized fluorescence signal plotted against different candidate sequences for urea coupled to magnetic beads. All of the

candidate sequences had affinity for urea, but U38 sequence demonstrated a marked difference in its binding capability with highest fluorescence value compared to other sequences which showed significantly less or negligible fluorescence value. FITC labelled RDL sequences were used a control.

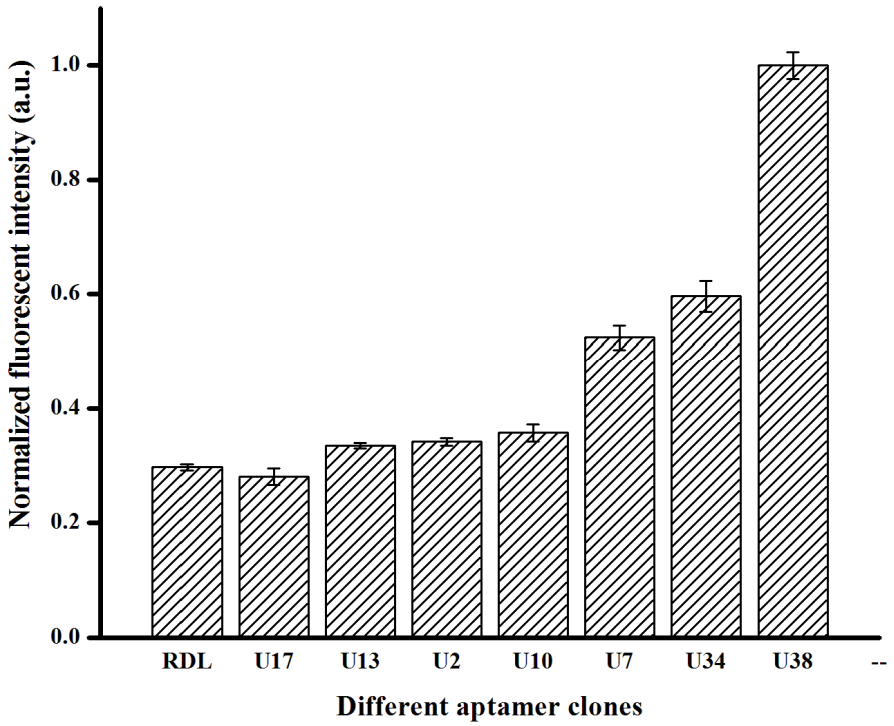

Fig 4.4 Binding assay for individual candidate sequences: FITC labelled sequences from each representative category (U2, U7, U10, U13, U17, U23, U34 and U38) were assessed for the highest binding affinity towards UCB. Representative sequence U38 of group 8 displayed maximum affinity as compared to the other candidate sequences and the FITC-RDL

4.5. Determination of dissociation constant (Kd) of urea aptamer (U-38)

Apparent dissociation constant (Kd) was calculated to quantify the binding affinity of aptamer to its target. To determine the Kd, fluorescence assay was carried out using the SELEX conditions as mentioned earlier by incubating varying concentrations of FITC labelled U38 (0-350 nM) against fixed concentration of urea-CMB (2.0 mg).Thereafter, the aptamer-urea-CMB complex was washed twice and fluorescence of the eluted aptamers was measured for each sample. The fluorescence values obtained were fitted in saturation curve using the nonlinear regression by GraphPad prism software (version 6.0, San Diego, CA, USA). The dissociation constant of U38 aptamer for urea was calculated to be 238nM (Fig 4.5). In comparison to the Kd of U38 aptamer the dissociation constant for previously studied aptamers against diverse small molecules such as PCB 72 [234], kanamycin [57], PCB 106 [234],

Sialyllactose [382], thalidomide [201], ibuprofen [202], PCB 77 [25],dopamine [230] and codeine [227] fall in the range of 85.6 nM- 4.9 μM, suggesting a strong binding to its cognate target molecule.

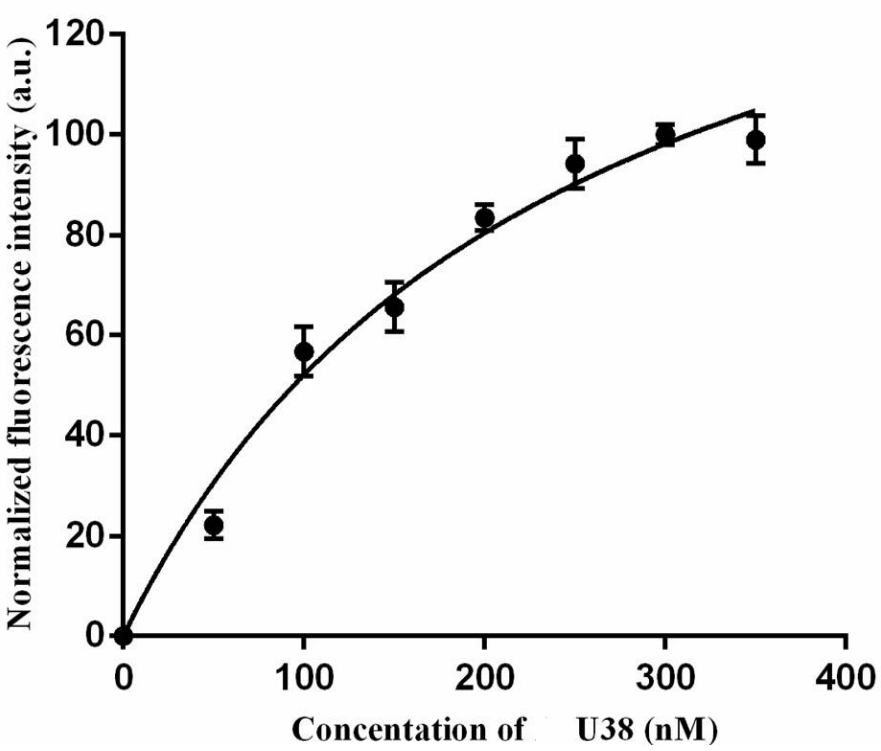

Fig 4.5 Determination of binding affinity, Kd value of the DNA aptamer U38 by fluorescence based assay: The apparent dissociation constant (Kd) of an aptamer representing group 8 (clone U38) was determined by fluorescence based assay using FITC labelled U38 aptamer. The average mean fluorescence intensity of the eluted FITC labelled U 38 aptamer obtained was plotted to determine dissociation constant Kd. The experiment was repeated thrice and an error bar represents the standard deviation.

4.6. Structural Analysis by Circular Dichroism (CD) Spectroscopy

CD is a biophysical tool which has been used for the study of secondary structure and conformational variations adopted by aptamers in presence of target molecules [60, 383, 384]. CD study was performed to investigate the structural changes accompanied by the U38 aptamer in the presence of urea and glycine when compared to the free U38 aptamer by monitoring the changes in CD signal in terms of ellipticity (θ) mdeg. The CD spectrum in Fig. 4.6.1 shows that the free U38 aptamer displayed positive maxima peaks at 276 nm probably due to base stacking and strong π-π* interaction of bases and a negative minima peak at 248 nm due to helicity, which are the characteristic of DNA in B-form [385, 386]. A substantial change in the ellipticity (θ) was observed on addition of 100 mM urea to U38 aptamer. An increase in the positive peak at 276 nm signifies the strong interaction of urea with U38 aptamer and thereby stabilizing the secondary structure. This strong interaction coincides well with the melting curve analysis (Fig. 4.6.2), which shows an increase in melting temperature of U38 aptamer in

presence of 100 mM urea (57 °C) as compared to U38 aptamer alone (48.5 °C). In presence of 100 mM glycine Tm was calculated to be 49.7 °C showing no significant change in the CD spectrum. These spectral changes indicates that a conformational change in U38 aptamer is urea specific

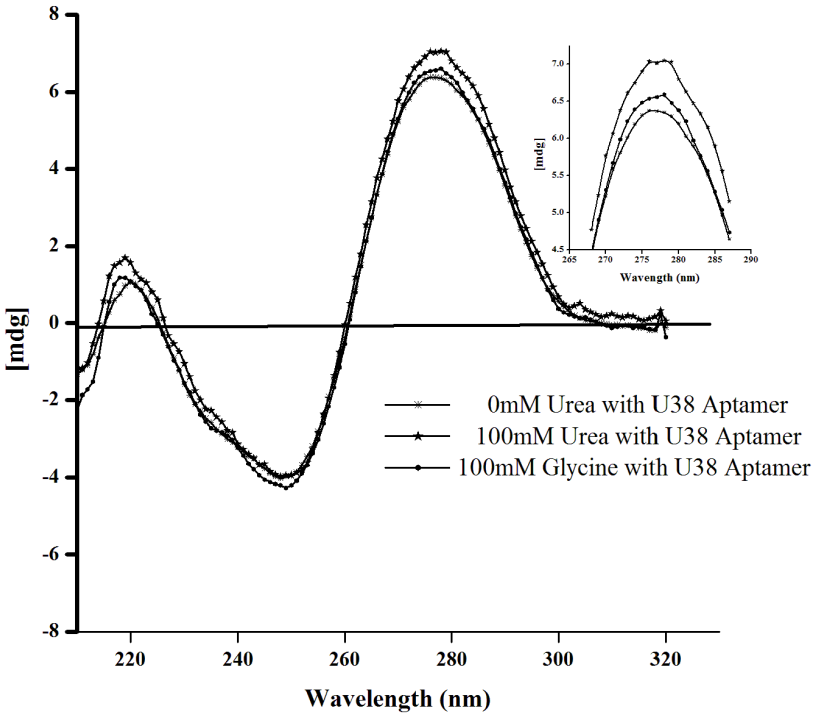

Fig 4.6.1 Circular dichroism spectra: 5µM U38 aptamer in absence (—✳—), in presence of 100mM urea (—★—) and in presence of 100mM glycine (—●—).

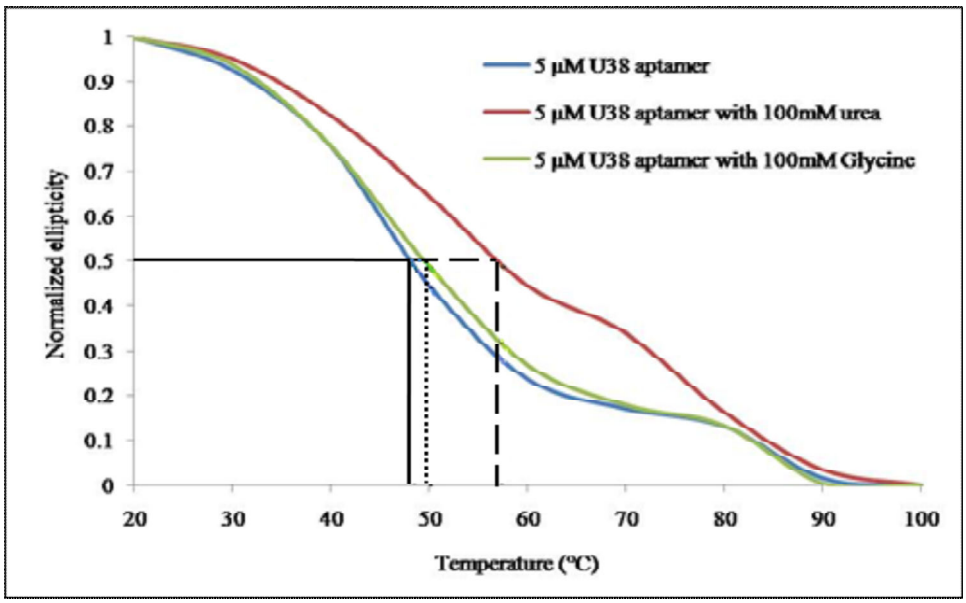

Fig 4.6.2 Melting curve analysis: Melting temperatures of free U38 aptamer (T_m = 48.5°C), U38 aptamer in presence of urea (T_m= 57°C) and U38 aptamer in presence of glycine (T_m= 49.7°C). Melting is monitored by Δε changes at 276 nm.

4.7. Synthesis and characterization of prepared gold nanoparticles (AuNPs)

Chemical reduction method was used for synthesis of citrate capped gold nanoparticles. $HAuCl_4$ was used as the precursor salt and citrate acted both as reducing and capping agent. Fig. 4.7 shows characterization of AuNPs by (A) UV-Vis absorbance spectrum, (B) Transmission Electron Microscopy, (C) Dynamic Light Scattering (DLS) and (D) Atomic Force Microscopy (AFM). UV-Vis scan of AuNPs revealed a characteristic absorbance peak at 520 nm which reflects surface plasmon resonance absorption band for wine red nanoparticles. TEM analysis showed that the AuNPs synthesised were of average size 13 ± 2.5 nm. DLS of gold nanoparticles was performed and average zeta potential was determined to be -39.6 ± 12.3, which reflected on the relative stability of the nanoparticles. AFM of the gold nanoparticles demonstrated the average size to be 18.73 nm. All of the above characterization techniques reveal that the gold nanoparticles are mono dispersed with high stability.

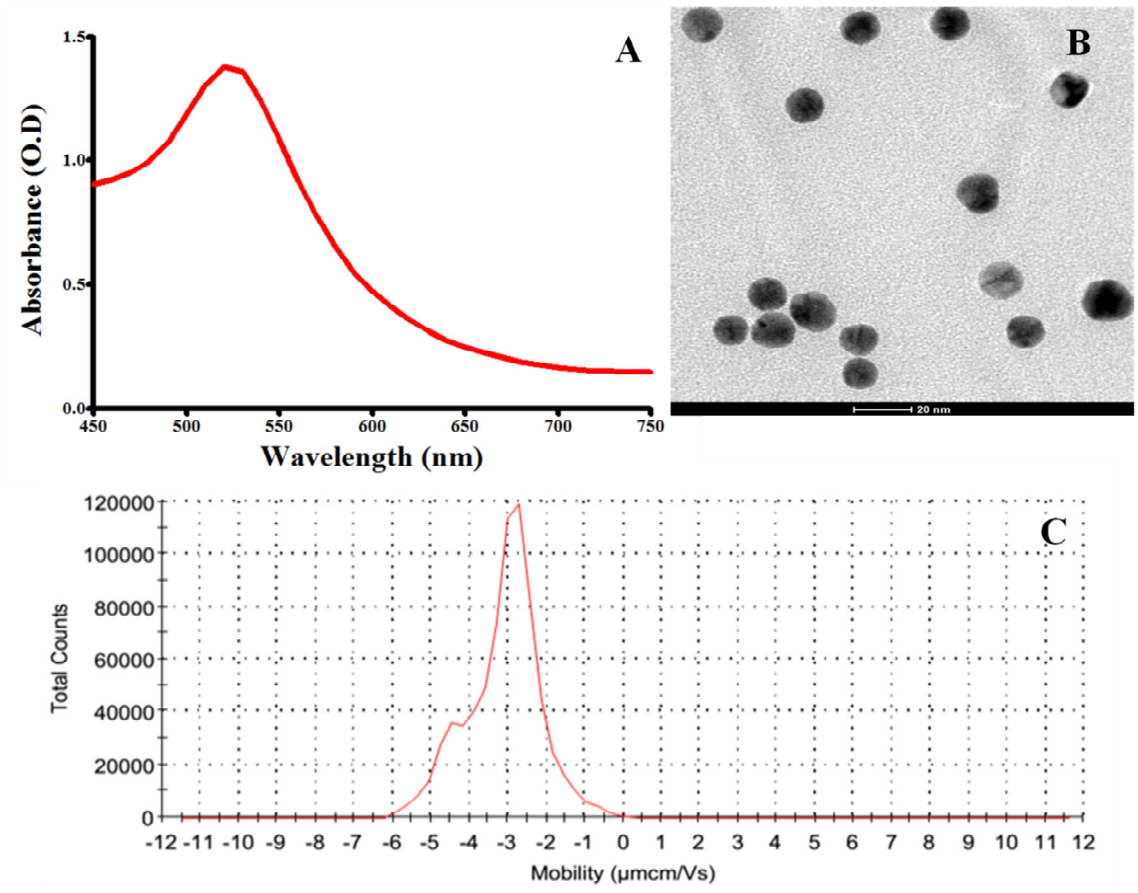

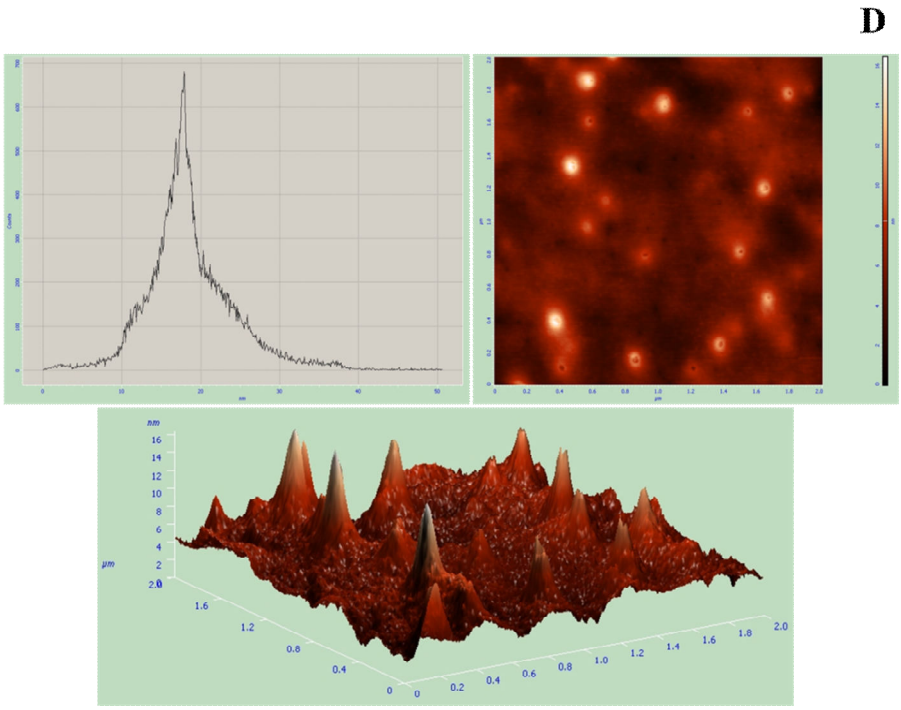

Fig 4.7 Characterization of citrate capped gold nanoparticles: (A) UV-Vis spectrum, (B) Transmission Electron Microscope and (C) Dynamic Light Scattering, (D) Atomic force microscopy.

4.8. Milk sample preparation

Milk is a complex biological secretion with approximately 10,000 different molecules in it. Owing to the heterogeneous nature of milk, various components can interfere with detection methods. It becomes necessary to get rid of these interfering species from the milk. To remove the interfering species, like protein in the milk sample, different reagents have been used for precipitation of milk. Tri-chloro acetic acid (TCA) alone or in combination with chloroform is known to be the method of choice for most of the protein precipitation steps used to prepare various analytical samples. Milk samples thus prepared by precipitation using TCA were not feasible for the aptamer-AuNPs assay, as this method suffers from the drawback of pH adjustment prior its use. To negate this additional step of neutralizing the precipitated sample, a simple and rapid method for precipitation was optimized for preparing milk samples. This method uses 99% methanol for cold precipitation of proteins. The supernatant of post precipitated milk was further used for detection purpose and showed no interference in aptamer-AuNPs based assay. The present method of milk sample preparation offers advantages of being simple and rapid over other complex and time consuming methods used by Song *et al.*, 2012 [387] and Liang *et al.*, 2011 [388] for detecting small molecules by AuNPs based optical detection method.

4.9. Detection of urea using aptamer-AuNPs visual based approach

The combination of gold nanoparticles with DNA offers opportunities to develop new biosensors based on optical (colorimetric and fluorescence), electrochemical, surface-enhanced Raman scattering (SERS), SPR and mass spectroscopy [41]. Recently optical based functionalised AuNPs-aptasensors, specifically colorimetric based sensors have been developed for detection of various different analytes [253, 256]. These aptasensors have myriad applications in fields ranging from environmental monitoring, bio-medical diagnosis and food industries.

Gold nanoparticles prepared by citrate reduction method showed characteristic chemical and physical properties, which were exploited for developing a visual based assay for detection of urea. The unmodified AuNPs remain as colloidal suspension due to the electrostatic repulsion of capping agent (*i: e* citrate) and the Van der Waals force of attraction between the AuNPs [50, 52, 168, 389], displays high extinction coefficient with characteristic surface plasmon resonance absorbance peak based on the distance dependent optical properties. The SPR peak of AuNPs is influenced by change in pH or high salt concentration, resulting in aggregation of nanoparticles due to the electrostatic screening effect. A red shift in the absorption peak (SPR) is observed when the interparticle distances in the aggregates are reduced to an average particle size resulting in electric dipole-dipole interaction and plasmon coupling of particles [390].

Further, it has been documented [391] that ssDNA is sufficiently flexible to form random coils exposing the nitrogen atoms of the base to interact strongly with the AuNPs, thereby enhancing the stability of the AuNPs against the salt induced aggregation. However, the lack of exposed bases in single stranded DNA (forming rigid tertiary structure) and double-stranded DNA prevents their adsorption on the AuNPs making them vulnerable to salt induced aggregation. Moreover, several studies have been reported on the use of aptamer based detection of analytes using unmodified nanoparticles as the signal transducer [51-61, 262, 392-396]. Inspired by the above observation, an aptamer-AuNPs based optical detection assay was developed. Based on the results of fluorescence binding assay (section 4.4), three different aptamer candidature sequences (U7, U34, and U38) exhibiting the best binding affinity was chosen for the developing an aptamer-AuNPs based optical assay for urea detection.

In a separate experiment, the aptamer candidates and a control random DNA sequence were incubated with AuNPs so as to cover the surface of AuNPs thus preventing them from the salt induced aggregation. Subsequently, the addition of processed urea spiked milk sample to

the DNA-AuNPs complex results in binding of the putative aptamer candidates to urea by virtue of ligand induced conformational changes. This binding event leaves the AuNPs vulnerable to high salt induced aggregation which is observed by a change in color from red to purple or blue, as shown in schematic representation of Fig. 4.9.1 whereas the no color change is observed in case of controls (milk sample without urea and random DNA sequence). Fig.4.9.2 shows the TEM images of corresponding normal AuNPs and salt induced aggregates of AuNPs on addition of urea spiked milk sample.

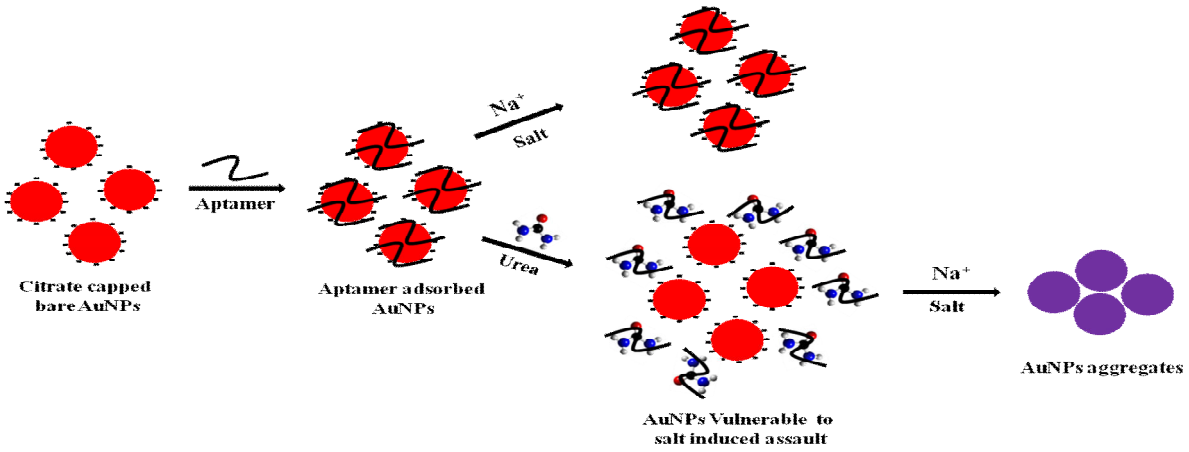

Fig 4.9.1 Schematic representation of Aptamer-AuNPs based visual detection assay for urea

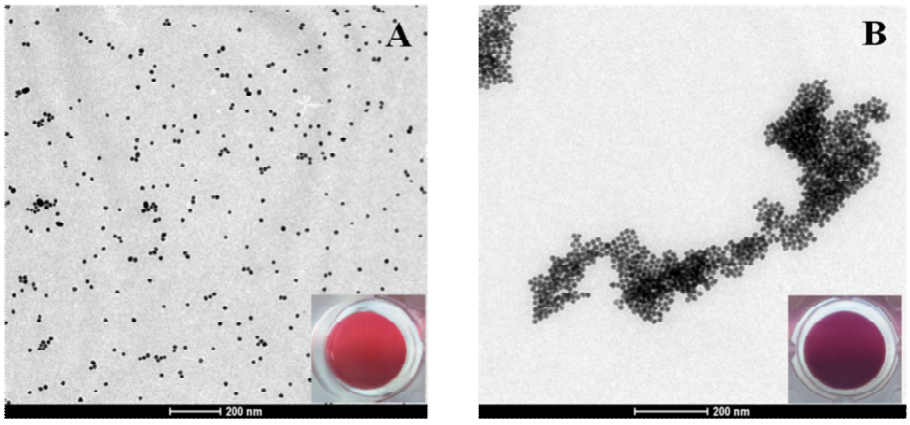

Fig 4.9.2 Color and TEM images of AuNPs (2.7 nM) with U38 aptamer (250 nM) supplemented by NaCl (250 mM) in (A) absence of urea (red wine color, no aggregation) and (B) in presence of 100 mM urea (purple color, aggregation).

Fig. 4.9.3A, demonstrates a color change in presence of urea (test) for selected aptamer candidates (U38, U34 and U7) with respect to their controls (in absence of urea). Whereas, the AuNPs adsorbed with control random sequence exhibited no such conformational changes on addition of the processed urea spiked milk sample, thus protecting the AuNPs against salt induced aggregation. Absorption spectra of all the samples show a dip in the intensity at 520 nm and an increase at 620 nm in samples with aptamer candidates, whereas no spectral changes with random DNA sequence was observed (Fig. 4.9.3B). The intensity of the color change was

measured by calculating the A_{620}/A_{520} nm absorbance ratio which correlates to the degree of AuNPs aggregates formed (Fig 4.9.3 box inset). Furthermore, this result indicates that the U38 aptamer displayed the maximum binding affinity for urea, which is in agreement with the result of fluorescence based binding assay (Fig. 4.4).

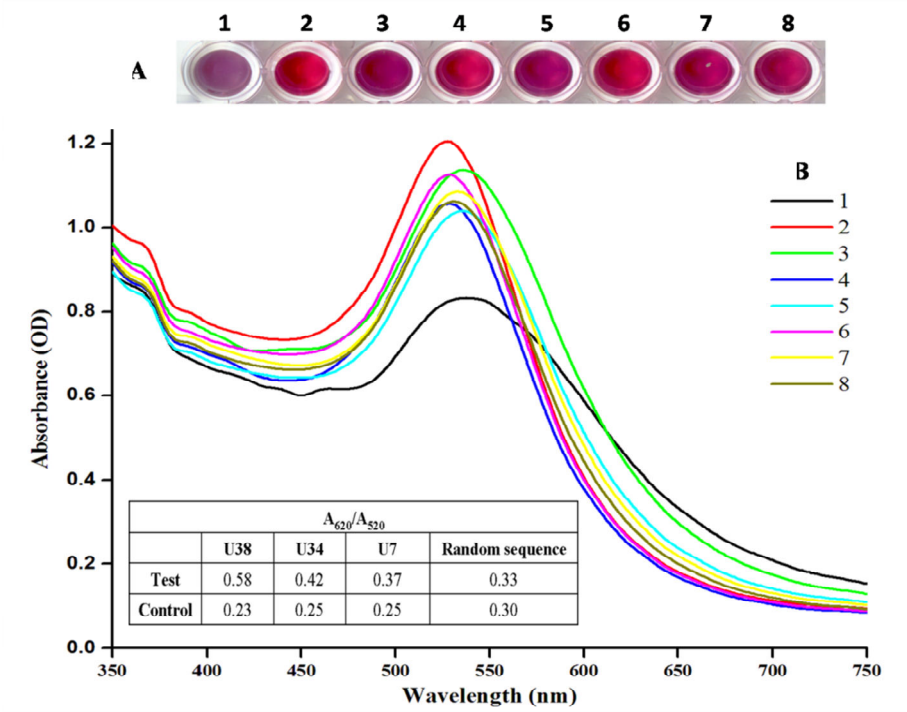

A_{620}/A_{520}

	U38	U34	U7	Random sequence
Test	0.58	0.42	0.37	0.33
Control	0.23	0.25	0.25	0.30

Fig 4.9.3 Development of Aptamer-AuNPs based detection assay: Screening of best aptamer candidate (A) color images of (1) U38-T, (2) U38-C, (3) U34-T, (4) U34-C, (5) U7-T, (6) U7-C, (7) random sequence-T, (8) random sequence-C. (B) UV-visible spectra (350-750 nm) of all the samples tested. (Tabular inset) A_{620}/A_{520} ratio gives a direct correlation of the color changes observed in presence of urea. Test (T) = AuNPs (2.7 nM) + aptamer candidate (250 nM) + processed urea spiked milk sample (50 µl) + NaCl (250 mM), control (C) = without urea. U38 shows best color and spectral changes.

4.10. Effect of truncation of U38 on aptamer-AuNPs aptasensor

In order to identify the functional motifs of the U38 aptamer sequence, truncation study was carried out and its effect on the performance of aptasensor was evaluated. The results in Fig.4.10.1 shows a red shift for different truncated variants of aptamer U38 in presence of urea. In Fig.4.10.2 the normalized absorbance A_{620}/A_{520} for U38, derived from Fig.4.10.1 is comapred with differenent truncated versions; FTU38, RTU38 and FRTU38. The result show that RTU38 oligo displayed 93% of color change, whereas the FRTU38 and FTU38 showed 77% and 73 % color change as compared to the U38; the full length aptamer. The data shows that the reverse primer truncation of U38 has the least effect on the performance of the aptamer-AuNPs biosensor. Whereas, FTU38-AuNPs biosesnor was least responsive in detecting urea when compared to the U38 aptamer-AuNPs biosesnor. The Mfold analysis of truncated and full length aptamer (Fig. 4.10.3) reveal that the hairpin domain of U38

(Fig.4.10.3) extending from 26–43 base (highlighted as yellow; region 1) along with a haipin domain extending from 11-23 base (highlighted as pink; region 2) are likely to be the the functional domains of the urea speicific aptamer. The deletion of the forward primer domain (FTU38 and FRTU38) seems to be the reason for the reduction in the performance of the visual asssay developed for detection of urea.

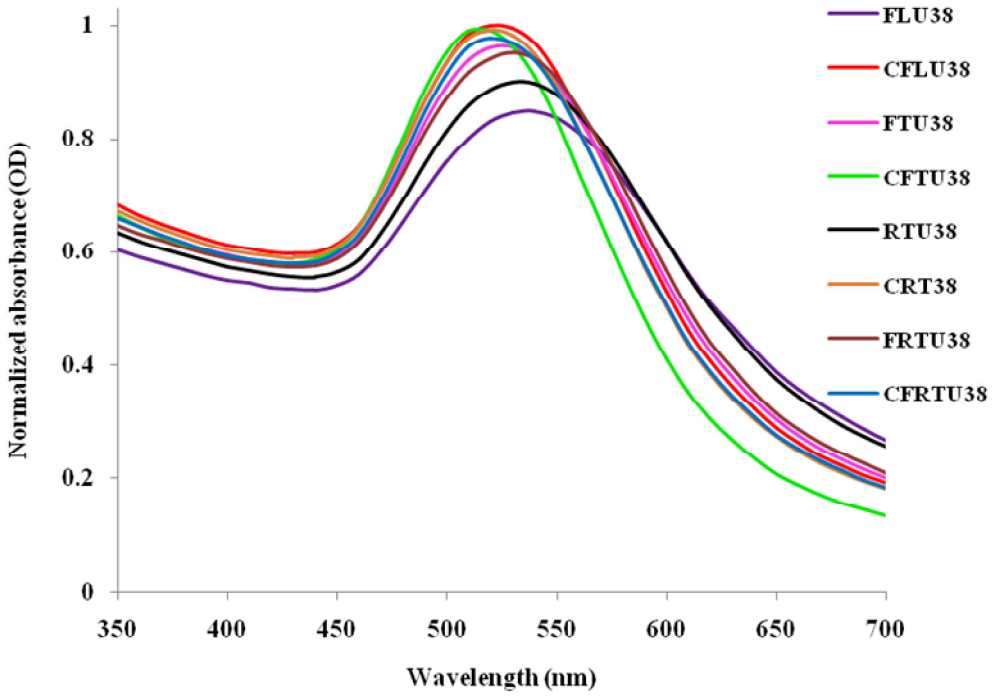

Fig 4.10.1 UV-Visible absorbance spectra of different truncated variants of U38 aptamer.

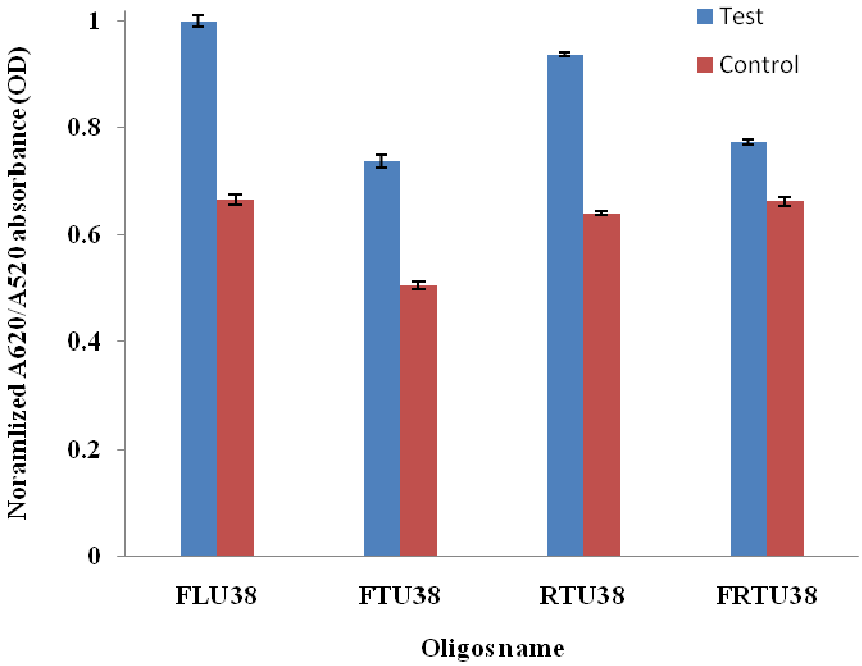

Fig 4.10.2 Change in the ratio of A_{620}/A_{520} a linear corelarion to colour change and the perfomance of the assay for truncated aptamer (FTU38, RTU38 and FRTU38) in comaprison to the full length U38 aptamer.

.

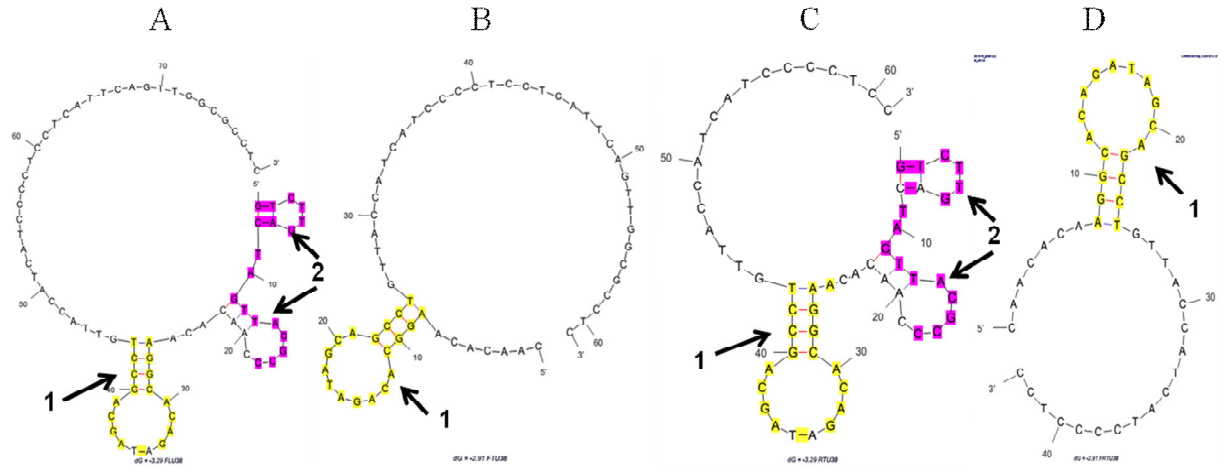

Fig 4.10.3 Secondary structure of truncated variants of U38 aptamer using Mfold software. (A) U38, (B) FTU38, (C) RTU38 and (D) FRTU38.

4.11. Specificty and interfernce studies of the urea aptasensor

Biosensors have been looked upon as the alternative to the conventional analytical detection methods as they offer rapid, specific detection of analytes without getting affected by the interfering molecules present in the sample matrices. We tested the specificity and the robustness of the urea aptasensor against the interfering molecules. The results in Fig.4.11.1, demonstrates the specificity of U38 aptamer-AuNPs assay for urea. The urea biosensor was tested in presence of structurally similar molecules like glycine (3), alanine (4), serine (5) and tyrosine (6) in same concentration and compared to the appropriate controls.

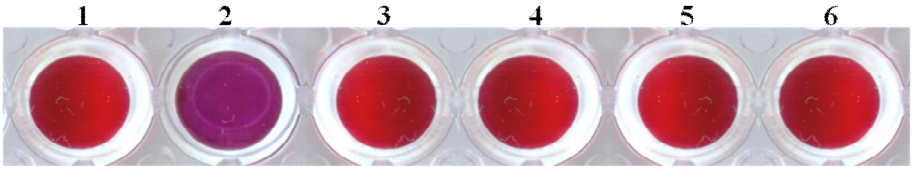

Fig 4.11.1 Specificity of the aptasensor in milk for urea and against structural analogs of urea: Color of AuNPs solution with 250 nM U38 aptamer (lane 1- processed normal milk sample, lane 2- processed 100 mM urea spiked milk sample, lane 3- processed 100 mM alanine spiked milk samples, lane4- processed 100 mM glycine spiked milk sample, lane 5- processed 100 mM serine spike milk sample, and lane 6- processed 100 mM tyrosine spiked milk samples) and NaCl (250 mM).

Additionally the developed method was investigated for other interfering agents present in synthetic milk such as sodium chloride (500 µM); glucose (600 µM); sodium bicarbonate (20 mM) and Tween-20 (1%; v/v) in the presence of urea were tested for visual color change. The result in Fig.4.11.2 show similar color change for sodium chloride (C), glucose (D), Sodium bicarbonate (E) and 1% v/v Tween 20 (F) in presence of urea, when compared to the 100 mM urea (B) positive control and negative control (A) sample.

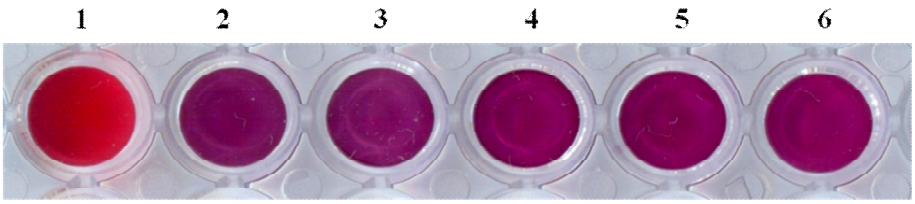

Fig 4.11.2 Colorimetric response of urea aptasensor in presence of different common interfering agents: Color of AuNPs solution with 250 nM U38 aptamer (lane 1- processed normal milk sample, lane 2- processed 100 mM urea spike milk sample, lane 3- processed 100 mM urea + 500 µM NaCl spiked milk sample, lane 4- processed 100 mM urea + 600 µM glucose spiked milk samples, lane5- processed 100 mM urea + 20 mM sodium bicarbonate spiked milk sample, lane 6- processed 100 mM urea + 1% Tween 20 spiked milk sample) and NaCl (250 mM)

4.12. Fluorescence recovery assay

The characteristic of AuNPs to adsorb ssDNA [52, 397] along with its high fluorescence quenching efficiency [384, 398-400] has been used to further confirm the specificity of the U38 aptamer. In this study, the FITC labeled U38 aptamer (FITC-U38) was incubated with the AuNPs and processed milk sample spiked with urea (as a test) and glycine (as a control) were added separately. After 10 min of incubation, fluorescence reading of each sample was taken with an Ex_{490nm} and Em_{525nm}. As shown in the Fig. 4.12 the fluorescence of FITC labeled U38 is quenched by 47.9 % as compared to FITC labeled aptamer alone. This result corroborates with the fact that the adsorbed FITC-U38 aptamer exhibits a Fluorescence Resonance Energy Transfer phenomena (FRET) whereby the emitted energy is transferred to AuNPs, thus resulting in decreased fluorescence signal. With the additions of the processed urea spiked milk samples a recovery of 85.8% of quenched fluorescence was observed (44). This result reveals that upon urea binding a conformational change in FITC-U38 aptamer leads to the displacement of the aptamer from the AuNPs surface as a consequence the distance between the fluorophore and the AuNPs is significantly increased, thereby enhancing the fluorescence signal of FITC-U38 aptamer.

The specificity of the aptamer was tested further by evaluating the fluorescence response in presence of structurally similar small molecule, glycine. Fig. 4.12 result shows that the fluorescence recovery in presence of glycine was insignificant 15.65% as compared to urea (85.8%). To further demonstrate the specificity of the aptamer, the milk sample spiked with urea was incubated for 10 min with urease enzyme. Subsequently, urease treated urea spiked milk sample was added to FITC-U38-AuNPs complex and the fluorescence reading was recorded after 10 min of incubation. The Fig. 4.12 shows a fluorescence recovery of only 47.1% which shows that the fluorescence signal directly accounts to the amount of urea present in the sample after urease treatment. The fluorescence recovery assay along with the U38

aptamer-AuNPs visual detection and CD spectra results further proves the property of U38 aptamers to detect urea specifically.

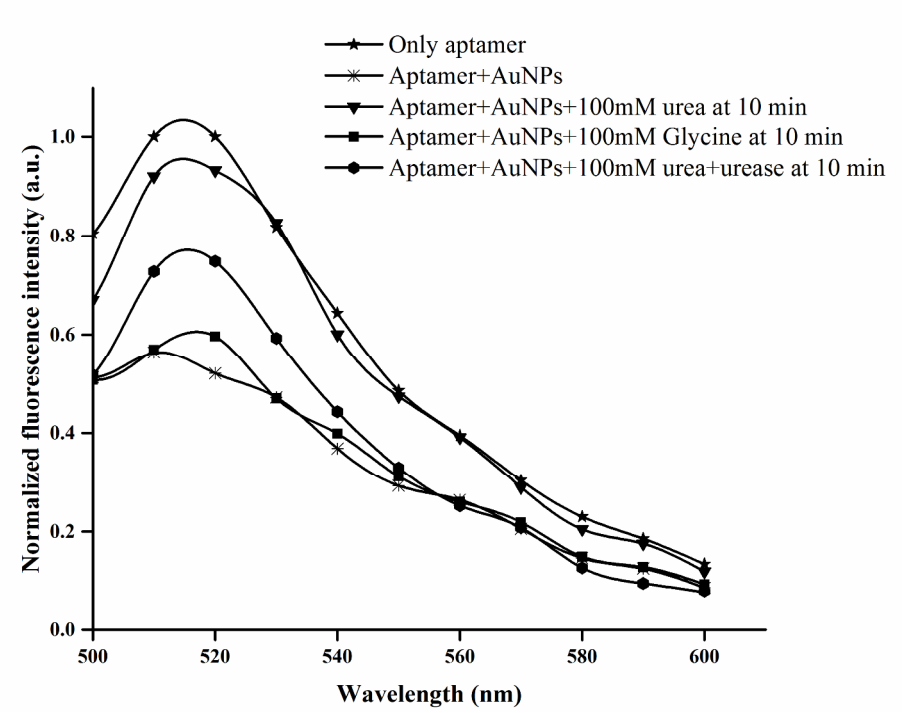

Fig 4.12 Fluorescence recovery assay based on the fluorescence quenching of FITC-labeled aptamer in vicinity of GNPs. Fluorescence emission spectra of FITC-labeled U38 aptamer alone (—★—), FITC-labeled U38 aptamer with GNPs (—✳—), FITC-labeled U38 aptamer with GNPs and 100 mM urea (—▼—), FITC-labeled U38 aptamer with GNPs and 100mM glycine as a control (—■—) and FITC-labeled U38 aptamer with GNPs and 100mM urea incubated with 100 unit of Jack bean urease (—●—).

4.13. Limit of detection by absorbance and fluorescence spectroscopy

As aforementioned, a highly specific aptamer-AuNPs based method for urea detection was developed in this study. To further test the detection limit of this method urea specific aptamer (250 nM) was incubated with 2.75 nM AuNPs and subsequently samples of varying concentration of urea ranging from 0-250 mM were added to the aptamer-AuNPs complex. With the change in the ionic strength of the solution, the aggregation of AuNPs was observed which corresponds to the color change accompanied by the change in the absorbance spectra and fluorescence spectra of the AuNPs. As shown in the Fig. 4.13.1, 20 mM urea sample was unable to induce any visual color change as compared to the control sample without any urea. Further, visible color change was observed with the sample containing a range between 50-250 mM of urea.

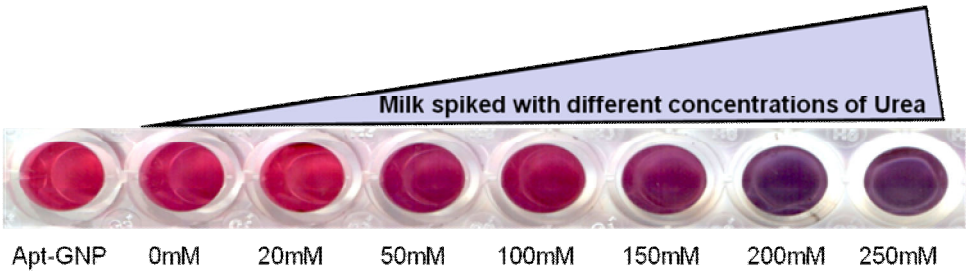

Fig 4.13.1 Limit of detection of urea on visual basis: Color change (red to violet) observed by naked eye in presence of increasing concentration of urea.

The UV-visible spectra of the samples exhibited significant changes in the absorbance values with increasing concentration of urea in the sample. As the concentration of the urea in the sample increases, the intensity of peak at 520 nm decreases slightly and a new peak appears with an increased intensity. A negligible change in the UV-visible spectrum was seen as the urea concentration in the sample reached 250 mM indicating the saturation limit of the method. A quantitative detection limit was achieved by establishing the relationship between the absorbance ratio A_{620}/A_{520} and urea concentration. As shown in the inset of Fig. 4.13.2 a linear correlation was observed between absorbance ratio A_{620}/A_{520} and urea concentration ranging from 20-150 mM (R^2 value of 0.995). From these observations, it can be inferred that the lower limit of detection for the developed aptamer–AuNPs method is 50 mM.

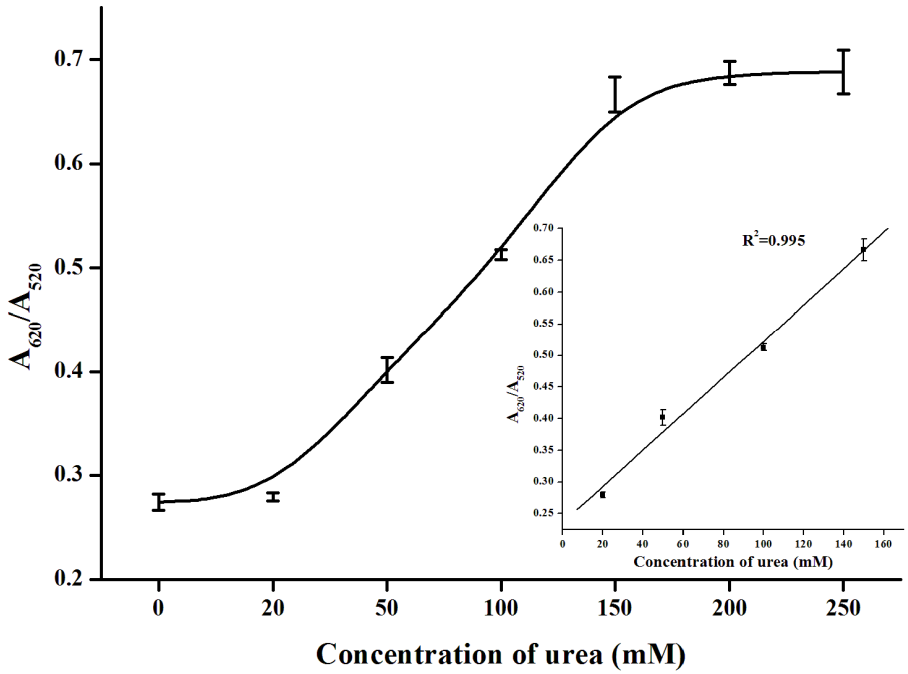

Fig 4.13.2 Limit of detection by spectral changes in absorbance ratio of A_{620}/A_{520}: Plot of urea concentration versus absorbance ratio (620/520) for quantification of urea in milk. The inset figure shows, a linearly fitted absorption spectra of the AuNPs solution containing the U38 aptamer versus the concentration of urea (0-250mM).

By using similar experimental conditions as above, the effect of increasing urea concentration on the intrinsic fluorescence of AuNPs was studied. The emission spectra of the AuNPs were recorded in the range 600-780 nm by excitation at 340 nm (Fig. 4.13.3). The fluorescence intensity at λ_{max}=700 nm was plotted as a function of urea concentration (20-150 mM) which illustrated a linear correlation (with regression value of 0.991).

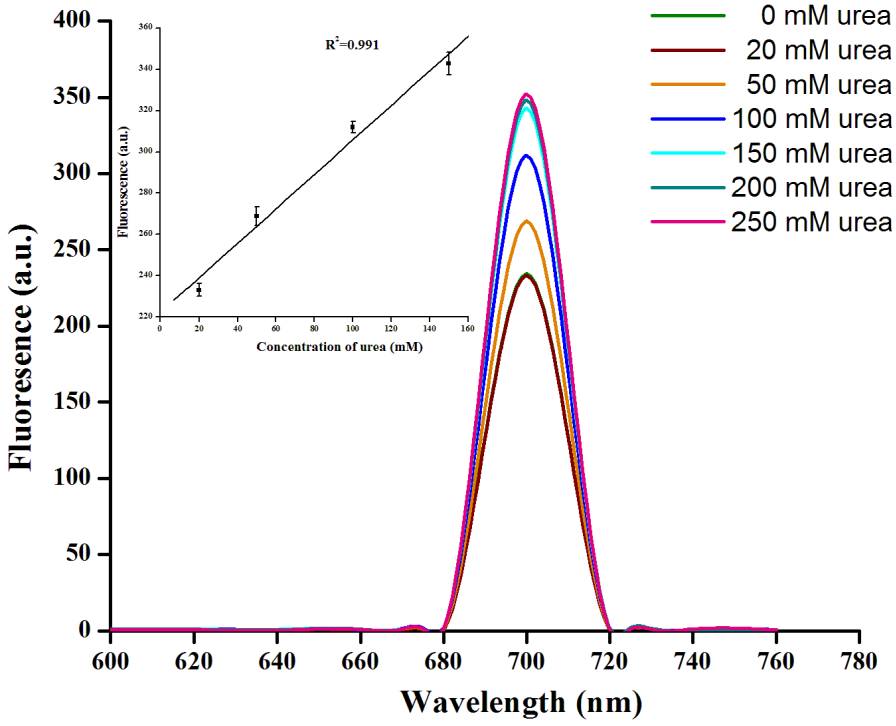

Fig 4.13.3 Limit of detection by fluorescence measurement: Fluorescence spectra of aptasensor in presence of unlabeled U38 aptamer and different concentration of urea (0-250mM). The inset indicates dose dependent changes in fluorescence intensity of the AuNPs solution over different concentration of urea

4.14. Conclusion

In this study, a urea specific aptamer was selected using Flu-Mag SELEX. Flu-Mag SELEX offers to be an excellent matrix for selection of ssDNA by allowing convenient and efficient separation of nonspecific ssDNA molecules. The fluorescence binding assay study demonstrated highest binding affinity for U38 aptamer with dissociation constant of 238 nM. Interaction study by circular dichroism (CD) clearly showed significant structural changes accompanied by U38 in presence of urea as compared to controls (glycine or U38 aptamer alone). Also, the interaction study complements with the increase in the melting temperature by ~9 °C for U38-urea complex. Based on the observation of ligand induced structural changes by CD, the U38 aptamer was taken further for the development of an aptamer-AuNPs based visual detection assay for urea in milk. A simple, rapid and user friendly method for milk sample

preparation by methanol precipitation was standardized. Regions of the aptamer interacting with the urea molecule were determined by carrying out the truncation studies, which highlighted the role of a hair-pin motif present in the forward primer to be responsible for the optimum performance of U38-aptamer-AuNPs colorimetric assay.

The aptamer-AuNPs biosensor thus developed was specific for urea as compared to other structural analogs such as alanine, glycine, serine and tyrosine. Further, the robustness of the developed assay for different interfering substance present in synthetic milk was evaluated and it was found to be unaffected in presence of salt (500 µM), sodium bicarbonate (20 mM), glucose (600 µM) and detergent (1%). A recovery of 85.8 % fluorescence of FAM-labeled U38 aptamer in presence of urea as compared to the 15.65 % recovery for glycine, further affirmed the specificity of the assay. Urease treated milk sample showed a decreased fluorescence recovery of 47.1 % suggesting the recovery of fluorescence to be urea dependent. The lower detection limit of the assay was established to be 50 mM and the saturation limit was set to be 200 mM. While the method offers advantages of being rapid, simple and specific for detecting high concentration of urea in milk, it can be further improved for increasing the sensitivity

Since detection of urea is also important in some pathological conditions (diabetes, nephritis, renal dysfunctions and urinary tract obstructions), it becomes imperative to think that this urea biosensor can also be adapted for pathological samples. Apart from this a third generation urea biosensors can be developed, by functionalizing aptamers onto the carbon nanotubes for a point of care devices from clinical point of view.

CHAPTER 5

DEVELOPMENT OF DNA APTAMER FOR HEMORRHAGIC COLI PILIN (HcpA) OF *Escherichia coli* O157:H7

5.1. Bioinformatics analysis of Hemorrhagic Coli Pilus (HCP) of *E. coli* O157:H7

The bioinformatics study for HcpA of *E. coli* O157:H7 (Gene ID: 8214675, Protein reference number- YP_003076080.1) was performed with non-redundant protein sequences of the rest of bacterial species by protein-Basic Local Alignment Search Tool (pBLAST) of National Centre for Biotechnology Information (NCBI). The BLAST results in Fig.5.1.1 show the conserved nature of HcpA in the Enterobacteriaceae family. Most of the hit sequences belong to the pathogenic strains of the Enterobacteriaceae family, which highlights the importance of this pilin protein in pathogenicity. Further, *in-vitro* data with cell lines has shown that the HcpA is expressed only in pathogenic strains as it is the first contact point of the pathogen with the host cell receptor [271]. Hemorrhagic coli pilus (HCP) of *E. coli* O157:H7 is composed of pilin subunit called HcpA which has been well characterized for its potential role in pathogenesis and therefore was chosen as the target for aptamer generation.

Select: All None Selected:0

Alignments Download GenPept Graphics Distance tree of results Multiple alignment

Description	Max score	Total score	Query cover	E value	Ident	Accession
MULTISPECIES: major pilin subunit [Escherichia coli O157:H7 str. EDL933]	303	303	100%	4e-103	100%	WP_000360900.1
major pilin subunit [Shigella flexneri 2a str. 301]	302	302	100%	1e-102	99%	WP_000360918.1
Prelipin peptidase dependent protein [Escherichia coli D6-113.11]	301	301	100%	2e-102	99%	CDP65000.1
MULTISPECIES: major pilin subunit [Escherichia coli str. K-12 substr. MG1655]	301	301	100%	2e-102	99%	WP_000360904.1
major pilin subunit [Escherichia coli]	301	301	100%	2e-102	99%	WP_001041684.1
major pilin subunit [Escherichia coli]	301	301	100%	2e-102	99%	WP_000360908.1
major pilin subunit [Shigella flexneri]	301	301	100%	2e-102	99%	WP_025757453.1
MULTISPECIES: major pilin subunit [Escherichia]	301	301	100%	3e-102	99%	WP_000360899.1
major pilin subunit [Escherichia coli]	300	300	100%	5e-102	99%	WP_029392818.1
major pilin subunit [Escherichia coli]	300	300	100%	6e-102	99%	WP_000360905.1
prepilin-type N-terminal cleavage/methylation domain protein [Escherichia coli 1-182-04_S3_C3]	300	300	100%	6e-102	99%	EZJ80300.1
prepilin-type N-terminal cleavage/methylation domain protein [Shigella flexneri 1235-66]	300	300	100%	6e-102	99%	EIQ77792.1
major pilin subunit [Escherichia coli P12b]	300	300	100%	7e-102	99%	WP_000360901.1
major pilin subunit [Escherichia coli 042]	300	300	100%	8e-102	99%	WP_000360907.1
major pilin subunit [Escherichia coli]	300	300	100%	8e-102	99%	WP_000360906.1
major pilin subunit [Shigella boydii]	300	300	100%	8e-102	99%	WP_000360909.1
major pilin subunit [Escherichia coli E24377A]	300	300	100%	8e-102	99%	WP_000360902.1
MULTISPECIES: major pilin subunit [Escherichia coli UTI89]	300	300	100%	9e-102	99%	WP_000360914.1
major pilin subunit [Escherichia coli]	300	300	100%	9e-102	99%	WP_020233150.1
prepilin-type N-terminal cleavage/methylation domain protein [Escherichia coli]	300	300	100%	9e-102	99%	WP_001727303.1
major pilin subunit [Escherichia coli SE11]	299	299	100%	1e-101	99%	WP_000360895.1

Fig 5.1 Bioinformatics analysis of HcpA pilin protein of *E. coli* O157:H7 using pBLAST.

5.2. Amplification and cloning of *hcpA* locus from *E. coli* O157:H7 genomic DNA

The Fig.5.2.1 shows a schematic representation of cloning of hcpA gene in pET28 (a) vector. For cloning, the *hcpA* locus encoding for the HCP protein was amplified using Pfu DNA polymerase (Fermentas, USA) from *E. coli* O157:H7 genomic DNA. The amplified and double digested PCR product of hcpA gene was cloned in pET28(a) an expression and cloning vector, double digested with similar enzymes as the PCR product. The ligated vector was transformed in and *E. coli* DH5α and the clones thus obtained were screened for the presence of *hcpA* insert. Fig.5.2.2 shows the conformation of the clone with the *hcpA* insert of 452bp run along with 100bp ladder.

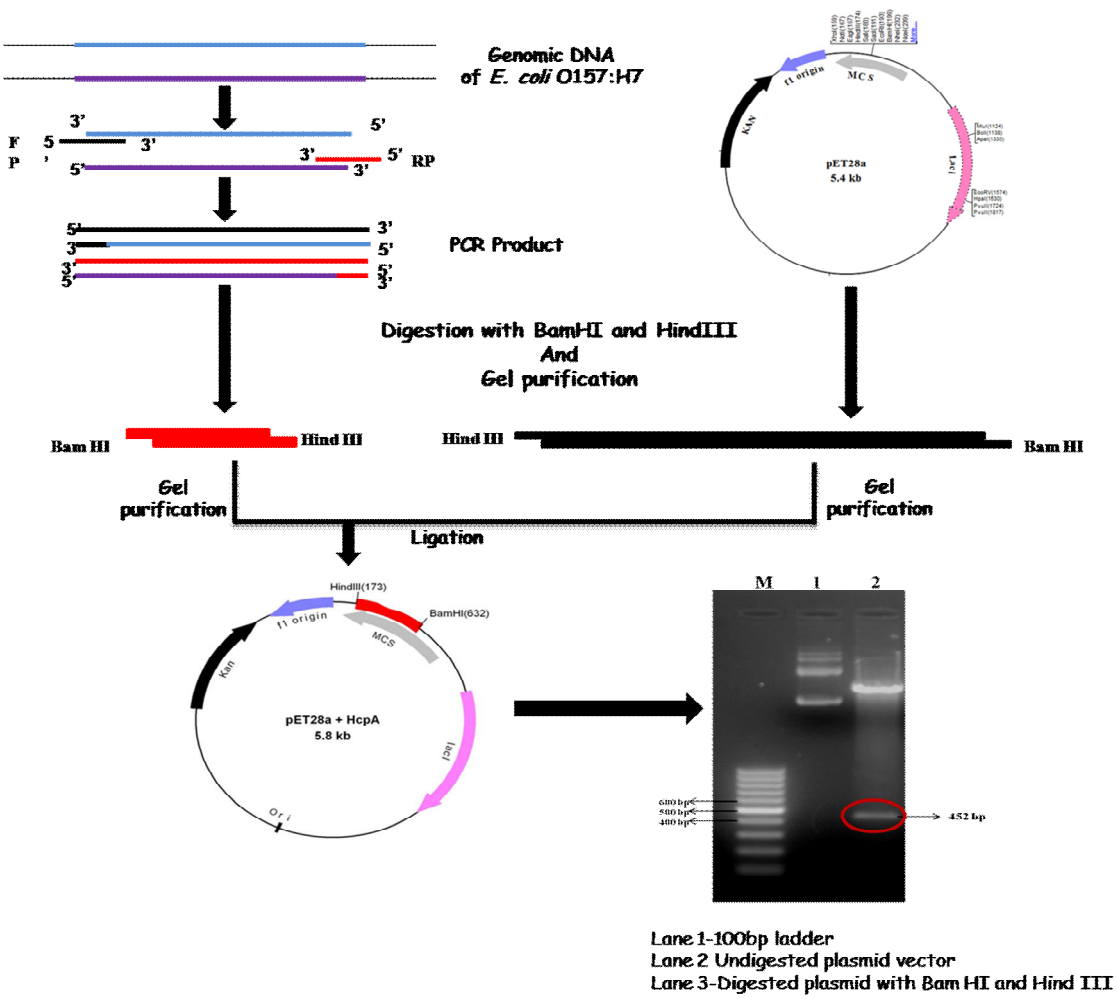

Fig 5.2.1 Strategy for cloning *hcpA* in pET28 (a): Amplification of hcpA from *E. coli* O157:H7, digestion of *hcpA* PCR product and pET28(a) with BamHI and HindIII restriction enzyme and ligation of both the digested products were performed to yield a recombinant hcpA-pET28(a) vector.

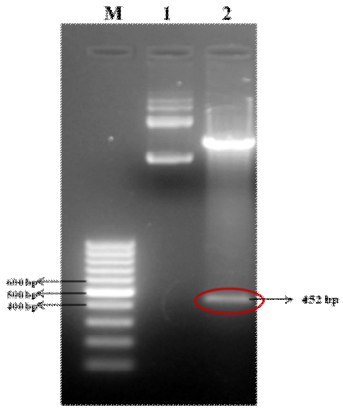

Fig 5.2.2 1% agarose gel for restriction digestion analysis of *hcpA* transformants: M- 100bp marker, 1- undigested vector of a clone, 2- digested vector with BamHI and HindIII restriction enzyme, with a fragment of ~ 452bp of hcpA gene.

5.3. Expression, purification and quantification of His-HcpA

The hcpA gene of *E. coli* O157:H7 encodes for a 19 kDa HcpA pilin monomer protein [271]. The cloning strategy adapted in this study was based on the previous report [273], and thus the HcpA monomers translated from the *hcpA*-pET28(a) recombinant vector contains additional amino acids including a 6 residues of histidine amino acid at the N-terminal. This leads to an increase in the molecular weight to 22kDa of the HcpA monomer [79, 273]. To further investigate the expression of His-HcpA, the *hcpA*-pET28(a) recombinant vector was transformed in *E. coli* BL21 (DE3). The samples for both induced and uninduced cultures were prepared by boil prep method as mentioned in the section 3.2.16. Fig. 5.3.1 represents an initial verification of protein expression on 15% SDS-PAGE for the induced and uninduced bacterial samples. The lane 2 distinctly shows a band of approximately 22 kDa molecular weight compared to the protein standard marker in lane M. The uniduced sample (lane 1) shows no band corresponding to the induced lane.

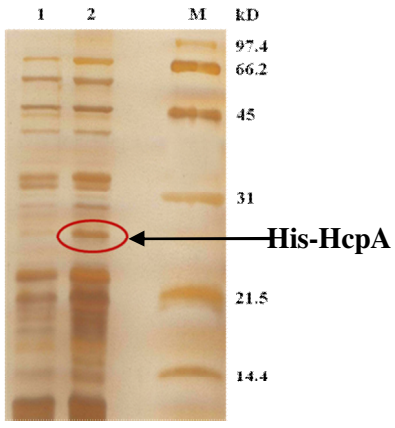

Fig 5.3.1 Overexpression study of His-HcpA in *E. coli* BL21 (DE3): Lane1-uninduced, Lane2- induced, Lane M- protein standard marker.

After verifying the expression of the His-HcpA protein, two litres of culture of *hcpA*-pET28(a) harbouring *E. coli* BL21 (DE3) was induced under optimum conditions. The induced cells were lysed and processed as per the instruction in the section 3.2.17 to release the overexpressed protein. Purification of the His-HcpA was carried out by Ni-NTA column under optimum conditions of binding, washing and elution steps. After the purification step, different aliquots of eluted product (Fig.5.3.2) were analysed for presence of His-HcpA by running 15% SDS-PAGE. The eluted fractions of 2-6 were pooled and passed through a 3 kDa cut off filter device to remove excess of imidazole and to concentrate the protein. After the buffer exchange, the concentrated protein was again passed through a 30 kDa cut off filter to eliminate the high molecular weight protein impurities. Fig 5.3.3 demonstrates the purity of the HCP protein attained after removal of other protein impurities.

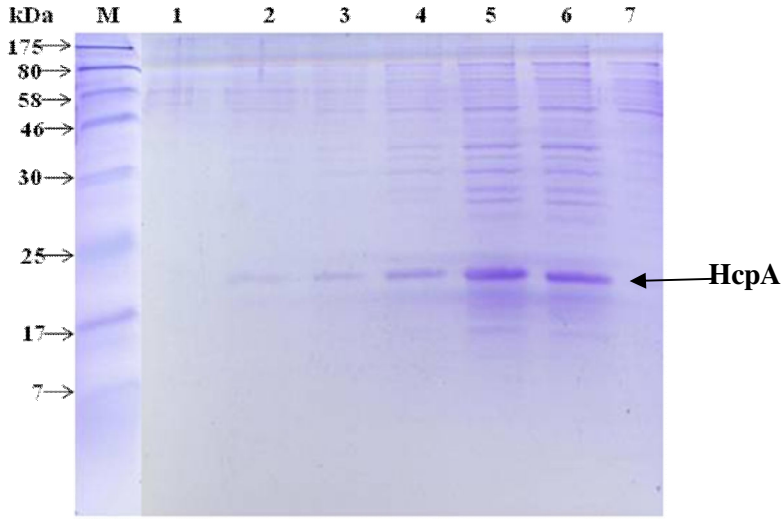

Fig 5.3.2 Ni-NTA purification of His-HcpA: Lane M- standard protein marker, fractions eluted with 250 mM imidazole in lane1- 9th , lane3- 7th, lane5- 5th, lane6- 2nd, and lane7- 1st eluted fraction with 150 mM imidazole.

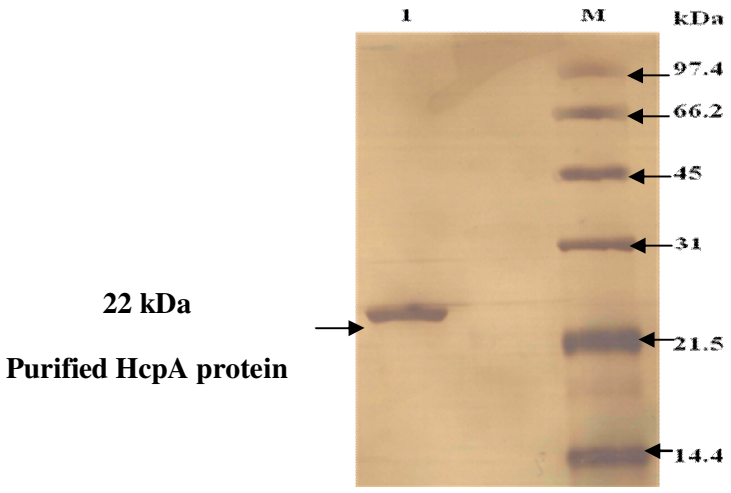

Fig 5.3.3 15% SDS-PAGE of purified 22 kDa His-HcpA (lane 1) alongside a standard protein marker (M).

The protein concentration for the purified His-HcpA was determined by using Micro BCA™ Protein Assay Kit (Thermo Scientific, Pierce, USA), as per manufacturers instruction and was found to be 30 mg/ml.

5.4. SELEX process for HcpA aptamer selection and preliminary binding study by electrophoretic mobility shift assay (EMSA)

Selection process starts with binding of ssDNA library to the target, with subsequent portioning of the nonspecific DNA sequence and finally eluting the specific DNA and performing PCR for enrichment of target specific DNA sequences. Following these principle steps which are well illustrated in Fig.5.4.1, an affinity chromatography based selection strategy was carried out as presented in the table 3.4. Aptamer selection for HcpA was performed using His-HcpA immobilized Ni-NTA beads. For development of HcpA specific aptamer in presence of the background of the non-target affinity matrix, a negative selection step against the Ni-NTA beads was introduced after initial three rounds of selection. This step eliminated the non-specific DNA binding to the Ni-NTA affinity matrix used for protein immobilization. In addition, the stringency of the process was increased with every single round of selection by decreasing the target protein concentration for selection, reducing the incubation time for binding in the positive selection steps, consequently increasing the binding reaction time for the negative selection steps, increase in the washing steps and increase in the concentration of the blocking agents (yeast t-RNA and bovine serum albumin).

After 10^{th} round of selection, binding study for the pool of DNA of selected 8^{th} and 10^{th} round was carried out by performing EMSA in comparison with RDL as the control pool of DNA. The result in Fig.5.4 clearly demonstrates a shift in the mobility of 10^{th} round pool of DNA in presence of HcpA (lane 6), suggesting the interaction/binding of DNA with HcpA to form DNA-HcpA complex of higher molecular weight thus retarding the mobility of free DNA pool (lane 5). Whereas the pool of DNA developed from 8^{th} round of selection (lane 4) and from the RDL (lane 2) showed no shift in the mobility of DNA in presence of HcpA from their respective control of free DNA (lane 3 and 1).

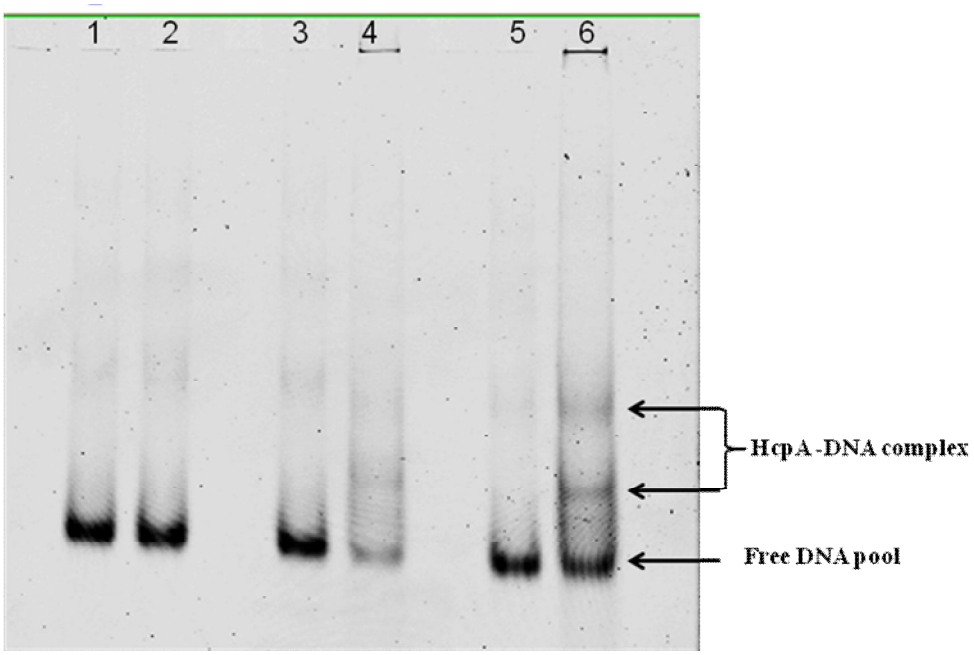

Fig 5.4 Electrophoretic mobility shift assay for HcpA in 8% native PAGE: Lane 1,3,5- only DNA, lane 2,4,6- DNA with HcpA, lane 1,2- RDL, lane 3,4- 8th round pool of DNA, lane 5,6- 10th round pool of DNA.

5.5. Cloning of DNA pool from selected round and alignment of cloned sequences using BioEdit software and Mfold derived structure of different putative aptamer sequences

The selected pool of DNA sequences from the 10th round of selection was PCR amplified and cloned into T/A cloning vector as mentioned in section 3.2.4. Seventy white colonies were picked from the IPTG-XGal plates based on blue white selection screening and were sent for sequencing. The sequences thus obtained were categorized in to 14 different categories using BioEdit software based on sequence similarity as shown in Fig. 5.5.1

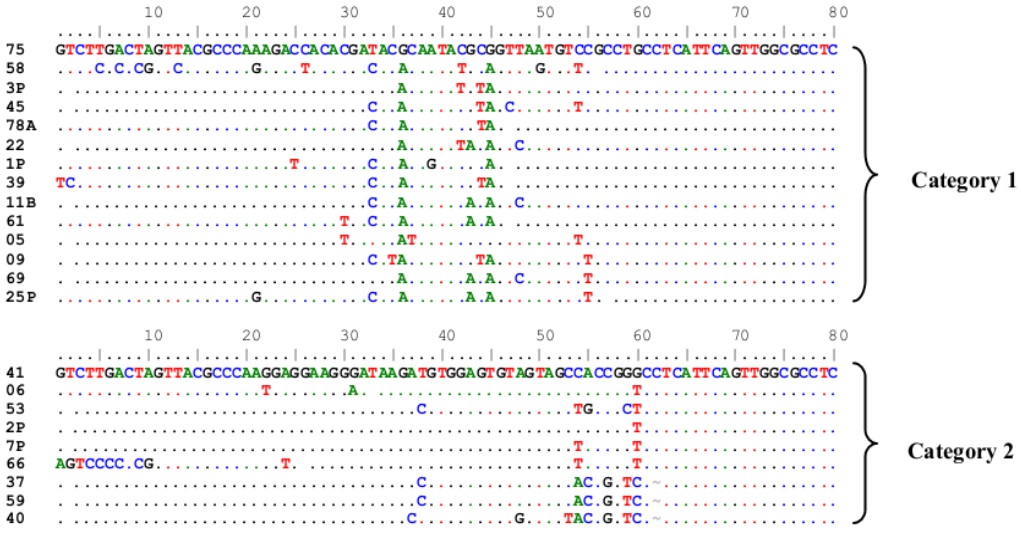

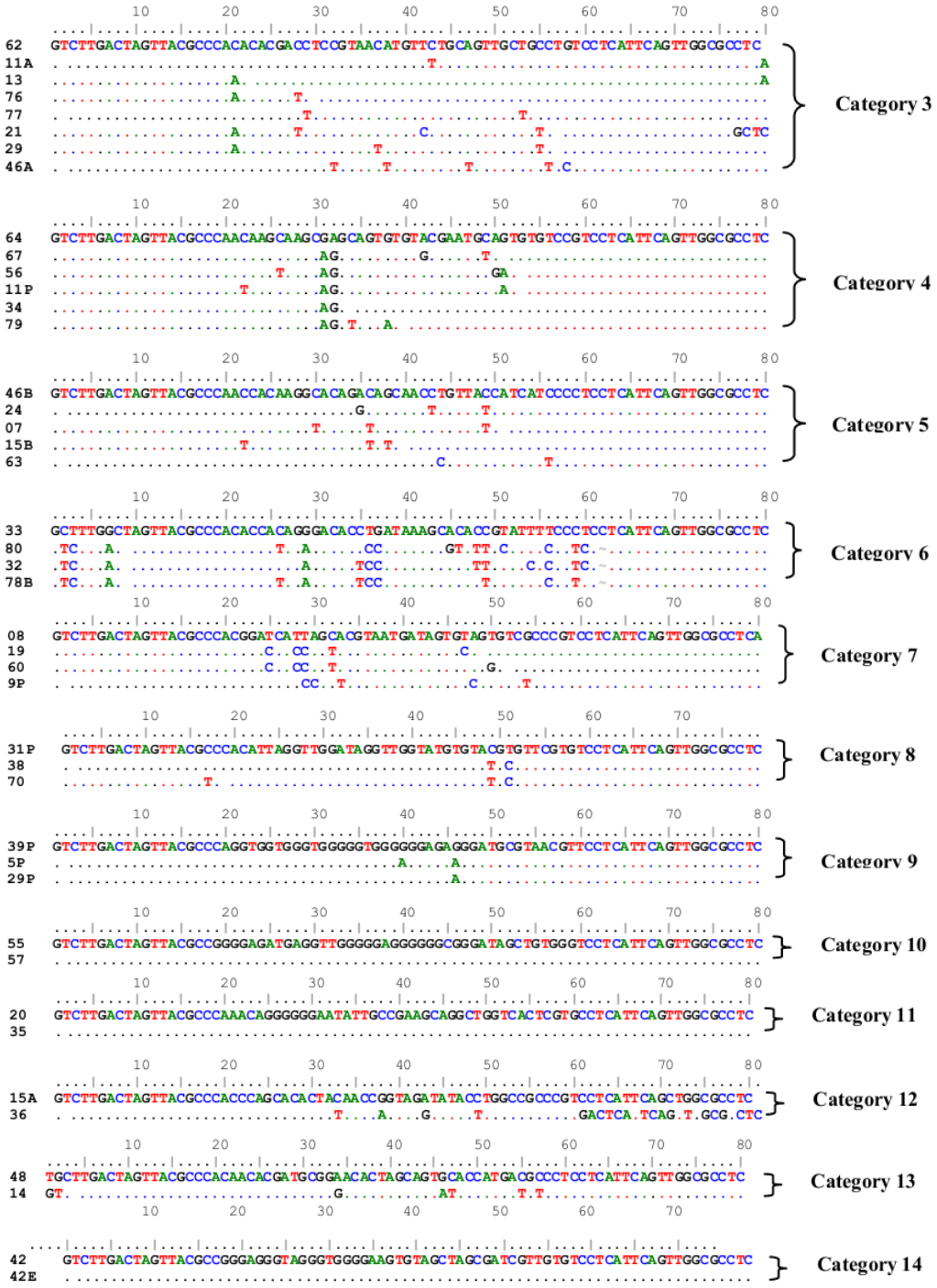

Fig 5.5.1 Sequence alignment sequences by BioEdit software: Cloned sequences of 10th round of urea selection were cloned and categorized based on sequence similarities obtained from BioEdit software.

Different aptamer candidates from top eight categories were analyzed by Mfold software for predicting the secondary structural folding (Fig. 5.5.2). Sequences were allowed to analyze for their possible folding using predefined salt conditions used in the selection procedures, while other parameters were set at default.

HcpA-62

GTCTTGACTAGTTACGCCCACACACGACCTCCGTAACATGTTCTGCAGTTGCTGCCTGTCCT
CATTCAGTTGGCGCCTC

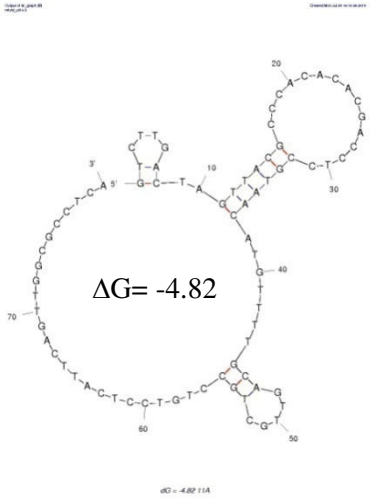

HcpA-75

GTCTTGACTAGTTACGCCCAAAGACCACACGATACGCAATACGCGGTTAATGTCCGCCTGC
CTCATTCAGTTGGCGCCTC

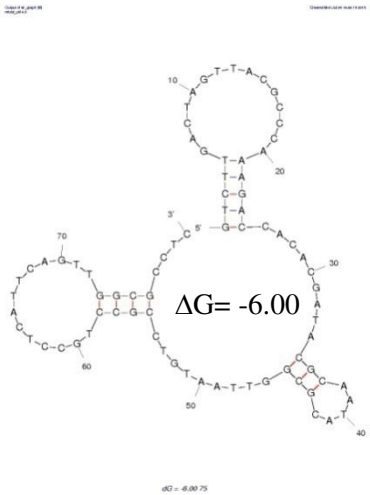

HcpA-41

GTCTTGACTAGTTACGCCCAAGGAGGAAGGGATAAGATGTGGAGTGTAGTAGCCACCGGG
CCTCATTCAGTTGGCGCCTC

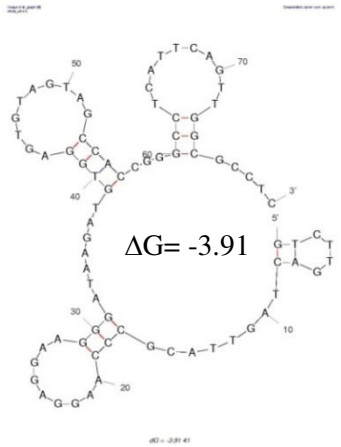

HcpA-64

GTCTTGACTAGTTACGCCCAACAAGCAAGCGAGCAGTGTGTACGAATGCAGTGTGTCCGTC
CTCATTCAGTTGGCGCCTC

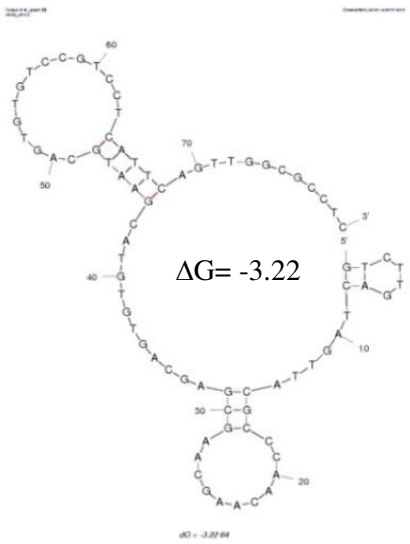

HcpA-24

GTCTTGACTAGTTACGCCCAACCACAAGGCACAGGCAGCAACTTGTTATCATCATCCCCTC
CTCATTCAGTTGGCGCCTC

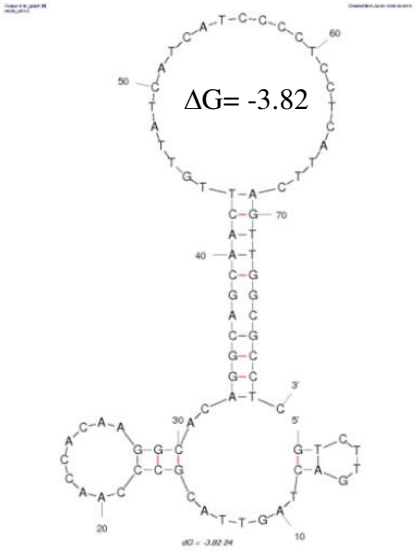

HcpA-33

GCTTTGGCTAGTTACGCCCACACCACAGGGACACCTGATAAAGCACACCGTATTTTCCCTC
CTCATTCAGTTGGCGCCTC

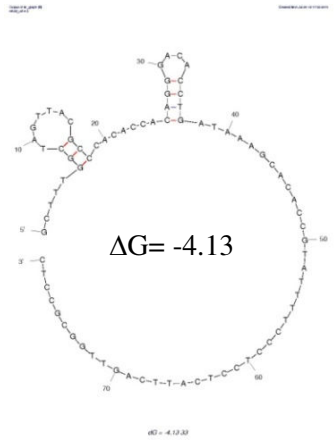

HcpA-8

GTCTTGACTAGTTACGCCCACGGATCATTAGCACGTAATGATAGTGTAGTGTCGCCCGTCC
TCATTCAGTTGGCGCCTCA

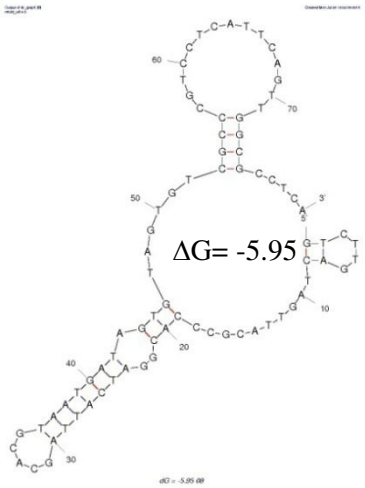

HcpA-38

GTCTTGACTAGTTACGCCCACATTAGGTTGGATAGGTTGGTATGTGTATGCGTTCGTGTCCT
CATTCAGTTGGCGCCTC

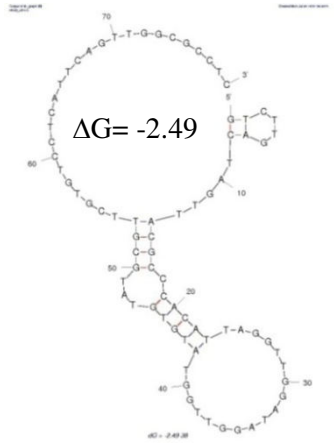

Fig 5.5.2 Secondary structure folding of aptamer candidature sequences (HcpA-62, 75, 41, 33, 24, 64, 8 and 38) along with the respective free energy (ΔG) in kcal/mol.

5.6. Binding confirmation of putative aptamer with HcpA using electrophoretic mobility gel shift assay (EMSA)

The putative aptamers from each category were synthesized with FITC tag at 5' end and studied for their HcpA binding potential. The result in the Fig 5.6 shows the confirmation of binding of putative aptamers HcpA-38, 41, 64 and 75 with HcpA protein target, on 8% native PAGE.

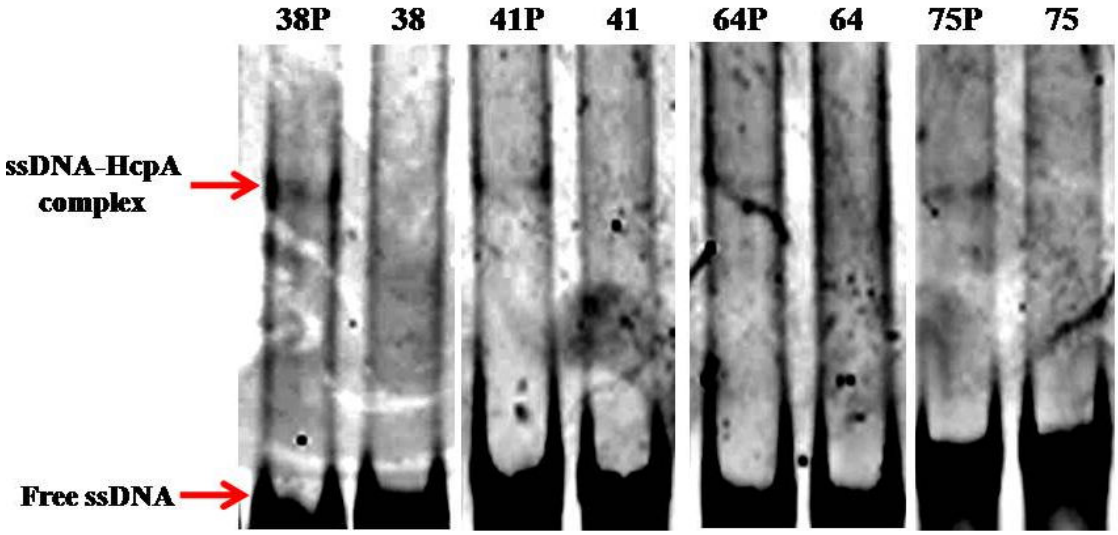

Fig 5.6 Binding confirmation of putative aptamers selected for HcpA on 8% native PAGE: Putative aptamers with protein (38-P, 41-P, 64-P, 75-P) displays a shift in the mobility as compared to the free ssDNA (38, 41, 64, 75).

5.7. Conclusion

The bioinformatics data suggests that the amino acid sequences of HcpA of *E. coli* O157:H7 is similar to the type IV pili a product of prepilin peptidase-dependent gene, possessing similar features with a distinct shorter leader sequence followed by a peptidase cleavage site along with invariable glycine residue [401]. The BLAST results also confirm conserved nature of HcpA in other bacterial species of Enterobacteriaceae family. *Shigella flexneri* (GenBank accession number-WP000360918.1) showed the maximum identity of 99% while, *Salmonella enterica* (GenBank Aaccession number- WP000414991.1) displayed 88% identity. Also type IV pili are present in other bacterial pathogens including PilA of *Pseudomonas aeruginosa* (55%, GenBank accession number AY113185), PilA of *Moraxella catarrhalis* (61%, GenBank accession number AY647185), and PilE of *Neisseria gonorrhoeae* (62%, GenBank accession number AF043652) [271]. Although the HcpA like protein are present in the commensal and pathogenic species of *E. coli*, studies in *E. coli* K12 have shown its inability to assemble the pili on its own [402, 403].

A detailed study carried by Ledesma *et al*., 2007 investigated the potential role of purified native HcpA (19 kDa) and recombinant His-HcpA (22 kDa) in modulating the immune response through the release of pro-inflammatory molecules by the epithelial cells [79, 271]. This study revealed a similar immunomodulatory response for both native HcpA and recombinant His-HcpA, suggesting the feasible use of recombinant protein for carrying out SELEX. Affinity chromatography based selection was carried out for HcpA aptamer development. Screening of populations of different rounds using EMSA evolved better DNA sequences with HcpA binding ability in the 10^{th} round of selection as compared to the 8^{th} round pool. Selected 10^{th} round of pool of DNA was cloned, sequenced and aligned. Using BioEdit software the sequences were categorized on the basis of sequence similarity. Putative aptamers from top eight groups exhibiting highest stability in terms of free energy were selected and synthesized with a fluorescence tag. Selected putative aptamers were screened for their binding confirmation by performing EMSA. The results confirm the binding of putative HcpA-38, 41, 64 and 75 aptamers with HcpA pilin protein.

Future experiments need to be carried, to determine binding affinity in terms of dissociation constant (Kd) for HcpA pilin protein. Kd can be calculated using either fluorescence binding assay, isothermal calorimetry (ITC) or EMSA. Experiments involving truncation of primer domains to shorten the aptamer length will enable us to get a smaller version of HcpA aptamers for development of nano-aptasesnor. Moreover, HcpA is specifically expressed and detected in serum of patients suffering from hemolytic uremic syndrome (HUS), and not in normal human serum [271]. Therefore, HcpA could be used as the marker for detecting *E. coli* O157:H7 infection in symptomatic patients. This can be achieved by combining aptamer with nanotechnology (based on gold nanoparticles, magnetic nanoparticles or single walled carbon nanotubes) for detecting *E. coli* O157:H7 [307, 319, 404-406].

Apart from being the signature protein for *E. coli* O157: H7, HcpA also plays an important role in pathogenesis [79, 273]. It is tempting to test the possible therapeutic role of HcpA aptamer for its inhibitory role in preventing the adherence of the *E. coli* O157H:7 cells in augmenting the infection once in contact with the intestinal epithelial cells [407].

CHAPTER 6

NANO BASED STRATEGIES FOR PATHOGEN CONTROL

Increasing incidences of nosocomial infections due to multiple drug resistant (MDR) pathogens have become a serious concern. To tackle such infections there is a need for discovering a new antibacterial chemical matter. However, dearth of new antibiotics for treating such antibiotic resistant bacteria has led researchers to think of exploiting antimicrobial metals in innovative ways for combating such infections. In the present part silver nanoparticles capped with an antibacterial peptide polymyxin B were synthesized using a facile method. The capping of the nanoparticles was characterized using biochemical and biophysical methods. The enhancement in antibacterial potency of coated silver nanoparticle and endotoxin removal capabilities from solution were assessed. Finally the ability of polymyxin B functionalized silver nanoparticles was shown to inhibit biofilm formation of *Pseudomonas aeruginosa*.

6.1. Characterization of bio-functionalized nanoparticles and evaluation of the antibacterial activity

A batch of experiments with varying concentrations of polymyxin B (0-100 µg/ml) and times (0-60 min) was carried out to determine the optimum concentration and incubation time for the synthesis of polymyxin B capped silver nanoparticles (PBSNPs). The solution of polymyxin B and silver nitrate turned yellow in 30 min. Fig 6.1.1 shows a schematic representation of PBSNPs synthesis. The PBSNPs thus formed were dialyzed against water and sonicated using water bath sonicator prior to further characterization studies.

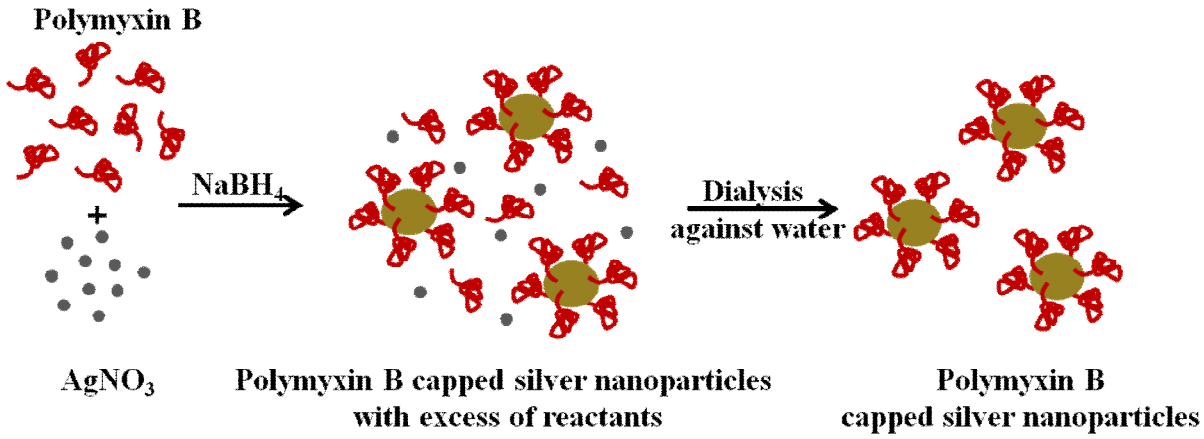

Fig 6.1.1Schematic representation of synthesis of the polymyxin capped silver nanoparticles (PBSNPs).

The results in Fig. 6.1.2 show the UV visible absorbance spectra of the PBSNPs formed after 30 min with varying concentration of polymyxin B (0- 100 µg/ml).The absorbance spectra of the nanoparticles synthesized using 60 µg/ml showed a characteristic SPR peak of silver nanoparticles at 414 nm which reveals that the majority of the nanoparticles to be in nano range [408]. TEM analysis revealed that the PBSNPs were mono dispersed and spherical in shape with a mean diameter of 10±5 nm (Fig. 6.1.3). However, an increase in nanoparticle size (~71.5±0.5 nm) with polymyxin capping as estimated by DLS was observed which is likely due to bimolecular layering on the nanoparticles (Fig. 6.1.4). These results are in agreement with the findings that the hydrodynamic size of the nano-bioconjugates (through DLS) is often more than that was observed under TEM [409].

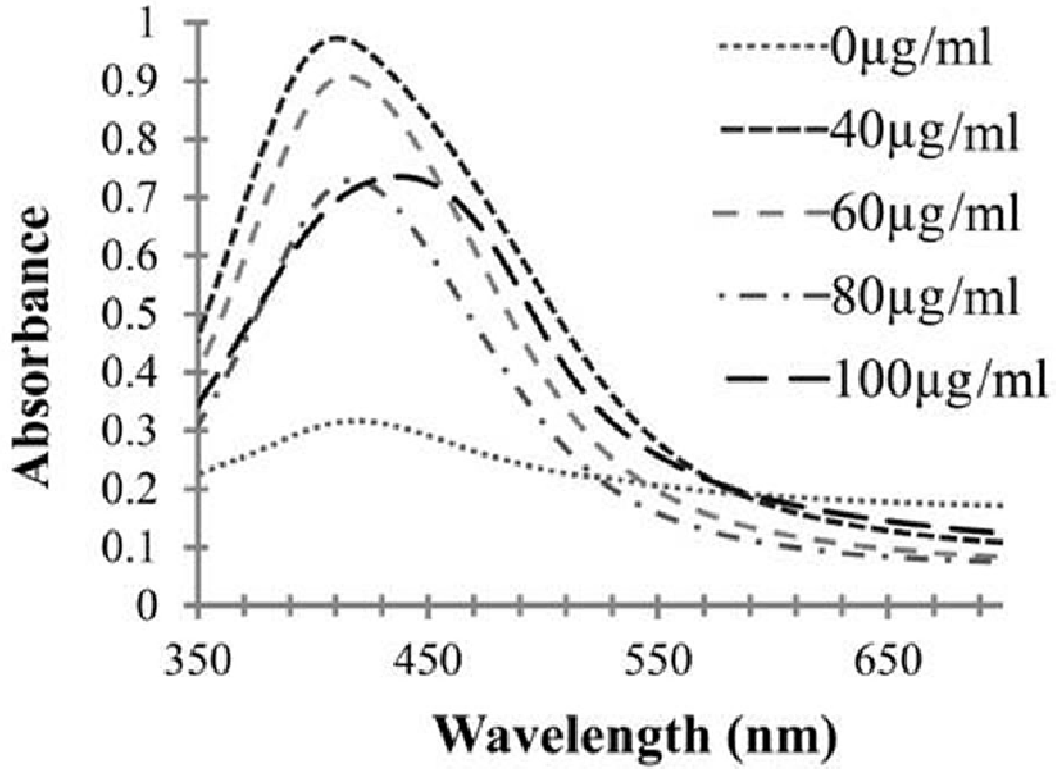

Figure 6.1.2 UV–visible absorbance spectra of polymyxin B capped silver nanoparticles prepared using varying concentration of polymyxin B.

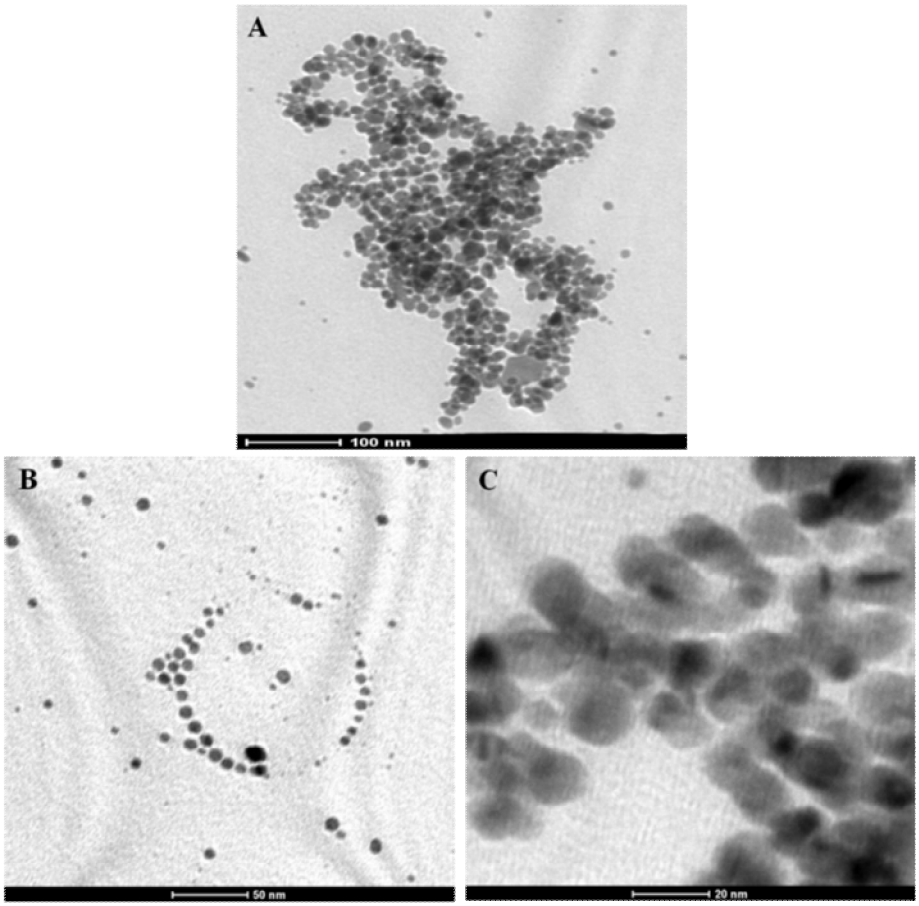

Fig 6.1.3 TEM images of PBSNPs at different scales: (A) 100 nm (B) 50 nm and (C) 20 nm revealing the size of PBSNPs to be 15±5 nm.

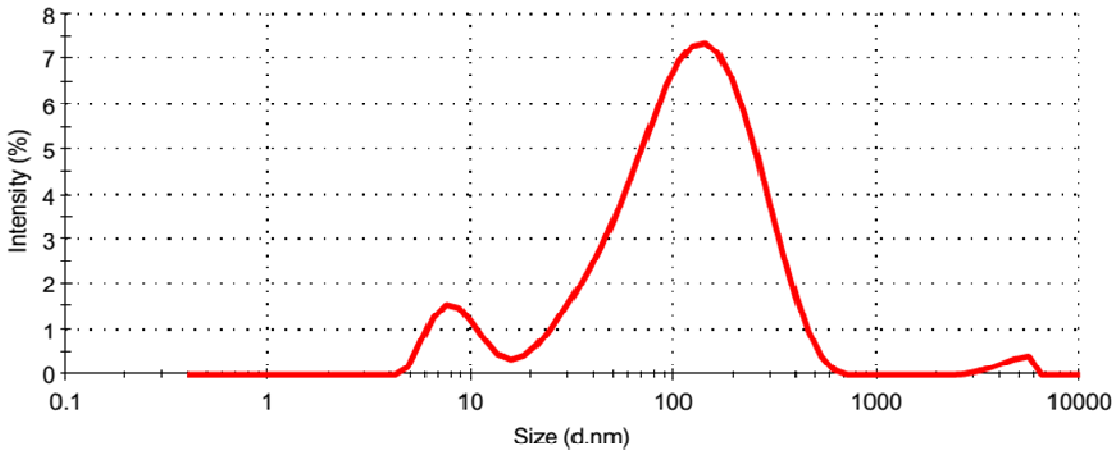

Fig 6.1.4 Dynamic Light Scattering: Size distribution analysis by DLS demonstrated the size of PBSNPs to be ~71.5±0.5 nm.

The zeta potential of PBSNPs and CSNPs was recorded to be 12.8±5.34 mV and -25.2 ±7.15mV respectively, indicating the stability of prepared nanoparticles (Fig. 6.1.5)

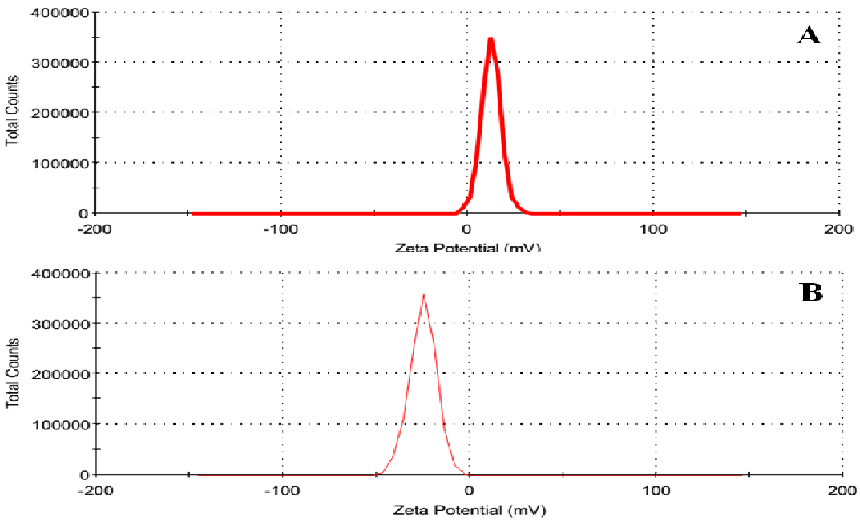

Fig 6.1.5 Zeta potential measurement of PBSNPs and citrate capped silver nanoparticles (CSNPs): Zeta potential distribution of (A) PBSNPs and (B) CSNPs was measured to be 12.8±5.34 mV and -25.2 ±7.15 mV respectively.

To determine the fate of polymyxin B used as the capping agent in the synthesis of biofunctionalized nanoparticles, FTIR analysis was performed. The FTIR data in Fig. 6.1.6 reveals that the spectrum of PBSNPs was similar to the spectrum of free polymyxin B. FTIR analysis provides evidence about any change in the secondary or tertiary structure of protein that alters the hydrogen bonding between the CO and NH groups in the peptide backbone, resulting in alterations of the primary, secondary or tertiary amine bands between 1200 and 1700/cm [410]. No such significant shifts were observed in this IR region of PBSNPs and free polymyxin B, as typical amide group peak was observed at 1635.85/cm in both the cases, indicating no major alterations occurred, in the functional groups of polymyxin B after capping on SNPs [411].

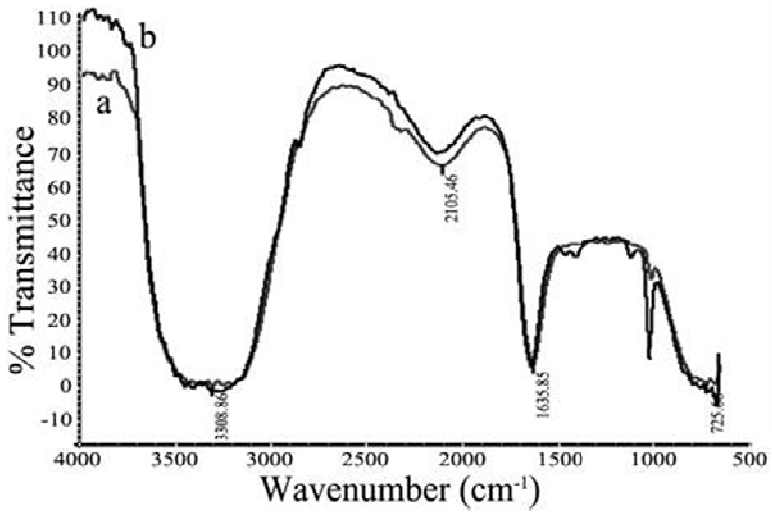

Fig 6.1.6 FTIR spectra for (a) pure polymyxin B (b) PBSNPs.

Further to confirm that polymyxin B preserved its secondary structure on the surface of biofunctionlized silver nanoparticles, CD spectra for free polymyxin B and PBSNPs were recorded. A negative peak typical of helix structures was observed at 200 nm (peptide π-π* transition) in the spectra of both the free polymyxin B in water and polymyxin B capped nanoparticles (Fig. 6.1.7) [412]. No such peaks were observed in case of CSNPs, which were used as control.

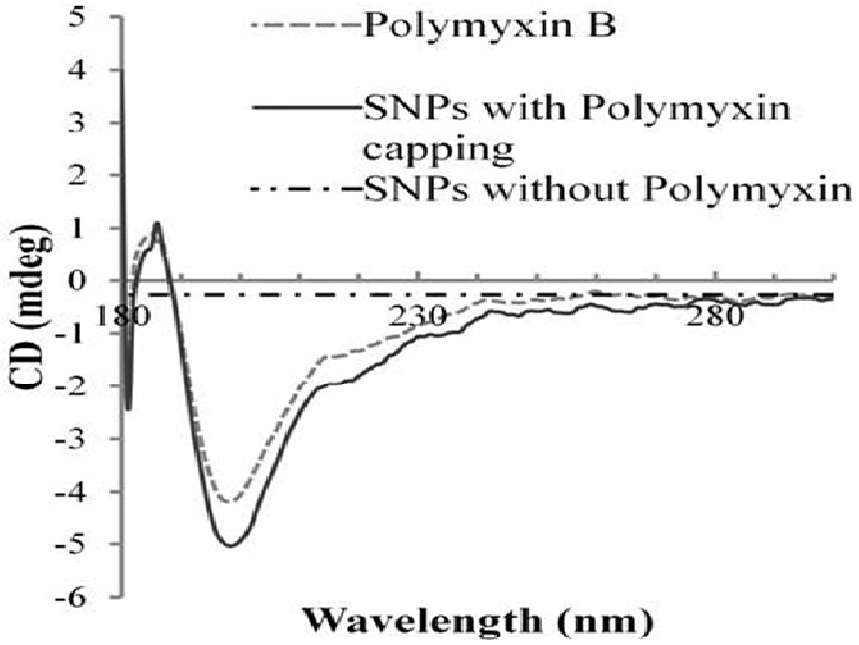

Fig 6.1.7 Circular dichroism spectra for polymyxin, PBSNPs and CSNPs.

It has been shown earlier that combined antibacterial action of silver nanoparticles and polymyxin B exerts synergistic effect on bacterial pathogens [413]. A simple method to immobilize polymyxin B on silver nanoparticles will be helpful to use these bio-functionalized nanoparticles as coatings for medical devices. Several studies have reported the conjugation of biomolecules via simple adsorption, covalent attachment, or electrostatic binding on the surface of nanoparticles for developing antibacterial surfaces [92, 360]. Recently, Soohyang et al. [414] reported antibacterial property of polymyxin B which was electrostatically conjugated to gold nanoparticles in a complex two step process. In the present study, the conditions optimized for capping silver nanoparticles with polymyxin B are facile thus leading to a stable and biologically relevant interaction of polymyxin B with nanoparticles.

Owing to the presence of an extra outer membrane which prevents antibiotics to cross the double layer, Gram-negative pathogens are known to be resistant to a variety of antibiotics. To overcome the aforementioned problem, Gram-negative antibacterial drugs are being discovered which may be effective even without crossing the inner layer [415]. Dearth of new antibiotics

and development of antibiotic resistance has led researchers to explore antimicrobial metals such as silver in innovative ways. The bio-functionalized SNPs used in this study clearly showed a decrease in MIC (4.5 µg/ml) as compared to CSNPs (12.5 µg/ml) for their antibacterial activity against both antibiotic resistant Gram negative bacteria. Bar graph in Fig. 6.1.8 demonstrates the anti bacterial activity of PBSNPs to be ~3 fold higher than CSNPs.

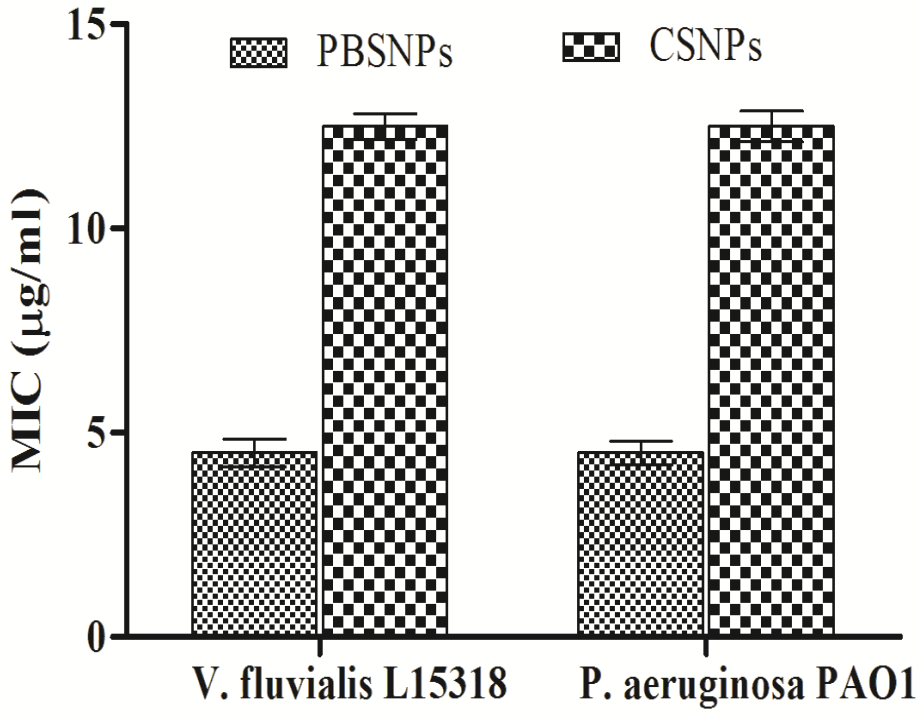

Fig 6.1.8 Minimum inhibitory concentration of PBSNPs and CSNPs: Against *Vibrio fluvialis* L15318 and *Pseudomonas aeruginosa* PAO1.

Further, the morphological effect of MIC of CSNPs and PBSNPs on both the cells was studied using SEM. The results in Fig.5.1.9 demonstrates an extensive damage to the cell membrane in presence of PBSNPs (c and f) as compared to CSNPs (b and e) and untreated cells (a and d).

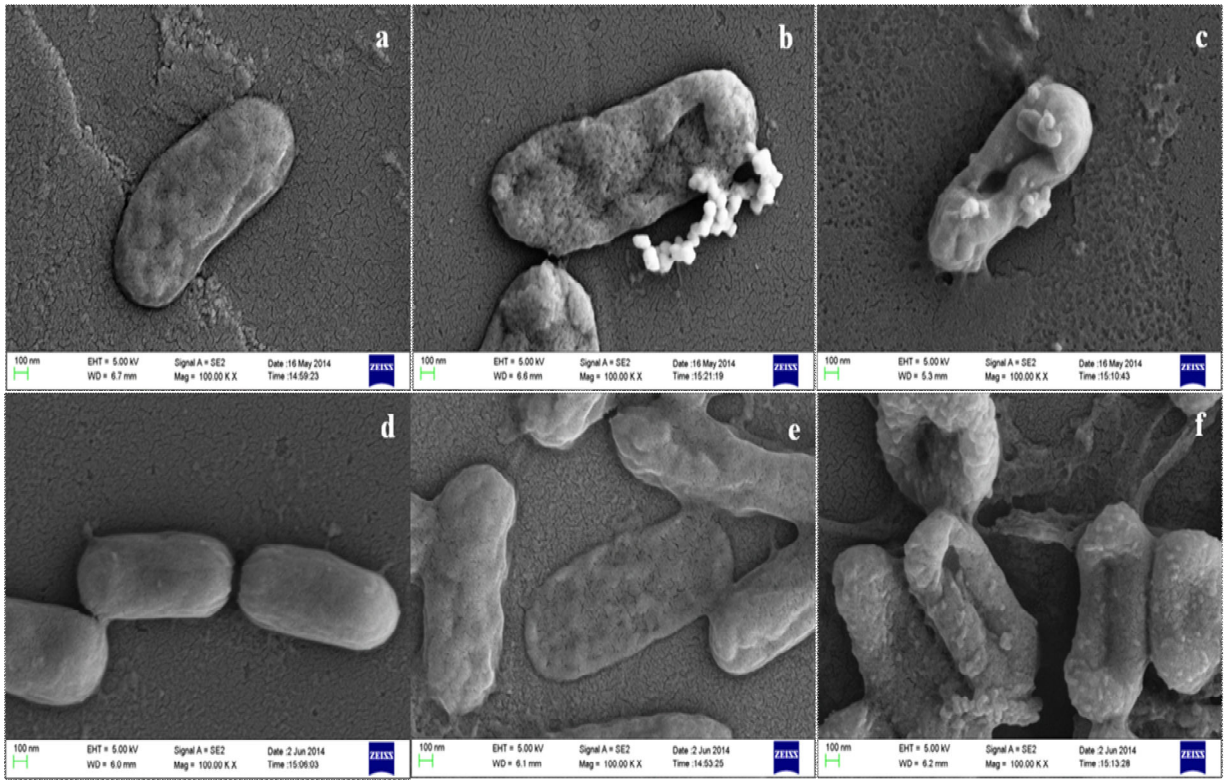

Fig 6.1.9 Scanning Electron Micrograph: Panels (a) and (d) shows control cells (without SNPs). Panels (b) and (e) shows CSNPs treated cells. Panels (c) and (f) PBSNPs treated cells. (a-c) *Vibrio fluvialis* L-15318 and (d-f) *Pseudomonas aeruginosa* PAO1.

Silver has been adored and appreciated for ages for its antibacterial activity has been appreciated, yet the exact mode of action of silver is an enigma to this world. While significant research has concluded that silver nanoparticles offer better antibacterial activity as they allow more effective contact with bacteria due to their large surface area property. The possible ways silver nanoparticles exert their antimicrobial activity after interacting with bacterial cells is by (a) release of silver ions and generation of reactive oxygen species (ROS); (b) interaction with membrane protein and disrupting its function; (c) disturbing the cell membrane permeability by accumulation; (d) entering into the cells, releasing the silver ions and generating ROS thus causing DNA damage [355, 356]. Fig. 6.1.10 shows a pictorial representation of the possible mode of action of PBSNPs.

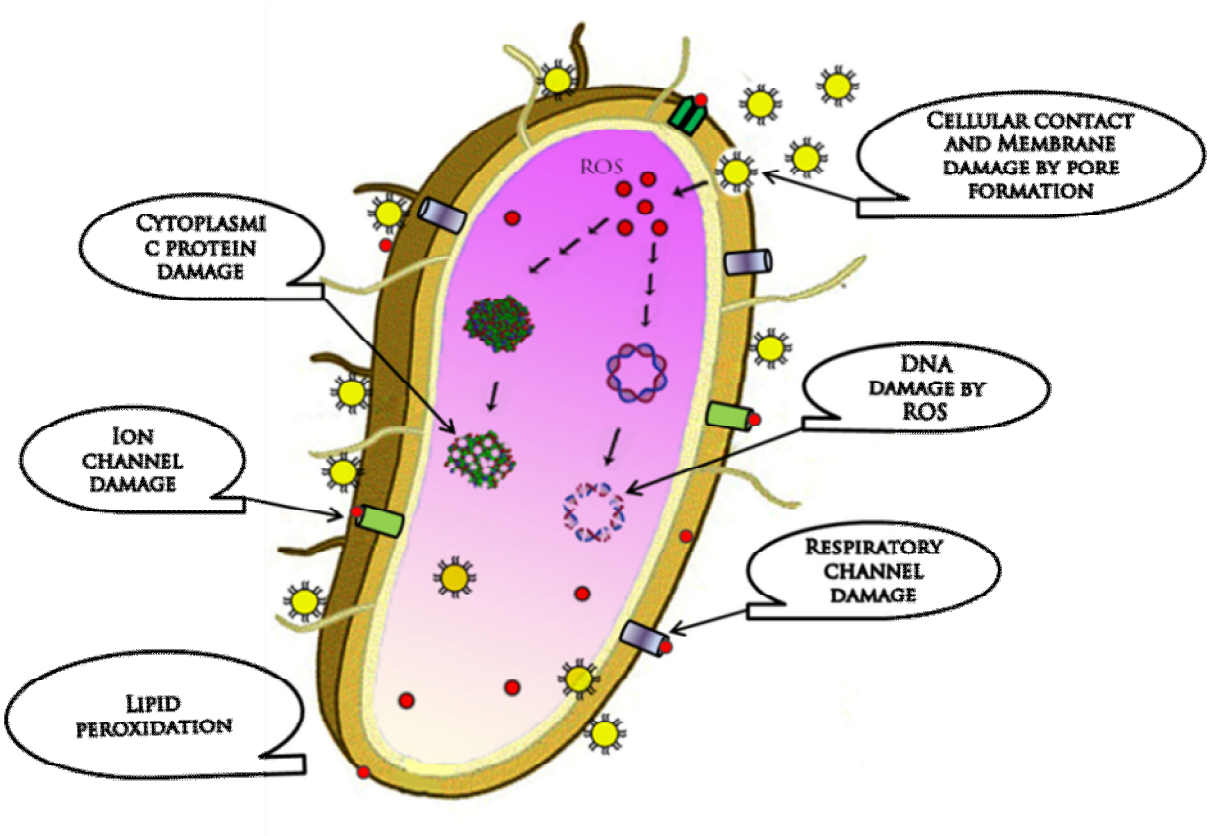

Fig 6.1.10 Different mode of action of PBSNPs: An attribute to its antibacterial activity against the bacterial cell.

The plausible explanation for the extensive damage caused by PBSNPs is that they get attached to bacterial surface making small and transient holes which disturb the functions of the bacterial membrane. Subsequently, disruption of bacterial membrane leads to the leakage of the cytoplasm resulting in wilting of the cells. These results indicate that the enhanced antibacterial activity of PBSNPs was due to the presence of a large number of polymyxin B molecules on the surface of SNPs. The interaction of these conjugates provided ample opportunity for both agents to act on the bacteria simultaneously, thus enhancing its inhibitory effect [413, 416]. SEM images of PBSNPs, CSNPs and untreated cells at different magnification for *Vibrio fluvialis* (Fig 6.1.11, 6.1.12 and 6.1.13) and *Pseudomonas aeruginosa* PAO1 (Fig 6.1.14, 6.1.15 and 6.1.16) are shown below

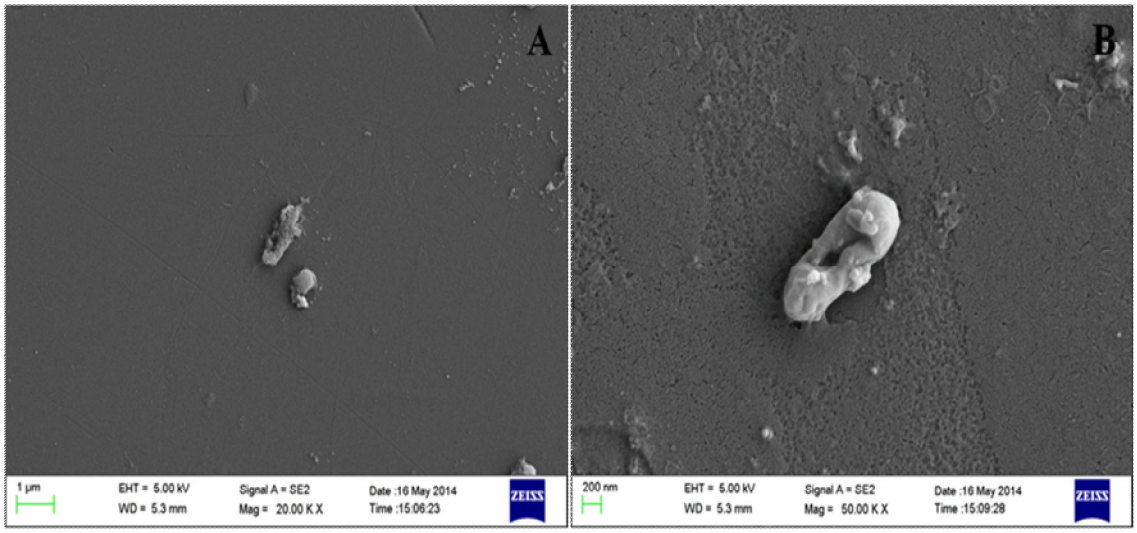

Fig 6.1.11 Scanning Electron Micrograph: PBSNPs treated *Vibrio fluvialis* L-15318 at different magnification (A) 20,000 X and (B) 50,000 X

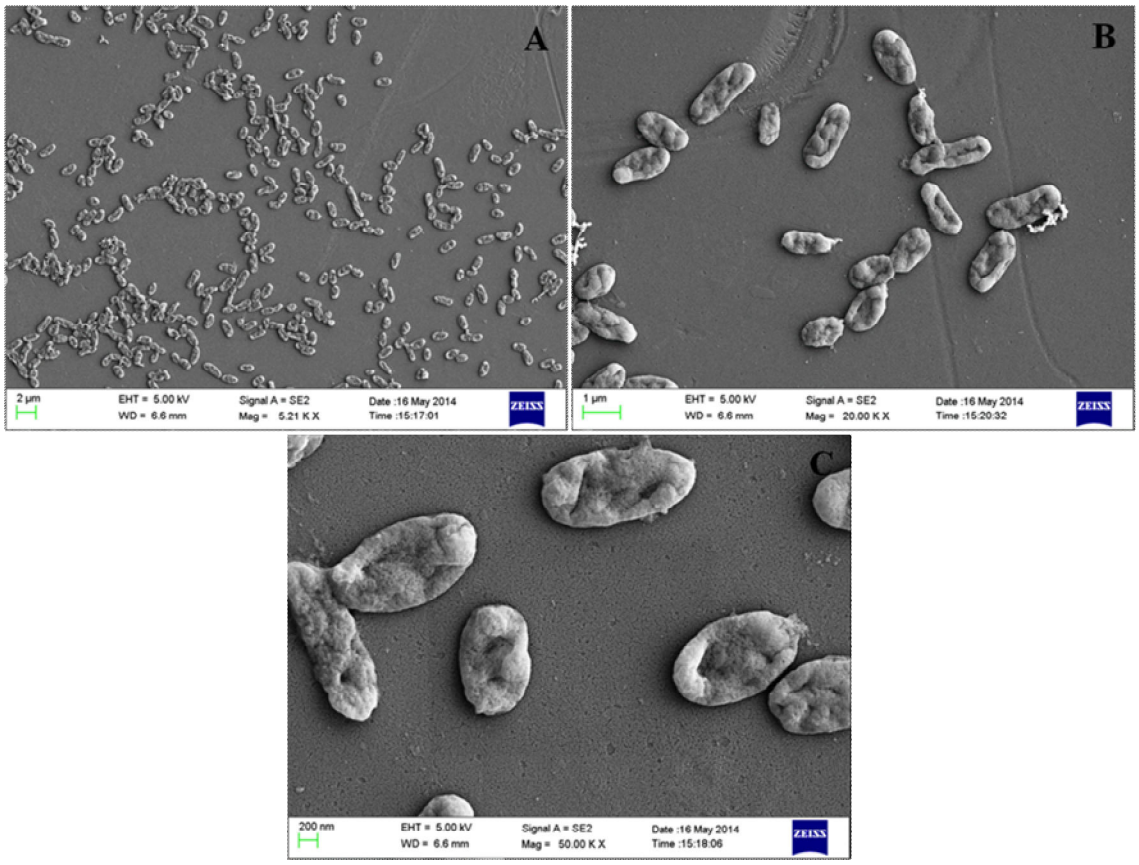

Fig 6.1.12 Scanning Electron Micrograph: CSNPs treated *Vibrio fluvialis* L-15318 at different magnification (A) 5000 X, (B) 20,000 X and (C) 50000 X.

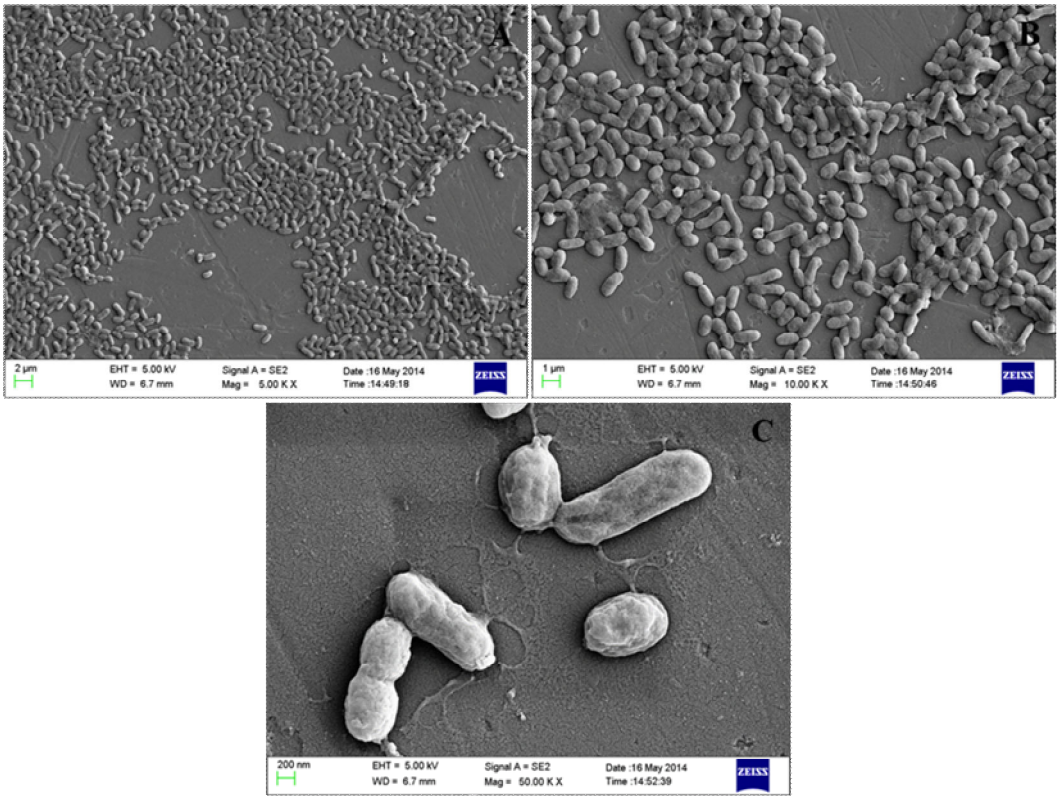

Fig 6.1.13 Scanning Electron Micrograph: Untreated *Vibrio fluvialis* L-15318 at different magnification (A) 5000 X, (B) 10,000 X and (C) 50000 X.

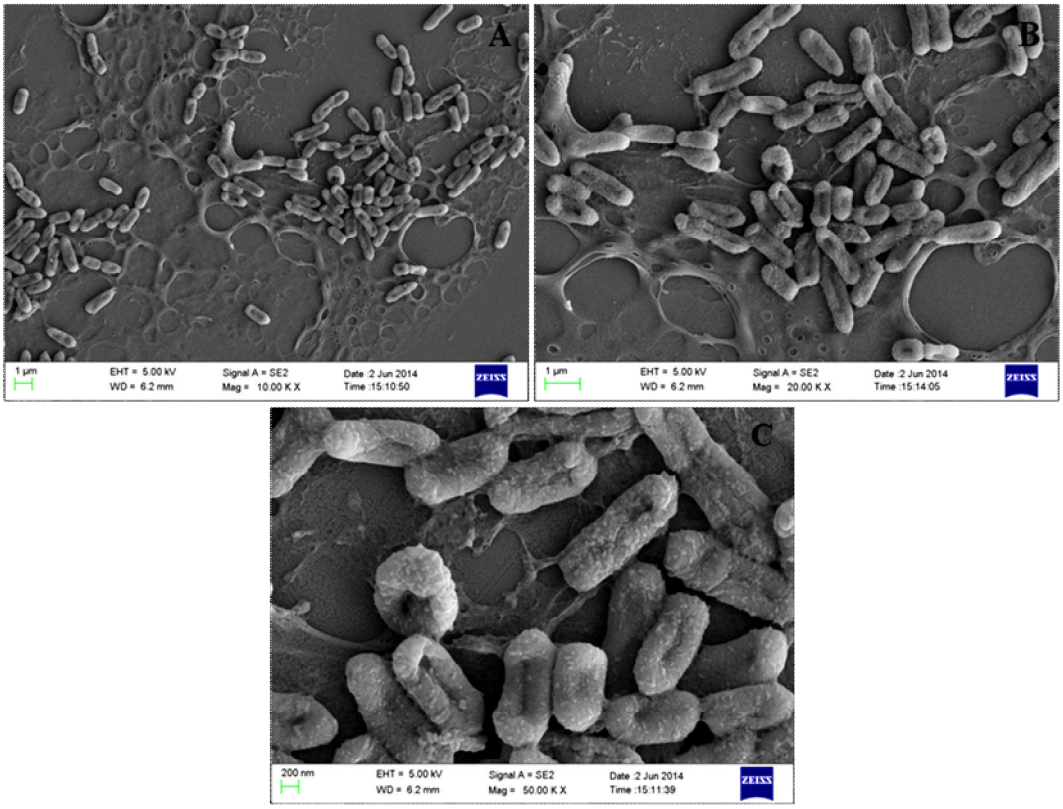

Fig 6.1.14 Scanning Electron Micrograph: PBSNPs treated *Pseudomonas aeruginosa* PAO1 at different magnification (A) 5,000 X (B) 10,000 X and (C) 50,000 X.

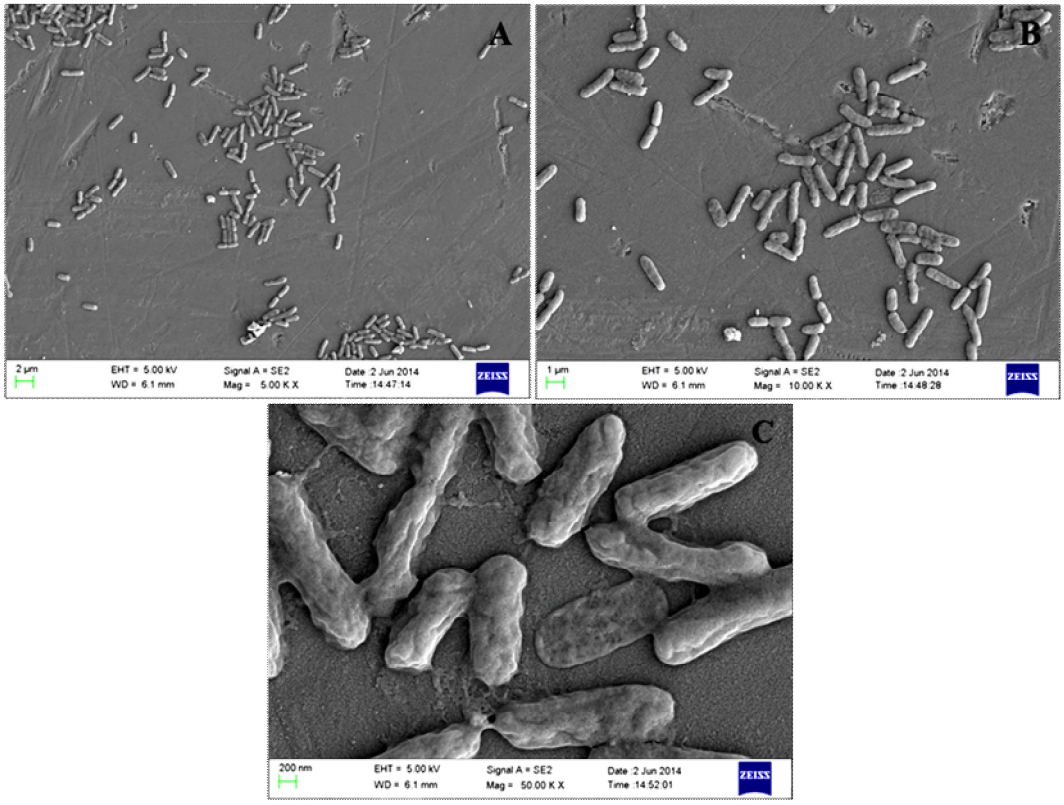

Fig 6.1.15 Scanning Electron Micrograph: CSNPs treated *Pseudomonas aeruginosa* PAO1 at different magnification (A) 5,000 X (B) 10,000 X and (C) 50,000 X.

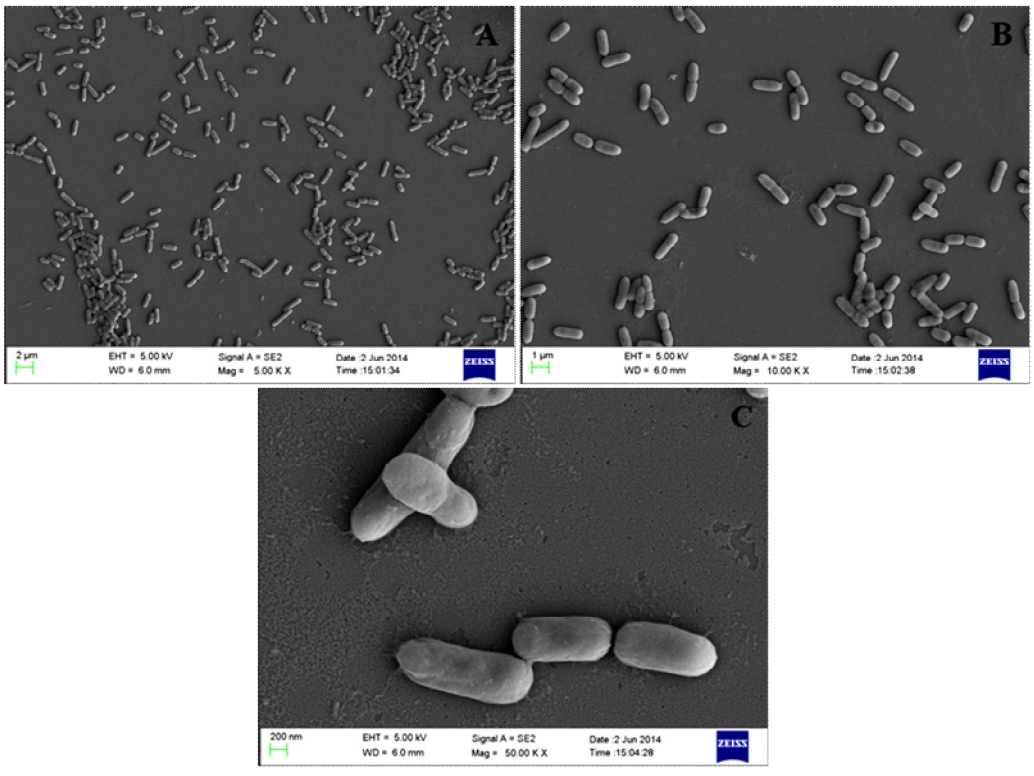

Fig 6.1.16 Scanning Electron Micrograph: Untreated *Pseudomonas aeruginosa* PAO1at different magnifications (A) 5,000 X (B) 10,000 X and (C) 50,000 X.

6.2. Effect of bio-functionalized nanoparticles on biofilm formation

Adhesion of planktonic cells on the surface of biomedical implants and devices is the primary and important step for initiation of biofilm formation [417, 418]. *P. aeruginosa* have been found associated with biofilms in hospital settings and other environment [419-421]. The activity of PBSNPs against *P. aeruginosa* prompted us to test the ability of these functionalized nanoparticles for their antibiofilm activity against *P. aeruginosa*. Fig. 6.2 shows that upon exposure of PAO1 cells to MIC of PBSNPs (4.5 µg Ag^0/ml, Fig. 3 A) and CSNPs (12.5 µgAg^0/ml, Fig. 3 B), a complete inhibition of bacterial growth ($O.D_{600}$) occurred, with no biofilm formation ($O.D_{550}$) after 6 h of incubation, as compared to the control. The above results reveal that PBSNPs display ~3 fold higher antibiofilm activity as compared to CSNPs, suggesting a paramount role being played by the capping agent; polymyxin B. Concurrent inhibition of planktonic cell growth and biofilm formation with increasing concentration of PBSNPs suggests that this formulation is refractory to the establishment of bacterial biofilm likely due to inhibition of planktonic cells.

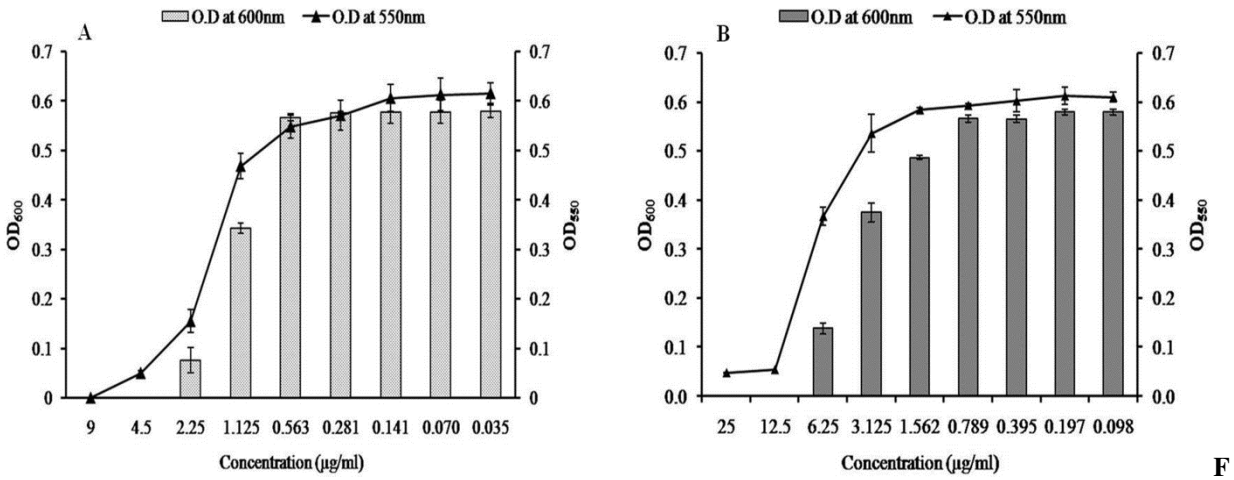

ig 6.2 Inhibition of biofilm formation: (A) Cells treated with PBSNPs; (B) cells treated with CSNPs. The line graph indicate the biofilm biomass at 550nm ($O.D_{550}$) and the bar graph represents the bacterial growth at 600 nm ($O.D_{600}$).

6.3. Live/Dead staining of bacteria in biofilm

To ascertain the antibiofilm activity of PBSNPs, *P. aeruginosa* PAO1 biofilm was assayed on the glass coverslip with MIC (4.5 µg Ag^0/ml) and sub-MIC concentration (2.25 µg Ag^0/ml) of PBSNPs under stationary conditions for 6 h. Viability of attached cells on the coverslip was evaluated by a mixture of SYTO9 (stains the total nucleic acid content of the cells; thus staining dead as well as live cells) and PI dye (unable to penetrate the intact cytoplasmic membrane of healthy cells; thus staining only the dead cells) [380, 422].

Although cells were able to adhere to the coverslip in MIC (4.5 µg Ag^0/ml) and sub-MIC (2.25 µg Ag^0/ml) treatments, yet the relative cell density was reduced as compared to the untreated cells thus demonstrating the inhibitory effect of PBSNPs. Fig 6.3 (A) shows the effect of MIC treated cells which resulted in death of most of the bacterial cells. The ratio of (i) live to (ii) dead cells was significantly higher in case of sub-MIC treated cells (B) as compared to the untreated cells (C) where the confluent layer of live cells on coverslip were stained green. The inhibitory effect of silver nanoparticle treatment on planktonic cells of *P. aeruginosa* PAO1 was also observed in a recent study [381]. The killing efficiency of PBSNPs in our study was found to be 2.5 times more effective than the reported values [381]. This highlights the importance of bio-functionalization of nanomaterials at surfaces for controlling infections.

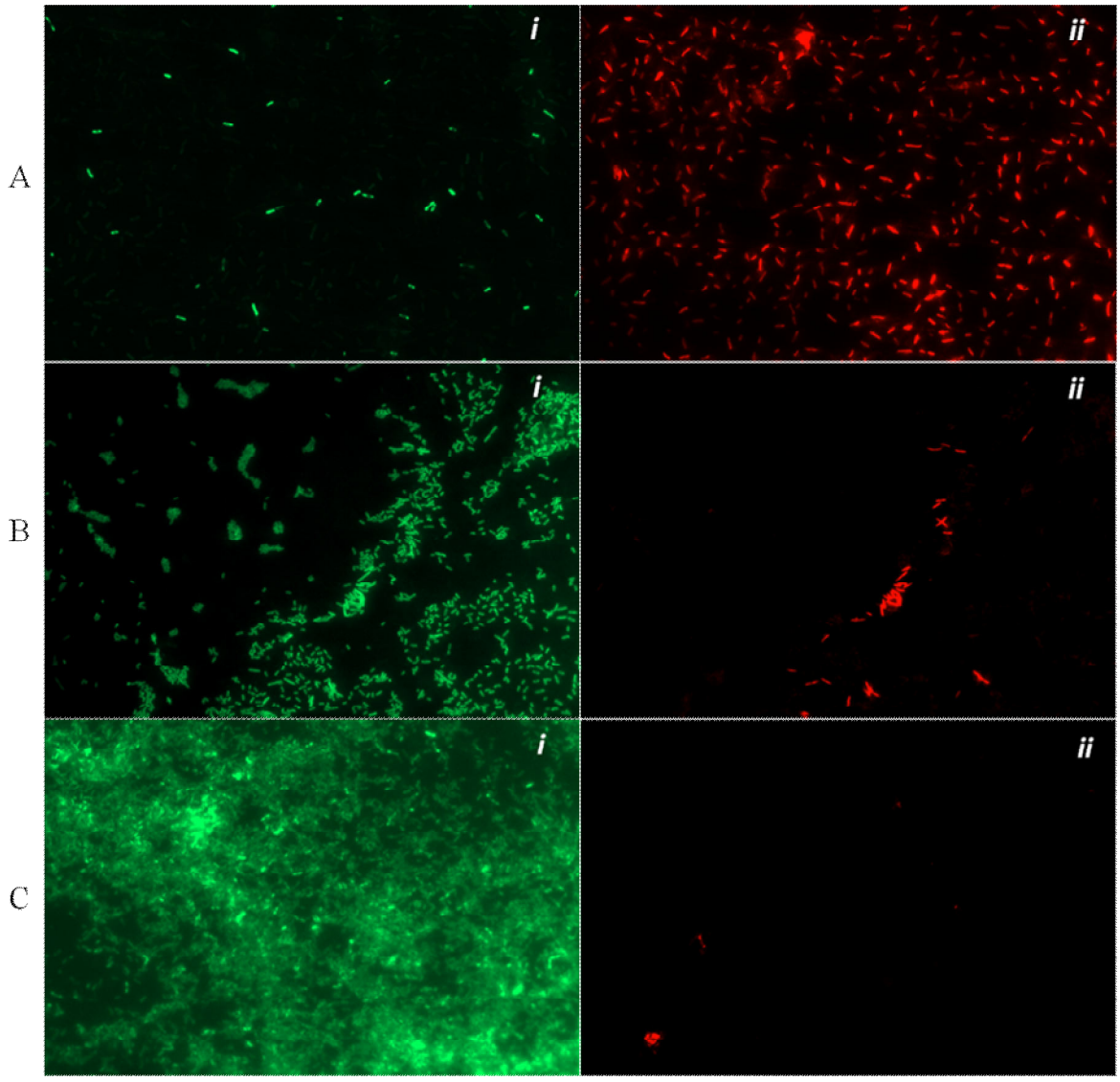

Fig 6.3 Live/Dead staining of biofilm on glass coverslips: (A) PBSNPs MIC treated cells, (B) PBSNPs sub-MIC treated cells and (C) untreated cells. (i) represents green cells as live and (ii) red cells as dead

6.4. Viability analysis of PBSNPs treated P. aeruginosa PAO1 using Flow cytometer

Viability analysis by standard plate assay may give a false impression on bactericidal nature of an antibacterial agent by reducing the cultivability of cells, while they remain dormant and recover later after a certain period of time. [423]. Further, to confirm the killing efficacy of PBSNPs against PAO1 planktonic cells, MIC treated cells were stained with Live/Dead stains and analyzed by flow cytometery, providing us a realtime assessment on bacterial viability [380, 381]. Fig. 6.4 shows the flow cytometry analysis of untreated unstained cells (A), untreated stained cells (B) and stained PBSNPs cells at MIC (C) as test sample. Based on the staining pattern the cells were divided in quadrants highlighting their viability status. In Fig. 6.4 A, 97.72% of untreated cells were gated in LL region of the scatter plot signifying the unstained nature of cells. Untreated stained cells (Fig. 6.4 B) showed an increase in green fluorescence signal representing 87.72% cells in UL quadrant as live. Whereas, 97.34% of PBSNPs treated cells at MIC levels displayed a clear shift in both green and red fluorescence signal and were observed in UR quadrant as dead cells take up both the stains (Fig. 6.4 C), thus indicating the killing efficiency of PBSNPs towards PAO1 cells.. The flow cytometry data is in agreement with the fluorescence microscopy for both untreated (Fig. 6.4 D) and treated (Fig. 6.4 E) stained cells. Overall, the data in this study strongly supports the bactericidal potency/nature of PBSNPs which can be exploited for other medical purpose.

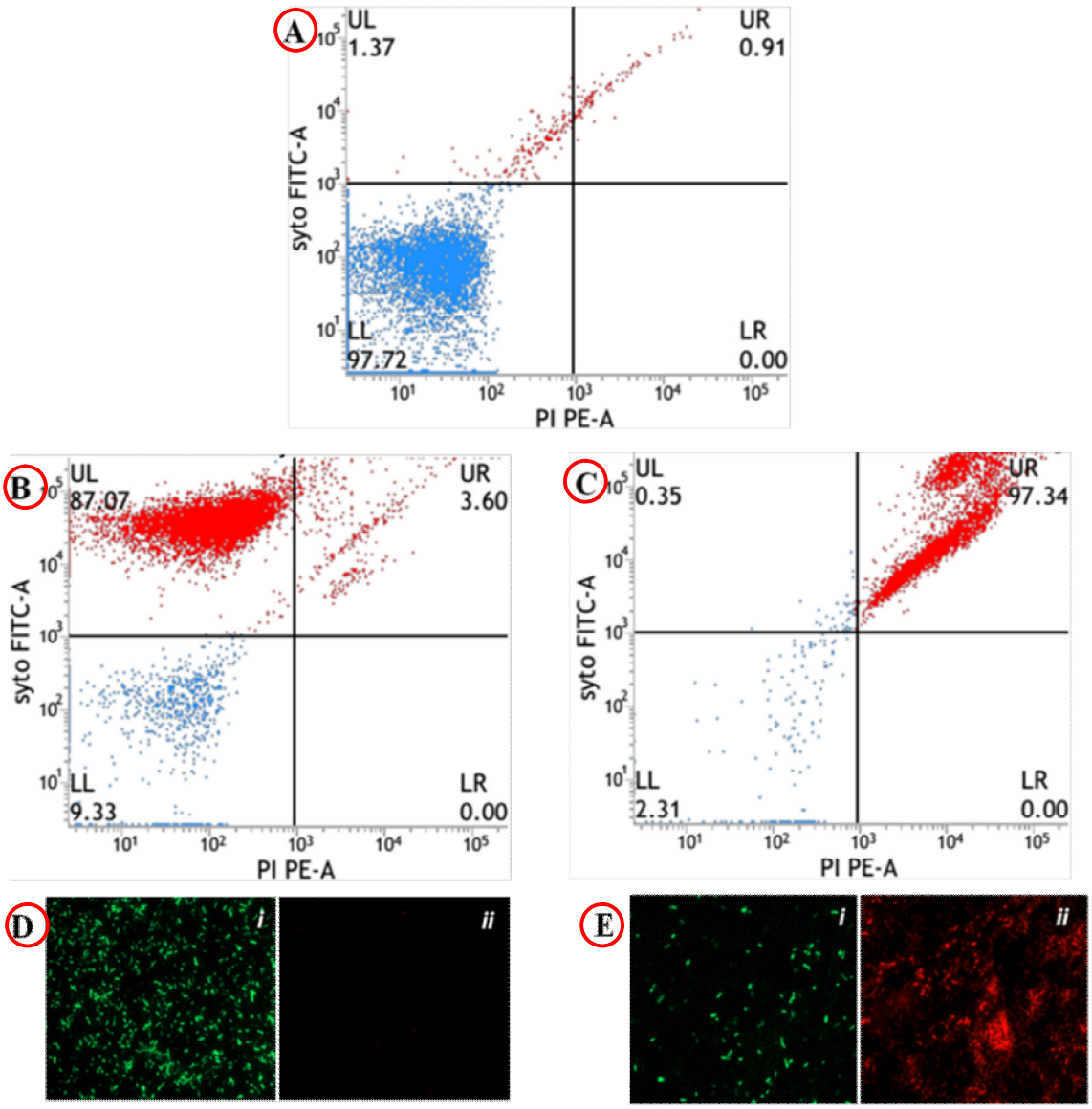

Fig 6.4 Live/Dead staining of planktonic *P aeruginosa PAO1* cells by flow cytometer and fluorescence microscopy: Flow cytometer scatter plot for (A) untreated unstained cells, (B) untreated SYTO9/PI stained and (C) PBSNPs MIC treated cells stained with SYTO/PI stains is represented .Different quadrants such as, lower left (LL) represents the unstained cells, upper left (UL) region represents live cells and dead cells are seen in upper right (UR) region. Fluorescence microscopy of (D) untreated stained cells and (E) PBSNPs MIC treated stained cells is represented, where (i) represents live cells stained as green, (ii) dead cells stained as red.

6.5. Antibacterial potency of PBSNPs coating

Antibacterial surfaces of materials used for medical devices can complement the fight against the pathogens which propagate in sessile stage. Since PBSNPs inhibited one of the biofilm associated pathogen *P. aeruginosa* PAO1 effectively, we tested if the functionalized nanoparticles could be adapted for coating on the surgical devices and if they could retain their inhibitory property following the composite coating. For this, PBSNPs were electroplated on stainless steel surgical blades to scrutinize their antibacterial potency. A uniform coating of PBSNPs onto the surgical blade was observed by AFM study (Fig. 6.5 A). The antibacterial

activity assayed by agar-diffusion test (Fig. 6.5 B) revealed that (a) PBSNP coated blades showed enhanced antibacterial activity as compared to blades coated with (b) CSNPs alone (smaller inhibition zone), (d) PBSNPs coated blade when treated with proteinase K (as broad spectrum serine-protease) exhibited significantly reduced antimicrobial activity and (c) uncoated blades (no inhibition zone). These results confirmed that the enhancement in antibacterial activity of PBSNPs coated surgical blades was due to polymyxin B.

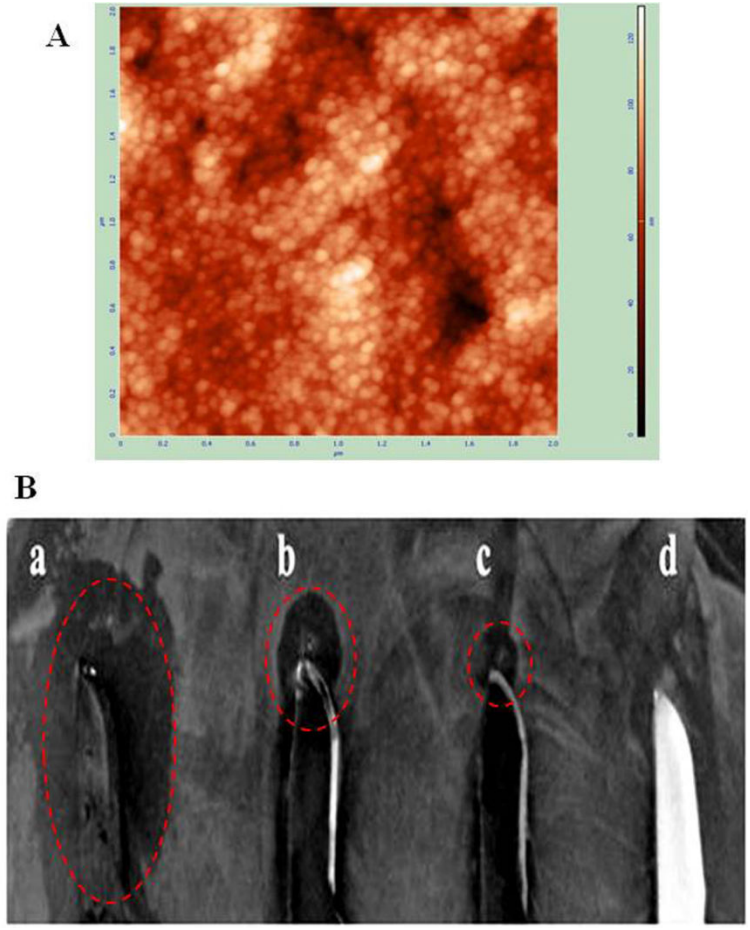

Fig 6.5 (A) AFM image of PBSNPs coated on surgical blade; (B) Antimicrobial assay measuring the antimicrobial activity of coated blade against *P. aeruginosa* PAO1. (a) Blade coated with PBSNPs. (b) Blade coated with CSNPs. (c) Blade coated with PBSNPs followed by proteinase K treatment. (d) Uncoated blade. Zone of inhibition are observed surrounding the blade (broken red circles).

6.6. Removal of endotoxin by PBSNPs

We expanded the utility of such bio-functionalized SNPs further in medical applications. Polymyxin B is known to interact with LPS part of lipid A of Gram-negative bacterial cell walls. LPS is also known as endotoxin which is shed by Gram-negative bacteria and is notorious in causing sepsis and septic shock [424]. Preservation of biological activity of the polymyxin B upon capping on SNPs prompted us to investigate the ability of such bio-functionalized nanoparticles to remove endotoxin from solutions which was tested using a

conventional chromogenic Limulus Amebocyte Lysate endotoxin assay (Fig. 6.6). The PBSNPs efficiently removed endotoxin from the test samples (~97%) as compared to control (~16%). The efficient removal of endotoxin could be attributed to the large number of polymyxin molecules present on SNPs due to their enhanced surface to volume ratio as compared to conventional column matrix. Herein, we have exploited PBSNPs as an efficient agent for endotoxin removal and could be developed further for removal of endotoxin from other biological fluids while keeping the infections under control.

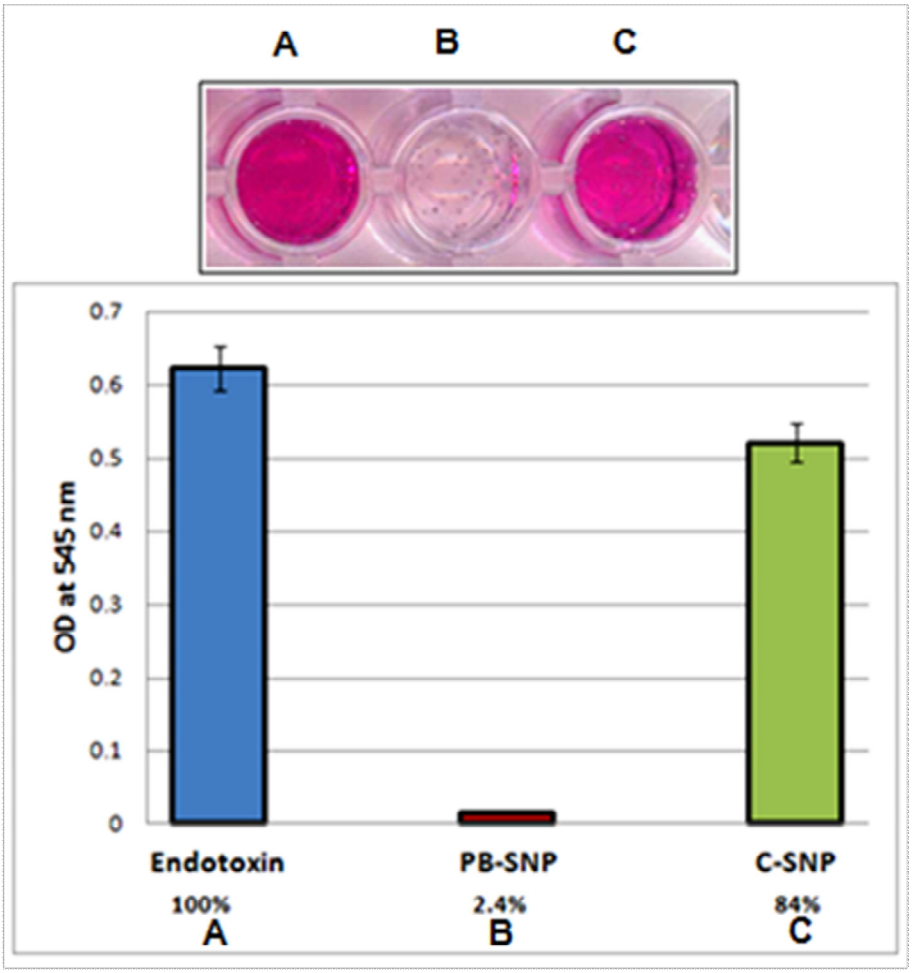

Fig 6.6 Endotoxin removal capability of PBSNPs: (A) Control endotoxin (no agent added); Removal by (B) PBSNPs; (C) CSNPs. Original picture of the wells (top inset) along with graphical representation (bottom). Percentage on X- axis represents the residual endotoxin after the treatment.

6.7. Conclusion

Due to multiple modes of action against bacterial pathogens, inability of the bacteria to develop resistance against silver is well established. In the present investigation, we have increased the potency of silver by synthesizing bio-functionalized silver nanoparticles (PBSNPs) using a facile method and have characterized them using various biophysical and analytical techniques. Due to a simple and straightforward method of synthesis, on decoration,

the antimicrobial peptide was found to retain its antibacterial property which was a problem as reported in a recent study [425]. The capping of polymyxin B on the silver nanoparticles enhanced the antimicrobial effectiveness of the nanoparticles. We have also explored various medically relevant applications of these bio-functionalized silver nanoparticles. The composite antimicrobial coating of PBSNPs on surgical blades via electrophoretic deposition proved effective in inhibiting the biofilm forming multiple antibiotic resistant bacterial strains. Biofilm formation on solid surfaces is a survival strategy of bacterial populations. These biofilms have been found to be associated with recalcitrant bacterial infections in medical devices and patients with compromised immune system [44]. Development of efficient antibacterial coating has been recognized as a major challenge to mitigate biofilm formation and controlling the infectious agents in the hospital settings. Polymyxin B capped nanoparticles reported in this study offer an opportunity to develop effective strategy to fight infectious agents in general and hospital acquired infections in specific. The usefulness of PBSNPs has also been extended to endotoxin removal from solutions, which widens the applications of these surface modified nanoparticles. Future challenges to this approach will be to study the stability and physical layering of the antimicrobial peptide coating on medical devices. Also, the performance of the antimicrobial coating under different pathological conditions including ability to resist biofilm formation needs detailed investigations before this approach can be tested at clinical stage.

REFERENCES

1. *Assuring Food Safety and Quality: Guidelines for Strengthening National Food Control Systems*. 2003; Available from: http://www.fao.org/docrep/006/y8705e/y8705e09.htm.
2. *U.S. Food and Drug Administration*. Available from: http://www.fda.gov/Food/GuidanceRegulation/RetailFoodProtection/FoodCode/ucm374275.htm.
3. *Milk production in India*. Available from: http://www.nddb.org/English/Statistics/Pages/Milk-Production.aspx. .
4. Souza, S.S., et al., *Monitoring the authenticity of Brazilian UHT milk: A chemometric approach.* Food Chemistry, 2011. **124**(2): p. 692-695.
5. *Food Safety and Standards Authority of India*. Available from: http://fssai.co.in/70-of-milk-in-delhi-country-is-adulterated/.
6. Ishler, V. and M.U.N. MUN, *Interpretation of milk urea nitrogen value*. 2008, DAS.
7. *Melamine-contaminated powdered infant formula in China*. 2008; Available from: http://www.who.int/csr/don/2008_09_19/en/.
8. Van Slyke, D.D., *Determination of urea by gasometric measurement of the carbon dioxide formed by the action of urease.* Journal of Biological Chemistry, 1927. **73**(2): p. 695-723.
9. Patton, C.J. and S. Crouch, *Spectrophotometric and kinetics investigation of the Berthelot reaction for the determination of ammonia.* Analytical chemistry, 1977. **49**(3): p. 464-469.
10. Ramsing, A., J. Růžička, and E. Hansen, *A new approach to enzymatic assay based on flow-injection spectrophotometry with acid-base indicators.* Analytica chimica acta, 1980. **114**: p. 165-181.
11. Roch-Ramel, F., *An enzymic and fluorophotometric method for estimating urea concentrations in nanoliter specimens.* Analytical biochemistry, 1967. **21**(3): p. 372-381.
12. Bashir, R., et al., *Biosensor and related method*. 2007, Google Patents.
13. Belkin, S., *Microbial whole-cell sensing systems of environmental pollutants.* Current Opinion in Microbiology, 2003. **6**(3): p. 206-212.
14. Cunningham, A.J., *Introduction to Bioanalytical Sensors*. 1998, John Wiley & Sons,New York/Chichester.

15. Eggins, B.R., *Analytical Techniques in the Sciences: Chemical Sensors and Biosensors*. Analytical Techniques in the Sciences 2007: John Wiley, Chichester.
16. Su, L., et al., *Microbial biosensors: a review.* Biosensors and bioelectronics, 2011. **26**(5): p. 1788-1799.
17. Dhawan, G., G. Sumana, and B. Malhotra, *Recent developments in urea biosensors.* Biochemical Engineering Journal, 2009. **44**(1): p. 42-52.
18. Meli, M., et al., *Adenine-Aptamer Complexes A BIPARTITE RNA SITE THAT BINDS THE ADENINE NUCLEIC BASE.* Journal of Biological Chemistry, 2002. **277**(3): p. 2104-2111.
19. áO'Sullivan, C.K., *Aptamer conformational switch as sensitive electrochemical biosensor for potassium ion recognition.* Chemical communications, 2006(32): p. 3432-3434.
20. Jo, M., et al., *Development of single-stranded DNA aptamers for specific bisphenol A detection.* Oligonucleotides, 2011. **21**(2): p. 85-91.
21. Mann, D., et al., *In vitro selection of DNA aptamers binding ethanolamine.* Biochemical and biophysical research communications, 2005. **338**(4): p. 1928-1934.
22. Li, L., et al., *Label-free aptamer-based colorimetric detection of mercury ions in aqueous media using unmodified gold nanoparticles as colorimetric probe.* Analytical and bioanalytical chemistry, 2009. **393**(8): p. 2051-2057.
23. Lauridsen, L.H. and R.N. Veedu, *Nucleic acid aptamers against biotoxins: a new paradigm toward the treatment and diagnostic approach.* Nucleic acid therapeutics, 2012. **22**(6): p. 371-379.
24. Ellington, A.D. and J.W. Szostak, *Selection in vitro of single-stranded DNA molecules that fold into specific ligand-binding structures.* 1992.
25. Xu, S., et al., *Selection of DNA aptamers against polychlorinated biphenyls as potential biorecognition elements for environmental analysis.* Analytical biochemistry, 2012. **423**(2): p. 195-201.
26. Hamula, C.L., et al., *Selection of aptamers against live bacterial cells.* Analytical chemistry, 2008. **80**(20): p. 7812-7819.
27. Jones, L.A., et al., *High-affinity aptamers to subtype 3a hepatitis C virus polymerase display genotypic specificity.* Antimicrobial agents and chemotherapy, 2006. **50**(9): p. 3019-3027.
28. Kwon, M., et al., *In vitro selection of RNA against kanamycin B.* Molecules and cells, 2001. **11**(3): p. 303-311.

29. Lozupone, C., et al., *Selection of the simplest RNA that binds isoleucine.* Rna, 2003. **9**(11): p. 1315-1322.
30. Orava, E.W., et al., *A Short DNA Aptamer That Recognizes TNFα and Blocks Its Activity in Vitro.* ACS chemical biology, 2012. **8**(1): p. 170-178.
31. Ruckman, J., et al., *2'-Fluoropyrimidine RNA-based aptamers to the 165-amino acid form of vascular endothelial growth factor (VEGF165) Inhibition of receptor binding and VEGF-induced vascular permeability through interactions requiring the exon 7-encoded domain.* Journal of Biological Chemistry, 1998. **273**(32): p. 20556-20567.
32. Saran, D., J. Frank, and D.H. Burke, *The tyranny of adenosine recognition among RNA aptamers to coenzyme A.* BMC evolutionary biology, 2003. **3**(1): p. 26.
33. Sefah, K., et al., *Molecular recognition of acute myeloid leukemia using aptamers.* Leukemia, 2009. **23**(2): p. 235-244.
34. Sekkai, D., et al., *In vitro selection of DNA aptamers against the HIV-1 TAR RNA hairpin.* Antisense and Nucleic Acid Drug Development, 2002. **12**(4): p. 265-274.
35. Allali-Hassani, A., et al., *Isolation of DNA Aptamers for CDP-Ribitol Synthase, and Characterization of Their Inhibitory and Structural Properties.* Chembiochem, 2007. **8**(17): p. 2052-2057.
36. Navani, N.K., W.K. Mok, and L. Yingfu, *In vitro selection of protein-binding DNA aptamers as ligands for biosensing applications*, in *Biosensors and Biodetection*. 2009, Springer. p. 399-415.
37. Ellington, A.D. and J.W. Szostak, *In vitro selection of RNA molecules that bind specific ligands.* nature, 1990. **346**(6287): p. 818-822.
38. Tuerk, C. and L. Gold, *Systematic evolution of ligands by exponential enrichment: RNA ligands to bacteriophage T4 DNA polymerase.* Science, 1990. **249**(4968): p. 505-510.
39. Rosi, N.L. and C.A. Mirkin, *Nanostructures in biodiagnostics.* Chemical reviews, 2005. **105**(4): p. 1547-1562.
40. Seydack, M., *Nanoparticle labels in immunosensing using optical detection methods.* Biosensors and bioelectronics, 2005. **20**(12): p. 2454-2469.
41. Tansil, N.C. and Z. Gao, *Nanoparticles in biomolecular detection.* Nano Today, 2006. **1**(1): p. 28-37.
42. Willets, K.A. and R.P. Van Duyne, *Localized surface plasmon resonance spectroscopy and sensing.* Annu. Rev. Phys. Chem., 2007. **58**: p. 267-297.
43. Alivisatos, A.P., et al., *Organization of'nanocrystal molecules' using DNA*. Nature, 1996. **382**(6592): p. 609-611.

44. Li, F., et al., *Adenosine detection by using gold nanoparticles and designed aptamer sequences.* Analyst, 2009. **134**(7): p. 1355-1360.
45. Liu, J. and Y. Lu, *Fast colorimetric sensing of adenosine and cocaine based on a general sensor design involving aptamers and nanoparticles.* Angewandte Chemie, 2006. **118**(1): p. 96-100.
46. Liu, J. and Y. Lu, *Non-base pairing DNA provides a new dimension for controlling aptamer-linked nanoparticles and sensors.* Journal of the American Chemical Society, 2007. **129**(27): p. 8634-8643.
47. Medley, C.D., et al., *Gold nanoparticle-based colorimetric assay for the direct detection of cancerous cells.* Analytical chemistry, 2008. **80**(4): p. 1067-1072.
48. Mirkin, C.A., et al., *A DNA-based method for rationally assembling nanoparticles into macroscopic materials.* Nature, 1996. **382**(6592): p. 607-609.
49. Zhao, W., et al., *Simple and rapid colorimetric biosensors based on DNA aptamer and noncrosslinking gold nanoparticle aggregation.* ChemBioChem, 2007. **8**(7): p. 727-731.
50. Zhao, W., et al., *DNA aptamer folding on gold nanoparticles: from colloid chemistry to biosensors.* Journal of the American Chemical Society, 2008. **130**(11): p. 3610-3618.
51. Li, H. and L.J. Rothberg, *Label-free colorimetric detection of specific sequences in genomic DNA amplified by the polymerase chain reaction.* Journal of the American Chemical Society, 2004. **126**(35): p. 10958-10961.
52. Wang, L., et al., *Unmodified gold nanoparticles as a colorimetric probe for potassium DNA aptamers.* Chem. Commun., 2006(36): p. 3780-3782.
53. Liu, X., et al., *Colorimetric Sensing of Adenosine Based on Aptamer Binding Inducing Gold Nanoparticle Aggregation.* Chinese Journal of Chemistry, 2009. **27**(10): p. 1855-1859.
54. Zhang, J., et al., *Visual cocaine detection with gold nanoparticles and rationally engineered aptamer structures.* Small, 2008. **4**(8): p. 1196-1200.
55. Wang, J., et al., *A Gold Nanoparticle-Based Aptamer Target Binding Readout for ATP Assay.* Advanced Materials, 2007. **19**(22): p. 3943-3946.
56. Kim, Y.S., et al., *A novel colorimetric aptasensor using gold nanoparticle for a highly sensitive and specific detection of oxytetracycline.* Biosensors and Bioelectronics, 2010. **26**(4): p. 1644-1649.
57. Song, K.-M., et al., *Gold nanoparticle-based colorimetric detection of kanamycin using a DNA aptamer.* Analytical biochemistry, 2011. **415**(2): p. 175-181.

58. Song, K.-M., et al., *Aptasensor for ampicillin using gold nanoparticle based dual fluorescence–colorimetric methods.* Analytical and bioanalytical chemistry, 2012. **402**(6): p. 2153-2161.

59. He, L., et al., *A Colorimetric Aptamer Biosensor Based on Gold Nanoparticles for the Ultrasensitive and Specific Detection of Tetracycline in Milk.* Australian Journal of Chemistry, 2013. **66**(4): p. 485-490.

60. Zheng, Y., Y. Wang, and X. Yang, *Aptamer-based colorimetric biosensing of dopamine using unmodified gold nanoparticles.* Sensors and Actuators B: Chemical, 2011. **156**(1): p. 95-99.

61. Chang, C.-C., et al., *Aptamer-based colorimetric detection of platelet-derived growth factor using unmodified goldnanoparticles.* Biosensors and Bioelectronics, 2013. **42**: p. 119-123.

62. Stacy M. Crim, M., Martha Iwamoto, MD1, Jennifer Y. Huang, MPH1, Patricia M. Griffin, MD1, Debra Gilliss, MD2, Alicia B. Cronquist, MPH3, Matthew Cartter, MD4, Melissa Tobin-D'Angelo, MD5, David Blythe, MD6, Kirk Smith, DVM7, Sarah Lathrop, PhD8, Shelley Zansky, PhD9, Paul R. Cieslak, MD10, John Dunn, DVM11, Kristin G. Holt, DVM12, Susan Lance, DVM13, Robert Tauxe, MD1, Olga L. Henao, PhD1, *Incidence and Trends of Infection with Pathogens Transmitted Commonly Through Food — Foodborne Diseases Active Surveillance Network, 10 U.S. Sites, 2006–2013.* Morbidity and Mortality Weekly Report (MMWR), 2014. **63**(15): p. 328-332.

63. Vemula, S.R., R.N. Kumar, and K. Polasa, *Foodborne diseases in India–a review.* British Food Journal, 2012. **114**(5): p. 661-680.

64. *Timeline for Reporting Cases of E. coli O157 Infection*. Centre for Disease Control and Prvenetion; Available from: http://www.cdc.gov/ecoli/reporting-timeline.html.

65. Buchanan, A., *Foodborne disease significance of Escherichia coli O157: H7 and other enterohemorrhagic E. coli.* Food technology (USA), 1997.

66. Etcheverría, A.I. and N.L. Padola, *Shiga toxin-producing Escherichia coli: Factors involved in virulence and cattle colonization.* Virulence, 2013. **4**(5): p. 366.

67. Karmali, M.A., *Infection by verocytotoxin-producing Escherichia coli.* Clinical Microbiology Reviews, 1989. **2**(1): p. 15-38.

68. Law, D., *Virulence factors of Escherichia coli O157 and other Shiga toxin-producing E. coli.* Journal of Applied Microbiology, 2000. **88**(5): p. 729-745.

69. Swaminathan, B. and P. Feng, *Rapid detection of food-borne pathogenic bacteria.* Annual Reviews in Microbiology, 1994. **48**(1): p. 401-426.
70. Chapman, P.A., *Methods available for the detection of Escherichia coli O157 in clinical, food and environmental samples.* World Journal of Microbiology and Biotechnology, 2000. **16**(8-9): p. 733-740.
71. Gracias, K.S. and J.L. McKillip, *A review of conventional detection and enumeration methods for pathogenic bacteria in food.* Canadian journal of microbiology, 2004. **50**(11): p. 883-890.
72. Deisingh, A. and M. Thompson, *Strategies for the detection of Escherichia coli O157: H7 in foods.* Journal of applied microbiology, 2004. **96**(3): p. 419-429.
73. Banerjee, P. and A.K. Bhunia, *Cell-based biosensor for rapid screening of pathogens and toxins.* Biosensors and Bioelectronics, 2010. **26**(1): p. 99-106.
74. Leonard, P., et al., *Advances in biosensors for detection of pathogens in food and water.* Enzyme and Microbial Technology, 2003. **32**(1): p. 3-13.
75. Banada, P.P., et al., *Label-free detection of multiple bacterial pathogens using light-scattering sensor.* Biosensors and Bioelectronics, 2009. **24**(6): p. 1685-1692.
76. Killard, A.J., et al., *Antibodies: production, functions and applications in biosensors.* TrAC Trends in Analytical Chemistry, 1995. **14**(6): p. 257-266.
77. Byrne, B., et al., *Antibody-based sensors: principles, problems and potential for detection of pathogens and associated toxins.* Sensors, 2009. **9**(6): p. 4407-4445.
78. DeVinney, R., et al., *Enterohemorrhagic Escherichia coliO157: H7 produces Tir, which is translocated to the host cell membrane but is not tyrosine phosphorylated.* Infection and immunity, 1999. **67**(5): p. 2389-2398.
79. Ledesma, M.A., et al., *The hemorrhagic coli pilus (HCP) of Escherichia coli O157: H7 is an inducer of proinflammatory cytokine secretion in intestinal epithelial cells.* PloS one, 2010. **5**(8): p. e12127.
80. Wodtke, J. and J. Löhr, *Das infizierte Implantat.* Der Orthopäde, 2008. **37**(3): p. 257-269.
81. Hellmann, M., et al., *The estimated magnitude and direct hospital costs of prosthetic joint infections in the United States, 1997 to 2004.* The Journal of arthroplasty, 2010. **25**(5): p. 766-771. e1.
82. Sampedro, M.F. and R. Patel, *Infections associated with long-term prosthetic devices.* Infectious disease clinics of North America, 2007. **21**(3): p. 785-819.

83. Tokarczyk, A.J., S.B. Greenberg, and J.S. Vender, *Death, dollars, and diligence: Prevention of catheter-related bloodstream infections must persist!**. Critical care medicine, 2009. **37**(7): p. 2320-2321.

84. Magill, S.S., et al., *Multistate Point-Prevalence Survey of Health Care–Associated Infections.* New England Journal of Medicine, 2014. **370**(13): p. 1198-1208.

85. Smith, A.W., *Biofilms and antibiotic therapy: is there a role for combating bacterial resistance by the use of novel drug delivery systems?* Advanced drug delivery reviews, 2005. **57**(10): p. 1539-1550.

86. Levy, S.B. and B. Marshall, *Antibacterial resistance worldwide: causes, challenges and responses.* Nature medicine, 2004. **10**: p. S122-S129.

87. Knetsch, M.L. and L.H. Koole, *New strategies in the development of antimicrobial coatings: the example of increasing usage of silver and silver nanoparticles.* Polymers, 2011. **3**(1): p. 340-366.

88. Chen, M., Q. Yu, and H. Sun, *Novel strategies for the prevention and treatment of biofilm related infections.* International journal of molecular sciences, 2013. **14**(9): p. 18488-18501.

89. Hetrick, E.M. and M.H. Schoenfisch, *Reducing implant-related infections: active release strategies.* Chemical Society Reviews, 2006. **35**(9): p. 780-789.

90. Goodman, S.B., et al., *The future of biologic coatings for orthopaedic implants.* Biomaterials, 2013. **34**(13): p. 3174-3183.

91. Lara, H.H., et al., *Silver nanoparticles are broad-spectrum bactericidal and virucidal compounds.* J Nanobiotechnology, 2011. **9**(1): p. 30.

92. Veerapandian, M. and K. Yun, *Functionalization of biomolecules on nanoparticles: specialized for antibacterial applications.* Applied microbiology and biotechnology, 2011. **90**(5): p. 1655-1667.

93. Ernest, V., et al., *Enhanced activity of lysozyme-AgNP conjugate with synergic antibacterial effect without damaging the catalytic site of lysozyme.* Artificial Cells, Nanomedicine, and Biotechnology, 2013(0): p. 1-8.

94. Brown, A.N., et al., *Nanoparticles functionalized with ampicillin destroy multiple-antibiotic-resistant isolates of Pseudomonas aeruginosa and Enterobacter aerogenes and methicillin-resistant Staphylococcus aureus.* Applied and environmental microbiology, 2012. **78**(8): p. 2768-2774.

95. Liu, L., et al., *Self-assembled cationic peptide nanoparticles as an efficient antimicrobial agent.* Nature nanotechnology, 2009. **4**(7): p. 457-463.

96. Wang, H., et al., *The efficacy of self-assembled cationic antimicrobial peptide nanoparticles against Cryptococcus neoformans for the treatment of meningitis.* Biomaterials, 2010. **31**(10): p. 2874-2881.

97. Hancock, R.E. and H.-G. Sahl, *Antimicrobial and host-defense peptides as new anti-infective therapeutic strategies.* Nature biotechnology, 2006. **24**(12): p. 1551-1557.

98. Petty, J.T., et al., *DNA-templated Ag nanocluster formation.* Journal of the American Chemical Society, 2004. **126**(16): p. 5207-5212.

99. Jones, M.R., et al., *Templated techniques for the synthesis and assembly of plasmonic nanostructures.* Chemical reviews, 2011. **111**(6): p. 3736-3827.

100. *History of Cow's Milk from the Ancient World to the Present.* Milk Pros and Cons, 2013.

101. India, F.S.a.S.A.o., *Adulteration in milk and Milk products.*

102. Paradkar, M.M., R.S. Singhal, and P.R. Kulkarni, *An approach to the detection of synthetic milk in dairy milk: 1. Detection of urea.* International journal of dairy technology, 2000. **53**(3): p. 87-91.

103. Trivedi, U., et al., *Potentiometric biosensor for urea determination in milk.* Sensors and Actuators B: Chemical, 2009. **140**(1): p. 260-266.

104. PFA, *The Prevention of Food Adulteration Act 1954 (Act No. 37 of 1954) with the prevention of food adulteration rules, 1955 and notifications.* Allahabad: Law Publishers (India), 2006.

105. Spencer, K., *Analytical reviews in clinical biochemistry: the estimation of creatinine.* Annals of clinical biochemistry, 1986. **23**: p. 1-25.

106. Jenkins, D., et al., *Refinement of the pressure assay for milk urea nitrogen.* Journal of dairy science, 2000. **83**(9): p. 2042-2048.

107. Della Ciana, L. and G. Caputo, *Robust, reliable biosensor for continuous monitoring of urea during dialysis.* Clinical chemistry, 1996. **42**(7): p. 1079-1085.

108. Singh, M., et al., *Urea biosensors.* Sensors and Actuators B: Chemical, 2008. **134**(1): p. 345-351.

109. Renny, E., et al., *Enzyme based sensor for detection of urea in milk.* Biotechnology & Biotechnological Equipment, 2005. **19**(2): p. 198-201.

110. Jonker, J., R. Kohn, and R. Erdman, *Using milk urea nitrogen to predict nitrogen excretion and utilization efficiency in lactating dairy cows.* Journal of dairy science, 1998. **81**(10): p. 2681-2692.

111. Kohn, R., *Caution needed when interpreting MUN.* Hoard's Dairyman, 2000. **145**(2): p. 58.

112. Lima, J.L., C. Delerue-Matos, and M.C.V. Vaz, *Flow injection system with potentiometric detection for the determination of urea content in milks.* Journal of Agricultural and Food Chemistry, 1998. **46**(4): p. 1386-1389.

113. Lefier, D., *Analytical Methods for the Determination of the Urea Content in Milk.* Bulletin of the IDF No. 315/1996 - UHT cream 1996: p. 58.

114. Ormsby, A.A., *A direct colorimetric method for the determination of urea in blood and urine.* Journal of Biological Chemistry, 1942. **146**(2): p. 595-604.

115. Butler, A.R. and D. Walsh, *Colorimetric non-enzymic methods for the determination of urea: Consideration of the chemical principles upon which an analytical method is based is an essential step in the optimization of that method. It can also contribute to the simplification of procedures used and hence cut the costs of many routine analyses.* TrAC Trends in Analytical Chemistry, 1982. **1**(5): p. 120-124.

116. Francis, P.S., S.W. Lewis, and K.F. Lim, *Analytical methodology for the determination of urea: current practice and future trends.* TrAC trends in analytical chemistry, 2002. **21**(5): p. 389-400.

117. Fearon, V., *Urea determination.* Biochem J, 1939. **43**: p. 305-310.

118. Wheatley, V., *An improved diacetyl reaction for the estimation of urea in blood.* Biochemical Journal, 1948. **43**(3): p. 420.

119. Rosenthal, H.L., *Determination of urea in blood and urine with diacetyl monoxime.* Analytical Chemistry, 1955. **27**(12): p. 1980-1982.

120. Evans, R., *Manual and automated methods for measuring urea based on a modification of its reaction with diacetyl monoxime and thiosemicarbazide.* Journal of clinical pathology, 1968. **21**(4): p. 527.

121. Sullivan, D. and J. Havlin, *Flow injection analysis of urea nitrogen in soil extracts.* Soil Science Society of America Journal, 1991. **55**(1): p. 109-113.

122. Mulvenna, P.F. and G. Savidge, *A modified manual method for the determination of urea in seawater using diacetylmonoxime reagent.* Estuarine, coastal and shelf science, 1992. **34**(5): p. 429-438.

123. Malhotra, B.D., A. Chaubey, and S. Singh, *Prospects of conducting polymers in biosensors.* Analytica Chimica Acta, 2006. **578**(1): p. 59-74.

124. Şehitoğullari, A. and A.H. Uslan, *Preparation of a potentiometric immobilized urease electrode and urea determination in serum.* Talanta, 2002. **57**(6): p. 1039-1044.

125. Lakard, B., et al., *Urea potentiometric biosensor based on modified electrodes with urease immobilized on polyethylenimine films.* Biosensors and Bioelectronics, 2004. **19**(12): p. 1641-1647.
126. Kuralay, F., H. Özyörük, and A. Yıldız, *Potentiometric enzyme electrode for urea determination using immobilized urease in poly (vinylferrocenium) film.* Sensors and Actuators B: Chemical, 2005. **109**(2): p. 194-199.
127. Marzadori, C., et al., *Immobilization of jack bean urease on hydroxyapatite: urease immobilization in alkaline soils.* Soil Biology and Biochemistry, 1998. **30**(12): p. 1485-1490.
128. Ruzicka, J., et al., *Enzymic determination of urea in serum based on pH measurement with the flow injection method.* Analytical chemistry, 1979. **51**(2): p. 199-203.
129. Vadgama, P., K. Alberti, and A. Covington, *Determination of urea in blood plasma by enzyme-pH electrode.* Analytica Chimica Acta, 1982. **136**: p. 403-406.
130. Eggenstein, C., et al., *A disposable biosensor for urea determination in blood based on an ammonium-sensitive transducer.* Biosensors and Bioelectronics, 1999. **14**(1): p. 33-41.
131. Guilbault, G.G. and J.G. Montalvo Jr, *Urea-specific enzyme electrode.* Journal of the American Chemical Society, 1969. **91**(8): p. 2164-2165.
132. Petersson, B.A., *Enzymatic determination of urea in undiluted whole blood by flow injection analysis using an ammonium ion-selective electrode.* Analytica chimica acta, 1988. **209**: p. 239-248.
133. Alegret, S. and E. Martínez-Fàbregas, *Biosensors based on conducting filled polymer all-solid-state PVC matrix membrane electrodes.* Biosensors, 1989. **4**(5): p. 287-297.
134. Rosario, S., et al., *Use of ionomer membranes to enhance the selectivity of electrode-based biosensors in flow-injection analysis.* Analytical chemistry, 1990. **62**(22): p. 2418-2424.
135. Wałcerz, I., et al., *Enzyme biosensors for urea determination based on an ionophore free pH membrane electrode.* Analytica chimica acta, 1995. **315**(3): p. 289-296.
136. Tinkilic, N., O. Cubuk, and I. Isildak, *Glucose and urea biosensors based on all solid-state PVC–NH_2 membrane electrodes.* Analytica chimica acta, 2002. **452**(1): p. 29-34.
137. Kovács, B., et al., *Optical biosensor for urea with improved response time.* Biosensors and Bioelectronics, 2003. **18**(2): p. 111-118.
138. Foulds, N.C. and C.R. Lowe, *Enzyme entrapment in electrically conducting polymers. Immobilisation of glucose oxidase in polypyrrole and its application in amperometric*

glucose sensors. Journal of the Chemical Society, Faraday Transactions 1: Physical Chemistry in Condensed Phases, 1986. **82**(4): p. 1259-1264.

139. Fortier, G., E. Brassard, and D. Belanger, *Optimization of a polypyrrole glucose oxidase biosensor.* Biosensors and Bioelectronics, 1990. **5**(6): p. 473-490.
140. Wolowacz, S.E., B. Yon Hin, and C.R. Lowe, *Covalent electropolymerization of glucose oxidase in polypyrrole.* Analytical chemistry, 1992. **64**(14): p. 1541-1545.
141. Kaku, T., H.I. Karan, and Y. Okamoto, *Amperometric glucose sensors based on immobilized glucose oxidase-polyquinone system.* Analytical chemistry, 1994. **66**(8): p. 1231-1235.
142. de Marcos, S., et al., *Characterization of a urea optical sensor based on polypyrrole.* Microchimica Acta, 1999. **130**(4): p. 267-272.
143. Komaba, S., et al., *Potentiometric biosensor for urea based on electropolymerized electroinactive polypyrrole.* Electrochimica acta, 1997. **42**(3): p. 383-388.
144. Adeloju, S., S. Shaw, and G. Wallace, *Pulsed-amperometric detection of urea in blood samples on a conducting polypyrrole-urease biosensor.* Analytica chimica acta, 1997. **341**(2): p. 155-160.
145. Adeloju, S.B., S.J. Shaw, and G.G. Wallace, *Polypyrrole-based amperometric flow injection biosensor for urea.* Analytica chimica acta, 1996. **323**(1): p. 107-113.
146. Bisht, V., W. Takashima, and K. Kaneto, *A novel thin film urea biosensor based on copolymer poly (N-3-aminopropylpyrrole-co-pyrrole) film.* Surface and Coatings Technology, 2005. **198**(1): p. 231-236.
147. Adeloju, S., S. Shaw, and G. Wallace, *Polypyrrole-based potentiometric biosensor for urea: Part 2. Analytical optimisation.* Analytica Chimica Acta, 1993. **281**(3): p. 621-627.
148. Pandey, P.C. and G. Singh, *Tetraphenylborate doped polyaniline based novel pH sensor and solid-state urea biosensor.* Talanta, 2001. **55**(4): p. 773-782.
149. Massafera, M.P. and S.I. Torresi, *Urea amperometric biosensors based on a multifunctional bipolymeric layer: Comparing enzyme immobilization methods.* Sensors and Actuators B: Chemical, 2009. **137**(2): p. 476-482.
150. Chirizzi, D. and C. Malitesta, *Potentiometric urea biosensor based on urease immobilized by an electrosynthesized poly (o-phenylenediamine) film with buffering capability.* Sensors and Actuators B: Chemical, 2011. **157**(1): p. 211-215.

151. Lakard, B., et al., *Urea potentiometric enzymatic biosensor based on charged biopolymers and electrodeposited polyaniline.* Biosensors and Bioelectronics, 2011. **26**(10): p. 4139-4145.
152. Huang, C.-Y., et al., *Urinalysis with molecularly imprinted poly (ethylene-co-vinyl alcohol) potentiostat sensors.* Biosensors and Bioelectronics, 2009. **24**(8): p. 2611-2617.
153. Alizadeh, T. and A. Akbari, *A capacitive biosensor for ultra-trace level urea determination based on nano-sized urea-imprinted polymer receptors coated on graphite electrode surface.* Biosensors and Bioelectronics, 2013. **43**: p. 321-327.
154. Lee, W.-Y., et al., *Sol–gel-derived thick-film conductometric biosensor for urea determination in serum.* Analytica chimica acta, 2000. **404**(2): p. 195-203.
155. Tsai, H.-c. and R.-a. Doong, *Simultaneous determination of pH, urea, acetylcholine and heavy metals using array-based enzymatic optical biosensor.* Biosensors and Bioelectronics, 2005. **20**(9): p. 1796-1804.
156. Sahney, R., et al., *A comparative study of immobilization techniques for urease on glass-pH-electrode and its application in urea detection in blood serum.* Analytica chimica acta, 2006. **578**(2): p. 156-161.
157. Singhal, R., et al., *Immobilization of urease on poly (N-vinyl carbazole)/stearic acid Langmuir–Blodgett films for application to urea biosensor.* Biosensors and Bioelectronics, 2002. **17**(8): p. 697-703.
158. Zhang, A., et al., *Mixed urease/amphiphile LB films and their application for biosensor development.* Bioelectrochemistry, 2002. **56**(1): p. 157-158.
159. Han, B.Q., E.J. Lavernia, and F.A. Mohamed, *Mechanical properties of nanostructured materials.* Rev. Adv. Mater. Sci, 2005. **9**(1): p. 1-16.
160. Bell, A.T., *The impact of nanoscience on heterogeneous catalysis.* Science, 2003. **299**(5613): p. 1688-1691.
161. Rieth, M., W. Schommers, and S. Baskoutas, *Thermal Stability and Specific Material Properties of Nanosystems.* Modern Physics Letters B, 2000. **14**(17n18): p. 621-629.
162. Atwater, H.A. and A. Polman, *Plasmonics for improved photovoltaic devices.* Nature materials, 2010. **9**(3): p. 205-213.
163. Baetzold, R., *Electronic properties of metal clusters: Size effects.* Inorganic Chemistry, 1981. **20**(1): p. 118-123.

164. Kim, W.Y., et al., *Application of quantum chemistry to nanotechnology: electron and spin transport in molecular devices.* Chemical Society Reviews, 2009. **38**(8): p. 2319-2333.

165. Pandey, P., M. Datta, and B. Malhotra, *Prospects of nanomaterials in biosensors.* Analytical Letters, 2008. **41**(2): p. 159-209.

166. Asefa, T., C.T. Duncan, and K.K. Sharma, *Recent advances in nanostructured chemosensors and biosensors.* Analyst, 2009. **134**(10): p. 1980-1990.

167. Yang, Y., et al., *Inhibitive determination of mercury ion using a renewable urea biosensor based on self-assembled gold nanoparticles.* Sensors and Actuators B: Chemical, 2006. **114**(1): p. 1-8.

168. Grabar, K.C., et al., *Preparation and characterization of Au colloid monolayers.* Analytical chemistry, 1995. **67**(4): p. 735-743.

169. Tiwari, A., et al., *An amperometric urea biosensor based on covalently immobilized urease on an electrode made of hyperbranched polyester functionalized gold nanoparticles.* Talanta, 2009. **78**(4): p. 1401-1407.

170. Tyagi, M., M. Tomar, and V. Gupta, *NiO nanoparticle-based urea biosensor.* Biosensors and Bioelectronics, 2013. **41**: p. 110-115.

171. Tyagi, M., M. Tomar, and V. Gupta, *Glad assisted synthesis of NiO nanorods for realization of enzymatic reagentless urea biosensor.* Biosensors and Bioelectronics, 2014. **52**: p. 196-201.

172. Huang, C.-P., Y.-K. Li, and T.-M. Chen, *A highly sensitive system for urea detection by using CdSe/ZnS core-shell quantum dots.* Biosensors and Bioelectronics, 2007. **22**(8): p. 1835-1838.

173. Duong, H.D. and J.I. Rhee, *Use of CdSe/ZnS luminescent quantum dots incorporated within sol–gel matrix for urea detection.* Analytica chimica acta, 2008. **626**(1): p. 53-61.

174. Lian, H.-T., et al., *A urea electrochemical sensor based on molecularly imprinted chitosan film doping with CdS quantum dots.* Analytical biochemistry, 2012. **426**(1): p. 40-46.

175. Azadbakht, A. and M.B. Gholivand, *Covalent attachment of Ni-2, 3-pyrazine dicarboxylic acid onto gold nanoparticle gold electrode modified with penicillamine-CdS quantum dots for electrocatalytic oxidation and determination of urea.* Electrochimica Acta, 2014. **125**: p. 9-21.

176. Sawicka, K., P. Gouma, and S. Simon, *Electrospun biocomposite nanofibers for urea biosensing.* Sensors and Actuators B: Chemical, 2005. **108**(1): p. 585-588.
177. Jin, J.H., Paek, S.H., Lee, C.W., Min, N.K., Hong, S.I., *Fabrication of amperometric urea sensor based on nano-porous silicon technology* Journal of the Korean Physical Society, 2003. **42**(SPEC.,): p. S735-S738.
178. Yun, D.H., Song, M.J., Hong, S.I. , Kang, M.S., Min, N.K., *Highly sensitive and renewable amperometric urea sensor based on self-assembled monolayer using porous silicon substrate.* Journal of the Korean Physical Society, 2005. **47**(SUPPL. 3): p. S445-S449.
179. Shalini, J., et al., *An amperometric urea bisosensor based on covalent immobilization of urease on N_2 incorporated diamond nanowire electrode.* Biosensors and Bioelectronics, 2014. **56**: p. 64-70.
180. Gabrovska, K., et al., *Immobilization of urease on nanostructured polymer membrane and preparation of urea amperometric biosensor.* International journal of biological macromolecules, 2011. **48**(4): p. 620-626.
181. Bhatia, P. and B.D. Gupta, *Fabrication and characterization of a surface plasmon resonance based fiber optic urea sensor for biomedical applications.* Sensors and Actuators B: Chemical, 2012. **161**(1): p. 434-438.
182. Yang, Z. and C. Zhang, *Single-enzyme nanoparticles based urea biosensor.* Sensors and Actuators B: Chemical, 2013. **188**: p. 313-317.
183. Berens, C., A. Thain, and R. Schroeder, *A tetracycline-binding RNA aptamer.* Bioorganic & medicinal chemistry, 2001. **9**(10): p. 2549-2556.
184. Duan, N., et al., *In vitro selection of a DNA aptamer targeted against Shigella dysenteriae.* Journal of microbiological methods, 2013. **94**(3): p. 170-174.
185. Ferreira, C., C. Matthews, and S. Missailidis, *DNA aptamers that bind to MUC1 tumour marker: design and characterization of MUC1-binding single-stranded DNA aptamers.* Tumor Biology, 2006. **27**(6): p. 289-301.
186. Sun, W., L. Du, and M. Li, *Aptamer-based carbohydrate recognition.* Current pharmaceutical design, 2010. **16**(20): p. 2269-2278.
187. Fang, X. and W. Tan, *Aptamers generated from cell-SELEX for molecular medicine: a chemical biology approach.* Accounts of chemical research, 2009. **43**(1): p. 48-57.
188. Tang, Z., et al., *Selection of aptamers for molecular recognition and characterization of cancer cells.* Analytical chemistry, 2007. **79**(13): p. 4900-4907.
189. Mascini, M., *Aptamers in bioanalysis*. 2009: John Wiley & Sons.

190. Fowler, C.C. and Y. Li, *Aptamers and small molecules play tug of war.* Chemistry & biology, 2007. **14**(7): p. 736-738.
191. Jayasena, S.D., *Aptamers: an emerging class of molecules that rival antibodies in diagnostics.* Clinical chemistry, 1999. **45**(9): p. 1628-1650.
192. Cho, M.J. and R. Juliano, *Macromolecular versus smallmolecule therapeutics: drug discovery, development and clinical considerations.* Trends in biotechnology, 1996. **14**(5): p. 153-158.
193. Ashour, M.L. and M. Wink, *Genus Bupleurum: a review of its phytochemistry, pharmacology and modes of action.* Journal of Pharmacy and Pharmacology, 2011. **63**(3): p. 305-321.
194. Roemer, T., et al., *Bugs, drugs and chemical genomics.* Nature chemical biology, 2012. **8**(1): p. 46-56.
195. Mascini, M., I. Palchetti, and S. Tombelli, *Nucleic acid and peptide aptamers: fundamentals and bioanalytical aspects.* Angewandte Chemie International Edition, 2012. **51**(6): p. 1316-1332.
196. Jenison, R.D., et al., *High-resolution molecular discrimination by RNA.* Science, 1994. **263**(5152): p. 1425-1429.
197. Michaud, M., et al., *A DNA aptamer as a new target-specific chiral selector for HPLC.* Journal of the American Chemical Society, 2003. **125**(28): p. 8672-8679.
198. Famulok, M. and J.W. Szostak, *Stereospecific recognition of tryptophan agarose by in vitro selected RNA.* Journal of the American Chemical Society, 1992. **114**(10): p. 3990-3991.
199. Famulok, M., *Molecular recognition of amino acids by RNA-aptamers: an L-citrulline binding RNA motif and its evolution into an L-arginine binder.* Journal of the American Chemical Society, 1994. **116**(5): p. 1698-1706.
200. Geiger, A., et al., *RNA aptamers that bind L-arginine with sub-micromolar dissociation constants and high enantioselectivity.* Nucleic acids research, 1996. **24**(6): p. 1029-1036.
201. Shoji, A., et al., *Modified DNA aptamer that binds the (R)-isomer of a thalidomide derivative with high enantioselectivity.* Journal of the American Chemical Society, 2007. **129**(5): p. 1456-1464.
202. Kim, Y.S., et al., *Isolation and characterization of enantioselective DNA aptamers for ibuprofen.* Bioorganic & medicinal chemistry, 2010. **18**(10): p. 3467-3473.

203. Carothers, J.M., et al., *Selecting RNA aptamers for synthetic biology: investigating magnesium dependence and predicting binding affinity.* Nucleic acids research, 2010: p. gkq082.
204. Mandal, M., et al., *Riboswitches Control Fundamental Biochemical Pathways in< i> Bacillus subtilis</i> and Other Bacteria.* Cell, 2003. **113**(5): p. 577-586.
205. Welz, R. and R.R. Breaker, *Ligand binding and gene control characteristics of tandem riboswitches in Bacillus anthracis.* Rna, 2007. **13**(4): p. 573-582.
206. Butler, E.B., et al., *Structural basis of cooperative ligand binding by the glycine riboswitch.* Chemistry & biology, 2011. **18**(3): p. 293-298.
207. Burgstaller, P. and M. Famulok, *Isolation of RNA aptamers for biological cofactors by in vitro selection.* Angewandte Chemie International Edition in English, 1994. **33**(10): p. 1084-1087.
208. Lato, S.M., A.R. Boles, and A.D. Ellington, *In vitro selection of RNA lectins: using combinatorial chemistry to interpret ribozyme evolution.* Chemistry & Biology, 1995. **2**(5): p. 291-303.
209. Lauhon, C.T. and J.W. Szostak, *RNA aptamers that bind flavin and nicotinamide redox cofactors.* Journal of the American Chemical Society, 1995. **117**(4): p. 1246-1257.
210. Huizenga, D.E. and J.W. Szostak, *A DNA aptamer that binds adenosine and ATP.* Biochemistry, 1995. **34**(2): p. 656-665.
211. Harada, K. and A.D. Frankel, *Identification of two novel arginine binding DNAs.* The EMBO journal, 1995. **14**(23): p. 5798.
212. Mannironi, C., et al., *In vitro selection of dopamine RNA ligands.* Biochemistry, 1997. **36**(32): p. 9726-9734.
213. Majerfeld, I. and M. Yarus, *An RNA pocket for an aliphatic hydrophobe.* Nature Structural & Molecular Biology, 1994. **1**(5): p. 287-292.
214. Wallace, S.T. and R. Schroeder, *In vitro selection and characterization of streptomycin-binding RNAs: recognition discrimination between antibiotics.* Rna, 1998. **4**(1): p. 112-123.
215. Majerfeld, I. and M. Yarus, *Isoleucine: RNA sites with associated coding sequences.* Rna, 1998. **4**(4): p. 471-478.
216. Baugh, C., D. Grate, and C. Wilson, *2.8 Å crystal structure of the malachite green aptamer.* Journal of molecular biology, 2000. **301**(1): p. 117-128.
217. Koizumi, M. and R.R. Breaker, *Molecular recognition of cAMP by an RNA aptamer.* Biochemistry, 2000. **39**(30): p. 8983-8992.

218. Jhaveri, S., M. Rajendran, and A.D. Ellington, *In vitro selection of signaling aptamers.* Nature biotechnology, 2000. **18**(12): p. 1293-1297.

219. Mannironi, C., et al., *Molecular recognition of amino acids by RNA aptamers: the evolution into an L-tyrosine binder of a dopamine-binding RNA motif.* Rna, 2000. **6**(4): p. 520-527.

220. Gebhardt, K., et al., *RNA aptamers to S-adenosylhomocysteine: kinetic properties, divalent cation dependency, and comparison with anti-S-adenosylhomocysteine antibody.* Biochemistry, 2000. **39**(24): p. 7255-7265.

221. Cowan, J., et al., *Recognition of a cognate RNA aptamer by neomycin B: quantitative evaluation of hydrogen bonding and electrostatic interactions.* Nucleic acids research, 2000. **28**(15): p. 2935-2942.

222. Vianini, E., M. Palumbo, and B. Gatto, *In vitro selection of DNA aptamers that bind L-tyrosinamide.* Bioorganic & medicinal chemistry, 2001. **9**(10): p. 2543-2548.

223. Roychowdhury-Saha, M., et al., *Flavin recognition by an RNA aptamer targeted toward FAD.* Biochemistry, 2002. **41**(8): p. 2492-2499.

224. Vaish, N.K., et al., *A novel, modification-dependent ATP-binding aptamer selected from an RNA library incorporating a cationic functionality.* Biochemistry, 2003. **42**(29): p. 8842-8851.

225. Goertz, P.W., J.C. Cox, and A.D. Ellington, *Automated selection of aminoglycoside aptamers.* Journal of the Association for Laboratory Automation, 2004. **9**(3): p. 150-154.

226. Sazani, P.L., R. Larralde, and J.W. Szostak, *A small aptamer with strong and specific recognition of the triphosphate of ATP.* Journal of the American Chemical Society, 2004. **126**(27): p. 8370-8371.

227. Win, M.N., J.S. Klein, and C.D. Smolke, *Codeine-binding RNA aptamers and rapid determination of their binding constants using a direct coupling surface plasmon resonance assay.* Nucleic acids research, 2006. **34**(19): p. 5670-5682.

228. Niazi, J.H., et al., *ssDNA aptamers that selectively bind oxytetracycline.* Bioorganic & medicinal chemistry, 2008. **16**(3): p. 1254-1261.

229. Cruz-Aguado, J.A. and G. Penner, *Determination of ochratoxin A with a DNA aptamer.* Journal of agricultural and food chemistry, 2008. **56**(22): p. 10456-10461.

230. Walsh, R. and M.C. DeRosa, *Retention of function in the DNA homolog of the RNA dopamine aptamer.* Biochemical and biophysical research communications, 2009. **388**(4): p. 732-735.

231. Joeng, C.B., et al., *ssDNA aptamers that recognize diclofenac and 2-anilinophenylacetic acid.* Bioorganic & medicinal chemistry, 2009. **17**(15): p. 5380-5387.

232. Yang, X., et al., *Characterization and application of a DNA aptamer binding to L-tryptophan.* Analyst, 2011. **136**(3): p. 577-585.

233. Barthelmebs, L., et al., *Enzyme-linked aptamer assays (ELAAs), based on a competition format for a rapid and sensitive detection of ochratoxin A in wine.* Food control, 2011. **22**(5): p. 737-743.

234. Mehta, J., et al., *Selection and characterization of PCB-binding DNA aptamers.* Analytical chemistry, 2012. **84**(3): p. 1669-1676.

235. Wilson, C. and J.W. Szostak, *Isolation of a fluorophore-specific DNA aptamer with weak redox activity.* Chemistry & biology, 1998. **5**(11): p. 609-617.

236. Yao, C., et al., *Aptamer-based piezoelectric quartz crystal microbalance biosensor array for the quantification of IgE.* Biosensors and Bioelectronics, 2009. **24**(8): p. 2499-2503.

237. Hu, J. and C.J. Easley, *A simple and rapid approach for measurement of dissociation constants of DNA aptamers against proteins and small molecules via automated microchip electrophoresis.* Analyst, 2011. **136**(17): p. 3461-3468.

238. Nguyen, T.-H., et al., *Measuring single small molecule binding via rupture forces of a split aptamer.* Journal of the American Chemical Society, 2011. **133**(7): p. 2025-2027.

239. Arghya, S., et al., *Aptasensors in Health, Environment and Food Safety Monitoring.* Open Journal of Applied Biosensor, 2012. **2012**.

240. Babu, P.J., et al., *Green synthesis of biocompatible gold nanoparticles using Fagopyrum esculentum leaf extract.* Frontiers of Materials Science, 2011. **5**(4): p. 379-387.

241. Chauhan, A., et al., *Fungus-mediated biological synthesis of gold nanoparticles: potential in detection of liver cancer.* International journal of Nanomedicine, 2011. **6**: p. 2305.

242. Chen, T., et al., *Aptamer-conjugated nanomaterials for bioanalysis and biotechnology applications.* Nanoscale, 2011. **3**(2): p. 546-556.

243. Khan, A., et al., *Gold Nanoparticles: Synthesis and Applications in Drug Delivery.* Tropical Journal of Pharmaceutical Research, 2014. **13**(7): p. 1169-1177.

244. Menon, S.K., et al., *Analytical detection and method development of anticancer drug Gemcitabine HCl using gold nanoparticles.* Spectrochimica Acta Part A: Molecular and Biomolecular Spectroscopy, 2012. **94**: p. 235-242.
245. Das, R.K., et al., *Synthesis of gold nanoparticles using aqueous extract of Calotropis procera latex.* Materials Letters, 2011. **65**(4): p. 610-613.
246. Lodha, A., et al., *Melamine modified gold nanoprobe for "on-spot" colorimetric recognition of clonazepam from biological specimens.* Analyst, 2013. **138**(18): p. 5411-5416.
247. CooperáStevenson, P., *A study of the nucleation and growth processes in the synthesis of colloidal gold.* Discussions of the Faraday Society, 1951. **11**: p. 55-75.
248. Pandey, P., et al., *Application of thiolated gold nanoparticles for the enhancement of glucose oxidase activity.* Langmuir, 2007. **23**(6): p. 3333-3337.
249. Frens, G., *Particle size and sol stability in metal colloids.* Kolloid-Zeitschrift und Zeitschrift für Polymere, 1972. **250**(7): p. 736-741.
250. Frens, G., *Controlled nucleation for the regulation of the particle size in monodisperse gold suspensions.* Nature, 1973. **241**(105): p. 20-22.
251. Perrault, S.D. and W.C. Chan, *Synthesis and surface modification of highly monodispersed, spherical gold nanoparticles of 50− 200 nm.* Journal of the American Chemical Society, 2009. **131**(47): p. 17042-17043.
252. Brust, M., et al., *Synthesis of thiol-derivatised gold nanoparticles in a two-phase liquid–liquid system.* J. Chem. Soc., Chem. Commun., 1994(7): p. 801-802.
253. Du, Y., B. Li, and E. Wang, *Analytical potential of gold nanoparticles in functional aptamer-based biosensors.* Bioanalytical Reviews, 2010. **1**(2-4): p. 187-208.
254. Shenoy, D., et al., *Surface functionalization of gold nanoparticles using hetero-bifunctional poly (ethylene glycol) spacer for intracellular tracking and delivery.* International journal of nanomedicine, 2006. **1**(1): p. 51.
255. Thomas, K.G. and P.V. Kamat, *Chromophore-functionalized gold nanoparticles.* Accounts of chemical research, 2003. **36**(12): p. 888-898.
256. Zeng, S., et al., *A review on functionalized gold nanoparticles for biosensing applications.* Plasmonics, 2011. **6**(3): p. 491-506.
257. Chen, S.-J., et al., *Colorimetric determination of urinary adenosine using aptamer-modified gold nanoparticles.* Biosensors and Bioelectronics, 2008. **23**(11): p. 1749-1753.

258. Liu, J. and Y. Lu, *Adenosine-dependent assembly of aptazyme-functionalized gold nanoparticles and its application as a colorimetric biosensor.* Analytical chemistry, 2004. **76**(6): p. 1627-1632.

259. Liu, J. and Y. Lu, *Smart nanomaterials responsive to multiple chemical stimuli with controllable cooperativity.* Advanced Materials, 2006. **18**(13): p. 1667-1671.

260. Sato, K., K. Hosokawa, and M. Maeda, *Rapid aggregation of gold nanoparticles induced by non-cross-linking DNA hybridization.* Journal of the American Chemical Society, 2003. **125**(27): p. 8102-8103.

261. Zhang, Z., C. Chen, and X. Sheng Zhao, *A Simple and Sensitive Biosensor Based on Silver Enhancement of Aptamer-Gold Nanoparticle Aggregation.* Electroanalysis, 2009. **21**(11): p. 1316-1320.

262. Yang, C., et al., *Aptamer-based colorimetric biosensing of Ochratoxin A using unmodified gold nanoparticles indicator.* Biosensors and Bioelectronics, 2011. **26**(5): p. 2724-2727.

263. Mei, Z., et al., *Ultrasensitive one-step rapid visual detection of bisphenol A in water samples by label-free aptasensor.* Biosensors and Bioelectronics, 2013. **39**(1): p. 26-30.

264. Robinson, A.L. and J.L. McKillip, *Biology of Escherichia coli O157: H7 in human health and food safety with emphasis on sublethal injury and detection.* Current research, technology and education topics in applied microbiology and microbial biotechnology, 2010. **2**: p. 1096-1105.

265. Paton, J.C. and A.W. Paton, *Pathogenesis and diagnosis of Shiga toxin-producing Escherichia coli infections.* Clinical microbiology reviews, 1998. **11**(3): p. 450-479.

266. Nataro, J.P. and J.B. Kaper, *Diarrheagenic escherichia coli.* Clinical microbiology reviews, 1998. **11**(1): p. 142-201.

267. McKee, M.L., et al., *Enterohemorrhagic Escherichia coli O157: H7 requires intimin to colonize the gnotobiotic pig intestine and to adhere to HEp-2 cells.* Infection and Immunity, 1995. **63**(9): p. 3739-3744.

268. Torres, A.G. and J.B. Kaper, *Multiple elements controlling adherence of enterohemorrhagic Escherichia coli O157: H7 to HeLa cells.* Infection and immunity, 2003. **71**(9): p. 4985-4995.

269. Perna, N.T., et al., *Genome sequence of enterohaemorrhagic Escherichia coli O157: H7.* Nature, 2001. **409**(6819): p. 529-533.

270. Low, A.S., et al., *Analysis of fimbrial gene clusters and their expression in enterohaemorrhagic Escherichia coli O157: H7.* Environmental microbiology, 2006. **8**(6): p. 1033-1047.

271. Xicohtencatl-Cortes, J., et al., *Intestinal adherence associated with type IV pili of enterohemorrhagic Escherichia coli O157: H7.* Journal of Clinical Investigation, 2007. **117**(11): p. 3519-3529.

272. Rendón, M.a.A., et al., *Commensal and pathogenic Escherichia coli use a common pilus adherence factor for epithelial cell colonization.* Proceedings of the National Academy of Sciences, 2007. **104**(25): p. 10637-10642.

273. Xicohtencatl-Cortes, J., et al., *The type 4 pili of enterohemorrhagic Escherichia coli O157: H7 are multipurpose structures with pathogenic attributes.* Journal of bacteriology, 2009. **191**(1): p. 411-421.

274. March, S.B. and S. Ratnam, *Sorbitol-MacConkey medium for detection of Escherichia coli O157: H7 associated with hemorrhagic colitis.* Journal of Clinical Microbiology, 1986. **23**(5): p. 869-872.

275. Silk, T.M. and C.W. Donnelly, *Increased detection of acid-injured Escherichia coli O157: H7 in autoclaved apple cider by using nonselective repair on trypticase soy agar.* Journal of Food Protection®, 1997. **60**(12): p. 1483-1486.

276. Adams, M.R.a.M., M.O., *Food Microbiology.* Cambridge:The Royal Society of Chemistry, 1995.

277. Cebula, T.A., W.L. Payne, and P. Feng, *Simultaneous identification of strains of Escherichia coli serotype O157: H7 and their Shiga-like toxin type by mismatch amplification mutation assay-multiplex PCR.* Journal of Clinical Microbiology, 1995. **33**(1): p. 248-250.

278. Paton, A.W. and J.C. Paton, *Detection and Characterization of Shiga ToxigenicEscherichia coli by Using Multiplex PCR Assays forstx 1, stx 2, eaeA, Enterohemorrhagic E. coli hlyA, rfb O111, andrfb O157.* Journal of Clinical Microbiology, 1998. **36**(2): p. 598-602.

279. Fratamico, P.M., et al., *Detection of Escherichia coli O157: H7 by multiplex PCR.* Journal of Clinical Microbiology, 1995. **33**(8): p. 2188-2191.

280. Bellin, T., et al., *Rapid detection of enterohemorrhagic escherichia coliby real-time pcr with fluorescent hybridization probes.* Journal of clinical microbiology, 2001. **39**(1): p. 370-374.

281. Kim, J.S., et al., *A novel multiplex PCR assay for rapid and simultaneous detection of five pathogenic bacteria: Escherichia coli O157: H7, Salmonella, Staphylococcus aureus, Listeria monocytogenes, and Vibrio parahaemolyticus.* Journal of Food Protection®, 2007. **70**(7): p. 1656-1662.

282. Iqbal, S.S., et al., *A review of molecular recognition technologies for detection of biological threat agents.* Biosensors and Bioelectronics, 2000. **15**(11): p. 549-578.

283. Sunwoo, H.H., W.W. Wang, and J.S. Sim, *Detection of Escherichia col O157: H7 using chicken immunoglobulin Y.* Immunology letters, 2006. **106**(2): p. 191-193.

284. Sewell, A., et al., *The development of an efficient and rapid enzyme linked fluorescent assay method for the detection of Listeria spp. from foods.* International journal of food microbiology, 2003. **81**(2): p. 123-129.

285. Schneid, A.d.S., et al., *Evaluation of an indirect ELISA for the detection of Salmonella in chicken meat.* Brazilian Journal of Microbiology, 2006. **37**(3): p. 350-355.

286. Owen, J.A., et al., *Kuby immunology*. 2013: WH Freeman New York.

287. Zhang, Y., et al., *Sensitive chemiluminescence immunoassay for E. coli O157: H7 detection with signal dual-amplification using glucose oxidase and laccase.* Analytical chemistry, 2014. **86**(2): p. 1115-1122.

288. Carvalho, R.N., et al., *PCR and ELISA (VIDAS ECO O157®) Escherichia coli O157: H7 identification in Minas Frescal cheese commercialized in Goiânia, GO.* Brazilian Journal of Microbiology, 2014. **45**(1): p. 07-10.

289. Gehring, A.G. and S.-I. Tu, *Enzyme-linked immunomagnetic electrochemical detection of live Escherichia coli O157: H7 in apple juice.* Journal of Food Protection®, 2005. **68**(1): p. 146-149.

290. Bennett, A., S. MacPhee, and R. Betts, *The isolation and detection of Escherichia coli O157 by use of immunomagnetic separation and immunoassay procedures.* Letters in applied microbiology, 1996. **22**(3): p. 237-243.

291. Zhu, P., et al., *Detection of E. col O157: H7 by immunomagnetic separation coupled with fluorescence immunoassay.* Biosensors and Bioelectronics, 2011. **30**(1): p. 337-341.

292. Gehring, A.G., et al., *Antibody Microarray Detection of Escherichia c oli O157: H7: Quantification, Assay Limitations, and Capture Efficiency.* Analytical chemistry, 2006. **78**(18): p. 6601-6607.

293. Disney, M.D. and P.H. Seeberger, *The use of carbohydrate microarrays to study carbohydrate-cell interactions and to detect pathogens.* Chemistry & biology, 2004. **11**(12): p. 1701-1707.
294. Wu, C.-F., et al., *DNA microarray for discrimination between pathogenic 0157: H7 EDL933 and non-pathogenic Escherichia col strains.* Biosensors and Bioelectronics, 2003. **19**(1): p. 1-8.
295. Woodbury, R.G., et al., *Construction of biosensors using a gold-binding polypeptide and a miniature integrated surface plasmon resonance sensor.* Biosensors and Bioelectronics, 1998. **13**(10): p. 1117-1126.
296. Fratamico, P., et al., *Detection of Escherichia coli 0157: H7 using a surface plasmon resonance biosensor.* Biotechnology Techniques, 1998. **12**(7): p. 571-576.
297. Ferreira, A., M. Werneck, and R. Ribeiro, *Aerobiological pathogen detection by evanescent wave fibre optic sensor.* Biotechnology techniques, 1999. **13**(7): p. 447-452.
298. Ziegler, C., *Cantilever-based biosensors.* Analytical and bioanalytical chemistry, 2004. **379**(7-8): p. 946-959.
299. Ilic, B., et al., *Mechanical resonant immunospecific biological detector.* Applied Physics Letters, 2000. **77**(3): p. 450-452.
300. Dzyadevych, S.V., et al., *Amperometric enzyme biosensors: past, present and future.* Irbm, 2008. **29**(2): p. 171-180.
301. Mata, D., et al., *Screen-printed integrated microsystem for the electrochemical detection of pathogens.* Electrochimica Acta, 2010. **55**(14): p. 4261-4266.
302. Barreiros dos Santos, M., et al., *Highly sensitive detection of pathogen< i> Escherichia coli</i> O157: H7 by electrochemical impedance spectroscopy.* Biosensors and Bioelectronics, 2013. **45**: p. 174-180.
303. Pérez-López, B. and A. Merkoçi, *Nanomaterials based biosensors for food analysis applications.* Trends in Food Science & Technology, 2011. **22**(11): p. 625-639.
304. McKeague, M., A. Giamberardino, and M. DeRosa, *Advances in aptamer-based biosensors for food safety.* Environmental Biosensors. New York: In Tech, 2011: p. 17-42.
305. ZHU, W.-q., et al., *Advance in Aptamer-based Biosensors.* Chinese Journal of Veterinary Drug, 2011. **7**: p. 016.
306. Tombelli, S., M. Minunni, and M. Mascini, *Aptamers-based assays for diagnostics, environmental and food analysis.* Biomolecular Engineering, 2007. **24**(2): p. 191-200.

307. Joshi, R., et al., *Selection, characterization, and application of DNA aptamers for the capture and detection of Salmonella enterica serovars.* Molecular and cellular probes, 2009. **23**(1): p. 20-28.

308. Duan, N., et al., *Dual-color upconversion fluorescence and aptamer-functionalized magnetic nanoparticles-based bioassay for the simultaneous detection of Salmonella Typhimurium and Staphylococcus aureus.* Analytica chimica acta, 2012. **723**: p. 1-6.

309. Duan, N., et al., *Selection, identification and application of a DNA aptamer against Listeria monocytogenes.* Food Control, 2013. **33**(1): p. 239-243.

310. Cao, X., et al., *Combining use of a panel of ssDNA aptamers in the detection of Staphylococcus aureus.* Nucleic acids research, 2009. **37**(14): p. 4621-4628.

311. Savory, N., et al., *Selection of DNA aptamers against uropathogenic Escherichia coli NSM59 by quantitative PCR controlled Cell-SELEX.* Journal of microbiological methods, 2014. **104**: p. 94-100.

312. Bruno, J.G., et al., *Plastic-adherent DNA aptamer-magnetic bead and quantum dot sandwich assay for Campylobacter detection.* Journal of fluorescence, 2009. **19**(3): p. 427-435.

313. Chen, F., et al., *Aptamer from whole-bacterium SELEX as new therapeutic reagent against virulent Mycobacterium tuberculosis.* Biochemical and biophysical research communications, 2007. **357**(3): p. 743-748.

314. Boshoff, H.I. and K. Tahlan, *Mechanisms underlying mycobacterial infections.* Drug discovery today. Disease mechanisms, 2010. **7**(1): p. e1.

315. Stratis-Cullum, D.N., S. McMasters, and P.M. Pellegrino, *Evaluation of relative aptamer binding to campylobacter jejuni bacteria using affinity probe capillary electrophoresis.* Analytical Letters, 2009. **42**(15): p. 2389-2402.

316. So, H.M., et al., *Detection and Titer Estimation of Escherichia coli Using Aptamer-Functionalized Single-Walled Carbon-Nanotube Field-Effect Transistors.* Small, 2008. **4**(2): p. 197-201.

317. Vivekananda, J. and J.L. Kiel, *Anti-Francisella tularensis DNA aptamers detect tularemia antigen from different subspecies by aptamer-linked immobilized sorbent assay.* Laboratory investigation, 2006. **86**(6): p. 610-618.

318. Queirós, R.B., et al., *A label-free DNA aptamer-based impedance biosensor for the detection of< i> E. coli</i> outer membrane proteins.* Sensors and Actuators B: Chemical, 2013. **181**: p. 766-772.

319. Wu, W., et al., *An aptamer-based biosensor for colorimetric detection of Escherichia coli O157: H7.* PloS one, 2012. **7**(11): p. e48999.

320. Anderson, J.M. and R.E. Marchant, *Biomaterials: factors favoring colonization and infection.* Infections associated with biomedical devices, 3rd ed. ASM Press, Washington, DC, 2000: p. 89-109.

321. Weber, W.P., et al., *Economic burden of surgical site infections at a European university hospital.* infection control and hospital epidemiology, 2008. **29**(7): p. 623-629.

322. Perencevich, E.N., et al., *Health and economic impact of surgical site infections diagnosed after hospital discharge.* Emerging infectious diseases, 2003. **9**(2): p. 196.

323. System, N.N.I.S., *National Nosocomial Infections Surveillance (NNIS) System Report, data summary from January 1992 through June 2004, issued October 2004.* American journal of infection control, 2004. **32**(8): p. 470.

324. Prevention, C.f.D.C.a. *Pseudomonas aeruginosa in Healthcare Settings*. 2013; Available from: http://www.cdc.gov/hai/organisms/pseudomonas.html.

325. Mah, T.-F., et al., *A genetic basis for Pseudomonas aeruginosa biofilm antibiotic resistance.* Nature, 2003. **426**(6964): p. 306-310.

326. Stewart, P.S. and J. William Costerton, *Antibiotic resistance of bacteria in biofilms.* The Lancet, 2001. **358**(9276): p. 135-138.

327. Davey, M.E. and G.A. O'toole, *Microbial biofilms: from ecology to molecular genetics.* Microbiology and molecular biology reviews, 2000. **64**(4): p. 847-867.

328. Drenkard, E. and F.M. Ausubel, *Pseudomonas biofilm formation and antibiotic resistance are linked to phenotypic variation.* Nature, 2002. **416**(6882): p. 740-743.

329. Hoyle, B.D. and J.W. Costerton, *Bacterial resistance to antibiotics: the role of biofilms*, in *Progress in Drug Research/Fortschritte der Arzneimittelforschung/Progrès des recherches pharmaceutiques*. 1991, Springer. p. 91-105.

330. Aloush, V., et al., *Multidrug-resistant Pseudomonas aeruginosa: risk factors and clinical impact.* Antimicrobial agents and chemotherapy, 2006. **50**(1): p. 43-48.

331. Fridkin, S.K. and R.P. Gaynes, *Antimicrobial resistance in intensive care units.* Clinics in chest medicine, 1999. **20**(2): p. 303-316.

332. Desrousseaux, C., et al., *Modification of the surfaces of medical devices to prevent microbial adhesion and biofilm formation.* Journal of Hospital Infection, 2013. **85**(2): p. 87-93.

333. Monteiro, D.R., et al., *The growing importance of materials that prevent microbial adhesion: antimicrobial effect of medical devices containing silver.* International journal of antimicrobial agents, 2009. **34**(2): p. 103-110.

334. Zobell, C.E. and E.C. Allen, *The significance of marine bacteria in the fouling of submerged surfaces.* Journal of bacteriology, 1935. **29**(3): p. 239.

335. Zobell, C.E., *The effect of solid surfaces upon bacterial activity.* Journal of bacteriology, 1943. **46**(1): p. 39.

336. Bazaka, K., et al., *Efficient surface modification of biomaterial to prevent biofilm formation and the attachment of microorganisms.* Applied microbiology and biotechnology, 2012. **95**(2): p. 299-311.

337. Warnes, S. and C. Keevil, *Mechanism of copper surface toxicity in vancomycin-resistant enterococci following wet or dry surface contact.* Applied and environmental microbiology, 2011. **77**(17): p. 6049-6059.

338. Hasan, J., R.J. Crawford, and E.P. Ivanova, *Antibacterial surfaces: the quest for a new generation of biomaterials.* Trends in biotechnology, 2013. **31**(5): p. 295-304.

339. Ivanova, E.P., et al., *Natural bactericidal surfaces: mechanical rupture of Pseudomonas aeruginosa cells by cicada wings.* Small, 2012. **8**(16): p. 2489-2494.

340. Ivanova, E.P., et al., *Differential attraction and repulsion of Staphylococcus aureus and Pseudomonas aeruginosa on molecularly smooth titanium films.* Scientific reports, 2011. **1**.

341. Whitehead, K.A., J. Colligon, and J. Verran, *Retention of microbial cells in substratum surface features of micrometer and sub-micrometer dimensions.* Colloids and Surfaces B: Biointerfaces, 2005. **41**(2): p. 129-138.

342. Van der Mei, H., R. Bos, and H. Busscher, *A reference guide to microbial cell surface hydrophobicity based on contact angles.* Colloids and surfaces B: Biointerfaces, 1998. **11**(4): p. 213-221.

343. Ahamed, M., et al., *Green synthesis, characterization and evaluation of biocompatibility of silver nanoparticles.* Physica E: Low-dimensional Systems and Nanostructures, 2011. **43**(6): p. 1266-1271.

344. De, M., P.S. Ghosh, and V.M. Rotello, *Applications of nanoparticles in biology.* Advanced Materials, 2008. **20**(22): p. 4225-4241.

345. Panáček, A., et al., *Silver colloid nanoparticles: synthesis, characterization, and their antibacterial activity.* The Journal of Physical Chemistry B, 2006. **110**(33): p. 16248-16253.

346. Pal, S., Y.K. Tak, and J.M. Song, *Does the antibacterial activity of silver nanoparticles depend on the shape of the nanoparticle? A study of the gram-negative bacterium Escherichia coli.* Applied and environmental microbiology, 2007. **73**(6): p. 1712-1720.

347. Sharma, V.K., R.A. Yngard, and Y. Lin, *Silver nanoparticles: green synthesis and their antimicrobial activities.* Advances in colloid and interface science, 2009. **145**(1): p. 83-96.

348. Pillai, Z.S. and P.V. Kamat, *What factors control the size and shape of silver nanoparticles in the citrate ion reduction method?* The Journal of Physical Chemistry B, 2004. **108**(3): p. 945-951.

349. Wang, H., et al., *Preparation of silver nanoparticles by chemical reduction method.* Colloids and Surfaces A: Physicochemical and Engineering Aspects, 2005. **256**(2): p. 111-115.

350. Zhu, J., et al., *Shape-controlled synthesis of silver nanoparticles by pulse sonoelectrochemical methods.* Langmuir, 2000. **16**(16): p. 6396-6399.

351. Farazuddin, M., et al., *Amoxicillin-bearing microparticles: potential in the treatment of Listeria monocytogenes infection in Swiss albino mice.* Bioscience reports, 2011. **31**: p. 265-272.

352. Adwan, G. and M. Mhanna, *Synergistic effects of plant extracts and antibiotics on Staphylococcus aureus strains isolated from clinical specimens.* Middle-East Journal of Scientific Research, 2008. **3**(3): p. 134-139.

353. Kwong, T., et al., *5S clavam biosynthesis is controlled by an atypical two-component regulatory system in Streptomyces clavuligerus.* Antimicrobial agents and chemotherapy, 2012. **56**(9): p. 4845-4855.

354. Tahlan, K., et al., *Two sets of paralogous genes encode the enzymes involved in the early stages of clavulanic acid and clavam metabolite biosynthesis in Streptomyces clavuligerus.* Antimicrobial agents and chemotherapy, 2004. **48**(3): p. 930-939.

355. Damm, C., H. Münstedt, and A. Rösch, *The antimicrobial efficacy of polyamide 6/silver-nano-and microcomposites.* Materials Chemistry and Physics, 2008. **108**(1): p. 61-66.

356. Neal, A.L., *What can be inferred from bacterium–nanoparticle interactions about the potential consequences of environmental exposure to nanoparticles?* Ecotoxicology, 2008. **17**(5): p. 362-371.

357. Strohal, R., et al., *Nanocrystalline silver dressings as an efficient anti-MRSA barrier: a new solution to an increasing problem.* Journal of Hospital Infection, 2005. **60**(3): p. 226-230.

358. Zhang, W., X. Qiao, and J. Chen, *Synthesis of silver nanoparticles—effects of concerned parameters in water/oil microemulsion.* Materials Science and Engineering: B, 2007. **142**(1): p. 1-15.

359. Mohanpuria, P., N.K. Rana, and S.K. Yadav, *Biosynthesis of nanoparticles: technological concepts and future applications.* Journal of Nanoparticle Research, 2008. **10**(3): p. 507-517.

360. Eby, D.M., H.R. Luckarift, and G.R. Johnson, *Hybrid antimicrobial enzyme and silver nanoparticle coatings for medical instruments.* ACS applied materials & interfaces, 2009. **1**(7): p. 1553-1560.

361. Taglietti, A., et al., *Antibacterial activity of glutathione-coated silver nanoparticles against gram positive and gram negative bacteria.* Langmuir, 2012. **28**(21): p. 8140-8148.

362. Nam, K.T., et al., *Peptide-mediated reduction of silver ions on engineered biological scaffolds.* Acs Nano, 2008. **2**(7): p. 1480-1486.

363. Mei, L., et al., *Bioconjugated nanoparticles for attachment and penetration into pathogenic bacteria.* Biomaterials, 2013. **34**(38): p. 10328-10337.

364. Golubeva, O.Y., et al., *Synthesis and study of antimicrobial activity of bioconjugates of silver nanoparticles and endogenous antibiotics.* Glass Physics and Chemistry, 2011. **37**(1): p. 78-84.

365. Jaiswal, S., et al., *Enhancement of the antibacterial properties of silver nanoparticles using β-cyclodextrin as a capping agent.* International journal of antimicrobial agents, 2010. **36**(3): p. 280-283.

366. Wei, Q., et al., *Norvancomycin-capped silver nanoparticles: synthesis and antibacterial activities against E. coli.* Science in China Series B: Chemistry, 2007. **50**(3): p. 418-424.

367. Stoltenburg, R., C. Reinemann, and B. Strehlitz, *FluMag-SELEX as an advantageous method for DNA aptamer selection.* Analytical and bioanalytical chemistry, 2005. **383**(1): p. 83-91.

368. Bruno, J.G., et al., *Development of DNA aptamers for cytochemical detection of acetylcholine.* In Vitro Cellular & Developmental Biology-Animal, 2008. **44**(3-4): p. 63-72.

369. Storhoff, J.J., et al., *One-pot colorimetric differentiation of polynucleotides with single base imperfections using gold nanoparticle probes.* Journal of the American Chemical Society, 1998. **120**(9): p. 1959-1964.

370. Zuker, M., *Mfold web server for nucleic acid folding and hybridization prediction.* Nucleic acids research, 2003. **31**(13): p. 3406-3415.

371. Sergeev, B., et al., *Synthesis of protein A conjugates with silver nanoparticles.* Colloid Journal, 2003. **65**(5): p. 636-638.

372. Munro, C., et al., *Characterization of the surface of a citrate-reduced colloid optimized for use as a substrate for surface-enhanced resonance Raman scattering.* Langmuir, 1995. **11**(10): p. 3712-3720.

373. Ferraro, M.J., *Methods for dilution antimicrobial susceptibility tests for bacteria that grow aerobically.* 2000.

374. Ghosh, I.N., et al., *Synergistic action of cinnamaldehyde with silver nanoparticles against spore-forming bacteria: a case for judicious use of silver nanoparticles for antibacterial applications.* International journal of nanomedicine, 2013. **8**: p. 4721.

375. Bendaoud, M., et al., *Broad-spectrum biofilm inhibition by Kingella kingae exopolysaccharide.* Journal of bacteriology, 2011. **193**(15): p. 3879-3886.

376. Inbakandan, D., et al., *Silver nanoparticles with anti microfouling effect: a study against marine biofilm forming bacteria.* Colloids and Surfaces B: Biointerfaces, 2013. **111**: p. 636-643.

377. George, A., *Microtiter dish biofilm formation assay.* Journal of Visualized Experiments, 2011(47).

378. O'Toole, G.A., et al., *Genetic approaches to study of biofilms.* 1999.

379. Barraud, N., et al., *Mannitol enhances antibiotic sensitivity of persister bacteria in Pseudomonas aeruginosa biofilms.* PloS one, 2013. **8**(12): p. e84220.

380. Hall-Stoodley, L., J.W. Costerton, and P. Stoodley, *Bacterial biofilms: from the natural environment to infectious diseases.* Nature Reviews Microbiology, 2004. **2**(2): p. 95-108.

381. Radzig, M., et al., *Antibacterial effects of silver nanoparticles on gram-negative bacteria: influence on the growth and biofilms formation, mechanisms of action.* Colloids and Surfaces B: Biointerfaces, 2013. **102**: p. 300-306.

382. Mehedi Masud, M., et al., *Sialyllactose-binding modified DNA aptamer bearing additional functionality by SELEX.* Bioorganic & medicinal chemistry, 2004. **12**(5): p. 1111-1120.

383. Neumann, O., et al., *Direct optical detection of aptamer conformational changes induced by target molecules.* Analytical chemistry, 2009. **81**(24): p. 10002-10006.

384. Jin, Y., J. Bai, and H. Li, *Label-free protein recognition using aptamer-based fluorescence assay.* Analyst, 2010. **135**(7): p. 1731-1735.

385. Ramakrishnan, S. and M. Palaniandavar, *Mixed-ligand copper (II) complexes of dipicolylamine and 1, 10-phenanthrolines: The role of diimines in the interaction of the complexes with DNA.* J Chem Sci, 2005. **117**: p. 179-186.

386. Kypr, J., et al., *Circular dichroism and conformational polymorphism of DNA.* Nucleic acids research, 2009. **37**(6): p. 1713-1725.

387. Song, K.-M., S. Lee, and C. Ban, *Aptamers and their biological applications.* Sensors, 2012. **12**(1): p. 612-631.

388. Liang, X., et al., *Colorimetric detection of melamine in complex matrices based on cysteamine-modified gold nanoparticles.* Analyst, 2010. **136**(1): p. 179-183.

389. Tasset, D.M., M.F. Kubik, and W. Steiner, *Oligonucleotide inhibitors of human thrombin that bind distinct epitopes.* Journal of molecular biology, 1997. **272**(5): p. 688-698.

390. Mocanu, A., et al., *Self-assembly characteristics of gold nanoparticles in the presence of cysteine.* Colloids and Surfaces A: Physicochemical And Engineering Aspects, 2009. **338**(1): p. 93-101.

391. Li, H. and L. Rothberg, *Colorimetric detection of DNA sequences based on electrostatic interactions with unmodified gold nanoparticles.* Proceedings of the National Academy of Sciences of the United States of America, 2004. **101**(39): p. 14036-14039.

392. Wang, H., et al., *Gold nanoparticle-based colorimetric and "turn-on" fluorescent probe for mercury (II) ions in aqueous solution.* Analytical chemistry, 2008. **80**(23): p. 9021-9028.

393. Wang, Y., F. Yang, and X. Yang, *Colorimetric biosensing of mercury (II) ion using unmodified gold nanoparticle probes and thrombin-binding aptamer.* Biosensors and Bioelectronics, 2010. **25**(8): p. 1994-1998.

394. Yu, M., *Colorimetric Detection of Trace Arsenic (III) in Aqueous Solution Using Arsenic Aptamer and Gold Nanoparticles.* Australian Journal of Chemistry, 2014. **67**(5): p. 813-818.

395. Wei, H., et al., *Simple and sensitive aptamer-based colorimetric sensing of protein using unmodified gold nanoparticle probes.* Chem. Commun., 2007(36): p. 3735-3737.

396. Liu, A., et al., *Gold nanoparticle-based colorimetric detection of staphylococcal enterotoxin B using ssDNA aptamers.* European Food Research and Technology, 2013. **237**(3): p. 323-329.

397. Li, H., et al., *Selective quenching of fluorescence from unbound oligonucleotides by gold nanoparticles as a probe of RNA structure.* RNA, 2007. **13**(11): p. 2034-2041.

398. Dubertret, B., M. Calame, and A.J. Libchaber, *Single-mismatch detection using gold-quenched fluorescent oligonucleotides.* Nature biotechnology, 2001. **19**(4): p. 365-370.

399. Darbha, G.K., A. Ray, and P.C. Ray, *Gold nanoparticle-based miniaturized nanomaterial surface energy transfer probe for rapid and ultrasensitive detection of mercury in soil, water, and fish.* Acs Nano, 2007. **1**(3): p. 208-214.

400. Jennings, T., M. Singh, and G. Strouse, *Fluorescent lifetime quenching near d= 1.5 nm gold nanoparticles: probing NSET validity.* Journal of the American Chemical Society, 2006. **128**(16): p. 5462-5467.

401. Blattner, F.R., et al., *The complete genome sequence of Escherichia coli K-12.* science, 1997. **277**(5331): p. 1453-1462.

402. Francetić, O., S. Lory, and A.P. Pugsley, *A second prepilin peptidase gene in Escherichia coli K-12.* Molecular microbiology, 1998. **27**(4): p. 763-775.

403. Strom, M. and S. Lory, *Structure-function and biogenesis of the type IV pili.* Annual Reviews in Microbiology, 1993. **47**(1): p. 565-596.

404. Wu, W.-h., et al., *Aptasensors for rapid detection of Escherichia coli O157: H7 and Salmonella typhimurium.* Nanoscale research letters, 2012. **7**(1): p. 1-7.

405. Ozalp, V.C., et al., *Pathogen detection by core–shell type aptamer-magnetic preconcentration coupled to real-time PCR.* Analytical biochemistry, 2014. **447**: p. 119-125.

406. Zelada-Guillén, G.A., et al., *Immediate detection of living bacteria at ultralow concentrations using a carbon nanotube based potentiometric aptasensor.* Angewandte Chemie International Edition, 2009. **48**(40): p. 7334-7337.

407. Pan, Q., et al., *Aptamers that preferentially bind type IVB pili and inhibit human monocytic-cell invasion by Salmonella enterica serovar typhi.* Antimicrobial agents and chemotherapy, 2005. **49**(10): p. 4052-4060.

408. Mock, J., et al., *Shape effects in plasmon resonance of individual colloidal silver nanoparticles.* The Journal of Chemical Physics, 2002. **116**(15): p. 6755-6759.

409. Dhawan, A. and V. Sharma, *Toxicity assessment of nanomaterials: methods and challenges.* Analytical and bioanalytical chemistry, 2010. **398**(2): p. 589-605.

410. Socrates, G., *Infrared and Raman characteristic group frequencies: tables and charts*. 2004: John Wiley & Sons.

411. Formaggio, F., et al., *The First Water-Soluble 310-Helical Peptides.* Chemistry-A European Journal, 2000. **6**(24): p. 4498-4504.

412. Toniolo, C., et al., *Circular dichroism spectrum of a peptide 310-helix.* Journal of the American Chemical Society, 1996. **118**(11): p. 2744-2745.

413. Ruden, S., et al., *Synergistic interaction between silver nanoparticles and membrane-permeabilizing antimicrobial peptides.* Antimicrobial agents and chemotherapy, 2009. **53**(8): p. 3538-3540.

414. Park, S., et al., *Antimicrobial activity and cellular toxicity of nanoparticle–polymyxin B conjugates.* Nanotechnology, 2011. **22**(18): p. 185101.

415. Pathania, R., et al., *Chemical genomics in Escherichia coli identifies an inhibitor of bacterial lipoprotein targeting.* Nature chemical biology, 2009. **5**(11): p. 849-856.

416. Bondarenko, O., et al., *Particle-cell contact enhances antibacterial activity of silver nanoparticles.* PloS one, 2013. **8**(5): p. e64060.

417. Sauer, K., et al., *Pseudomonas aeruginosa displays multiple phenotypes during development as a biofilm.* Journal of bacteriology, 2002. **184**(4): p. 1140-1154.

418. Palmer, J., S. Flint, and J. Brooks, *Bacterial cell attachment, the beginning of a biofilm.* Journal of industrial microbiology & biotechnology, 2007. **34**(9): p. 577-588.

419. Raymond, J., *[Pseudomonas aeruginosa and hospital-acquired infections].* Archives de pediatrie: organe officiel de la Societe francaise de pediatrie, 2006. **13**: p. S2-4.

420. Driscoll, J.A., S.L. Brody, and M.H. Kollef, *The epidemiology, pathogenesis and treatment of Pseudomonas aeruginosa infections.* Drugs, 2007. **67**(3): p. 351-368.

421. Kerr, K. and A. Snelling, *Pseudomonas aeruginosa: a formidable and ever-present adversary.* Journal of Hospital Infection, 2009. **73**(4): p. 338-344.

422. Berney, M., et al., *Assessment and interpretation of bacterial viability by using the LIVE/DEAD BacLight Kit in combination with flow cytometry.* Applied and environmental microbiology, 2007. **73**(10): p. 3283-3290.

423. Gião, M.S., et al., *Validation of SYTO 9/propidium iodide uptake for rapid detection of viable but noncultivable Legionella pneumophila.* Microbial ecology, 2009. **58**(1): p. 56-62.

424. Davies, B. and J. Cohen, *Endotoxin removal devices for the treatment of sepsis and septic shock.* The Lancet infectious diseases, 2011. **11**(1): p. 65-71.

425. Héquet, A., et al., *Optimized grafting of antimicrobial peptides on stainless steel surface and biofilm resistance tests.* Colloids and Surfaces B: Biointerfaces, 2011. **84**(2): p. 301-309.